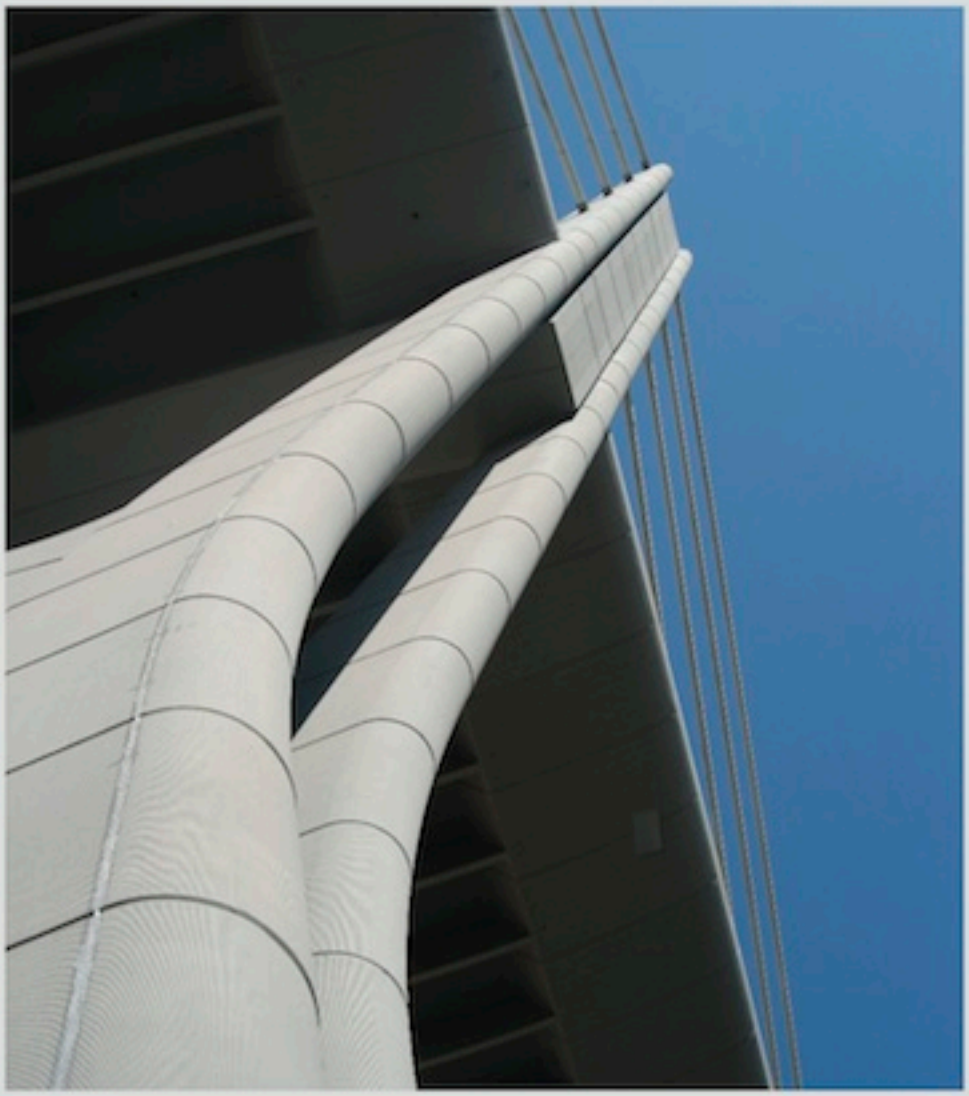
bulletin 54

manual – textbook

fib
CEB-FIP



Structural Concrete

Textbook on behaviour, design and performance

Second edition

Volume 4

Structural Concrete

Textbook

on behaviour, design and performance

Second edition

Volume 4

October 2010

Subject to priorities defined by the Technical Council and the Presidium, the results of ***fib***'s work in Commissions and Task Groups are published in a continuously numbered series of technical publications called 'Bulletins'. The following categories are used:

category	minimum approval procedure required prior to publication
Technical Report	approved by a Task Group and the Chairpersons of the Commission
State-of-Art Report	approved by a Commission
Manual, Guide (to good practice) or Recommendation	approved by the Technical Council of ***fib***
Model Code	approved by the General Assembly of ***fib***

Any publication not having met the above requirements will be clearly identified as preliminary draft.

This Bulletin N° 54 was approved as an ***fib*** Manual by the Technical Council in June 2009.

This fourth volume of the Structural Concrete Textbook, second edition, was drafted by the following authors:

György L. Balázs* (Budapest Univ. of Technology and Economics, Hungary)	Editor
Karl R. Kordina †	Chapter 6
Giuseppe Mancini* (Politecnico Torino, Italy)	Sections 7.1, 7.2, 7.4
Kurt Schäfer (Germany)	Section 7.3
Angelika Schieβl (Germany)	Chapter 8
Konrad Zilch* (Technische Univ. München, Germany)	Chapter 8

* member of Special Activity Group 2, "Dissemination of knowledge", Working Group "Textbook".

Full address details of Commission/Task Group members may be found in the ***fib*** Directory or through the online services on ***fib's*** website, www.fib-international.org.

Cover image: Wadi Abdoun Bridge, Jordan, one of the winners of the 2010 *fib* Awards for Outstanding Concrete Structures [photo courtesy of Dar Al-Handasah (Shair & Partners)].

© fédération internationale du béton (***fib***), 2010

Although the International Federation for Structural Concrete ***fib*** - fédération internationale du béton - does its best to ensure that any information given is accurate, no liability or responsibility of any kind (including liability for negligence) is accepted in this respect by the organisation, its members, servants or agents.

All rights reserved. No part of this publication may be reproduced, modified, translated, stored in a retrieval system, or transmitted in any form or by any means, electronic, mechanical, photocopying, recording, or otherwise, without prior written permission.

First published in 2010 by the International Federation for Structural Concrete (*fib*)
Postal address: Case Postale 88, CH-1015 Lausanne, Switzerland
Street address: Federal Institute of Technology Lausanne - EPFL, Section Génie Civil
Tel +41 21 693 2747 • Fax +41 21 693 6245
fib@epfl.ch • www.fib-international.org

ISSN 1562-3610
ISBN 978-2-88394-094-9

Printed by DCC Document Competence Center Siegmar Kästl e.K., Germany

Copyright fib, all rights reserved. This PDF copy of fib Bulletin 54 is intended for use and/or distribution only within National Member Groups of fib.

Editor's remarks

Volumes 1, 2 and 3 of the second edition of *Structural Concrete Textbook on behaviour, design and performance* were recently published in *fib* Bulletin 51 (*Design of concrete structures, Conceptual design, Concrete, reinforcement and composite behaviour*), *fib* Bulletin 52 (*Structural analysis, Design format, Serviceability and ultimate limit state principles, Anchorage and detailing principles*) and *fib* Bulletin 53 (*Design of durable concrete structures*).

This *fib* Bulletin 54 is Volume 4 of the Textbook. A forthcoming Volume 5 on *Through life care and management of concrete structures – Assessment, protection, repair and strengthening* will be published as a separate bulletin.

Volume 4 of the *Structural Concrete Textbook* includes the following three areas:

Chapter 6 Design of concrete buildings for fire resistance was originally written by Karl Kordina. Regretfully, he passed away just after submitting his ideas about improvements for Chapter 6; nevertheless based on his guidance we were able to finalize this chapter. Serious cases of fire remind us again and again the importance of fire design. Chapter 6 includes guidance on progress of fire, modifications of material properties as a function of temperature (concrete, non-prestressed steel, prestressing steel), general design rules, design concept, robustness, spalling, thermal expansion, importance of joints, compartmentation, cooling and design examples for fire resistance.

Chapter 7 Design of members includes examples for linear members, slabs as well as deep beams and discontinuity regions.

The first example by Giuseppe Mancini in Chapter 7 gives all design details of a *box-culvert under crossing a railway line* for high speed trains. Particular attention is taken to the analysis and design of corner zones, detailing of reinforcement, anchorages, crack control and control of deformations. The second example also by Giuseppe Mancini gives the design of *a two dimensional prestressed concrete slab (a railway bridge deck)* that is a continuous slab on three supports with longitudinal and transverse prestressing. Details are included for the structural model, layout of prestressing reinforcement, analysis of initial or time dependent losses of prestressing, verification of serviceability and ultimate limit states and verification of bursting forces in the anchorage zones by using the symmetric prism analogy. A separate section was prepared by Giuseppe Mancini on reinforcement layouts of some typical elements. *Deep Beams and discontinuity regions* are presented by Kurt Schäfer including definition of D (discontinuity) regions, design of deep beams and discontinuity regions by strut-and-tie models with design examples.

Volume 4 is concluded by *Chapter 8 Practial aspects* by Konrad Zilch and Angelika Schießl. Details are included on definition of tolerances, effects of tolerances on durability, on serviceability, on appearance, on erection of precast structures. Quality requirements are given in the form of control methods of variation of material properties. Quality management, quality assurance plans, quality control, control levels, and influences on erection by the formwork and prestressing are also addressed.

Finally, I would like to express my thanks to the authors of the *Textbook* for their very valuable work in preparing their contributions. In addition, my special thanks are directed to Laura Thommen-Vidale in the *fib* secretariat in Lausanne for her careful work in finalizing the manuscripts, as well as to Dr. Éva Lublóy at my university in Budapest for her assistance to me.

György L. Balázs
Editor, Deputy-President, *fib*

Copyright fib, all rights reserved. This PDF copy of fib Bulletin 54 is intended for use and/or distribution only within National Member Groups of fib.

Contents

6 Design of concrete buildings for fire resistance 1

6.1 Fire risks 1

6.1.1 Objectives and design provisions 1

6.1.2 Costs and losses 2

6.2 Structural fire design 3

6.2.1 Fire severity 3

6.2.2 Progress of fire in a building 4

6.2.3 Structural response 6
(Spalling – Separating functions – Fire resistance design – Tabulated data)

6.3 Material properties 9

6.3.1 General aspects on the material properties 9

6.3.2 Concrete 10

6.3.3 Steel 12

6.4 General design rules and tables 14

6.4.1 General 14

6.4.2 Tabulated data 14
(Scope – General design rules)

6.5 Overall design 15

6.5.1 Concept design and detailing 15

6.5.2 Robust structures 16

6.5.2 Thermal expansion, restraint and behaviour of buildings in fire 17

6.5.4 Compartmentation 21

6.5.5 Fires in tunnels 22

6.6 Damage caused by fire exposure 24

6.6.1 Circumstances and indication at the place of the fire 24

6.6.2 Material damage 24

6.6.3 Structural damage 27

6.6.4 Determination of the degree of deterioration, method of repair 28

Annex to Chapter 6 30

A.1 General considerations 30

A.2 Columns 30

A.3 Load bearing solid walls 31

Copyright fib, all rights reserved. This PDF copy of fib Bulletin 54 is intended for use and/or distribution only within National Member Groups of fib.

A.4 Beams 31
(General – Simply supported beams – Continuous beams)

A.5 Simply supported slabs 32

A.6 Flat slabs 32

7 Design of members 37

7.1 Linear members 37

7.1.1 Description of the structures 37

7.1.2 Structural model 40

7.1.3 Actions 41

7.1.4 Combination for ULS and consequent internal actions 43
(Design of upper slab and foundation – Design of uprights)

7.1.5 Reinforcement layout 51

7.1.6 Verification at serviceability limit state 56
(Stress limitation – Crack width – Deformation)

7.2 Slabs 61

7.2.1 Description of the structure 61
(Material properties – Concrete cover)

7.2.2 Structural model 62
(Restraints – Prestressing forces – Time-dependent prestressing losses)

7.2.3 Actions 70

7.2.4 Combinations of actions 74

7.2.5 Verification at serviceability limit state 75
(Verification at tensioning – Verification of limit state of stress limitation in concrete – Verification of serviceability limit state of cracking – Deformation)

7.2.6 Verification of ultimate limit state 77
(Ultimate limit state of slab – Verification of bursting force – Verification of spalling force – Verification of punching action

7.3 Deep beams and discontinuity regions 88

7.3.1 Principles and methods of design 88
(Introduction to the design of deep beams and discontinuity regions – The design of D-regions with finite element computer programs (FEM) – Design of deep beams and discontinuity regions with strut-and-tie models)

7.3.2 Deep beams 106
(General – Numerical example of a deep beam)

7.3.3 Beam-column connections 116
(General behaviour – Beam-column connections with negative (closing) moment – Beam-column connections with positive (opening) moment – Rigid connection of column with continuous beam – Members with a kink and joints of profiled members)

Copyright fib, all rights reserved. This PDF copy of fib Bulletin 54 is intended for use and/or distribution only within National Member Groups of fib.

7.3.4 Corbels 125
(Load bearing behaviour and necessary checks – Standard design for a corbel (numerical example) – Corbels with suspended or indirect load)

7.4 Reinforcement layout of typical elements 132

8 Practical aspects 151

8.1 Introduction 151

8.2 Geometric tolerances 151

8.2.1 Definition and types 151

8.2.2 Effects on tolerances 152
(Effects on safety – Effects on durability – Effects on serviceability and structural appearance – Effects on erection of precast concrete structures – Admissible tolerances)

8.3 Quality requirements for material properties 161

8.3.1 Variations in material properties 161

8.3.2 Control methods of variations in material properties 163

8.3.3 Influences of variation in material properties 165
(Effects on safety – Effects on economy – Effects on serviceability and structural appearance)

8.4 Quality management 167

8.4.1 General 167

8.4.2 Concept of quality management 168

8.4.3 Quality assurance plant 169

8.4.4 Quality control 170
(General – Phases of control – Types of control – Control levels)

8.5 Aspects in erection of RC and PC structures 171

8.5.1 General 171

8.5.2 Formwork and falsework 172
(Formwork – Falsework)

8.5.3 Curing 175

8.6 Prestressing 177

8.6.1 Time of prestressing 178

8.6.2 Effects of prestressing during construction 178

8.7 Precast elements and structures 180

8.7.1 General 180

8.7.2 Joints 181

References to Chapter 8 181

Annex: List of notations 183

Copyright fib, all rights reserved. This PDF copy of fib Bulletin 54 is intended for use and/or distribution only within National Member Groups of fib.

6 Design of concrete buildings for fire resistance

by Karl R. Kordina †

Preface

Structural fire design and fire strategies need to be considered at a very early stage in the design of new buildings, and also in the renovation of existing buildings. Early planning can result in very significant cost savings. On the other hand, costs can become very high, if the first consideration of fire safety is given when the building work is nearing completion.

Fire protection is achieved through a range of measures, including planning of evacuation routes and protection against smoke toxic gases, as well as the fire design of load bearing members.

Specific fire design provisions depend on the type and function of the building. They also vary according to local and national standards. Therefore, this report focuses only on general aspects of fire safety in concrete buildings, and some additional information is given with respect to EN 1992-1-2: Structural fire design.

6.1 Fire risks

6.1.1 Objectives and design provisions

Fires in buildings occur with unwelcome frequency, but in spite of intensive efforts, it has not been possible to reduce the fire frequency substantially. Designers have a very important role to play in providing adequate fire safety in buildings. Through the appropriate choice of design details and materials, they must protect lives, minimize damage and economic loss, and apply measures in order to restrict the spread of fire.

National regulations for fire protection in buildings have a variety of aims, which can be summarized as follows:

- prevention of the outbreak of fire;
- avoid premature collapse of the structure;
- prevention of the spread of fire, smoke, hot and toxic gases beyond designated areas;
- safety of occupants in the zone, in other parts of the building and in adjacent buildings;
- evacuation of occupants from the immediate fire zone and other parts of the building;
- mitigation of damage to the building structure, the contents and to adjacent buildings;
- protection of life during fire fighting and rescue operations;
- the mitigation of property damage is looked after by insurance activities on a voluntary rather than a mandatory basis.

Government agencies are primarily interested in life safety, fire containment, and delaying the growth and spread of fire. They are also concerned with the possibility of general uncontrolled conflagration in built-up areas, and in ensuring that firefighting and rescue operations can proceed, even in buildings with difficult access such as large or high buildings.

Copyright fib, all rights reserved. This PDF copy of fib Bulletin 54 is intended for use and/or distribution only within National Member Groups of fib.

It is becoming apparent that some industrial installations also require national regulations because of special hazards which occur in the event of malfunction or accident. Examples are fires in nuclear power stations and in underwater tunnels.

Overall fire protection strategies involve both active and passive (or built-in) measures [National Building Regulations]. The passive built-in measures are preventive in character and remain permanently effective. Active measures, on the other hand, require the stimulus of the fire. They include detection, control by sprinklers or other installations, and fire fighting.

Buildings are usually classified according to intended use, occupancy, size and location; nevertheless, the fire regulations are aimed primarily at the safety of human occupants. If special circumstances apply and the owner requires additional standards, such as preservation of the structure, then these will be over and above the minimum regulatory requirements. In this respect there is currently a need for a more rational approach to the specification of fire safety in buildings, which takes account of risk, and aims at the optimum economic level of protection.

Since 90 % of all fatalities in fires occur as the result of smoke and toxic gases, it is particularly important for evacuation routes to be provided, with floors and staircases remaining free of smoke and properly illuminated. Smoke and fire doors should shut off floors and protect staircases. The distance from any room to a staircase should not be greater than about 30 m. Staircases must be designed to withstand a fire for 90 minutes. In all cases two evacuation routes must be provided. Up to a height of about 20 m, fire brigade ladders may be considered to provide a second escape route.

6.1.2 Costs and losses

Fortunately the risk of fire is generally low. While it remains so, people are reluctant to suffer too much inconvenience. Systems that are installed solely for the purpose of fire safety should therefore interfere with normal usage as little as possible, yet harmonize with public feelings on acceptable risks.

On the other hand, the risks of fire are not always obvious. As an example of unexpected risk, a person sleeping in a room adjacent to a fire is highly endangered because the concentrations of CO and CO_2 can rapidly reach fatal levels, well before the increase in temperature would wake the sleeper.

A major contribution to both fire prevention and fire protection is the development of an awareness of fire hazard in those who are in a position to do something to reduce it, be they the designer, the architect, legal authorities or members of the public (Fig. 6.1-1). Building requirements concentrate on fire protection on the assumption that fires will occur and that their consequences have to be mitigated.

Copyright fib, all rights reserved. This PDF copy of fib Bulletin 54 is intended for use and/or distribution only within National Member Groups of fib.

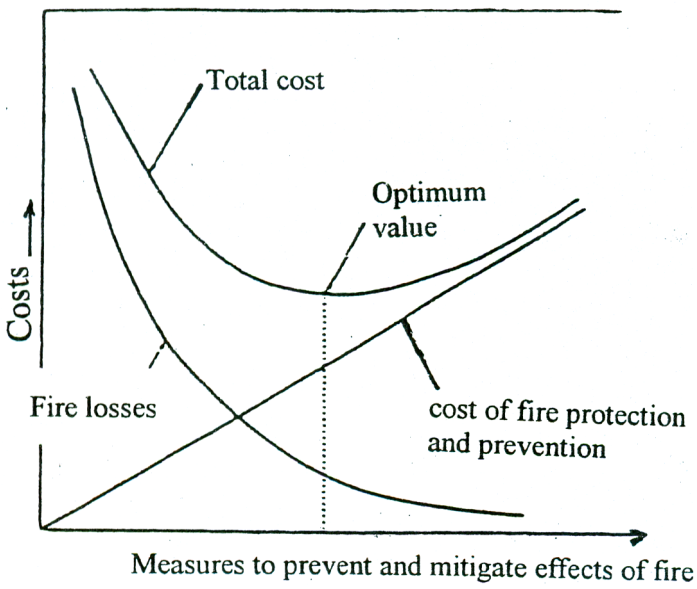


Fig. 6.1-1: Cost and losses (CEB 41, 1978)

6.2 Structural fire design

6.2.1 Fire severity

The severity of a fire in a structure is dependent on many factors. However, *building authorities assume for design purposes that a structure will be subjected to the worst-case fire*, and indeed this approach is supported by the conventional wisdom of fire brigade experience, which is that any kind of combustible material will eventually burn.

The severity of a fire depends on three main factors:

- available fuel;
- ventilation, i.e. air supply available to promote its growth;
- the characteristics of the compartment where the fire commences.

For a given fire load, the severity of the fire can vary by a factor of two or three depending on the ventilation and the configuration of the area.

For practical purposes fire severity is expressed in ISO 834 by means of a standardized temperature-time relationship which is also used in many national code regulations. Laboratory tests are conducted in furnaces using this relationship for the purpose of establishing the fire resistance of prototype structural elements (EN 1992-1-2). This experimental approach has also been used to investigate the effects of various design variables, and much of the information available for design is derived from this type of study. Standard furnace tests are the main source of tabulated data in design codes on the fire resistance of different single elements. Typical results from fire tests in a building are shown in Fig. 6.2-l.

Copyright fib, all rights reserved. This PDF copy of fib Bulletin 54 is intended for use and/or distribution only within National Member Groups of fib.

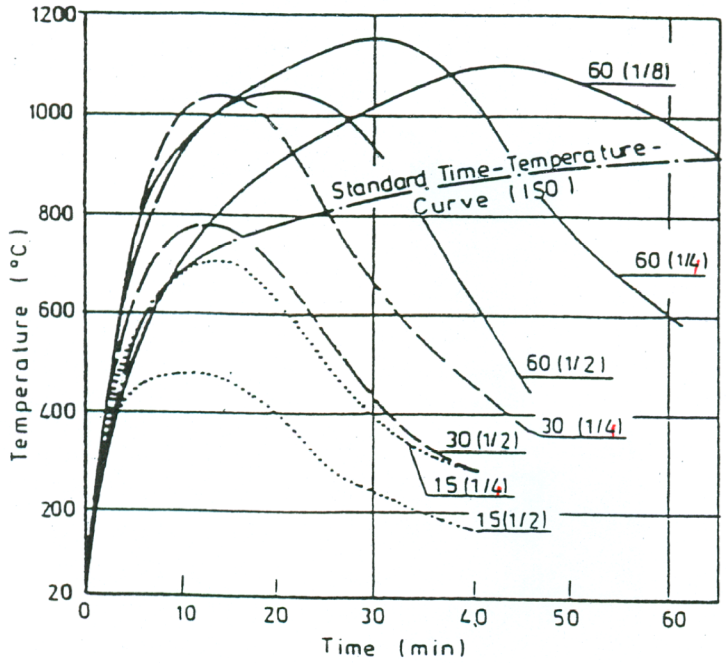


Fig. 6.2-1: Average temperature development with fire tests of wood cribs

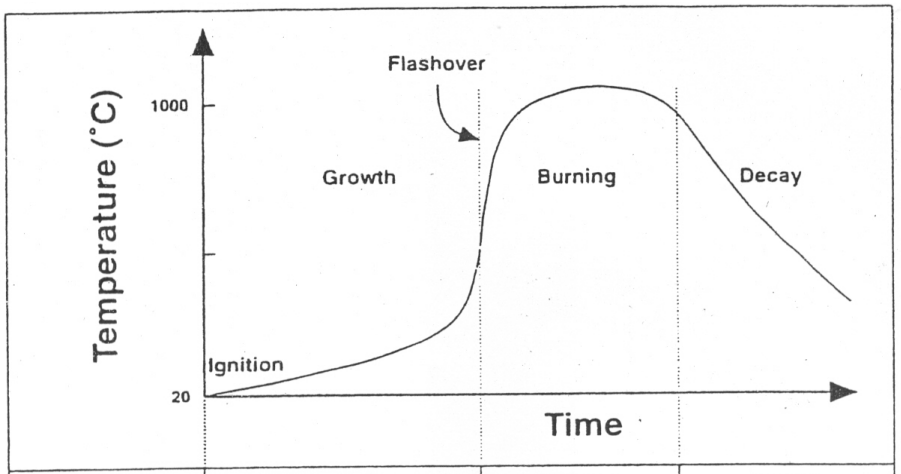
Current building controls in most countries express the standard of safety for a building in terms of the fire requirements for individual elements. The intention is to ensure that the building structure does not collapse and that the separating elements are maintained during fire. Fire resistance requirements are expressed for specified periods, ranging from 30 to 240 minutes.

According to the limit states philosophy a strength limit state is reached when a member can no longer carry its design load when combined with any additional thermally-induce loading. Other serviceability limit states may also have to be considered, such as those relating to the integrity of elements which provide horizontal or vertical barriers to the passage of fire. The latter may, for example, be required to prevent the progress of the fire through the gap between a floor slab and the suspended ceiling, or through holes provided in wall or floors for service pipes. A limit on deformation may also be used as a criterion for stability. In some special cases where re-use of the structure is important, additional criteria may be introduced which relate to reparability.

6.2.2 Progress of fire in a building

Most standards describe the progress of fire in a building in terms of four main phases, which may be termed *ignition, growth, the fully developed phase, and cooling*. Ignition takes place if sufficient energy is supplied to combustible material in the presence of oxygen. Energy may be provided by a short circuit, a burning cigarette, sparks from a welding operation, or by machinery which is not operating correctly. It is also possible for energy to be supplied by the combustible material itself, i.e. for self-ignition to occur. For the fire to develop into the growth and fully developed phases, air must be provided by some form of ventilation. In the growth phase, thermal energy is transferred by radiation and convection from the ignited material to other adjacent material, which becomes heated to the stage where it also ignites. Hot gases produced by the burning material can built up under the ceiling and cause a very rapid spread of fire. This process is called flame over. Smoke, toxic gases and heat may endanger life and property during the growth phase of the fire.

Copyright fib, all rights reserved. This PDF copy of fib Bulletin 54 is intended for use and/or distribution only within National Member Groups of fib.



Stage	Growth	Burning	Decay
Fire behaviour	Fuel controlled	Ventilation-controlled	Fuel-controlled
Human behaviour	Escape	Death	
Detection	Smoke detectors Heat detectors	External smoke and flame	
Active control	Extinguish by hand, sprinklers or Fire Service. Smoke control	Control by Fire Service	
Passive control	Flammability, surface spread of flame	Fire resistance, containment, collapse	

Fig. 6.2-2: Development of fire in a building [Kordina and Meyer-Ottens (1999)]

The ability of the load-bearing members to maintain structural adequacy in the presence of fire, and to resist the sustained loads acting, is of critical importance in the further sequence of events (Fig. 6.2-2). Very high ambient temperatures occur during the fully developed phase of the fire and produce sharp temperature gradients and an attenuated rise in temperature within the structural members. The increasing internal temperature causes a fall-off in the elastic modulus and the yield strength of the steel reinforcement. The effects of temperature on the steel properties become noticeable at 200°C; they are significant at 400°C and very serious at 600°C. The compressive strength and stiffness reductions are severe; the load-bearing capacity of individual members can fall to the level of the sustained loads, which are acting, so that local collapse occurs. Large deflections occur prior to collapse, owing to the loss of elastic stiffness in both the steel and concrete. At an even earlier stage, structural damage will commence with spalling of cover concrete at edges and corners due to temperature gradients. As the protective cover concrete is lost by spalling, the temperature of the steel reinforcement reaches a critical level very quickly and a condition of collapse can develop. If the structure is prone to progressive collapse, the loss of one member due to the effects of fire can trigger a general collapse. Good compartmentation is therefore crucial in minimizing fire risk.

Of particular interest is the possibility of a fire spreading outside of the building and along the facade, and attacking external load bearing columns. This is shown in Fig. 6.2-3.

Copyright fib, all rights reserved. This PDF copy of fib Bulletin 54 is intended for use and/or distribution only within National Member Groups of fib.

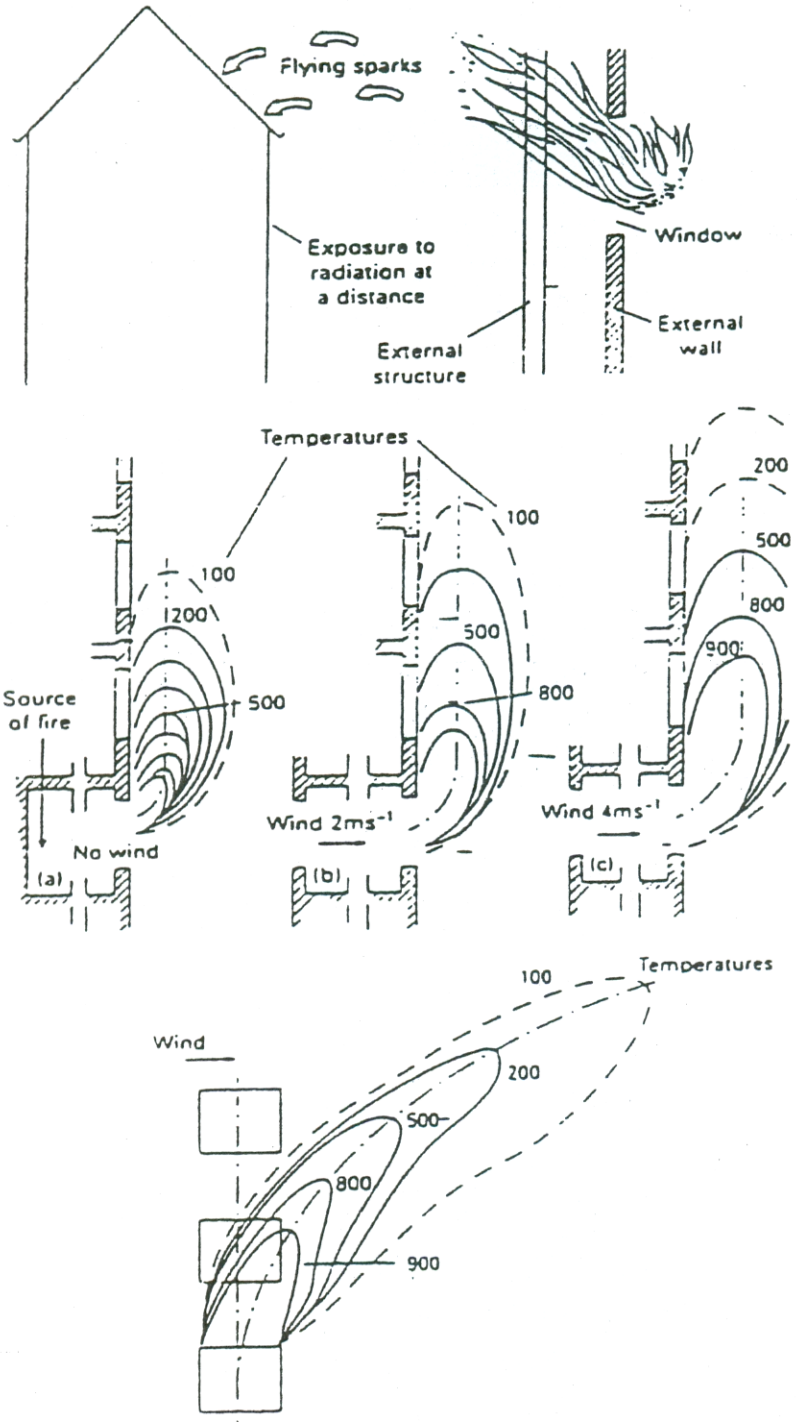


Fig. 6.2-3: Separated of fire trough openings on outside of building [Brechtold (1997)]

6.2.3 Structural response

Building regulations in most countries provide for a minimum fire-protection strategy. Additional standards contain design aids for fire in the form of tables for minimum dimensions and minimum concrete cover (axis distances of the main reinforcement to the member surface) of beams, slabs, columns, tension members and the like (EN 1992-1-2). New standards such as the Eurocodes allow for additional computational methods to predict the development of fire in buildings and the response of the structure to the fire [FIP/CEB (1978), Petterson (1978)].

Copyright fib, all rights reserved. This PDF copy of fib Bulletin 54 is intended for use and/or distribution only within National Member Groups of fib.

A structure designed for a specified fire resistance time may collapse after exposure to fire over the specified time and may require demolition. If reparability is a design requirement, then limits on acceptable damage, residual deformation and degradation of material properties need to be specified.

In the design of a concrete structure for fire, an assessment of the loads and heat exposure is required, together with an analysis of structural response and an appropriate choice of structural system and components, including joints and supports.

Material limit states for concrete and steel can be expressed in terms of a "critical temperature", at which a specified deformation or rate of deformation is exceeded in a fire test specimen under constant stress. If the critical temperature is reached in a critical area of load-bearing structural element, failure is initiated by compression, tension or bending.

Other failure modes also have to be considered, such as shear and bond, lack of rotation capacity over the interior supports of flexural systems, and explosive spalling especially with humid concrete (Fig. 6.2-4).

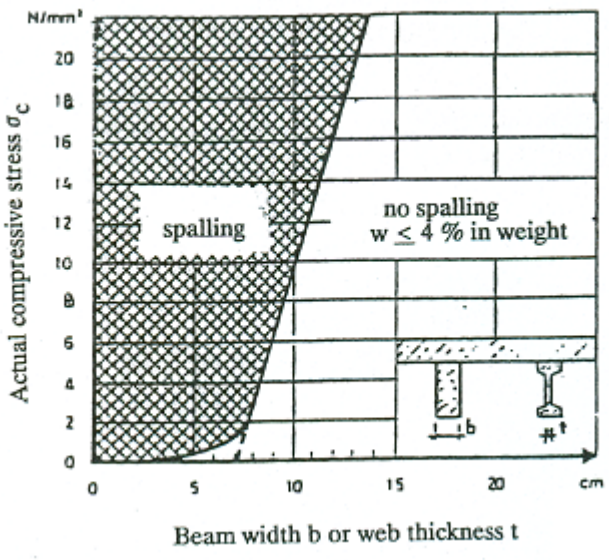


Fig. 6.2-4: Borderline between destructive and non-destructive spalling with plain and slightly reinforced concrete (C25/30-C35/45)

(1) Spalling

Explosive spalling can occur during the first 10-20 minutes of severe fire exposure. This is governed by the water content of the concrete, its porosity and the level of loading in conjunction with the restrained thermal expansions. Spalling may be avoided by limiting stresses and keeping the water content of the concrete to less than 4 % of the weight. Fig. 6.2-4 gives additional information. *High strength concrete (HSC) has a very small porosity and suffers by spalling more than normal concrete. Similar behaviour shows structural light weight concrete because of its relatively high water content stored by its porous aggregates which does not dry out under real conditions*. Admixtures of plastic fibres can reduce spalling also in HSC concrete. Fibres of that kind are melting under fire attack opening exits for steam under high pressure, which is the most important cause of spalling.

Copyright fib, all rights reserved. This PDF copy of fib Bulletin 54 is intended for use and/or distribution only within National Member Groups of fib.

(2) Separating functions

In treating the separating function of floors and walls, limit states are specified for thermal insulation and structural integrity against fire penetration. It needs to be emphasized that structural integrity cannot be checked by calculation, but only by test.

Integrity implies the absence of cracks, orifices or openings in separating elements through which flames and hot gases can pass, thus allowing the fire to break out on the other side. Retention of integrity is a design requirement for joints and junctions which should not open up as a result of excessive deformation of components. Occasionally, spalling of the concrete can lead to the formation of apertures in thin sections, with heat transfer through the construction. Information on such phenomena is available in many countries and provides the basis for many national codes.

(3) Fire resistance design

The current approach to fire-resistance design is dictated by the lack of simple and accurate methods for predicting structural behaviour in the presence of fire, and by the lack of adequate design data concerning both the variability in fire conditions and the effect of fire on material properties.

In a formal manner, three methods of assessment can be distinguished for use in structural fire design [EN 1992-1-2, FIP/CEB (1978)].

- *Assessment Method I.* This is based on the standard heating conditions as formulated in EN 1992-1-2 or in ISO 834. The design criterion is that the fire resistance time of a building component is equal to or grater than that required by the relevant regulation. For design, the dimensions of structural elements are obtained from tabulated data, taking into account the loads and the required fire resistance time. Tables of that kind are published in EN 1992-1-2.

- *Assessment Method II*. This is based on the concept of an equivalent fire exposure time which is used to relate the effects of a non-standard compartment fire to those of the ISO 834 standard fire and the related “standard heating conditions”. However, the design criterion is that the fire resistance of a structural component, determined either by experiment of calculation, is equal to or grater than the equivalent time of fire exposure. This equivalent time relates the non-standard compartment fire exposure to the standard heating conditions in such a way that the effect on the component is the same. Fig. 6.2-5 gives further details.

Copyright fib, all rights reserved. This PDF copy of fib Bulletin 54 is intended for use and/or distribution only within National Member Groups of fib.

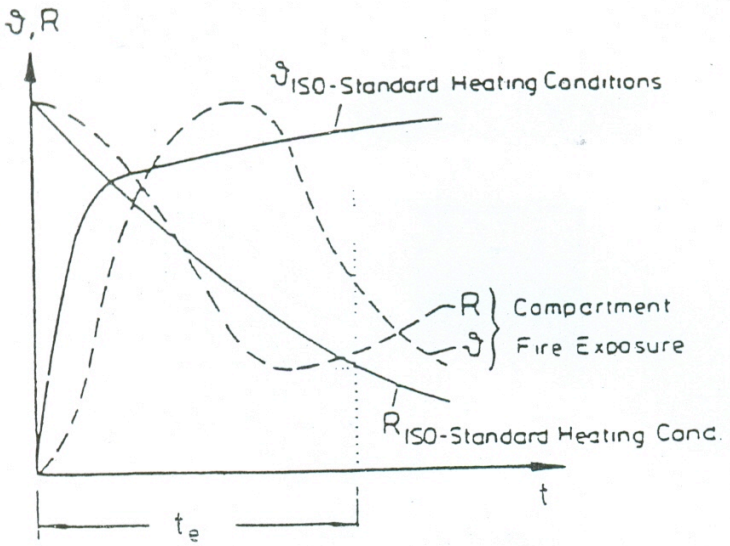


Fig. 6.2-5: Relation between "compartment fire exposure" and "standard heating conditions" (ISO 834), defining the "equivalent time of fire exposure"

- *Assessment Method III*. This method uses an analysis of the structure when subjected to a non-standard compartment fire exposure. Assessment of the temperature is based on heat and mass balance equations, and account is taken of factors such as the fire load characteristics, ventilation conditions and the thermal properties of the structural components surrounding the fire compartment.

National fire standards usually give basic information on the above three approaches. At the present time, evaluation according to methods I and II does not usually differ significantly; however, *assessment method III* needs expert help and approval. The use of most sophisticated computer programs is necessary; the results need very intensive critics with respect to their accord to reality. *Assessment method III* needs experience with real fires and laboratory test as well in order to avoid misleading results.

(4) Tabulated data

As a result of the analysis of fire tests, carried out in accordance with ISO 834 on a large number of structural components, tabulated data have been made available which simplify the assessment of the fire resistance of commonly used structural elements [CEB (1991), Kordina and Meyer-Ottens (1999)]. As a further design aid a simplified analysis can be made of the moment capacity of reinforced concrete members exposed to fire.

6.3 Material properties

6.3.1 General aspects on the material properties

Values for the reduction of the characteristic compressive strength of concrete, and of the characteristic strength of reinforcing and prestressing steels are given in this section. They may be used with the simplified calculation methods. These values may also be used for the evaluation of the critical temperature of reinforcement when adapting tabulated data for critical temperatures other than 500°C.

Copyright fib, all rights reserved. This PDF copy of fib Bulletin 54 is intended for use and/or distribution only within National Member Groups of fib.

The material laws given below should only be applied for heating rates similar to those appearing under standard fire exposure until the time of the maximum temperature [ISO 834].

The standard fire conditions are defined between 20°C and 1200°C, the properties are also defined between the same limits.

6.3.2 Concrete

The development of stress strain relations in function of temperature are given in Fig. 6.3-1.

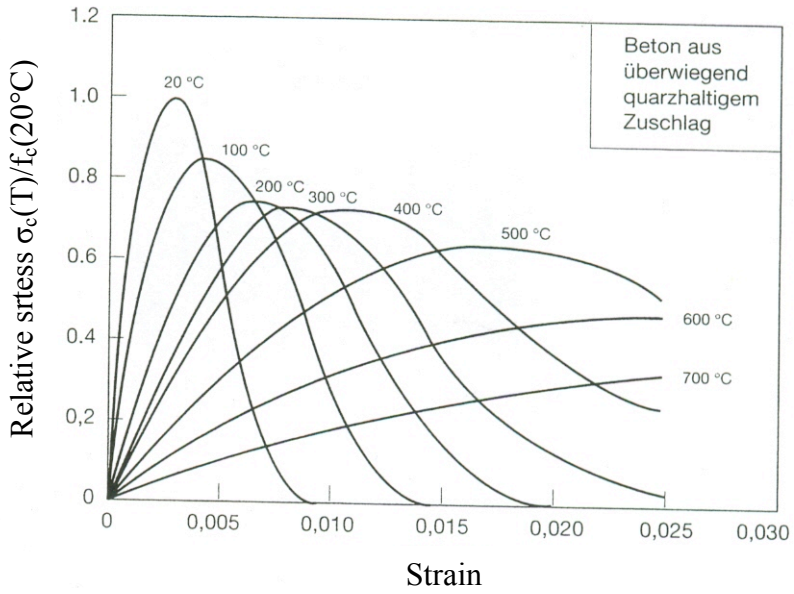


Fig. 6.3-1: Stress-strain relations of ordinary concrete with quartz aggregates

The reduction of the characteristic compressive strength of concrete as a function of the temperature using the coefficient $\kappa_c(\theta)$:

$$f_{ck}(\theta) = \kappa_c(\theta) f_{ck}(20°C). \qquad (6.3\text{-}1)$$

In the absence of more accurate information the following $\kappa_c(\theta)$ values, applicable to concretes with siliceous or calcareous aggregates, should be used (see Figure 6.3-2).

The development of total deformations of high-strength and ordinary concrete in function of temperature are given in Fig. 6.3-3.

In Fig. 6.3-4 are given the ISO temperatures in beams and plates with quartz gravel aggregates under three-side heating.

Copyright fib, all rights reserved. This PDF copy of fib Bulletin 54 is intended for use and/or distribution only within National Member Groups of fib.

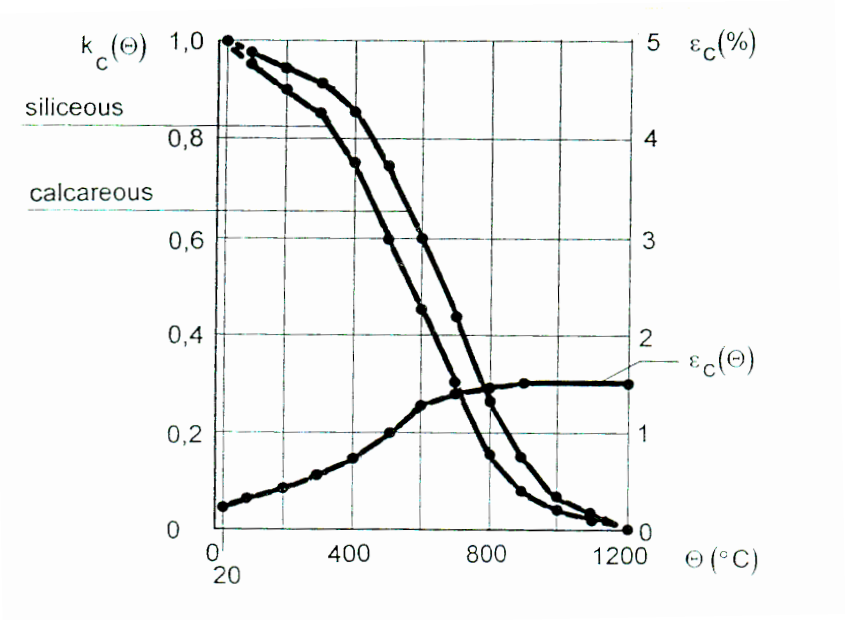


Fig. 6.3-2: Coefficient $\kappa_c(\theta)$ allowing for decrease of compressive strength (f_{ck}) of siliceous or calcareous concrete at elevated temperature (EN 1992-1-2)

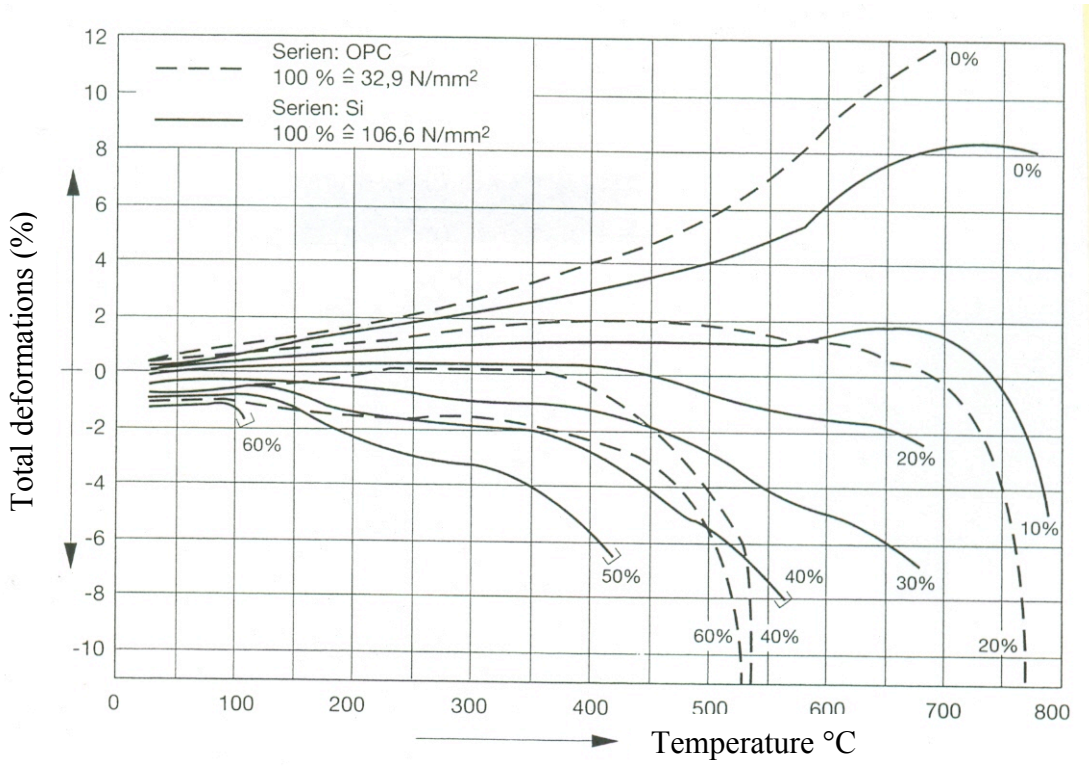


Fig. 6.3-3: Total deformations of high strength and ordinary concrete under non-stationary temperature conditions in creep test

Copyright fib, all rights reserved. This PDF copy of fib Bulletin 54 is intended for use and/or distribution only within National Member Groups of fib.

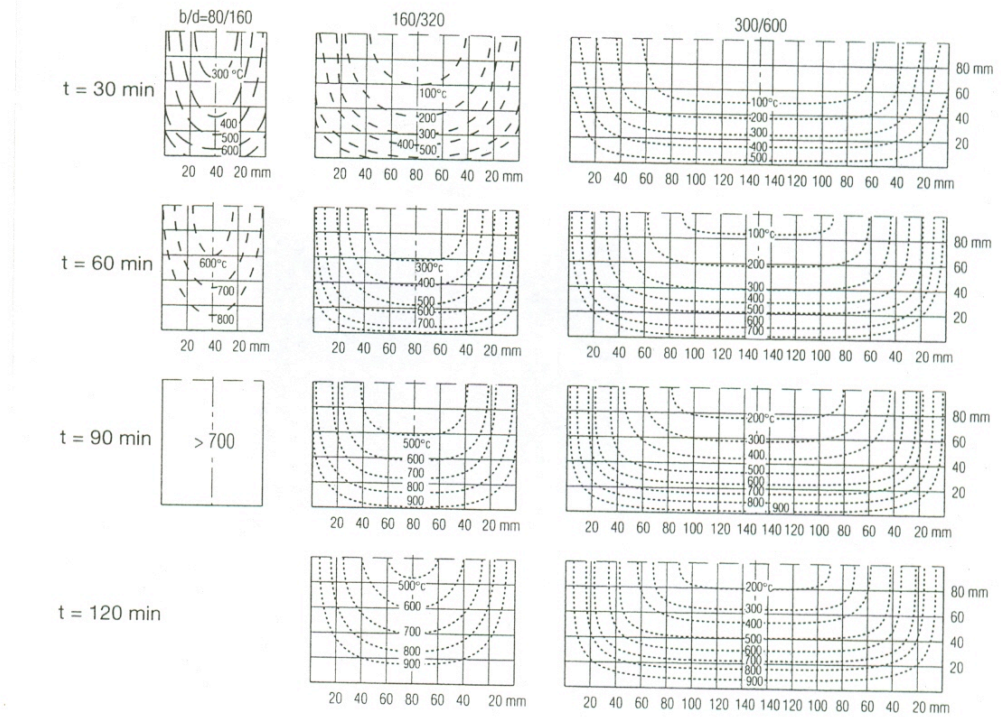


Fig. 6.3-4: ISO temperatures in beams and plates with quartz gravel aggregates under three-side heating

6.3.3 Steel

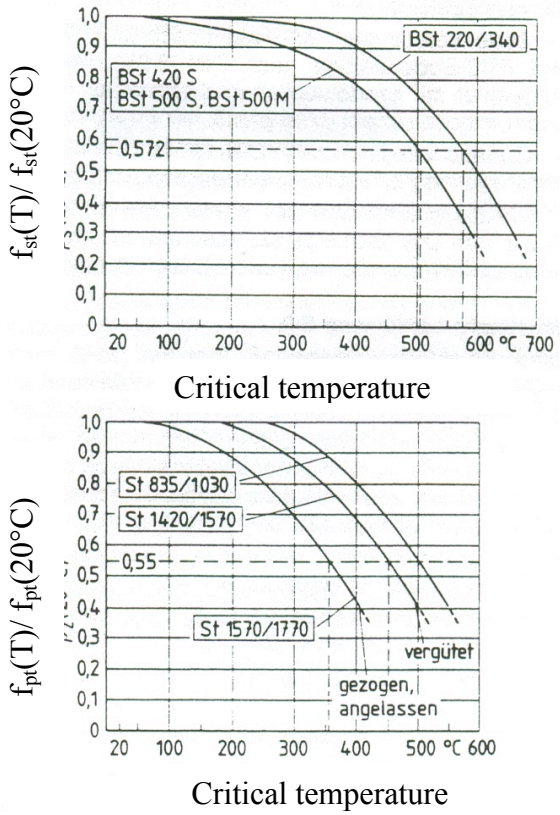


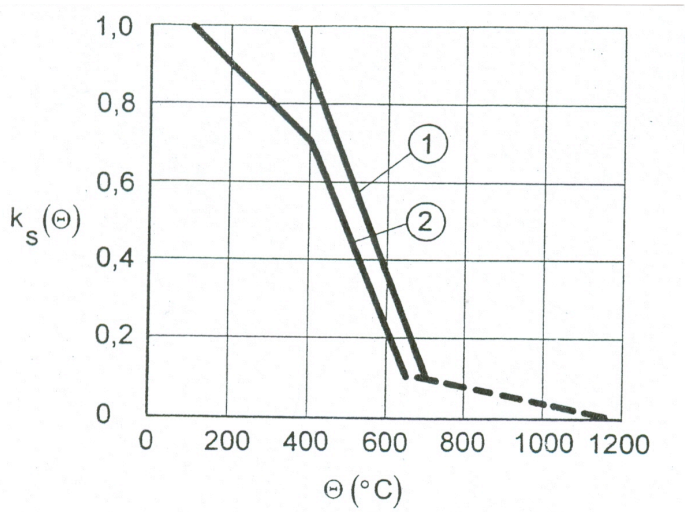
Fig. 6.3-5: Decrease of tensile strength of reinforcing bars and prestressing tendons as a function of temperature

In Fig. 6.3-5 decrease of tensile strength of reinforcing bars and prestressing tendons are given as a function of temperature.

Copyright fib, all rights reserved. This PDF copy of fib Bulletin 54 is intended for use and/or distribution only within National Member Groups of fib.

(1) The reduction of the characteristic strength of a reinforcing steel as a function of the temperature using for by the coefficient $\kappa_s(\theta)$ for which:

$$f_{sk}(\theta) = \kappa_s(\theta) f_{yk}(20°C) \qquad (6.3\text{-}2)$$

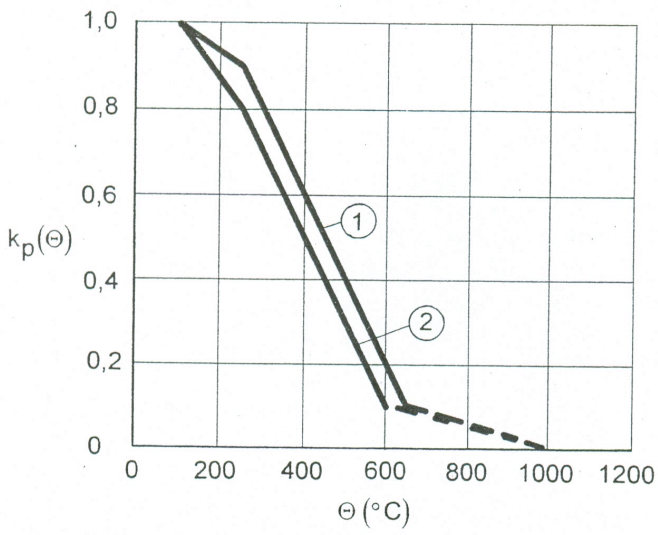


Curve (1): $\kappa_s(\theta)$ applicable for strains $\varepsilon_{s,fi} \geq 2.0$ %
Curve (2): $\kappa_s(\theta)$ applicable for strains $\varepsilon_{s,fi} \leq 2.0$ %

Fig. 6.3-6: Coefficient $\kappa_s(\theta)$ allowing for decrease of characteristic strength (f_{yk}) of reinforcing steels at elevated temperature (EN 1992-1-2)

(2) The reduction of the characteristic strength of a prestressing steel as a function of the temperature θ using the coefficient $\kappa_{p(\theta)}$ for which:

$$f_{pk}(\theta) = \kappa_p(\theta) f_{pk}(20°C) \qquad (6.3\text{-}3)$$



Curve (1): Bars
Curve (2): Wires and strands

Fig. 6.3-7: Coefficient $\kappa_p(\theta)$ allowing for decrease of characteristic strength (f_{pk}) of prestressing steels at elevated temperature (EN 1992-1-2)

Copyright fib, all rights reserved. This PDF copy of fib Bulletin 54 is intended for use and/or distribution only within National Member Groups of fib.

(3) Where $\kappa_s(\theta)$ and $\kappa_p(\theta)$ are taken from documented data they should be derived from tests performed under constant stress and variable temperature (transient tests). In the absence of more accurate information the following $\kappa_s(\theta)$ and $\kappa_p(\theta)$ values should be used for reinforcement (see Figs. 6.3-6 and 6.3-7).

It should be noted modern reinforcing steel recovers its original strength after a cooling down period nearly to 90%. Tests are recommended, if the heating period differs significantly of a welding procedure of the steel members in question.

6.4 General design rules and tables

6.4.1 General

This section deals with detailing according to recognized design solutions as tabulated data (see section 6.4.2).

Where necessary, explosive spalling shall be avoided by appropriate measures.

In the absence of more accurate data, the risk of explosive spalling can be assessed on the safe side by using Fig. 6.2-4. For more accurate assessments, moisture content, type of aggregate, tightness of concrete and heating rate should be considered.

Where local experience indicates increased susceptibility of lightweight concrete to explosive spalling relevant documents should be used to determine member size or additional protective linings.

6.4.2 Tabulated data

(1) Scope

(1.1) In absence of more precise methods for structural fire design (i.e. general calculation method, simplified calculation method), reference should be made to the tabulated data given in national codes. Examples are given in the annex.

The following rules refer to single member analysis. The tables apply for the standard fire exposure.

(1.2) The tables have been developed on an empirical basis confirmed by experience and theoretical evaluation tests.

(1.3) The values given in the tables apply to normal weight concrete made with siliceous aggregates (see EN 1992-1-1, 3.1.2.1).

If calcareous aggregates are used in beams and slabs either the minimum dimension of the cross-section or the minimum value of the axis distance, a, of reinforcement may be reduced by 10%.

Copyright fib, all rights reserved. This PDF copy of fib Bulletin 54 is intended for use and/or distribution only within National Member Groups of fib.

(1.4) The tabulated data takes into account requirements to prevent explosive spalling for all exposure classes and no further check is required. Examples of tables are given in the annex of this chapter.

(2) General design rules

(2.1) Requirements for separating function may be considered satisfied where the minimum thickness of walls or slabs according to standardized values.

(2.2) For load-bearing function (Criterion R), the minimum requirements concerning section sizes and heat protection (axis distance) of steel have been set up in the tables so that

$$E_{d,fi}/R_{d,fi} \leq 1.0 \qquad (6.4\text{-}1)$$

where:

$E_{d,fi}$ is the design effect of actions in the fire situation
$R_{d,fi}$ is the design load-bearing capacity (resistance) in the fire situation.

(2.3) In order to ensure the necessary steel protection (cover, axis distance) in tensile zones of simple supported members, the tables are based on a critical steel temperature of $\theta_{cr} = 500°C$. θ_{cr} is the critical temperature of reinforcement at which yielding becomes imminent under the actual steel stress $\sigma_{s,fi}$. This assumption corresponds approximately to $E_{d,fi} = 0.7\ E_d$ and $\gamma_s = 1.15$, where E_d denotes the design effect of actions according to EN 1992-1-1.

(2.4) For prestressing tendons the critical temperature for bars is assumed to be 400°C and for strands and wires to be 350°C. If no special check is made for prestressed members, beams and slabs the required axis distance, a, should be increased by

10 mm for prestressing bars, corresponding to $\theta_{cr} = 400°C$
15 mm for prestressing wires and strands, corresponding to $\theta_{cr} = 350°C$.

6.5 Overall design

6.5.1 Concept design and detailing

The normal steps in structural design namely

- conceptual design,
- detailed design calculations and
- detailing,

also need to be applied in the case of structural fire design.

The conceptual design and the detailing process together take care of those actions and situations which are unlikely to occur, and which are therefore not calculated in detail, but which require some consideration in design.

Copyright fib, all rights reserved. This PDF copy of fib Bulletin 54 is intended for use and/or distribution only within National Member Groups of fib.

For this reason the author consider that conceptual design and detailing are as important in fire design as the detailed design calculations under normal temperature. In this respect, designing and detailing for fire refer to the following:

- making the structure robust in relation to fire;
- designing for thermal expansions in the building;
- detailing for thermal expansions;
- compartmentation.

6.5.2 Robust structures

Where fire resistance requirements do not strictly apply to the load bearing system, as in a one-storey building or a building with automatic sprinkler systems, the structure nevertheless should not collapse due to a small, local fire. This requirement would often be satisfied automatically because of the inherent fire resistance of normal concrete members which are not too slender. Without observing specific fire design requirements, concrete members are likely to have 50 to 60 minutes of fire resistance for the standard exposure situation.

Although a structure may not survive a fully developed fire, gradual collapse, or collapse proceeded by visual and acoustic warning, is preferred in view of the safety of fire fighters. Stability failure may occur suddenly, and is undesirable in contrast with a strength failure preceded by large deformation.

Supports and joints:

Related to failure mode is the requirement that flexural failures should occur in span regions and not at supports or joints. Thus, members should not slip off supports, and the joints of prefabricated composite structures should be over designed (Fig. 6.5-1).

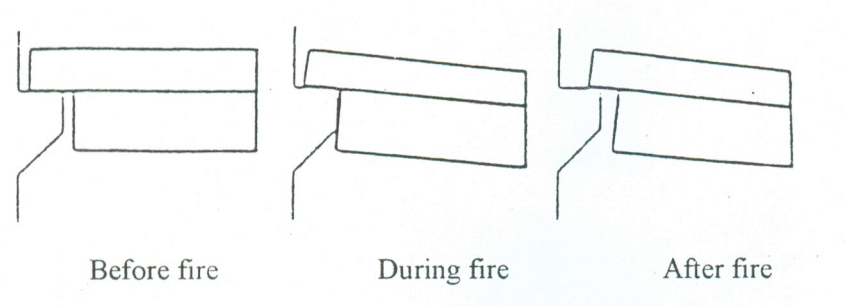


Fig. 6.5-1: Beam support area before, during and after fire exposure

Copyright fib, all rights reserved. This PDF copy of fib Bulletin 54 is intended for use and/or distribution only within National Member Groups of fib.

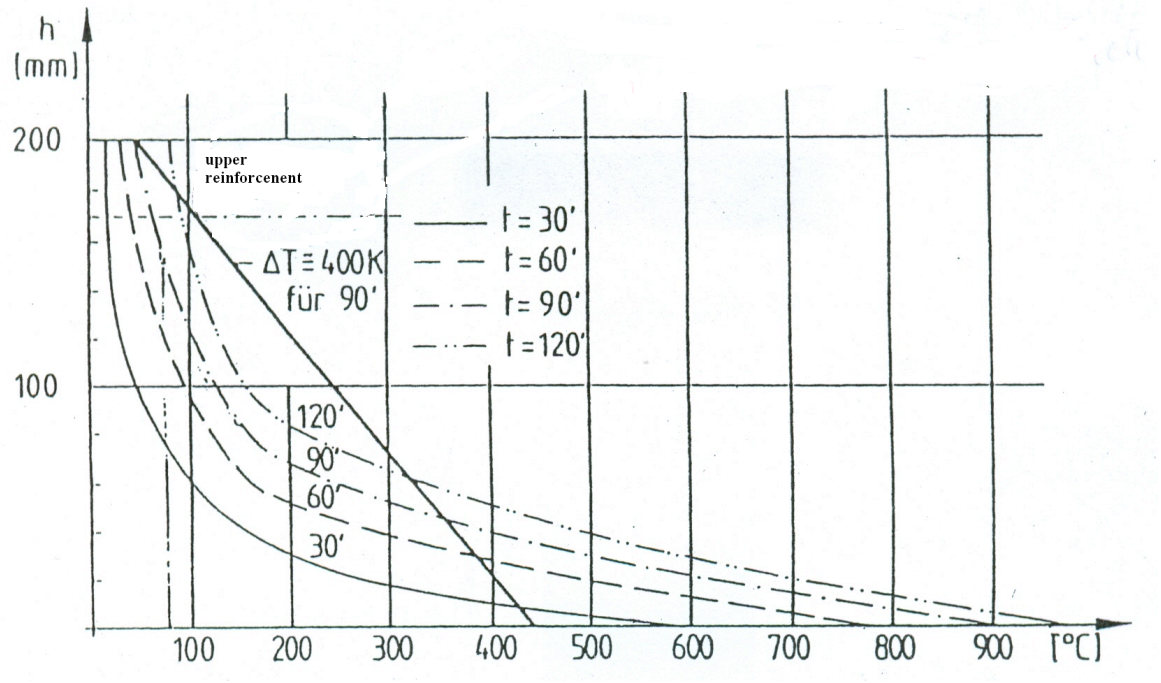


Fig. 6.5-2: Temperature gradient in concrete slabs after 30 to 120 minutes of standard fire exposure; upper reinforcement; assumed linear stress-strain relation

6.5.3 Thermal expansion, restraint and behaviour of buildings in fire

In principle, design for thermal expansion only requires rough estimates of how the structure will expand and deform under fire, although it may be necessary to consider also the cooling down period.

Thermal expansion and deformation depend mainly on the temperature increase in members during fire exposure. Figure 6.5-2 gives thermal gradients in concrete slabs under standard fire exposure, which may also be considered as an equivalent time for fire exposure.

The thermal expansion of concrete can be expressed as a function of temperature. Siliceous concrete has values of about $10 \times 10^{-6}\theta_c$ between 20 and 200°C and of about $12 \times 10^{-6}\ \theta_c$ for θ_c over 200°C. For steel average values are about $12 \times 10^{-6}\ \theta_s$.

For the simple assessment of normal reinforced concrete in fire, $\theta \approx 600$°C, we may take:

$$\frac{\Delta l}{l} = 14 \times 10^{-6}\theta_c,$$

for concrete made with lightweight aggregates

$$\frac{\Delta l}{l} = 8 \times 10^{-6}\theta_c,$$

Copyright fib, all rights reserved. This PDF copy of fib Bulletin 54 is intended for use and/or distribution only within National Member Groups of fib.

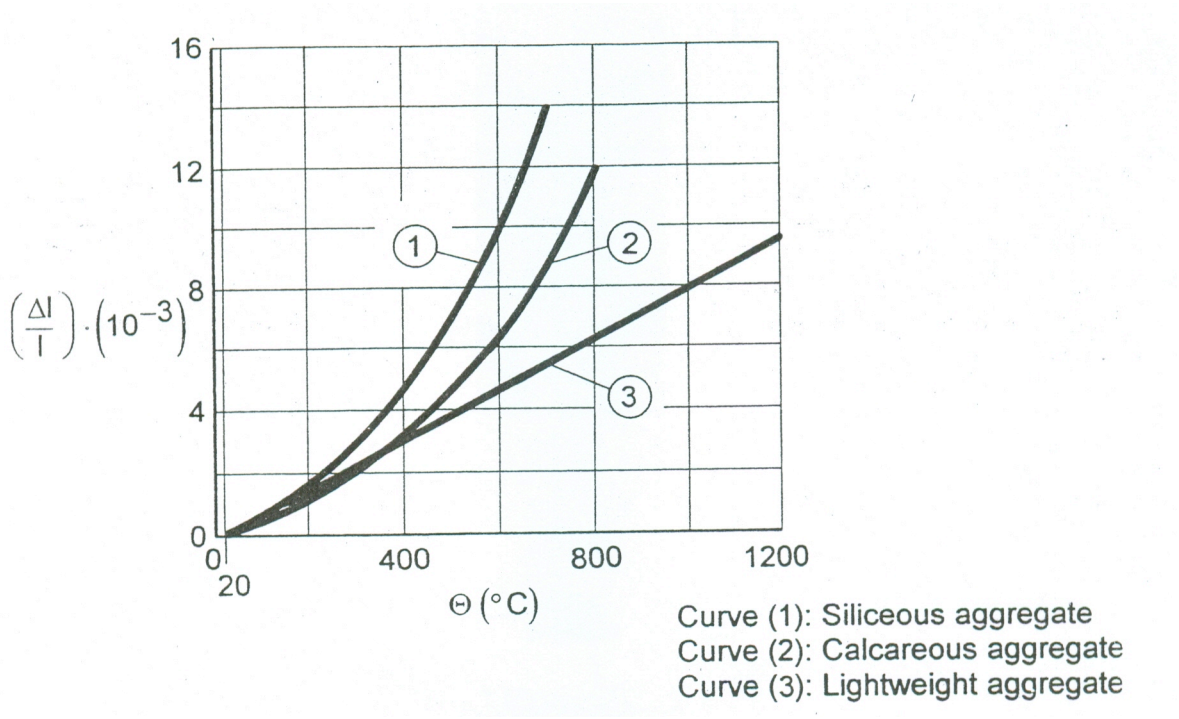


Fig. 6.5-3: Thermal elongation of concrete

Expansion joints:

As a rough guide, the minimum width e of an expansion joint for fire should be e = 40 mm, at 30 m spacing.

The joint filling material should have sufficient durability and must be non-combustible; the sealing material may be combustible (Fig. 6.5-4).

Further issues regarding expansion joints include the following. In Fig. 6.5-5 the top storey of the building is separated into relatively small fire compartments, while the lower storey has just one large compartment. It is interesting to compare the effects of a fire in the lower storey and in a compartment in the upper storey. If the average increase in temperature in the slab is 200°C the potential expansion is in the order of 300 mm in the slab above the ground floor, but only about 80 mm for the roof slab. These figures ignore constraints and effects of curvature. Irrespective of the exact expansion which occurs, expansion joints are clearly more important in the slab above the ground floor than in the roof slab.

Copyright fib, all rights reserved. This PDF copy of fib Bulletin 54 is intended for use and/or distribution only within National Member Groups of fib.

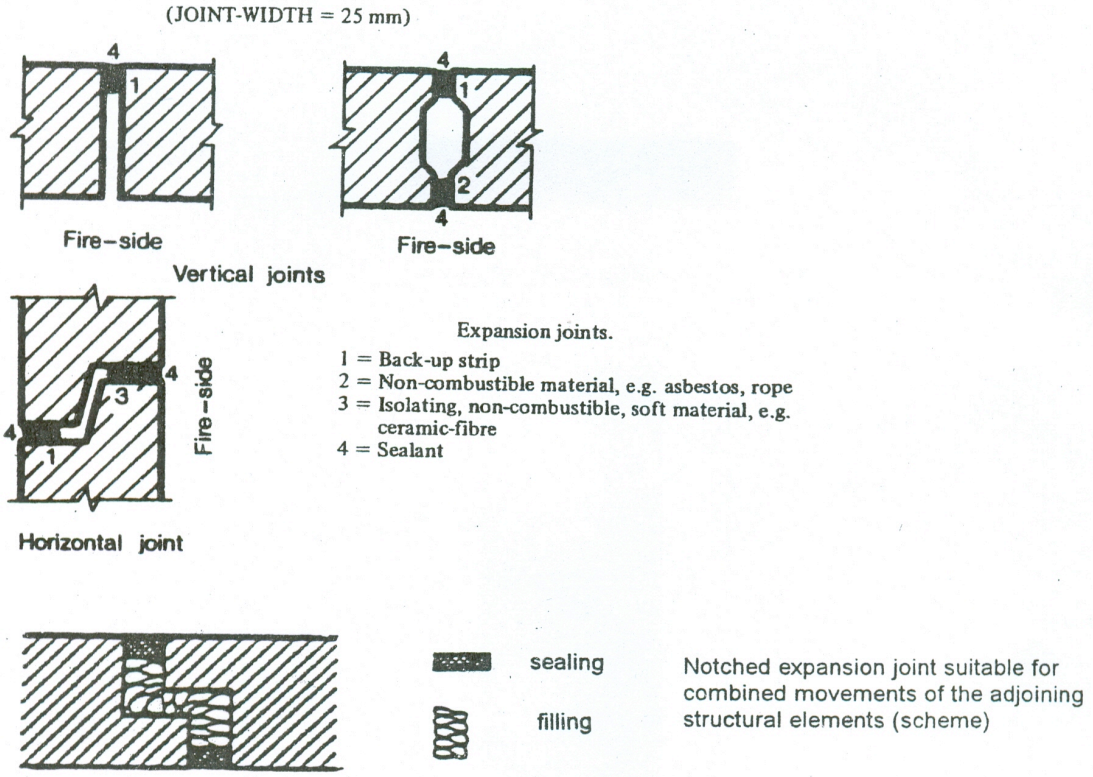


Fig. 6.5-4 a: Examples of expansion joints [FIP/CEB (1978)]

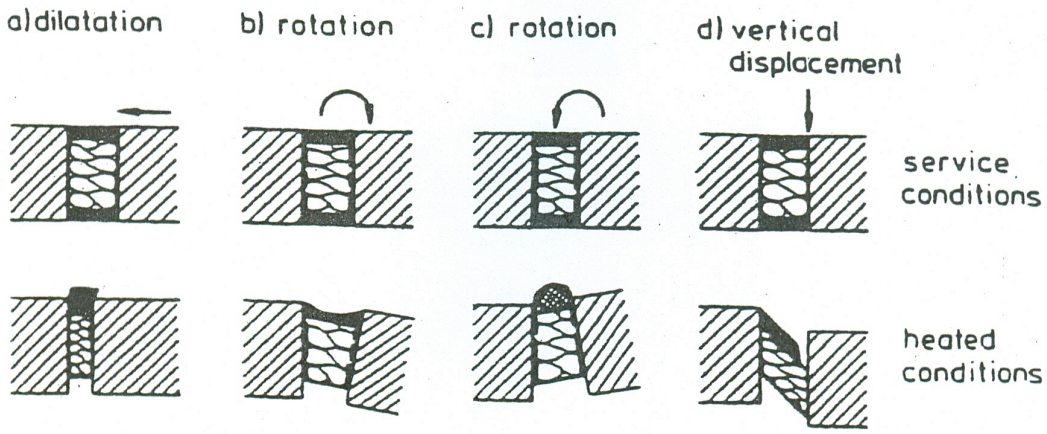


Fig. 6.5-4 b: Examples of expansion joints [CEB (1991)]

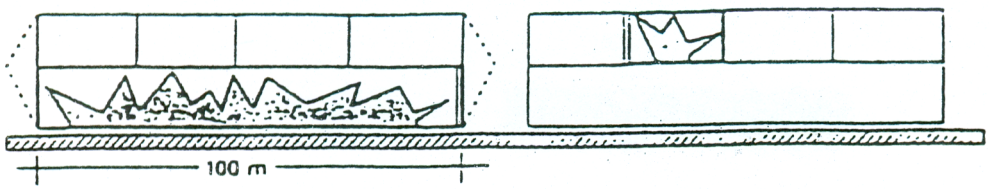


Fig. 6.5-5: Different situations connecting compartmentation [Kordina/Kersken-Brandley (1996)]

Copyright fib, all rights reserved. This PDF copy of fib Bulletin 54 is intended for use and/or distribution only within National Member Groups of fib.

We compare now two different configurations for the horizontal constraints acting in the floor-slabs (Fig. 6.5-6). In one case there is a single stairwell in the middle of the building, in the other case there are two stairwells, one at either ends of the building. The first arrangement clearly provides the minimum constraint to the slab and allows maximum expansion. The second case gives maximum constraint and minimum expansion. Disregarding the rest of the structure, no expansion joint would be required in the first case, whereas expansion joints would be needed in the second case to limit the compressive forces in the slab and the resultant forces on the stairwells. It should be noted that expansion joints in separating walls and slabs need special detailing.

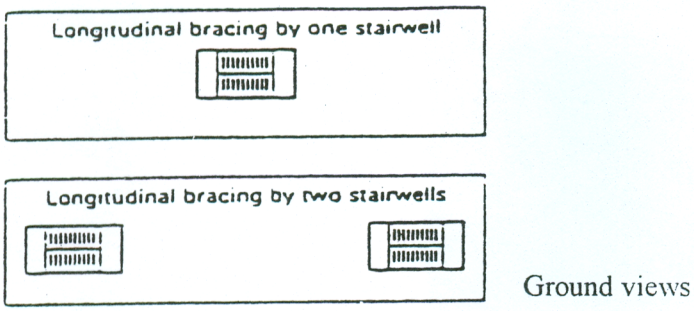


Fig. 6.5-6: Effect of horizontal resistance

Considering the columns supporting the slab in the case of the central constraint provided by the staircase, severe displacement at the column heads is likely to occur, as in Fig. 6.5-7, with horizontal forced acting on the columns. Expansion joints would be needed to protect the columns. On the other hand, in the design with stairwells at each end, the columns would be virtually unaffected, irrespective of the presence of expansion joints.

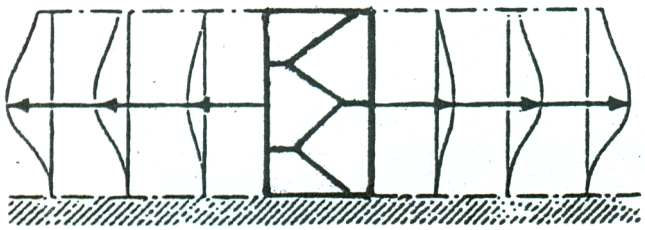


Fig. 6.5-7: Effect of central stairwell on surrounding columns (no expansion joint)

Tension members which are used for bracing or for supporting other members fail to fulfil their function when they are exposed to fire and expand. They need to become protected.

When exposed to fire a simply supported beam expands and also deflects because it is heated on three sides (Fig. 6.5-1). After cooling down, the expansion may disappear, but the deflection remains. The beam may slip off a support which is not large enough.

A severe fire can produce the temperature strains and gradients as shown in Fig. 6.5-2 in a slab and in Fig. 6.5-8 in a wall.

Copyright fib, all rights reserved. This PDF copy of fib Bulletin 54 is intended for use and/or distribution only within National Member Groups of fib.

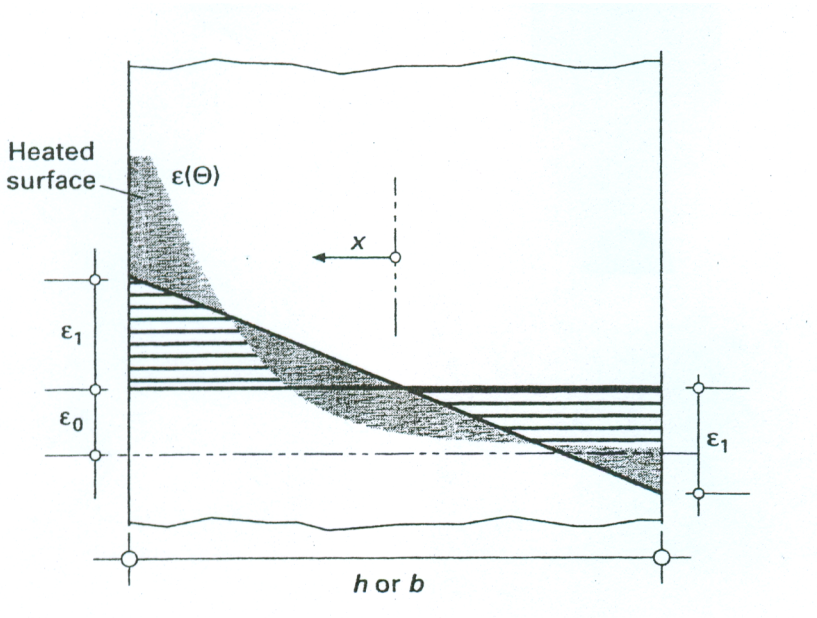


Fig. 6.5-8: Temperature-dependent strains [Kordina/Kersken-Brandley (1996)]

The temperature gradient produces internal stresses as well as curvature in the wall if exposed to a fire on one side. Strictly, expansion and curvature should be calculated on the basis of equilibrium of the internal stresses.

If a linear stress-strain relation is assumed and the dependency of the modulus of elasticity on temperature is ignored, then the resulting stress estimates are on the safe side. The error is larger for curvature than for expansion. If a non-load bearing wall is b = 250 mm thick equilibrium occurs with strains of around $\varepsilon_1 \pm 0.004$. This results in a radius of curvature of only about 30 m when calculated from $l/R = 2\,\varepsilon_1/b$.

Nevertheless, the full benefit of a large b value (equal to the column width b_c) is only achieved if the columns are on the cooler side of the wall, and not exposed to fire on three sides. Without systematic investigation, only the following tentative guidelines can be given.

- If the wall separates-areas with high fire loads on one side and low fire loads on the other, then the columns should be located in the low fire-load area.
- If this is not possible, protective layers can be applied to the column, so that full exposure only occurs on one side (this is not a typical “concrete” solution).
- The column should be designed and braced in such a way that plastification would occur at the column foot prior to failure of the bracing.

6.5.4 Compartmentation

Fire damage is mostly due to inadequate compartmentation, rather than to poor fire design of individual floors and walls, to achieve the separating functions. Providing fire resistance for concrete members as such is usually not very expensive, but where compartmentation requires openings in walls and floors to be secured (doors, ducts, shutters) the cost may be considerable and the result may turn out to be useless because of elementary mistakes made on site and during use, as well as in design.

Copyright fib, all rights reserved. This PDF copy of fib Bulletin 54 is intended for use and/or distribution only within National Member Groups of fib.

Frequent mistakes are geometrically incomplete compartments in areas where the geometry of the structure is not straightforward, and in particular where the possibility of fire propagation across facades and roofs has not been adequately considered (Fig. 6.5-9). Serious mistakes can be encountered in the design of air-conditioning systems and building services in general. This is mostly due to lack of communication between the structural designer and the designers of the building services.

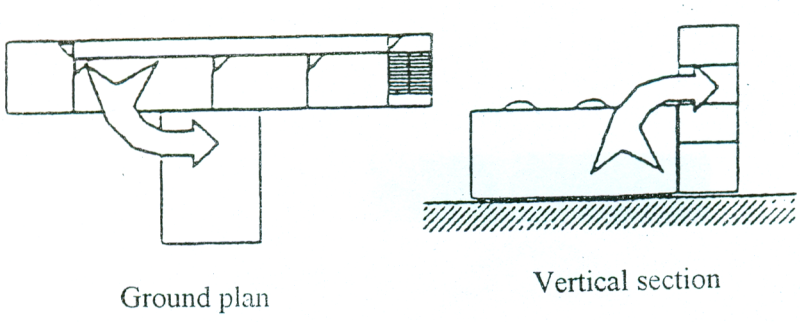


Fig. 6.5-9: Fire penetration from one part of the building to another part [Kordina/Kersken-Brandley (1996)]

The compartmentation as originally planned is often obstructed during use. The best-known example is the fire door which is forced to remain open to provide easy access. In buildings where electric or electronic cables are newly or repeatedly installed, it is common to forget to close the seals in compartment walls and floors. Maintenance of devices such as fire shutters is often not performed. Finally, in the course of time, the original compartmentation concept is simply forgotten, with the result that new installations such as ventilation ducts and transport systems are introduced without provision for the automatic barriers needed for fire.

Windows in facades are always a problem with regard to the horizontal and vertical compartmentation of a building. Breaching of fire compartments via windows is most effectively inhibited by fire-resistant parapets and balconies. Experience shows that traditional wall-window construction is also adequate, provided:

- fire-resistant parapets are used;
- the flashover distance is at least 1 m;
- no combustible materials are used in the construction of the facade.

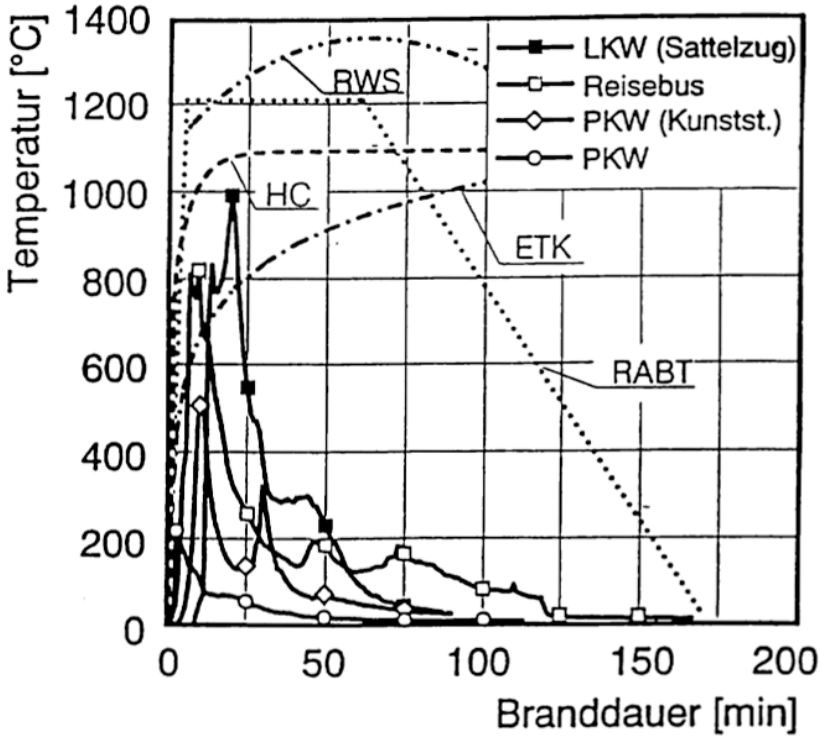
Nevertheless, with increasing building height, fire brigades are less likely to control fire propagation along the facade, so that flashover distances need to be increased for high-rise structures.

6.5.5 Fires in tunnels

Fires in a road or railway tunnel have two different dangerous aspects:

On the one hand heavy failures may occur in the concrete lining for instance by explosive spalling, on the other hand hot and toxic gases and dense smoke cannot escape in the free atmosphere and can thus become a heavy handicap to the tunnel users to find the escape routes. The gas-temperature during a tunnel fire goes up to 1000-1200°C within about 5 min as shown in Fig. 6.5-10, which also shows the temperature-time function according to different standards for designing tunnel linings [EUREKA-Bericht (1996)].

Copyright fib, all rights reserved. This PDF copy of fib Bulletin 54 is intended for use and/or distribution only within National Member Groups of fib.



ETK	=	Einheitstemperaturzeitkurve DIN 4102 = ISO-834-Curve
HC	=	Hydrocarbon-Curve (DIN EN 1363 Teil 2)
RABT	=	Instruction on Equipment and use of Tunnel (Richtlinie für Ausstattung und Betrieb von Tunneln)
RWS	=	Rijks Waterstraat, NL

Fig. 6.5-10: Maximal temperatures in tunnels

The wholes in concrete linings by spalling may reach 40 cm and more so that the rocks behind the lining become visible and the water-tightness of the tunnel structure may be lost. Measures against spalling under ISO-834 fire have been found very recently by the addition of plastic fibres of about 3 kg/m^3 [Diederichs/Jumppanen/Schneider (1995)]. Steeper increase of temperature as by ISO 834 should be investigated. Temperatures in the tunnel structure as well as restraining stresses in a fire can produce deformations and cracks for instance in a hollow bridge used for a subway or in the corners of a frame-shaped subway-tunnel [Haksever/Kordina (1981)].

Smoke and hot gases must be removed from the burning vehicles as quick as possible; longitudinal ventilation may be sufficient until tunnel length of about 1500 m; longer tunnels should get in addition a transverse ventilation for instance by an additional floor in the upper region of the tube with openings to the traffic way, where ventilation suck away the smoke. The openings should open above the burning vehicles automatically and very swift [Kordina (1998), Kordina (1997)].

Copyright fib, all rights reserved. This PDF copy of fib Bulletin 54 is intended for use and/or distribution only within National Member Groups of fib.

6.6 Damage caused by fire exposure

Reparability means the ability of a structure or a part thereof, to be restored to an agreed level of safety, in practical use comparable to that before the fire occurred. Its judgement in most cases will be influenced by economic considerations, but under specific circumstances, high financial expenses for the repair may be unjustifiable [CEB (1991)]. The evaluation of a structure after a fire is very similar when plans and material data are missing. Drilling of concrete cores, testing of samples of the reinforcement are the most important measures. Concrete surfaces after spalling have to be controlled, if they are free of cracks; see also 6.6.4.

More detailed information about the reparability of damaged structures may be taken from the literature [CEB (1991), Schneider/Nägele (1989), Warner/Ranyan/Hall (1989)]. The following chapters only give an introduction into this problem.

6.6.1 Circumstances and indications at the place of the fire

Judgement of reparability should start with the attempt to obtain an overall image of the event, the fire.

A visit to the place of the fire should be undertaken by an expert in fire design as soon as it seems possible without endangering any persons.

There are a number of indicators pointing to the fire severity, such as:

- charring depth of wooden elements,
- burnt away PVC (polyvinyl chloride) cable insulation (>300°C),
- blue heat tinting of steel surface (< 400°C),
- melted aluminium (> 650°C),
- melted usual silicate glass (> 1000°C),
- sintered brickwork (> 1200°C),
- net of cracks in the concrete surface (depth ca. 2 cm at ca. 1000°C),
- unburned fire load.

Not only the specific damages of the affected structural members, such as deformations, cracks, spalling and disintegration of concrete, etc., but the overall condition of the structure and the building should be carefully recorded.

6.6.2 Material damage

Residual mechanical properties of the materials used in concrete structures, after cooling depend on a number of parameters, such as:

- kind of steel (reinforcing, prestressing), hot rolled, cold worked, tempered,
- maximum temperature attained,
- stress-level during the manufacturing process,

and with lower importance:

- rate of heating and cooling (if not chilled by a hose stream),
- duration of maximum temperature level.

Copyright fib, all rights reserved. This PDF copy of fib Bulletin 54 is intended for use and/or distribution only within National Member Groups of fib.

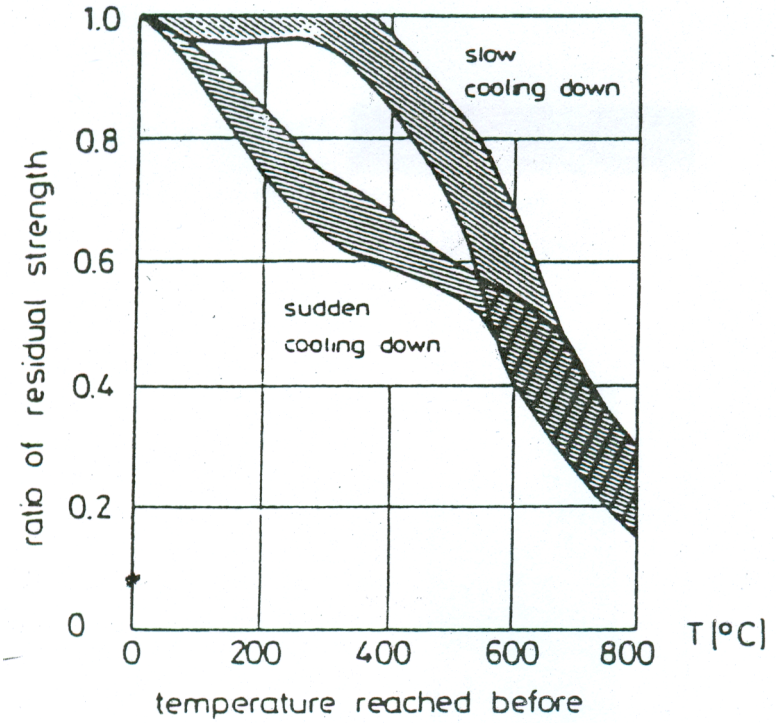


Fig. 6.6-1: Residual compressive strength of normal dense concrete as a function of the temperature reached and the cooling conditions [CEB (1991)]

Therefore, the following data and reference publications should only be regarded as basic information for a rough estimation of possible damages. They cannot compensate individual structural investigations, even more if the temperatures reached during the fire cannot be assessed with adequate reliability.

The residual compressive strength of concrete is normally not severely reduced if temperatures up to 300°C have not been exceeded, and no sudden cooling down, e.g. by extinguishing water, has occurred (see Fig. 6.6-1). Concrete heated by more than 100-150°C may loose its protective behaviour against corrosion. Application of additional layers could be necessary.

Hot rolled reinforcing steel recovers its original yield stress if the temperature does not exceed approx. 700°C. With cold worked steel, the work hardening effect which increases the strength of such types of reinforcement under normal temperature, suffers regression if exposed to temperatures > 400°C. The favourable influence of after treatments on the strength of prestressing steels decreases even if lower temperatures (ca. 300°C) are reached. These reductions are not fully recovered (see Fig. 6.6-2 and 6.6-3).

Copyright fib, all rights reserved. This PDF copy of fib Bulletin 54 is intended for use and/or distribution only within National Member Groups of fib.

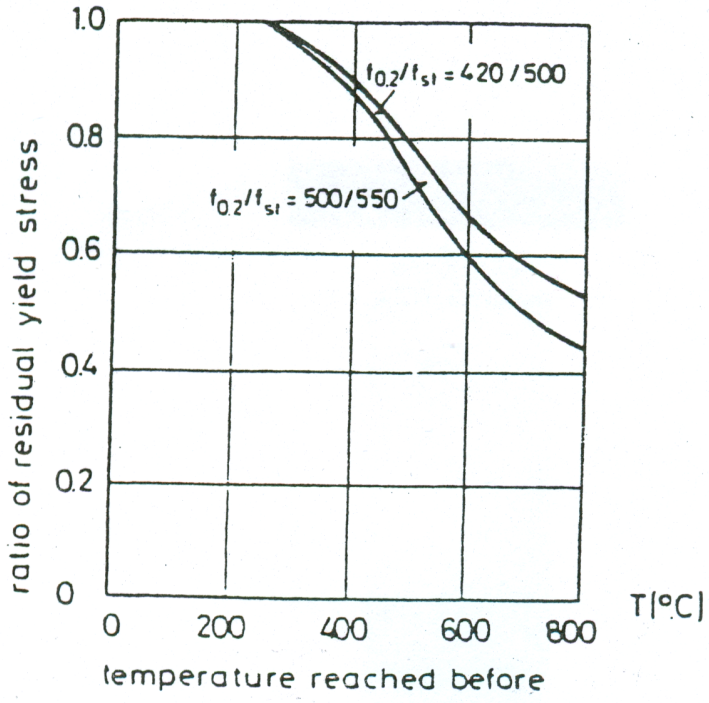


Fig. 6.6-2: Residual yield strength after heating of cold-worked reinforcing steel; exposure time to the maximum temperature 30 minutes[CEB (1991)]

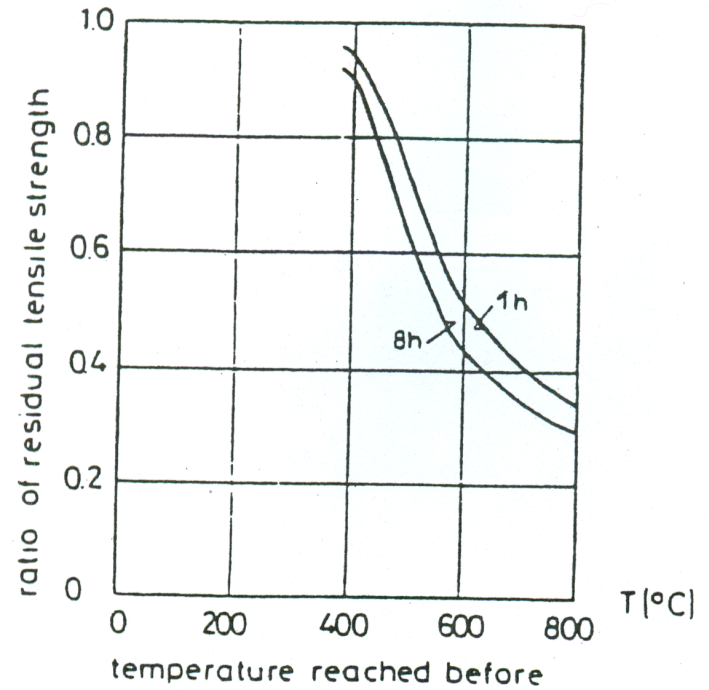


Fig. 6.6-3: Residual tensile strength after heating of high strength prestressing steel; (US-American); exposure time to the maximum temperature 31 or 8 hours [CEB (1991)]

Copyright fib, all rights reserved. This PDF copy of fib Bulletin 54 is intended for use and/or distribution only within National Member Groups of fib.

6.6.3 Structural damage

The bond between concrete and reinforcement may be affected by the heating process. The residual bond strength does not only depend on the temperature reached and on the exposure time, but in addition on the condition of the steel surface.

The prestress which possibly decreases during a fire, can partly be regained during the cooling down period. Fig. 6.6-4 shows, results derived from tests with high tensile prestressing wires of 9 mm diameter.

Cracks occur in any reinforced or prestressed concrete element when exposed to a heating, extinguishing and cooling down process. There are several reasons causing this phenomenon, such as:

- deformation due to mechanical influences and the thermal conditions,
- the temperature gradient in the cross section,
- the non-linearity of the temperature gradient,
- different temperature rise at the change of the size and shape of a cross section,
- different thermal elongation of the cement matrix and the aggregates,
- different thermal elongation of the concrete and the reinforcing steel,
- restraints of the re-contraction during the cooling-down process,
- sudden cooling-down by a fire extinguishing hose stream.

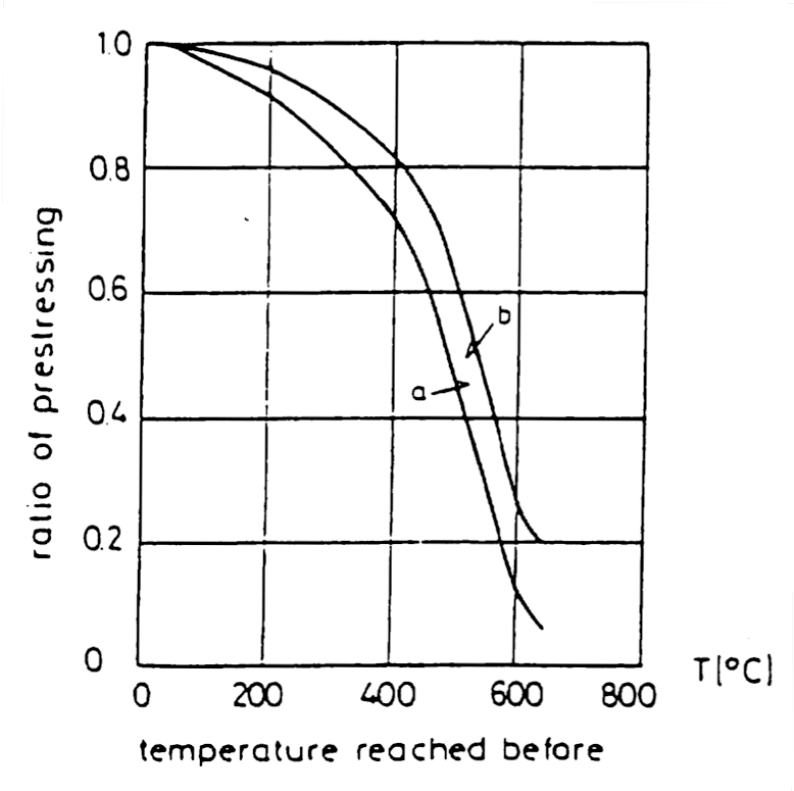


Fig. 6.6-4: Decrease of prestressing force under elevated temperature (a) and after cooling down (b)

Copyright fib, all rights reserved. This PDF copy of fib Bulletin 54 is intended for use and/or distribution only within National Member Groups of fib.

The kinds of cracks described above only concern the directly affected concrete structure. But, if monolithic structures are concerned, thermal deformation of structural members exposed to a fire cause stresses in the surrounding assembly, which may not be directly effected by the fire. Therefore, cracks may occur in these unaffected regions. This fact has to be taken into account, mainly when the damage of the fire-exposed part of the structure indicates a severe fire attack.

Explosive spalling (see 6.2.3)

Residual deformations of the load bearing concrete structure depend not only on the intensity of the fire attack but also on the static system involved. The decision to which degree these deformations may be tolerated must be regarded in connection with the system and in addition with other criteria such as the overall appearance etc.

In case of a fire, corrosive decomposition products may be released which can penetrate into concrete cross-sections and affect the reinforcement. Above all, this danger occurs if larger portions of polyvinyl chloride have been involved in the fire. It should be taken into account that long-term damages can be initiated if the transport of chloride into deeper areas of the concrete is not prevented by appropriate means early as possible. The highest amount of chloride may be found in areas not severely affected by the fire.

6.6.4 Determination of the degree of deterioration, methods of repair

The identification of the severity and degree of possible deterioration of a concrete structure after a fire, requires the same test methods, instrumentation and techniques as used for damages caused by other influences. It should be considered however, that a careful examination of the residual properties of reinforcing or prestressing members may be necessary, even if they do not show an obvious damage [CEB (1991), Harmathy (1986), Schneider/Nägele (1989)].

Methods of repair after a fire are similar to those used for repair measures for other causes. In the case that the restored building has to fulfil fire resistance of the structure.

Recalculation of the load bearing capacity of the repaired concrete structure may be necessary.

References to Chapter 6

Bechtold, R. (1977), *Zur thermischen Beanspruchung von Außenstützen im Brandfall (Thermal loading of outside columns during fire)*. Doctoral Dissertation, Technical University Braunschweig.

CEB Bulletin 208 (1991), *Fire design of concrete structures.* Comité Euro-International du Béton, Lausanne, Switzerland.

Diederichs, U.; Jumppanen, U.-M.; Schneider, U. (1995), *High Temperature Properties and Spalling Behaviour of High Performance Concrete: Material Properties and Design*. Freiburg; Aedificatio-Verlag.

EN 1992-1-2: *Structural Fire Design*.

Copyright fib, all rights reserved. This PDF copy of fib Bulletin 54 is intended for use and/or distribution only within National Member Groups of fib.

EUREKA-Bericht (1996), *Projekt "EU 499: Firetunn", Fires in Transport Tunnels*. Studiengesellschaft für Stahlanwendung e.V., Düsseldorf.

FIP/CEB (1978), *Report on methods of assessment of the fire resistance of concrete structural members* (1978). Fédération Internationale de la Précontrainte, London, UK.

Haksever, A.; Kordina, K. (1981), *Fire Engineering design of Wiener Reichsbrücke*, ACI-Journal.

Harmathy, T.Z. (1986), *Evaluation and Repair of Fire Damage to Concrete*. American Concrete Institute, Detroit, USA.

ISO 834, *Structural Fire design.*

Kordina, K. (1997), *Über das Brandverhalten punktgestützter Stahlbetonplatten*. Deutscher Ausschuss für Stahlbeton, H. 479.

Kordina, K. (1998), *Brandschäden und Entrauchungsprobleme bei langen Tunneln*. Bauingenieur 74, Heft 1.

Kordina, K. and Kersken-Bradley, M. (1996), *The Engineering considerations in large concrete buildings*, Longman.

Kordina, K.; Meyer-Ottens, C. (1999), *Beton Brandschutz Handbuch*. Verlag Bau + Technik, 2. Auflage.

Krampf, L. (1973), *Grundlagenversuche zum Verhalten von Konstruktionsleichtbeton unter Brandbeanspruchung*. Institut für Baustoffe, Massivbau und Brandschutz, Technical University Braunschweig.

Petterson O. (1978), *Assessment of fire severity by calculation*. FIP/CEB Report on methods of assessment of the fire resistance of concrete structural.

Schneider, U. (2001), *Ingenieurmethoden im Baulichen Brandschutz*. Expert Verlag Renningen.

Schneider, U.; Nägele, E. (1989), *Repairability of fire damaged structures*. CIB Report.

Schneider, U.; Horvath, J. (2003), *Behaviour of Ordinary Concrete at High Temperatures*. Institut für Baustofflehre, Bauphysik und Brandschutz, TU Wien.

Schneider, U.; Diederichs, U.; Weiß, R. (1975/1977), *Hochtemperaturverhalten von Festbeton*. SFB 148, Technische Universität Braunschweig.

Schneider, U.; Lebeda, C. (2000), *Baulicher Brandschutz*. Verlag W. Kohlhammer GmbH, Stuttgart.

Steinert, C. (1998), Brandverhalten von Tunnelauskleidungen aus Spritzbeton mit Faserzusatz. Bauingenieur 1/1998.

Warner, R. F.; Ranyan, B. V.; Hall A. S. (1998), *Reinforced Concrete*. Longman Cheshire, III Ed.

Copyright fib, all rights reserved. This PDF copy of fib Bulletin 54 is intended for use and/or distribution only within National Member Groups of fib.

Annex to Chapter 6

A.1 General considerations

Values given in the tables provide minimum dimensions for fire resistance in addition to the detailing rules required by ENV 1992-1-1. It must be stated that after the fire resistance time taken as a basis for design a failure of the member in question may occur. Some values of the axis distance of the steel, used in the tables are less than that required by ENV 1992-1-1 and should be considered for interpolation only.

Linear interpolation between the values given in the table is allowed.

Symbols used in the tables are defined in Fig. 6.A-1.

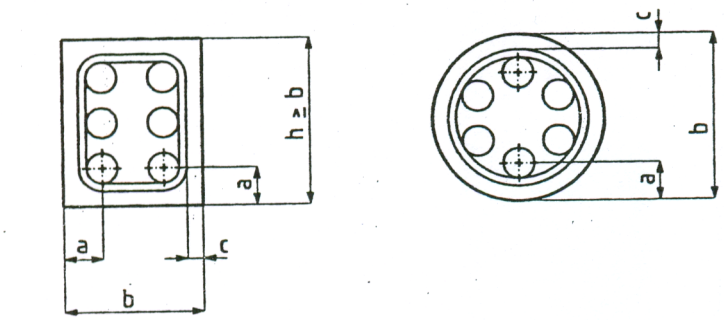


Fig. 6.A-1: Sections trough structural members, showing nominal axis distance a, and nominal concrete cover c to reinforcement

The nominal values of axis distance a to a steel bar, wire or tendon, should not be less than the minimum values given in the tables below.

The minimum axis distance for any individual bar should not be less than that required for R 30 and not less than half the average axis distance.

In tensile members, beams and slabs with concrete covers c ≥ 50 mm to the main longitudinal reinforcement, surface reinforcement should be provided in order to prevent the fall off of the concrete unless it can be justified, generally by tests, that falling off does not occur within the period of fire resistance. Where surface reinforcement is necessary, reference should be made to ENV 1992-1-1, 4.1.1.1 (6) and (7).

A.2 Columns

Fire resistance of reinforced concrete columns may be satisfied by the use of Table 6.A-1 and the following rules.

In Table 6.A-1 a load level n the fire situation l_{fi} has been introduced accounting for load combinations and the design column resistance to compression and, possibly bending including second order effects. The effective length l_o is assumed to be equal to the actual column length l_{col} (notation as in ENV 1992-1-1, 4.3.5).

Copyright fib, all rights reserved. This PDF copy of fib Bulletin 54 is intended for use and/or distribution only within National Member Groups of fib.

A.3 Load bearing solid walls

Adequate fire resistance of load-bearing reinforced concrete walls exposed on one side may be assumed if the following datas are applied.

REI 30 to 90: Cover as required by ENV 1992-1-1 thickness ≤ 120 mm.

A.4 Beams

(1) General

Adequate fire resistance of reinforced and prestressed concrete beams may be assumed if the data given in Tables 6.A-2 to 6.A-4 together with the following rules are used.

The Tables apply to beams which can be exposed to fire on three sides, i.e. the upper side is insulated by slabs or other elements which continue their insulating function during the whole fire resistance period.

For beams with varying width the minimum value b relates to the centroid of the tensile reinforcement.

Holes through the webs of beams do not affect the fire resistance provided that the remaining cross-sectional area of the member in the tensile zone is not less than $A_c = 2b^2$.

(2) Simply supported beams

Table 6.A-2 provides minimum values of axis distance to the soffit and sides of simply supported beams together with minimum values of the width of beam, for standard fire resistance of R 30 to R 240.

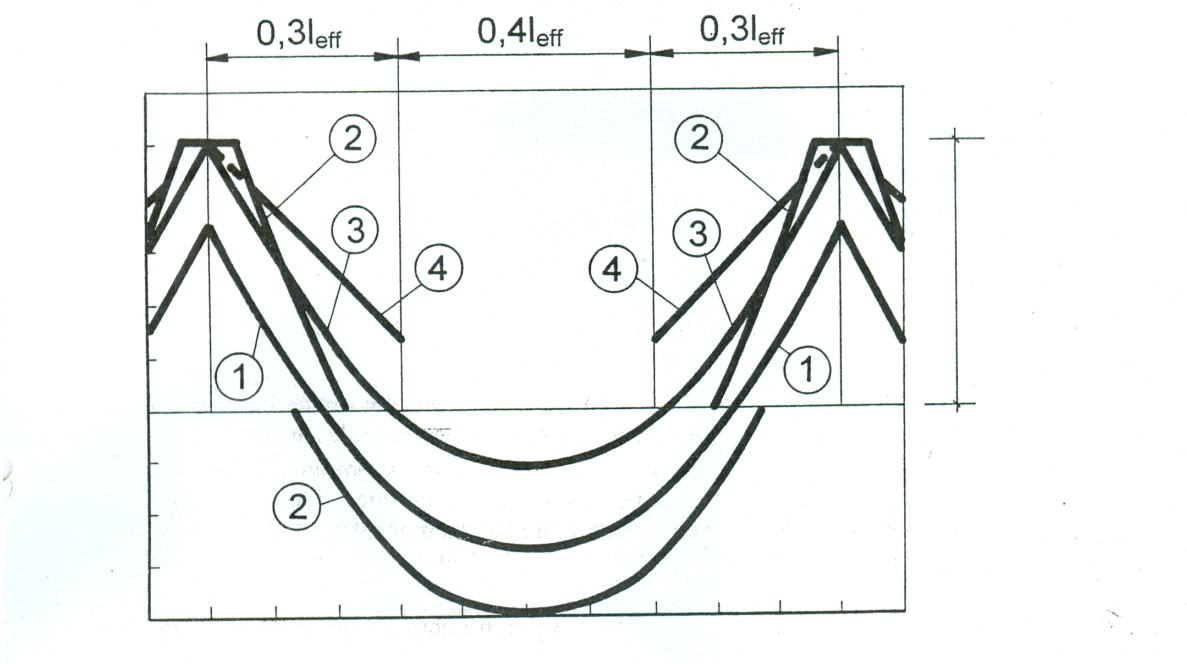
(3) Continuous beams

Table 6.A-3 provides minimum values of axis distance to the soffit and sides of continuous beams together with minimum values of the width of beam, for standard fire resistance of R 30 to R 240.

Table 6.A-3 and the following rule apply for beams where the moment redistribution according to ENV 1992-1-1, 2.5.3.4.2 does not exceed 15%. In the absence of a more rigorous calculation and where the redistribution exceeds 15%, or the detailing rules of this Part 1-2 are not followed, each span of a continuous beam should be assessed using Table 6.A-2 for simple supported beams.

The area of top reinforcement over each intermediate support for standard fire resistance of R 90 and above, for up to a distance of 0.3 1_{eff} (as defined in ENV 1992-1-1, 2.5.2.2.2) from the centre line of support (see Fig. 6.A-2).

Copyright fib, all rights reserved. This PDF copy of fib Bulletin 54 is intended for use and/or distribution only within National Member Groups of fib.



Key:

(1) Diagram of bending moments for the actions in a fire situation at t=0
(2) Envelope line of acting bending moments to be resisted by tensile reinforcement according to ENV 1992-1-1
(3) Diagram of bending moments in fire conditions
(4) Envelope line of resisting bending moments

Fig. 6.A-2: Envelope of resisting bending moments over supports in fire conditions

A.5 Simply supported slabs

Table 6.A-4 provides minimum values of axis distance to the soffit of simply supported slabs for standard fire resistance of R 30 to R 240.

In two-way spanning slabs, a denotes the axis distance of the reinforcement in the lower layer.

The values given in Table 6.A-4 (Columns 2 and 4) also apply to one-way or two-way continuous slabs.

A.6 Flat slabs

The following rules apply to flat slabs where the moment redistribution according to ENV 1992-1-1, 2.5.3.5.4 does not exceed 15%. Otherwise axis distances should be taken as for one-way slab (Column 3 in Table 6.A-4) and the minimum thickness from Table 6.A-5.

For fire ratings of REI 90 and above, at least 20% of the total top reinforcement in each direction over intermediate supports, required by ENV 1992-1-1, should be continuous over the full span. This reinforcement should be placed in the column strip.

Minimum slab-thickness should not be reduced (e.g. by taking floor finishes into account).

Copyright fib, all rights reserved. This PDF copy of fib Bulletin 54 is intended for use and/or distribution only within National Member Groups of fib.

The axis distance a denotes the axis distance of the reinforcement in the lower layer.

Table 6.A-1: Minimum dimensions and axis distances for reinforced concrete columns; rectangular and circular section

Standard fire resistance	Minimum dimensions (mm) Column width b_{min}/axis distance a			
	Column exposed on more than one side			Exposed on one side
	$\mu_{fi} = 0.2$	$\mu_{fi} = 0.5$	$\mu_{fi} = 0.7$	$\mu_{fi} = 0.7$
1	2	3	4	5
R 30	¦ 150/10¦*	¦ 150/10¦*	¦ 150/10¦*	¦ 100/10¦*
R 60	¦ 150/10¦*	¦ 180/10¦*	¦ 200/10¦*	¦ 120/10¦*
R 90	¦180/10¦*	¦210/10¦*	¦240/35¦*	¦140/10¦*
R 120	¦200/40¦	¦250/40¦	¦280/40¦	¦160/45¦
R 180	¦240/50¦	¦320/50¦	¦360/50¦	¦200/60¦
R 240	¦300/50¦	¦400/50¦	¦450/50¦	¦300/60¦
*Normally the cover required by ENV 1992-1-1 will control				

Copyright fib, all rights reserved. This PDF copy of fib Bulletin 54 is intended for use and/or distribution only within National Member Groups of fib.

Table 6.A-2: Minimum dimensions and axis distances for simply supported beams made with reinforced and prestressed concrete

Standard fire resistance	Minimum dimensions (mm)				
	Possible combinations of a and b_{min} where a is the avarege axis distance and b_{min} is the width of beam				Web thickness b_w
1	2	3	4	5	6
R 30	b_{min} = 80 a = 25	120 15*	160 10*	200 10*	80
R 60	b_{min} = 120 a = 40	160 35	200 30	300 25	100
R 90	b_{min} = 150 a = 55	200 45	250 40	400 35	100
R 120	b_{min} = 200 a = 65	240 55	300 50	500 45	120
R 180	b_{min} = 240 a = 80	300 70	400 65	600 60	140
R 240	b_{min} = 280 a = 90	350 80	500 75	500 70	160
$a_{sd} = a + 10$ mm (see note below)					

For prestressed beams the increase of axis distance according to 4.2.2(4) should be noted.

a_{sd} is the axis distance to the side of beam for the corner bars (tendon or wire) of beams with only one layer of reinforcement. For values of b_{min} greater than that given in Column 4 no increase of a is required.

*Normally the cover required by ENV 1992-1-1 will control.

Copyright fib, all rights reserved. This PDF copy of fib Bulletin 54 is intended for use and/or distribution only within National Member Groups of fib.

Table 6.A-3: Minimum dimensions and axis distances for continuous beams made with reinforced and prestressed concrete

Standard fire resistance	Minimum dimensions (mm)			
	Possible combinations of a and b_{min} where a is the avarege axis distance and b_{min} is the width of beam			Web thickness b_w
1	2	3	4	5
R 30	b_{min} = 80 a = 12*	160 12*	200 12*	80
R 60	b_{min} = 120 a = 25	200 12	300 12*	100
R 90	b_{min} = 150 a = 35	250 25	400 25	100
R 120	b_{min} = 220 a = 45	300 35	500 35	120
R 180	b_{min} = 380 a = 60	400 60	600 50	140
R 240	b_{min} = 480 a = 70	500 70	700 60	160
$a_{sd} = a + 10$ mm (see note below)				

For prestressed beams the increase of axis distance according to 4.2.2(4) should be noted.

a_{sd} is the axis distance to the side of beam for the corner bars (tendon or wire) of beams with only one layer of reinforcement. For values of b_{min} greater than that given in Column 3 no increase of a is required.

*Normally the cover required by ENV 1992-1-1 will control.

Copyright fib, all rights reserved. This PDF copy of fib Bulletin 54 is intended for use and/or distribution only within National Member Groups of fib.

Table 6.A-4: Minimum dimensions and axis distances for reinforced and prestressed concrete simply supported one-way and two-way slabs

Standard fire resistance	Minimum dimensions (mm)			
	slab thickness h_s (mm)	axis distance *a*		
		one way	two ways	
			$/_y/_x \leq 1.5$	$1.5 < /_y/_x \leq 2$
1	2	3	4	5
REI 30	60	10*	10*	10*
REI 60	80	20	10*	15*
REI 90	100	30	15*	20
REI 120	120	40	20	25
REI 180	150	55	30	40
REI 240	175	65	40	50

$/_x$ and $/_y$ are the spans of a two-way slab (two directions at right angles) where $/_y$ is the longer span.

For prestressed slabs the increase of axis distance according to 4.2.2(4) should be noted.

The axis distance *a* in Column 4 and 5 for two way slabs relate to slabs supported at all four edges. Otherwise, they should be treated as one-way spanning slab.

*Normally the cover required by ENV 1992-1-1 will control.

Table 6.A-5: Minimum dimensions and axis distances for reinforced and prestressed

Standard fire resistance	Minimum dimensions (mm)	
	slab thickness, h_s	axis distance *a*
1	2	3
REI 30	150	10*
REI 60	200	15*
REI 90	200	25
REI 120	200	35
REI 180	200	45
REI 240	200	50

*Normally the cover required by ENV 1992-1-1 will control.

Copyright fib, all rights reserved. This PDF copy of fib Bulletin 54 is intended for use and/or distribution only within National Member Groups of fib.

7 Design of members

The design of members is a synthesis process which requires the application of models and procedures presented within the previous chapters. Traditionally two different classes of structural members may be distinguished: linear members and two-dimensional members; as a consequence, in the following, two different structures, which may be considered as composed respectively by linear and two-dimensional members, are analysed. Of course, this distinction is not a sharp border, because in several cases two-dimensional structures may be designed as linear one and, conversely, sometimes a linear member may require a two-dimensional approach.

7.1 Linear members

by Giuseppe Mancini

A reinforced concrete frame on elastic ground is analysed as a linear member; the actual structure from which the frame is derived is described in the following section.

7.1.1 Description of the structure

The analysed structure consists of a 22.10 m long concrete box-culvert, undercrossing a railway line for high speed trains at a right angle and built to save the free flow of a stream. The railway consists of double tracks spaced of 5.0 m over a bed composed by ballast, sleepers and rails having an overall thickness of 80 cm.

A plan view of the structure is given in Fig. 7.1-1, where the bold lines represent the culvert dimensions. Two retaining walls are present at the extremities of the culvert in order to contain the railway back-fill.

In Fig. 7.1-2 the longitudinal section A-A and the transverse section B-B of the culvert are presented. The structure has a longitudinal gradient to allow the stream flowing; furthermore, a lean concrete bed is provided under the foundation, with a thickness of 200 mm. The upper slab of culvert is 2.50 m deep under the ballast level, so that an average earth cover was considered in the calculations.

The following material properties were considered:

– Concrete

Grade C30/37:	f_{ck} = 30.0 N/mm^2;
compressive design strength:	f_{cd} = 20.0 N/mm^2;
compressive resistance for uncracked zones:	f_{cd1} = 15.0 N/mm^2;
compressive resistance for cracked zones:	f_{cd2} = 10.6 N/mm^2;
mean value of tensile strength:	f_{ctm} = 2.9 N/mm^2;
modulus of elasticity of concrete:	E_c = 29.0 × 10^3 N/mm^2;

– Reinforcing steel:

Grade 500:	f_{yk} = 500.0 N/mm^2;
design strength:	f_{yd} = 434.8 N/mm^2;
modulus of elasticity:	E_s = 200.0 × 10^3 N/mm^2;

Copyright fib, all rights reserved. This PDF copy of fib Bulletin 54 is intended for use and/or distribution only within National Member Groups of fib.

– Soil:

internal friction angle:	ϕ =	30°;
modulus of subgrade reaction (vertical):	K_v =	20×10^{-3} N/mm^3;
modulus of subgrade reaction (horizontal):	K_h =	10×10^{-3} N/mm^3;
unit weight:	γ =	19 kN/m^3.

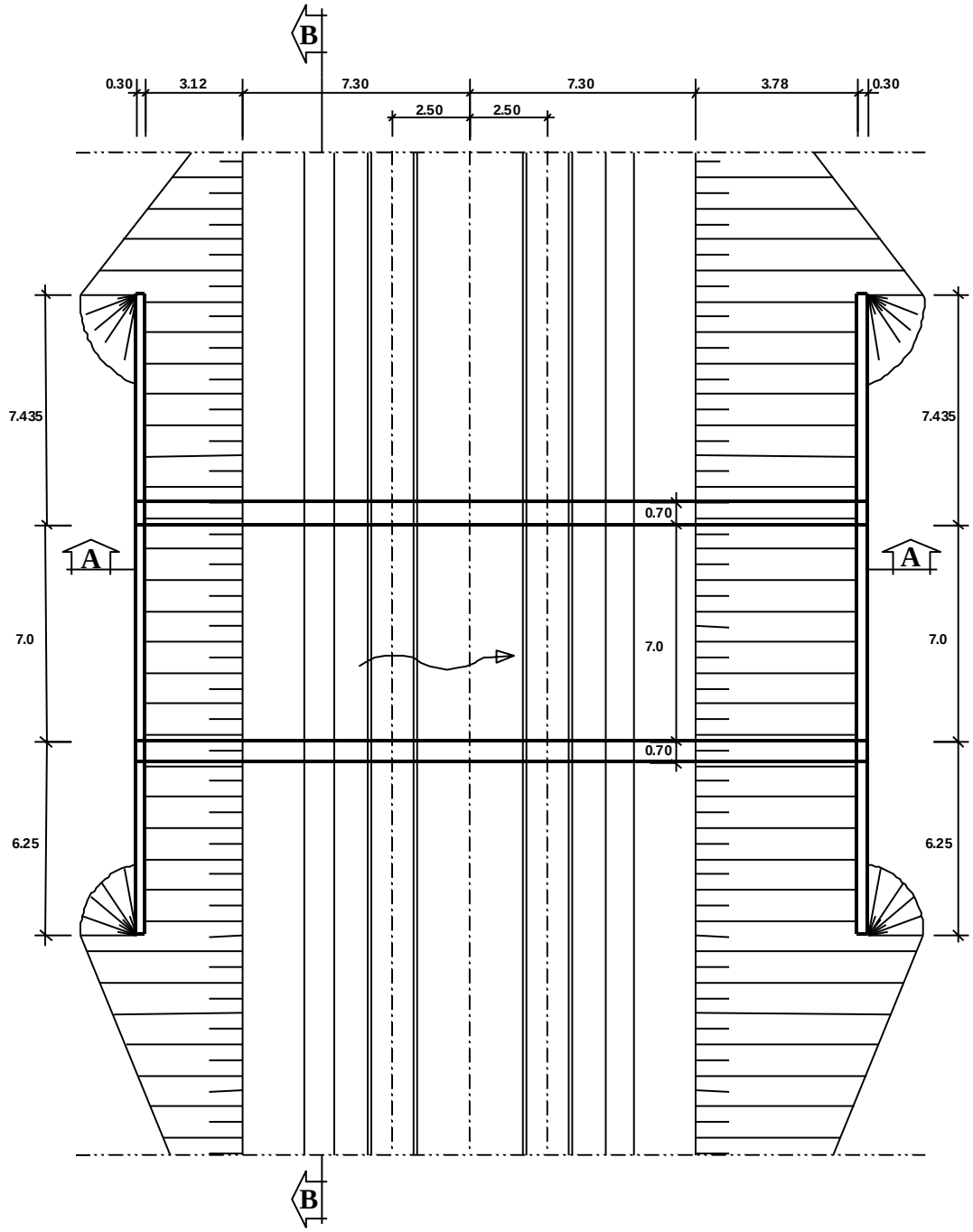


Fig. 7.1-1: Plan view of the structure (dimensions in meters)

(1) Concrete cover

For the environmental conditions, the Exposure Class 2 may be considered (humid environment without frost: components in non-aggressive soil).

Copyright fib, all rights reserved. This PDF copy of fib Bulletin 54 is intended for use and/or distribution only within National Member Groups of fib.

The minimum concrete cover for Class 2 is equal to 25 mm, which should be added to the tolerance value of 10 mm; as a consequence the nominal value for concrete cover results:

$c_{nom} = c_{min} + 10 = 25 + 10 = 35$ mm

adopted in the calculations.

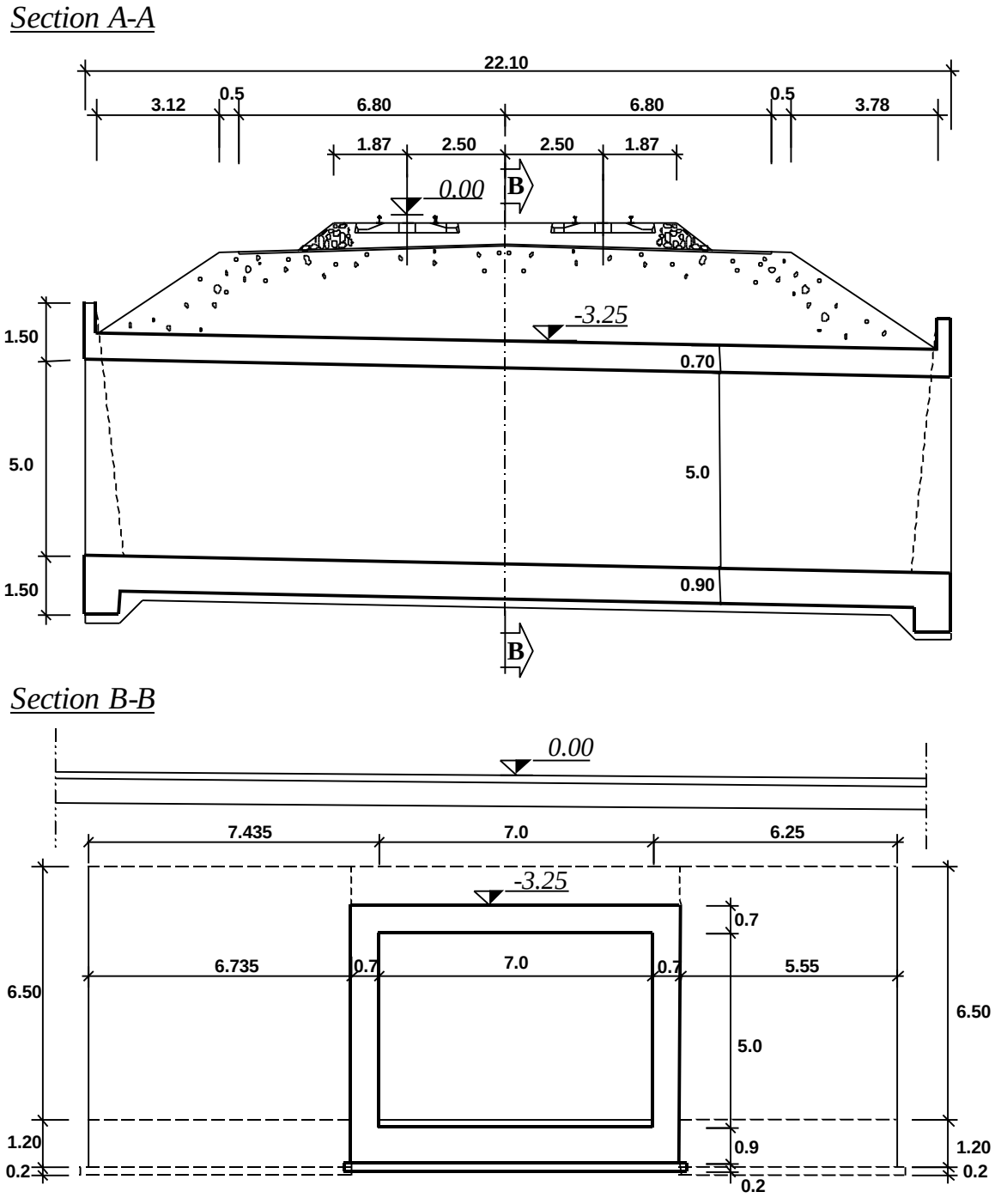


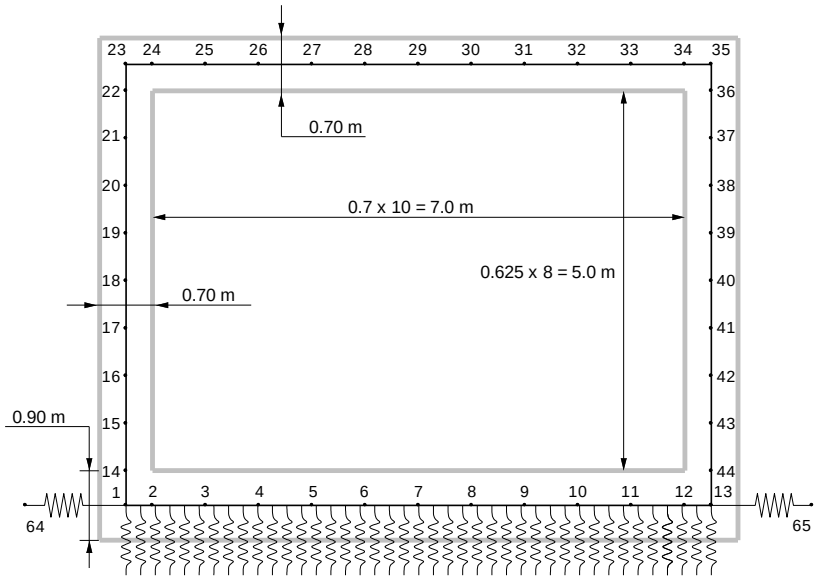
Fig. 7.1-2: Longitudinal and cross section of the culvert

Copyright fib, all rights reserved. This PDF copy of fib Bulletin 54 is intended for use and/or distribution only within National Member Groups of fib.

7.1.2 Structural model

A linear-elastic FEM analysis was performed in order to evaluate the internal actions on the structure produced by the applied loads. Due to earth cover, the train load is spread into the soil in both longitudinal and transverse directions so that a distributed load is acting on the upper slab of the culvert; consequently, calculations may be referred to a transverse strip having 1.0 m of width, adopting a plane frame to represent the culvert; so the two-dimensional problem may be reduced to a linear one.

a) Nodes



b) Elements

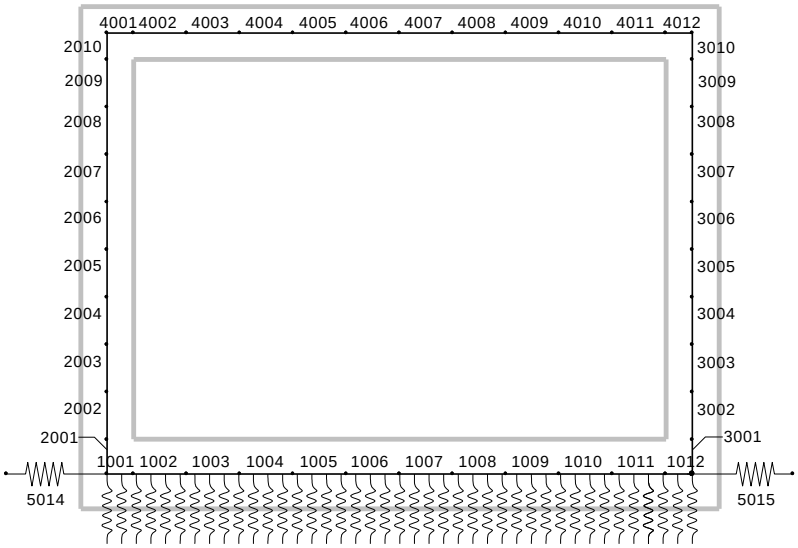


Fig. 7.1-3: FEM model

Fig. 7.1-3 represents the adopted FEM mesh, with both nodes and elements. The slab, the uprights and the foundation are modelled by means of beam elements with area and inertia characteristics related to a rectangular section of unit breadth and height coincident with each respective concrete thickness. The previous quantities are summarized in Table 7.1-1.

Copyright fib, all rights reserved. This PDF copy of fib Bulletin 54 is intended for use and/or distribution only within National Member Groups of fib.

The model may be restrained by means of spring elements representing the deforming ground, or can be assumed to rest on a continuous elastic bed. In this second case, of course, a B.E.F. (Beam on Elastic Foundation) element should be used and its elastic parameter is evaluated as product of K_v with the foundation breadth. If the spring elements are adopted, their elastic constant is calculated by the moduli of subgrade reaction; for the vertical restraints two different collaborating widths are assumed: 0.525 m and 0.70 m respectively for the external springs and for the internal ones.

Member	Area m^2	Inertia m^4
Upper Slab	0.700	0.02858
Uprights	0.700	0.02858
Foundation	0.900	0.06075

Table 7.1-1: Area and inertia of FEM beam elements

A spring element shall be used for the horizontal restraint; its elastic constant is related to the overall height of the culvert, and its value is obtained by multiplying the K_h value with an area of influence of 6.6×1.0 m. The elastic constants of each spring element (whether for vertical or horizontal restraints) are reported in Table 7.1-2, together with the subgrade constant of the B.E.F. element.

Element	Collaborating Area/Width $[m^2 – m]$	Elastic Constant $[kN/m – kN/m^2]$
Horizontal spring	6.600×1.0	6.60×10^3
Vertical spring (external)	0.525×1.0	10.50×10^3
Vertical spring (internal)	0.700×1.0	14.00×10^3
B.E.F.	1.000	20.00×10^3

Table 7.1-2: Spring constants

For these calculations, the B.E.F. approach was chosen.

7.1.3 Actions

In such a structure several combinations of actions should be considered in accordance with, for instance, the requirements of EN 1991-2 Traffic Load on Bridges. For the sake of simplicity in the following, only one a combination of actions is analysed, considering only the dead weights, the live load due to the trains, the lateral pressures exerted by earth and, of course, the subsequent subgrade reactions.

The external actions considered are loaded in the mathematical model in several different steps, as illustrated in the following:

- STEP 1: Self-weight: adopting a specific weight of $\gamma = 24.5$ kN/m^3;
- STEP 2: Gravity load on upper slab due to earth cover and ballast:

Copyright fib, all rights reserved. This PDF copy of fib Bulletin 54 is intended for use and/or distribution only within National Member Groups of fib.

By considering the cover weight and the ballast presence with a nominal height of 0.8 m (unit weight: $\gamma_{ballast}$ = 18 kN/m^3), the following uniformly distributed loads are obtained:

$g_{soil} = 19 \cdot 2.5 \cdot 1.0 = 47.5$ kN/m
$g_{ballast} = 18 \cdot 0.8 \cdot 1.0 = 14.4$ kN/m;

– STEP 3: Lateral earth pressure at rest.

This pressure is evaluated adopting a k_0 coefficient calculated as:

$k_0 = 1 - \sin\phi = 0.5$

A symmetric trapezoidal load diagram is obtained, acting on the two uprights with opposite sign. The top and bottom values are:

$p_{top} = 0.5 \cdot (47.5 + 14.4) = 30.95$ kN/m;
$p_{bottom} = 30.95 + 0.5 \cdot (19 \cdot 6.6 \cdot 1.0) = 93.65$ kN/m

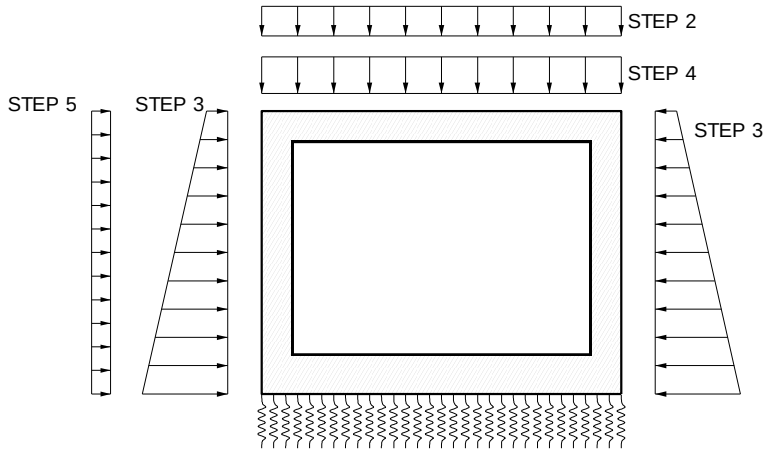


Fig. 7.1-4: Applied loads on structure

– STEP 4: Train load.

As railway load on track, a uniformly distributed live load, derived from Load Model 71 (LM71) of EN 1991-2, was adopted. This kind of load is composed by $\alpha \times 250$ kN point loads spaced of 1.6 m each other; thus the corresponding uniform load value is obtained by ($\alpha = 1.1$ according to the Italian national code):

$q_{LM71} = 1.1 \cdot 250 / 1.6 = 171.88$ kN/m.

A transverse spreading, with respect to the railway direction, may be evaluated to calculate the load acting on the upper slab of the culvert: starting from the sleeper width of 2.60 m, it may be considered a spread ratio of 4:1 within the ballast, of 2:1 within the earth cover and of 1:1 within the concrete up to the middle plane of the slab. So, the influence breadth results:

$b_{influence} = 2.6 + 2 \cdot (0.4/4 + 2.5/2 + 0.35/1) = 6.00$ m.

Copyright fib, all rights reserved. This PDF copy of fib Bulletin 54 is intended for use and/or distribution only within National Member Groups of fib.

Having two trains on the rails and being spaced of 5.0 m, the uniform load on the slab:

$q = 2 \cdot 171.88 / 6 = 57.3$ kN/m

This procedure may be certainly considered as conservative; in fact with a different approach the total live load may be distributed uniformly on a breadth of 3+5+3 = 11 m, taking into account the capability of the upper slab to distribute the load transversally.

For the dynamic allowance, according to the code indication, a coefficient of 1.3 was adopted. Finally, the value of train load results:

$q_{train} = 1.3 \cdot 57.3 = 74.50$ kN/m

– STEP 5: Lateral earth pressure from vertical live load.

The increase in the lateral earth pressure is conventionally evaluated considering a uniform surcharge of 40 kN/m^2 on one side of the earth adjacent to the culvert which results in a constant horizontal pressure acting on only one upright; the value of the lateral load is calculated as:

$q_{earth,variab} = k_0 \cdot 40 \cdot 1 = 0.5 \cdot 40 \cdot 1 = 20.0$ kN/m

Fig. 7.1-4 summarizes the applied loads on the structure.

7.1.4 Combination for ULS and consequent internal actions

The design is performed using the output of FEM analysis without any redistribution of internal actions (linear-elastic analysis). The following expression for combination of actions was used:

$$S_d = S\left\{\gamma_G\, G_k + \gamma_Q\, Q_k\right\} \qquad (7.1\text{-}1)$$

where:

G_k = permanent loads: self-weight, soil and ballast weight, lateral earth pressure at rest;
Q_k = variable loads: train load, lateral earth pressure from train load;
$\gamma_G = 1.35$;
$\gamma_Q = 1.50$.

The results of FEM analysis, in terms of internal actions combined according to Eq. (7.1-1) are represented in Fig. 7.1-5.

Copyright fib, all rights reserved. This PDF copy of fib Bulletin 54 is intended for use and/or distribution only within National Member Groups of fib.

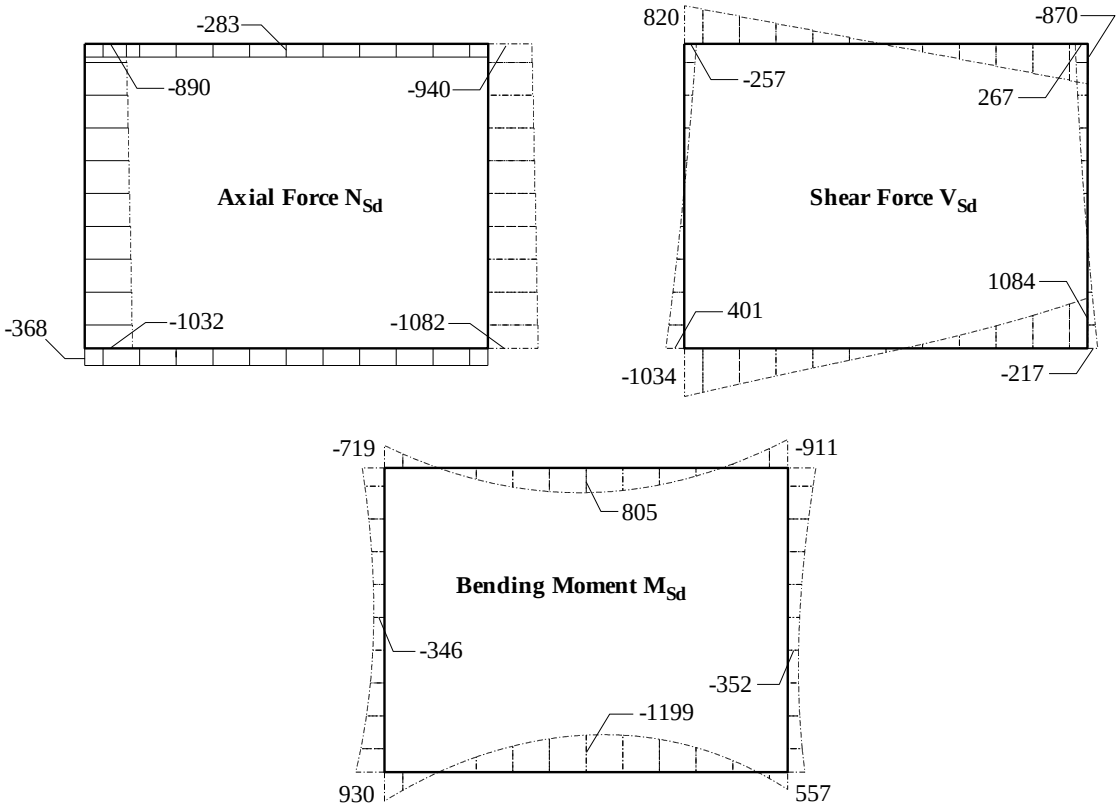


Fig. 7.1-5: Internal actions from FEM model at ULS

(1) Design of upper slab and foundation

Referring to Fig. 7.1-5, three different sections are investigated for the upper slab in order to evaluate the amount of reinforcing steel: at midspan, where maximum positive bending moment is present, and at corners where maximum shear force and negative bending moment are reached. Similarly, the same sections were chosen for the foundation. The internal actions at ULS are given in Table 7.1-3.

The following notation was adopted:

- b = breadth of the equivalent beam;
- h = overall depth of the section;
- d = distance of reinforcement centroid from the extreme compressive fibre.

	Section	b [m]	h [m]	d [m]	N_{Sd} [kN]	V_{Sd} [kN]	M_{Sd} [kNm]
Upper Slab	Left Corner	1.0	0.7	0.655	-283	820	-719
	Midspan	1.0	0.7	0.655	-283	-25	805
	Right Corner	1.0	0.7	0.655	-283	-870	-911
Foundation	Left Corner	1.0	0.9	0.855	-368	-1034	930
	Midspan	1.0	0.9	0.855	-368	-84	-1199
	Right Corner	1.0	0.9	0.855	-368	1084	557

Table 7.1-3: Internal actions on upper slab and foundation

Copyright fib, all rights reserved. This PDF copy of fib Bulletin 54 is intended for use and/or distribution only within National Member Groups of fib.

On the safety side, the axial forces were disregarded because earth pressure may not have a favourable effect on N_{Sd} values.

	Section	μ [-]	ω [-]	ξ [-]	ζ [-]	A_s [mm^2]	x [m]	z [m]
Upper Slab	Left Corner	0.085	0.0905	0.1620	0.9395	2714	0.106	0.613
	Midspan	0.095	0.1018	0.1745	0.9340	3052	0.114	0.609
	Right Corner	0.107	0.1155	0.1901	0.9268	3465	0.124	0.604
Foundation	Left Corner	0.064	0.0674	0.1362	0.9506	2640	0.116	0.810
	Midspan	0.083	0.0883	0.1596	0.9405	3459	0.136	0.801
	Right Corner	0.038	0.0394	0.1010	0.9642	1544	0.086	0.821

Table 7.1-4: Tension reinforcement from General Table

The amount of reinforcement required for bending is calculated, for the sake of simplicity and on the side of safety, without consideration of the compression reinforcement, using the General Table reported in CEB Bulletin 141 and reproduced in Table 7.1-5. So, for each investigated section, one has to enter the non-dimensional bending moment:

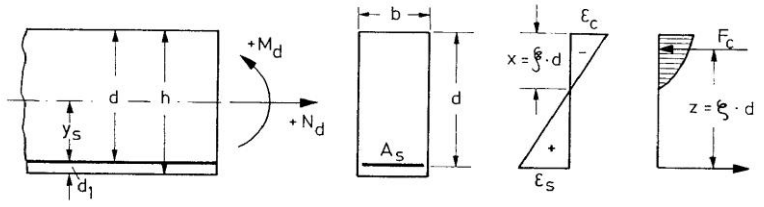
$$\mu = \frac{M_{Sd}}{b\,d^2\,f_{cd}}$$

in the General Table and obtain the following quantities:

$$\omega = \frac{A_s}{b\,d}\,\frac{f_{yd}}{f_{cd}} \qquad \xi = \frac{x}{d} \qquad \zeta = \frac{z}{d}$$

where *x* is the depth of neutral axis and *z* the internal lever arm; the obtained results are resumed in Table 7.1-4.

Copyright fib, all rights reserved. This PDF copy of fib Bulletin 54 is intended for use and/or distribution only within National Member Groups of fib.



μ_{sd}	ω	$\xi = \frac{x}{d}$	$\zeta = \frac{z}{d}$	ϵ_c [‰]	ϵ_s [‰]	σ_{sd} [MPa] S220	S400	S500
0.01	0.0102	0.050	0.983	-0.52	10.00	191	348	435
0.02	0.0205	0.072	0.975	-0.77	10.00			
0.03	0.0310	0.089	0.969	-0.98	10.00			
0.04	0.0415	0.104	0.963	-1.16	10.00			
0.05	0.0522	0.118	0.958	-1.34	10.00			
0.06	0.0630	0.131	0.953	-1.51	10.00			
0.07	0.0739	0.144	0.947	-1.68	10.00			
0.08	0.0849	0.156	0.942	-1.85	10.00			
0.09	0.0961	0.168	0.937	-2.03	10.00			
0.10	0.1074	0.181	0.931	-2.21	10.00			
0.11	0.119	0.194	0.925	-2.40	10.00			
0.12	0.131	0.207	0.919	-2.60	10.00			
0.13	0.143	0.220	0.912	-2.82	10.00			
0.14	0.155	0.233	0.905	-3.04	10.00			
0.15	0.167	0.247	0.899	-3.27	10.00			
0.16	0.179	0.261	0.892	-3.50	9.92			
0.17	0.192	0.280	0.884	-3.50	9.02			
0.18	0.206	0.299	0.878	-3.50	8.22			
0.19	0.219	0.318	0.868	-3.50	7.50			
0.20	0.233	0.338	0.859	-3.50	6.85			
0.21	0.247	0.359	0.851	-3.50	6.26			
0.22	0.261	0.380	0.842	-3.50	5.72			
0.23	0.276	0.401	0.833	-3.50	5.22			
0.24	0.291	0.423	0.824	-3.50	4.77			
0.25	0.307	0.446	0.814	-3.50	4.35			
0.26	0.323	0.470	0.805	-3.50	3.95			
0.27	0.340	0.494	0.795	-3.50	3.59			
0.28	0.357	0.519	0.784	-3.50	3.24			
0.29	0.375	0.545	0.773	-3.50	2.92			
0.30	0.394	0.572	0.762	-3.50	2.62			
0.31	0.413	0.600	0.750	-3.50	2.33			435
0.32	0.434	0.630	0.738	-3.50	2.05			410
0.33	0.455	0.662	0.725	-3.50	1.79		348	358
0.34	0.478	0.695	0.711	-3.50	1.54		308	308
0.35	0.503	0.731	0.696	-3.50	1.29		258	258
0.36	0.529	0.770	0.680	-3.50	1.05	191	210	210
0.37	0.559	0.812	0.662	-3.50	0.81	162	162	162
0.38	0.592	0.860	0.642	-3.50	0.57	104	104	104
0.39	0.630	0.915	0.619	-3.50	0.32	64	64	64

Table 7.1-5: General Table for the design of rectangular sections without compression reinforcement for bending with or without normal force

Considering shear effects, the amounts of A_s, previously calculated, should be increased to take into account the longitudinal component that shear force produces on tension chords; the further reinforcement is evaluated by:

$$\Delta A_s = \frac{V_{Sd}\left(\cot\theta - \cot\alpha\right)}{2\, f_{yd}} \tag{7.1-2}$$

Assuming $\theta = 30°$ and $\alpha = 90°$, the total longitudinal reinforcement can be found as reported in Table 7.1-6.

Copyright fib, all rights reserved. This PDF copy of fib Bulletin 54 is intended for use and/or distribution only within National Member Groups of fib.

	Section	A_s [mm^2]	ΔA_s [mm^2]	$A_{s,TOT}$ [mm^2]
Upper Slab	Left Corner	2714	1630	4344
	Midspan	3052	50	3102
	Right Corner	3465	1730	5195
Foundation	Left Corner	2640	2060	4700
	Midspan	3459	170	3629
	Right Corner	1544	2160	3704

Table 7.1-6: Total longitudinal reinforcement

The compression chord results are automatically verified since the term V_{Sd} /2 (cotθ–cotα) should be subtracted from the compression force, whose safety is controlled by using the General Table of CEB Bulletin 141.

Regarding the transverse web reinforcement, the amount of tension steel is evaluated by imposing the equality between the acting force and the resisting one:

$$\frac{V_{Sd}}{\sin\alpha} = \left(\frac{A_{sw}}{s}\right) f_{yd}\, z\, (\cot\theta + \cot\alpha). \qquad (7.1\text{-}3)$$

The values of A_{sw}/s for the investigated sections are given in Table 7.1-7.

	Section	V_{Sd} / sin α [kN]	A_{sw}/s [mm^2/m]
Upper Slab	Left Corner	820	1777
	Midspan	25	55
	Right Corner	870	1911
Foundation	Left Corner	1034	1696
	Midspan	84	139
	Right Corner	1084	1753

Table 7.1-7: Transverse web reinforcement

The compression in the concrete web is checked by calculating the acting force with the following formula:

$$F_{Scw} = \frac{V_{Sd}}{\sin\theta}\left(\frac{\cot\theta}{\cot\theta + \cot\alpha}\right)$$

which should be lesser or equal to the resisting force, according to:

$$F_{Scw} \le F_{Rcw} = f_{cd2}\, b\, z\, \cos\theta.$$

Table 7.1-8 reports the results for the investigated sections.

Copyright fib, all rights reserved. This PDF copy of fib Bulletin 54 is intended for use and/or distribution only within National Member Groups of fib.

	Section	F_{Scw} [kN]	F_{Rcw} [kN]	$\Delta F(F_{Rcw} - F_{Scw})$ [kN]
Upper Slab	Left Corner	1639.3	5601.9	3962.6
	Midspan	50.0	5569.2	5519.1
	Right Corner	1739.4	5526.2	3786.9
Foundation	Left Corner	2068.3	7406.8	5338.5
	Midspan	167.2	7328.1	7160.9
	Right Corner	2168.4	7512.8	5344.4

Table 7.1-8: Check of web compression

(2) Design of uprights

The verification of uprights should be performed considering the interaction of axial force and bending moment; but, for the case involved, the compression is less dominant on bending actions, so that the General Table approach is still valid. To be on the safe side, reinforcement design is performed considering only tension reinforcement, although a minimum amount of compressed reinforcement will be also provided.

To enter the General Table, the axial force should be referred to the centroid of tension reinforcement, so that a modified value of acting moment is obtained:

$$M^{*}_{Sd} = M_{Sd} + N_{Sd} \cdot (d - h/2)$$

for the evaluation of the non-dimensional moment μ. The reinforcement area should be calculated by the expression:

$$A_s = \omega\, b\, d\, \frac{f_{yd}}{f_{cd}} - \frac{N_{Sd}}{f_{yd}}$$

Referring to the most loaded upright, Table 7.1-9 reports the internal actions while in the Table 7.1-10 reinforcement design for all the section coincident with the FEM nodes is indicated.

Copyright fib, all rights reserved. This PDF copy of fib Bulletin 54 is intended for use and/or distribution only within National Member Groups of fib.

Section	Node	b [m]	h [m]	d [m]	N_{Sd} [kN]	V_{Sd} [kN]	M_{Sd} [kNm]	M^*_{Sd} [kNm]
2001	1	1.0	0.7	0.654	-1032	401	-930	1244
2002	14	1.0	0.7	0.654	-1017	335	-764	1073
2003	15	1.0	0.7	0.654	-1003	247	-583	888
2004	16	1.0	0.7	0.654	-988	164	-455	755
2005	17	1.0	0.7	0.654	-974	86	-377	673
2006	18	1.0	0.7	0.654	-959	13	-346	638
2007	19	1.0	0.7	0.654	-945	-55	-360	647
2008	20	1.0	0.7	0.654	-930	-118	-414	697
2009	21	1.0	0.7	0.654	-916	-176	-507	785
2010	22	1.0	0.7	0.654	-901	-229	-634	908
2010	23	1.0	0.7	0.654	-890	-257	-719	989

Table 7.1-9: Internal actions on left upright

Section	Node	μ [-]	ω [-]	ξ [-]	ζ [-]	A_s [mm^2]	x [m]	z [m]
2001	1	0.145	0.1610	0.240	0.902	2470	0.157	0.590
2002	14	0.125	0.1370	0.214	0.916	1782	0.140	0.599
2003	15	0.104	0.1120	0.186	0.929	1065	0.122	0.607
2004	16	0.088	0.0939	0.166	0.938	551	0.108	0.613
2005	17	0.079	0.0838	0.155	0.943	282	0.101	0.616
2006	18	0.075	0.0794	0.150	0.945	183	0.098	0.618
2007	19	0.076	0.0805	0.151	0.944	249	0.099	0.617
2008	20	0.082	0.0871	0.158	0.941	482	0.104	0.615
2009	21	0.092	0.0984	0.171	0.936	853	0.112	0.612
2010	22	0.106	0.1144	0.189	0.927	1368	0.123	0.607
2010	23	0.116	0.1262	0.202	0.921	1750	0.132	0.603

Table 7.1-10: Vertical reinforcement design for normal actions

As for upper slab and foundation design, an additional amount of tension reinforcement arises from shear action, evaluated by the (7.1-2) for the same values of θ and α angles; Table 7.1-11 reports the total longitudinal reinforcement for the investigated upright.

Copyright fib, all rights reserved. This PDF copy of fib Bulletin 54 is intended for use and/or distribution only within National Member Groups of fib.

Section	Node	A_s [cm^2]	ΔA_s [mm^2]	$A_{s,\,TOT}$ [mm^2]
2001	1	2470	800	3270
2002	14	1782	670	2452
2003	15	1065	490	1555
2004	16	551	330	881
2005	17	282	170	452
2006	18	183	30	213
2007	19	249	110	359
2008	20	482	240	722
2009	21	853	350	1203
2010	22	1368	460	1828
2010	23	1750	510	2260

Table 7.1-11: Total longitudinal reinforcement

Transverse reinforcement may be calculated according to Eq. (7.1-3) (see results in Table 7.1-12).

Section	Node	$V_{Sd} / \sin \alpha$ [kN]	A_{sw}/s [mm^2/m]
2001	1	401	903
2002	14	335	743
2003	15	247	540
2004	16	164	355
2005	17	86	185
2006	18	13	27
2007	19	55	119
2008	20	118	255
2009	21	176	382
2010	22	229	502
2010	23	257	566

Table 7.1-12: Transverse reinforcement design

The compression in the web may be checked in the same way as for the upper slab.

Due to the low values assumed by transverse shear within the uprights, there is no interaction between M, N and V.

Copyright fib, all rights reserved. This PDF copy of fib Bulletin 54 is intended for use and/or distribution only within National Member Groups of fib.

Section	Node	F_{Scw} [kN]	F_{Rcw} [kN]	$\Delta F(F_{Rcw} - F_{Scw})$ [kN]
2001	1	803	5395	4592
2002	14	670	5476	4806
2003	15	494	5554	5060
2004	16	328	5610	5283
2005	17	172	5637	5466
2006	18	25	5649	5624
2007	19	111	5646	5536
2008	20	237	5628	5392
2009	21	353	5597	5244
2010	22	458	5547	5088
2010	23	513	5511	4997

Table 7.1-13: Compression in the web concrete verification

7.1.5 Reinforcement layout

Some basic rules of detailing for structural members should be respected when designing reinforcement layout, in addition to the static requirements.

Firstly, at least minimum reinforcement area shall be provided. For this example, the provisions relative to linear members may be applied as a consequence of the chosen calculation models; the upper slab and the foundation may be treated as beam elements, whereas the uprights as columns. The criteria described below were respected to attain minimum areas for longitudinal and transverse reinforcement.

– Beams (Upper slab and foundation)

Longitudinal reinf.:	$\geq 0.0015\ b\ d$	for steel Grade 500;
Transverse reinf.:	$\rho_w = \frac{A_{sw}}{s\ b_w\ \sin\alpha} \geq 0.12\%$	for steel S500 and concrete C30/37;
Spacing of shear reinf.:	$s_{max} \leq \{0.6\ d\ ;\ 300\ mm\}$	for the considered range of web concrete compression;

– Columns (Uprights)

Vertical reinf.:	$A_s \geq 0.15\ N_{Sd} / f_{yd}$	with a minimum bar diameter of 12 mm
Transverse bar diam.:	$\varnothing_t \geq \varnothing_l /4\ ,\ 5mm$	where $\varnothing_l$ is the diameter of vertical diameter
Spacing of shear reinf.:	$s_{max} \leq \{12\ \varnothing_l\ ;b;\ 300\ mm\}$	where *b* is the smallest dimension of concrete section.

As second step, one has to assess the design length to bond the bar in concrete, whether for anchorage or overlap. The design value of the bond stress is evaluated with the following expression:

Copyright fib, all rights reserved. This PDF copy of fib Bulletin 54 is intended for use and/or distribution only within National Member Groups of fib.

$$f_{bd} = \eta_1\eta_2\eta_3 f_{ctd} = \begin{cases} 1.87\ \text{N/mm}^2 & \text{good bond conditions} \\ 2.67\ \text{N/mm}^2 & \text{bad bond conditions} \end{cases}$$

where:

f_{ctd} = 1.33 N/mm^2 design value of concrete tensile stress (for grade C30);
η_1 = 1.4 for intended bars;
η_2 = 1.0/0.7 good/bad bond conditions:
η_3 = 1.0 for bar diameter lesser of 32 mm

so that the basic length necessary for the transfer of the yield force of a bar of diameter ∅ results:

$$l_b = \frac{\varnothing}{4}\frac{f_{yd}}{f_{bd}} = \frac{434.8}{4f_{bd}}\varnothing \cong \begin{cases} 58\varnothing & \text{good bond conditions} \\ 83\varnothing & \text{bad bond conditions.} \end{cases}$$

The different values are relative to the position of each bar during concreting; good bond conditions may be referred to all the bars with an inclination of 45°–90° to the horizontal or with an inclination less than 45° to the horizontal, which are up to 250 mm from the bottom or at least 300 mm from the top of the concrete layer. So, with respect to the culvert, one should consider the upper reinforcement of both the slab and the foundation to be in bad bond condition, and all the other bars to be in good bond condition.

The design anchorage length $l_{b,net}$ can be calculated from the following equation:

$$l_{b,net} = \alpha_1\alpha_2\alpha_3\alpha_4\alpha_5 l_b \frac{A_{s,cal}}{A_{s,ef}} \tag{7.1-4}$$

with α_1 , α_2 , α_4 and α_5 assumed equal to 1.0 on the safety side, and α_3 evaluated considering the maximum adopted diameter (26 mm) and a straight bar, by means of:

$$\alpha_3 = 1 - 0.15\frac{c_d - \varnothing}{\varnothing} = 0.948 \qquad (c_d = \text{concrete cover})$$

thus the following operative value may be adopted for $l_{b,net}$:

$$l_{b,net} = 0.948 \cdot \begin{Bmatrix} 58\varnothing \\ 83\varnothing \end{Bmatrix} \cdot \frac{A_{s,cal}}{A_{s,ef}} = \frac{A_{s,cal}}{A_{s,ef}} \cdot \begin{Bmatrix} 55\varnothing \\ 79\varnothing \end{Bmatrix} \tag{7.1-5}$$

with $A_{s,cal}$ and $A_{s,ef}$ area of reinforcement required by calculation and effectively provided respectively. Two values are obtained with respect to the bond condition.

The design lap length is evaluated with Eq. (7.1-6):

$$l_0 = \alpha_1\alpha_3\alpha_4\alpha_5\alpha_6 l_b \frac{A_{s,cal}}{A_{s,ef}} = \frac{A_{s,cal}}{A_{s,ef}} \cdot \begin{Bmatrix} 110\varnothing \\ 158\varnothing \end{Bmatrix} \tag{7.1-6}$$

where:

α_1, α_3, α_4, α_5: calculated as above;

Copyright fib, all rights reserved. This PDF copy of fib Bulletin 54 is intended for use and/or distribution only within National Member Groups of fib.

$\alpha_6 = 2$: supposing that more than 50% of the total reinforcement is lapped.

It can be noted that a significant reduction of the design lengths $l_{b,net}$ and l_0 may be achieved if the amount of reinforcement provided is much greater than the requested one; so a minimum length shall be established, with respect to the following limits:

$l_{b,min} < \max\{0.3\, l_b ; 10\varnothing ; 100 \text{ mm}\}$; $l_{0,min} < \max\{0.3\, \alpha_6\, l_b ; 15\varnothing ; 200 \text{ mm}\}$.

In the design of secondary reinforcement one may provide a percentage of the primary one (20% for distributed loads) in order to cover the real two-dimensional behaviour, but, at least a minimum amount of reinforcement shall be arranged to avoid cracking by restrained shrinkage; the latter should be calculated by means of the following expression:

$$A_{s,min} = k_c\ k\ f_{ct,max}\ \frac{A_{ct}}{\sigma_{s2}} \qquad (7.1\text{-}7)$$

where the following values are considered, if pure tension is assumed to be active:

$f_{ct,max}$ = 2.39 N/mm^2:	upper fractile of concrete tensile strength for grade C30 at the moment when the first crack is expected to appear; because principal intrinsic imposed deformation is due to heat-curing, a time of 3 days is considered as reference to calculate concrete tensile strength;
σ_{s2} = 240 N/mm^2:	tension on steel limited to 240 N/mm^2 in order to satisfy the crack width limits if a bar diameter of 20 mm is adopted.
A_{ct} = 0.7 – 0.9 m^2:	area of the concrete tension zone coincident with a rectangular section with a breadth 0f 1.0 m and a depth equal to the thickness of each structural member (0.7 for the upper slab and uprights, 0.9 for the foundation);
k = 0.56 – 0.5 :	corrective factor equal to 0.56 for h = 0.7 m and to 0.5 for h = 0.9 m, in case of intrinsic imposed deformation on rectangular section;
k_c = 1.0 :	corrective factor that accounts for the scheme of tensile stress distribution, equal to 1.0 for pure tension.

So, for the structural member considered, the following quantities may be calculated:

- Upper slab and uprights: $A_{s,min} = 1 \times 0.56 \times 2.39 \times 0.7/240 \times 10^5 = 390.4$ mm^2/m;
- Foundation: $A_{s,min} = 1 \times 0.5 \times 2.39 \times 0.9/240 \times 10^5 = 448.1$ mm^2/m;

that shall be arranged in two layers. So for the upper slab and the uprights, a 20 mm diameter bar was disposed with a transverse spacing of 150 mm, whereas in the foundation a 22 mm bar diameter is provided with the same spacing.

Particular attention must be reserved to the corner zones, to complete design of primary reinforcement; in fact, in case of closing moment, the main reinforcement exercises a splitting effect on the concrete which may lead to local crushing; these forces shall be equilibrated by an additional reinforcement put within the node. By reference to Fig. 7.1-6 it is possible to determine the minimum diameter of the mandrel to bend the bars in order to avoid a reduction of the internal lever arm z (equal to 0.8 d).

Copyright fib, all rights reserved. This PDF copy of fib Bulletin 54 is intended for use and/or distribution only within National Member Groups of fib.

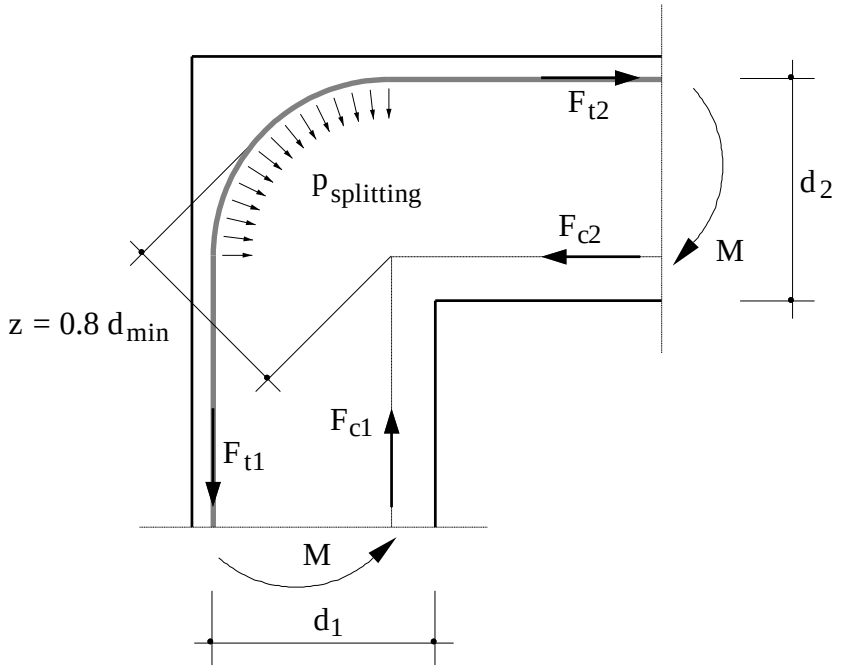


Fig. 7.1-6: Internal lever arm in the corner

The splitting force may be designed approximately for 25% of radial pressure produced by the main reinforcement, i.e.:

$$p_{splitting} = 0.25 \frac{F_{t1} + F_{t2}}{2} \frac{1}{0.8 d_{min}} \tag{7.1-8}$$

Considering the left corner between the upper slab and the upright, the tensile forces F_{t1} and F_{t2} are calculated multiplying the reinforcement areas, respectively from Table 7.1-5 and 7.1-10, with the design tensile strength f_{yd} . Being in this case $d_1 = d_2$, the total splitting force is evaluated as product of Eq. (7.1-8) for bent length:

$$F_{splitting} = p_{splitting} \frac{\pi}{2} 0.8 d_{min} = 0.25 \cdot \frac{22.6 + 43.4}{2} \cdot 434.78 \cdot \frac{\pi}{2} \cdot 10^{-1} = 563.43 \text{ kN}$$

from which the following steel area results:

$$A_{s,splitting} = \frac{F_{splitting}}{f_{yd}} = \frac{563.45}{434.78} \cdot 1000 = 1296 \text{ mm}^2$$

that was arranged by means of 10 bar with a diameter of 14 mm, disposed as indicated in Fig. 7.1-7.

Similarly, for the corner between the foundation and the uprights, the necessary area for splitting action results:

$A_{s,splitting} = 1567 \text{ mm}^2$.

Fig. 7.1-8 represents the main reinforcement layout for the culvert in the upper slab, in the foundation and only in the left upright, the right one being equally reinforced.

Copyright fib, all rights reserved. This PDF copy of fib Bulletin 54 is intended for use and/or distribution only within National Member Groups of fib.

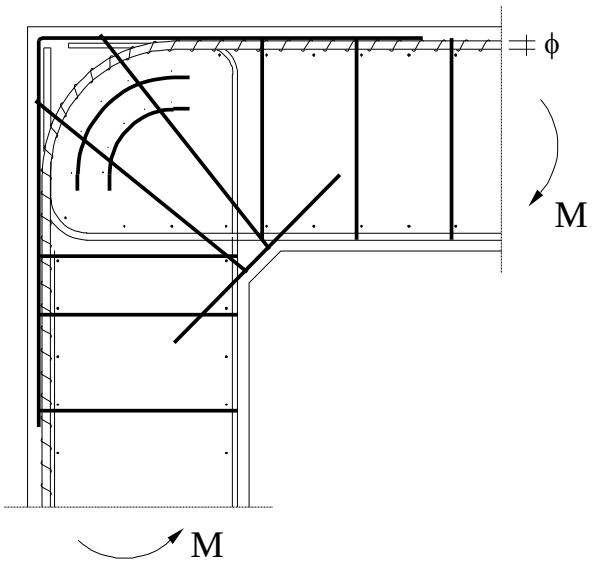


Fig. 7.1-7: Local reinforcement in the node to equilibrate the splitting action

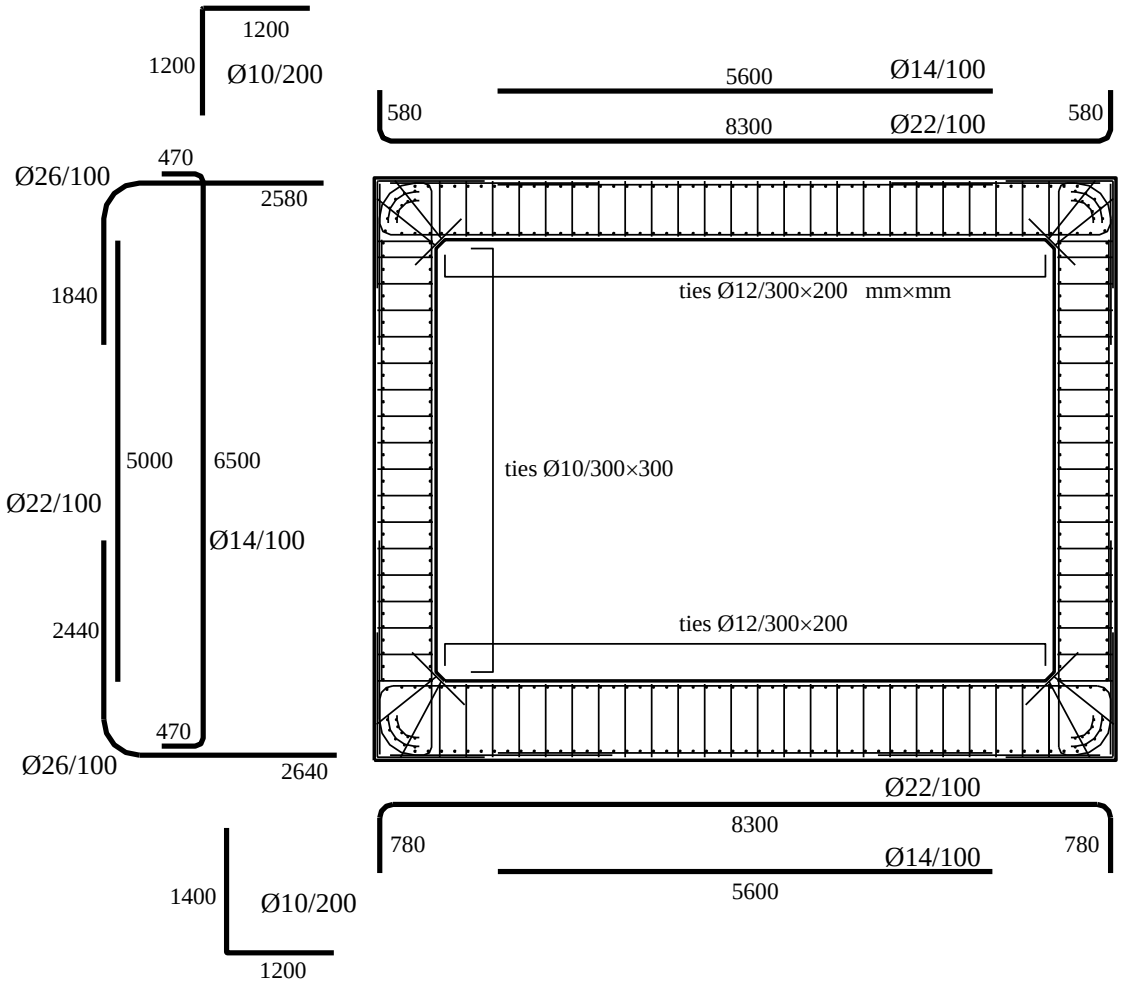


Fig. 7.1-8: Reinforcement layout

Copyright fib, all rights reserved. This PDF copy of fib Bulletin 54 is intended for use and/or distribution only within National Member Groups of fib.

7.1.6 Verification at serviceability limit state

The verification at serviceability limit state is related to the following conditions:
- stress limitation;
- crack widths;
- deformations.

Different combination of actions should be considered, according to the provisions of the adopted code; in this example, the adopted combinations are listed below together with the symbolic presentation:
- rare combination: $G_k + Q_k$
- quasi-permanent combination: $G_k + \Psi_2 Q_k$.

(1) Stress limitation

One has to check that, under the rare combination, the maximum concrete compressive stress does not exceed 0.6 f_{ck} = 18 N/mm^2 and that the tensile stress in ordinary reinforcement does not exceed 0.8 f_{yk} = 400 N/mm^2.

The diagrams of combined actions according to the rare combination are reported in Fig. 7.1 - 9, with respect to only bending moment and axial force.

The extreme stresses for the upper slab, the foundation and one of the two uprights are summarized in Table 7.1-14. The same sections investigated at ULS and the effective arranged reinforcement are considered.

These stresses, due to the SLS considered, were calculated by the modular ratio method.

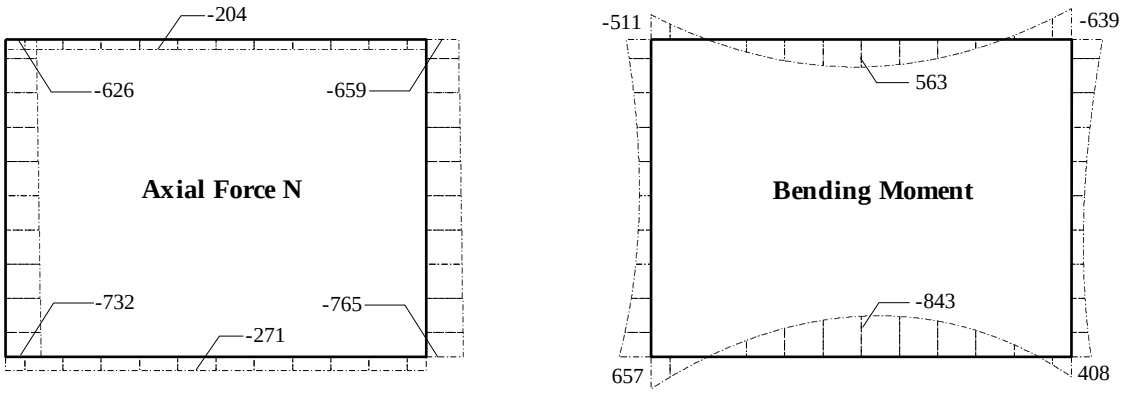


Fig. 7.1-9: Internal actions from FEM model at SLS in the rare combination

Copyright fib, all rights reserved. This PDF copy of fib Bulletin 54 is intended for use and/or distribution only within National Member Groups of fib.

Element	Node	Nk [kN]	Mk [kNm]	b [m]	h [m]	$A_{1,s}$ [mm^2]	$A_{2,s}$ [mm^2]	x [m]	σ_c [N/mm^2]	σ_s [N/mm^2]
4001	23	-204	-511	1.0	0.7	5309	3801	0.18	-9.1	142.7
4007	29	-204	563	1.0	0.7	3801	1539	0.16	-12.1	220.4
4012	35	-204	-639	1.0	0.7	5309	3801	0.17	-11.3	182.9
1001	1	-271	657	1.0	0.9	5309	3801	0.22	-7.7	133.0
1007	7	-271	-843	1.0	0.9	3801	1539	0.19	-11.9	245.4
1012	13	-271	408	1.0	0.9	5309	3801	0.24	-4.9	74.2
2001	1	-732	-657	1.0	0.7	3801	1539	0.19	-14.3	199.5
2002	14	-721	-538	1.0	0.7	3801	1539	0.21	-11.7	149.9
2003	15	-710	-407	1.0	0.7	3801	1539	0.23	-8.8	96.3
2004	16	-699	-316	1.0	0.7	3801	1539	0.26	-6.8	60.1
2005	17	-688	-260	1.0	0.7	3801	1539	0.29	-5.5	39.9
2006	18	-678	-239	1.0	0.7	3801	1539	0.31	-5.0	33.1
2007	19	-667	-250	1.0	0.7	3801	1539	0.29	-5.2	37.8
2008	20	-656	-290	1.0	0.7	3801	1539	0.26	-6.2	54.0
2009	21	-645	-357	1.0	0.7	3801	1539	0.23	-7.7	82.2
2010	22	-635	-449	1.0	0.7	3801	1539	0.21	-9.8	121.8
2010	23	-626	-511	1.0	0.7	3801	1539	0.20	-11.2	148.9

Table 7.1-14: Extreme stress on concrete and tension steel

where $A_{1,s}$ and $A_{2,s}$ are respectively the tension and compression reinforcement area. It can be noted that, in all the sections, verification is met.

(2) Crack width

The quasi-permanent combination of action is adopted to evaluate crack width, with a Ψ_2 coefficient equal to 0.6 as specified in the relevant code. The nominal width value relative to exposure class 2 is of 0.30 mm for reinforced concrete member with respect to both appearance and durability.

In Fig. 7.1-10 are sketched the diagrams of axial force and bending moment for the quasi-permanent combination.

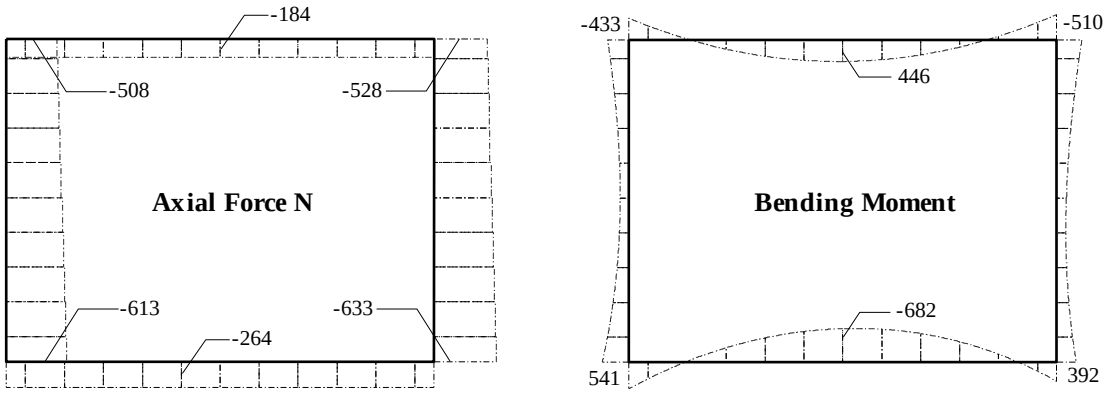


Fig. 7.1-10: Internal actions from FEM model at SLS in the quasi-permanent combination

Copyright fib, all rights reserved. This PDF copy of fib Bulletin 54 is intended for use and/or distribution only within National Member Groups of fib.

Crack width is calculated by means of the following expression:

$$w_k = l_{s,max}\left(\varepsilon_{s2} - \beta\,\varepsilon_{sr2} - \varepsilon_{cs}\right) \qquad (7.1\text{-}9)$$

where:

$l_{s,max} = \dfrac{\varnothing_s}{3.6\rho_{s,ef}}$ length over which slip between concrete and steel occurs;

$\varnothing_s$ diameter of the steel bar;

$\rho_{s,ef} = \dfrac{A_s}{A_{c,ef}}$ effective reinforcement ratio referred to concrete area in tension;

$\varepsilon_{s2} = \dfrac{\sigma_{s2}}{E_s}$ steel strain at the crack;

$\varepsilon_{sr2} = \dfrac{\sigma_{sr2}}{E_s}$ steel strain at the crack under forces causing f_{ctm} within $A_{c,ef}$;

$\beta = 0.38$ empirical factor to assess averaged strain within $l_{s,max}$;

$\varepsilon_{cs} = -0.385 \cdot 10^3$ concrete strain due to shrinkage.

Referring to the three sections of upper slab and foundation, and considering just two sections for the upright at nodal zone (higher bending moments), we can obtain Table 7.1-15 where the principal results are reported.

Elem.	Node	Nk [kN]	Mk [kNm]	M_{crack} [kNm]	b [m]	h [m]	$A_{1,s}$ [mm^2]	$A_{2,s}$ [mm^2]	x [m]	ϕ [mm]	$\rho_{s,ef}$ [-]	σ_{s2} [N/mm^2]	σ_{sr2} [N/mm^2]	$l_{s,max}$ [mm]	$\varepsilon_{s2} - \beta\varepsilon_{sr2}$ [x 1000]	w_k [mm]
4001	23	-184	-433	-259	1.0	0.7	5309	3801	0.18	26	0.044	119.6	65.4	163.2	0.47	0.14
4007	29	-184	446	259	1.0	0.7	3801	1539	0.16	22	0.033	171.0	90.3	184.9	0.68	0.20
4012	35	-184	-510	-259	1.0	0.7	5309	3801	0.18	26	0.044	143.6	65.4	163.2	0.59	0.16
1001	1	-264	541	433	1.0	0.9	5309	3801	0.22	26	0.044	105.9	80.3	163.2	0.38	0.12
1007	7	-264	-682	-433	1.0	0.9	3801	1539	0.19	22	0.033	192.5	110.9	184.9	0.75	0.21
1012	13	-264	392	433	1.0	0.9	5309	3801	*section uncracked*							
2001	1	-613	-541	-309	1.0	0.7	3801	1539	0.19	22	0.033	162.6	65.4	184.9	0.69	0.20
2010	23	-508	-433	-297	1.0	0.7	3801	1539	0.20	22	0.033	128.2	70.9	184.9	0.51	0.16

Table 7.1-15: Cracks opening evaluation

It can be noticed that the crack width limit of 0.3 mm was respected.

(3) Deformation

Deformation limitation is carried out to control the maximum vertical deflection for passengers comfort. The limit values δ/L (deflection/span Length) are given by EN 1991-2 as a function of the span and the train speed. For the analysed structure, it may be considered that the earth cover behaves like a rigid body so that it undergoes the same deflection of upper slab. The limit value for maximum vertical deflection is calculated considering a span of 7.7 m (uprights spacing) and a train speed over 280 km/h and, according to the provisions of the code, it results:

$$\frac{\delta}{L} = \frac{1}{1500}$$

Copyright fib, all rights reserved. This PDF copy of fib Bulletin 54 is intended for use and/or distribution only within National Member Groups of fib.

that should be multiplied by a factor 2 for structure with 1 span; finally, the following limit may be achieved:

$$\frac{\delta_{lim}}{L} = \frac{2}{1500} = \frac{1}{750}.$$

As a consequence of the transient nature of this event, the elastic deflection, calculated by the FEM model, is relative to the only live load; the check shall be performed loading only one track. Fig. 7.1-11 represents the applied load on FEM model (half of the train load plus the dynamic allowance together with the deformed shape of the structure).

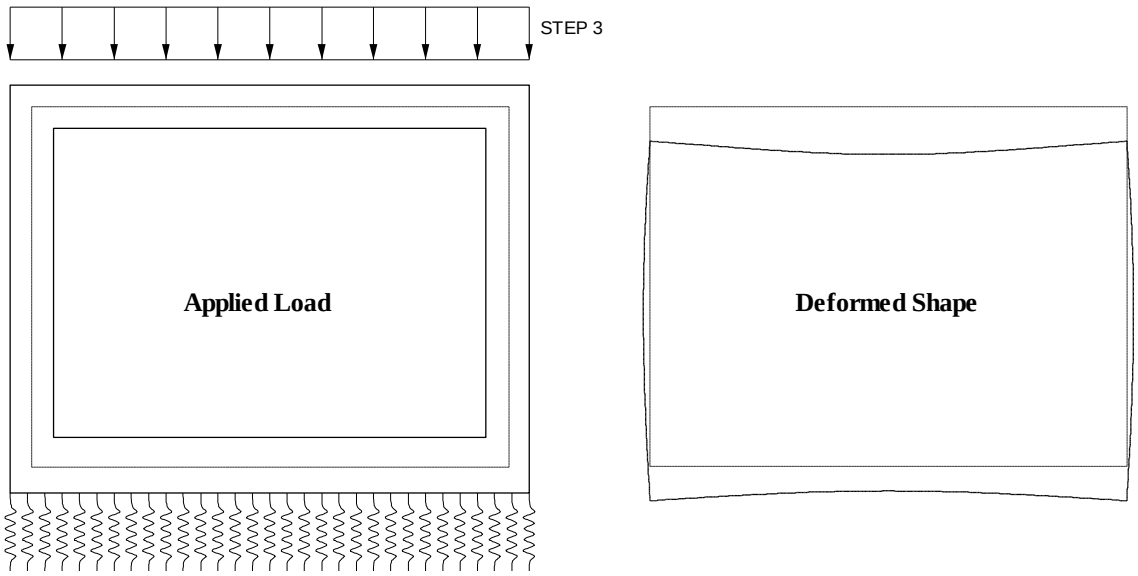


Fig. 7.1-11: Applied load and deformed shape for deflection check

According to the MC90, the deformations should be calculated from the curvatures through the principle of virtual work. For the sake of simplicity, the simplified method may be followed; it is based on a bilinear relationship between load and deflection, by applying the following expression:

$$\delta = \left(\frac{h}{d}\right)^3 \eta \left(1 - 20\rho_{cm}\right) \delta_c \qquad (7.1\text{-}10)$$

where:

δ_c = 0.0035 m	maximum elastic deflection of upper slab calculated with the FEM analysis;
η = 3.64	correction factor for cracking and creep effects;
ρ_{cm} = 0.0029	geometrical mean percentage of compressive reinforcement;
h = 0.700 m	depth of the upper slab;
d = 0.655 m	distance of centroid of reinforcement from the extreme concrete compressive fibre.

By applying the (7.1 - 10), for the node 29 of FEM model, the following value is obtained:

δ = 0.0146 m. (7.1-11)

The previous value shall be corrected by subtracting the creep influence, included in the η coefficient; in fact it is possible to estimate that the ordinary frequency of railway traffic

Copyright fib, all rights reserved. This PDF copy of fib Bulletin 54 is intended for use and/or distribution only within National Member Groups of fib.

corresponds, in the lifetime of the structure, to an equivalent application of the train as a sustained load for a period of two years. So, the amount of the deflection due to creep can be calculated by means of the following expression:

$$\delta_{c,creep} = \phi\, \delta_c = 1.69 \cdot 0.0035 = 0.0059 \text{ m}$$

where $\phi = 1.69$ is the creep coefficient calculated for a period of two years.

Finally, the obtained value should be subtracted from Eq. (7.1-11) so that the effective deflection results:

$$\delta_{effective} = \delta - \delta_{creep} = 0.0146 - 0.0059 = 0.0087$$

which leads to a deflection/span ratio of:

$$\frac{\delta_{effective}}{L} = \frac{0.0087}{7.70} = \frac{1}{885}$$

with a result that is lower than the corresponding limit.

References to Section 7.1

CEB Bulletin 141 (1982), *Manual on Bending and Compression*. Comité Euro-international du Béton, Lausanne, Switzerland.

CEB Bulletin 213/214 (1993), *CEB-FIP Model Code 1990*, published by Thomas Telford Ltd., UK. ("MC90")

EN 1991-2: *Traffic loads on bridges.*

EN 1992-1-1, Eurocode 2: *Design of concrete structures.*

Copyright fib, all rights reserved. This PDF copy of fib Bulletin 54 is intended for use and/or distribution only within National Member Groups of fib.

7.2 Slabs

by Giuseppe Mancini

As a two-dimensional member a prestressed concrete slab is analysed. The actual structure is described in the following section.

7.2.1 Description of the structure

The design example proposed in this section is related to a railway bridge deck made up by a continuous slab on three spans with two series of prestressing tendons (longitudinal and transverse prestressing). The slab is designed in category A (see Eurocode 2, Part 2, Table 4.118) for fatigue. The deck rests on abutments and circular piers and has a overall breadth of 13.60 m with two side-walks of 1.40 m width, two ballast retaining walls and, in the middle, two track spacing of 5.0 m. The slab presents a constant thickness of 1.50 m for a central zone 7.0 m width, and is tapered towards the extremity with a final height of 0.6 m. Figs. 7.2-1 and 7.2-2 represent the principal geometric dimensions of the slab bridge and support scheme.

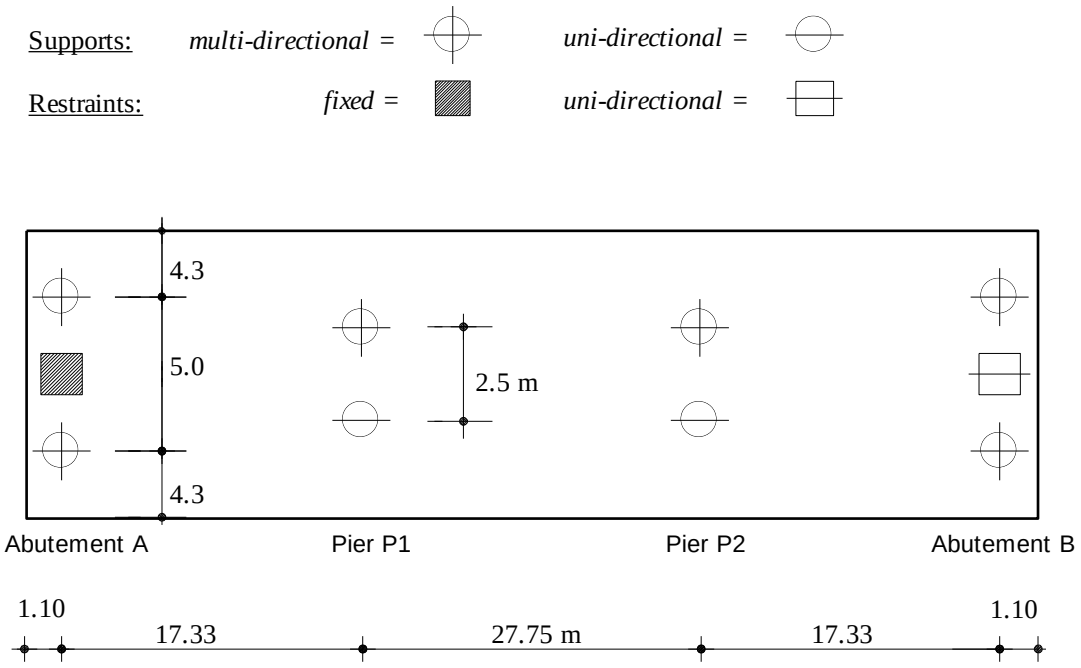


Fig. 7.2-1: Plan view of the structure and supports' scheme

(1) Material properties

The following material properties were considered:

– Concrete:

Grade 35/45:	f_{ck} =	35.00 N/mm^2;
compressive design strength:	f_{cd} =	23.30 N/mm^2;
compressive resistance for uncracked zones:	f_{cd1} =	17.10 N/mm^2;
compressive resistance for cracked zones:	f_{cd2} =	12.00 N/mm^2;

Copyright fib, all rights reserved. This PDF copy of fib Bulletin 54 is intended for use and/or distribution only within National Member Groups of fib.

mean value of tensile strength:	f_{ctm} =	3.23 N/mm^2;
modulus of elasticity:	E_c =	29.70 · 10^3 N/mm^2;
shear modulus:	G =	12.40 · 10^3 N/mm^2
Poisson ratio:	ν =	0.20

– Prestressing steel, (strands ∅ 0.6”):

0.1% proof–stress	$f_{p0.1k}$ =	1600 N/mm^2
total elongation at maximum load:	ε_{pu} >	35 ‰
modulus of elasticity:	E_p =	195.0 · 10^3 N/mm^2;

– Reinforcing steel:

Grade 500:	f_{yk} =	500.0 N/mm^2;
design strength:	f_{yd} =	434.8 N/mm^2;
modulus of elasticity:	E_s =	200.0 · 10^3 N/mm^2.

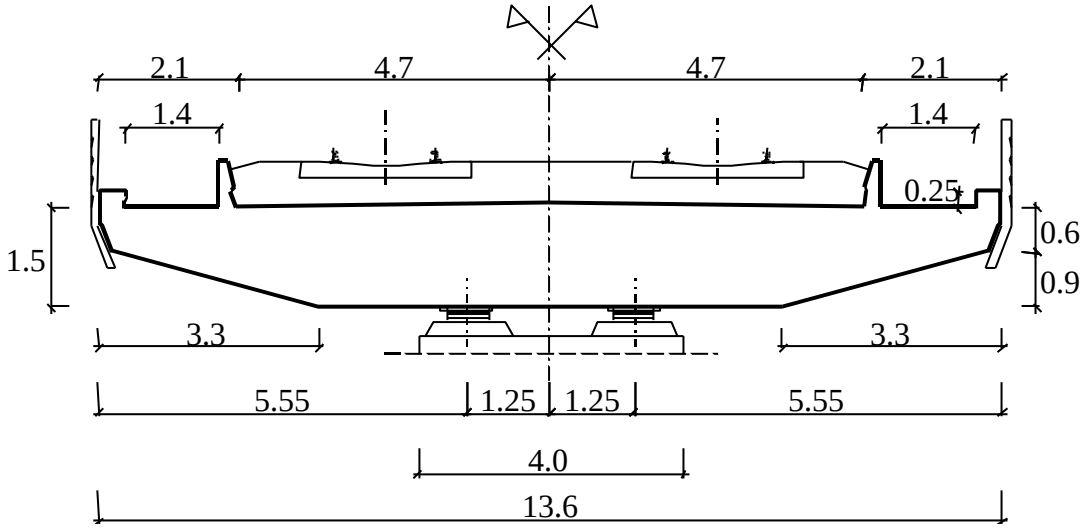


Fig. 7.2-2: Geometric dimensions of bridge cross section

(2) Concrete cover

For the environmental conditions, Exposure Class 2 may be considered (humid environment with frost: exterior components exposed to frost).

The minimum concrete cover for Class 2 is equal to 25 mm, which should be added to the tolerance value of 10mm; as a consequence the nominal value for concrete cover results:

$c_{nom} = c_{min} + 10 = 25 + 10 = 35$ mm

adopted in the calculations.

7.2.2 Structural model

To evaluate the internal actions of the structure a linear FEM analysis was performed adopting shell elements to represent the reinforced concrete slab; this kind of element takes into account all of the slab and plate components as well as the out-of-plane shear forces. The

Copyright fib, all rights reserved. This PDF copy of fib Bulletin 54 is intended for use and/or distribution only within National Member Groups of fib.

thickness of shell elements was assumed to be constant for the inner zone of the slab and stepped to accommodate the tapered extremity. In Figs. 7.2-3 and 7.2-4 the FEM model is shown and the different thicknesses of the elements are also reported.

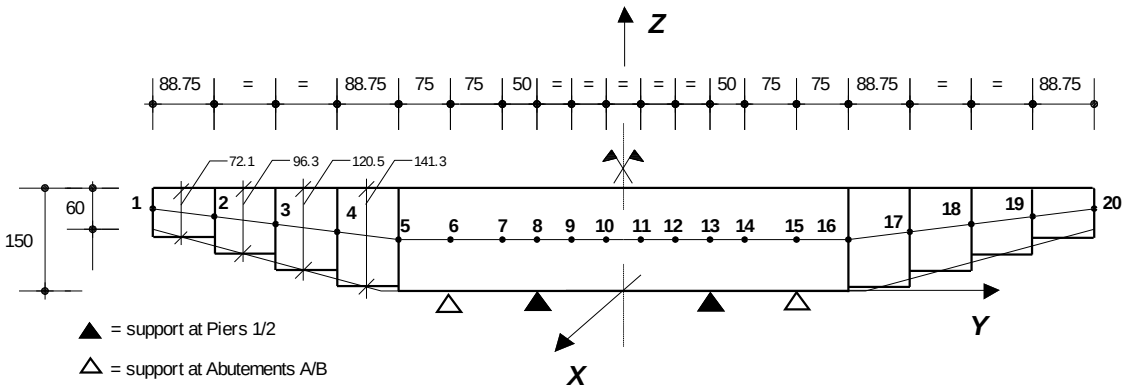


Fig. 7.2-3: Transverse view of FEM model

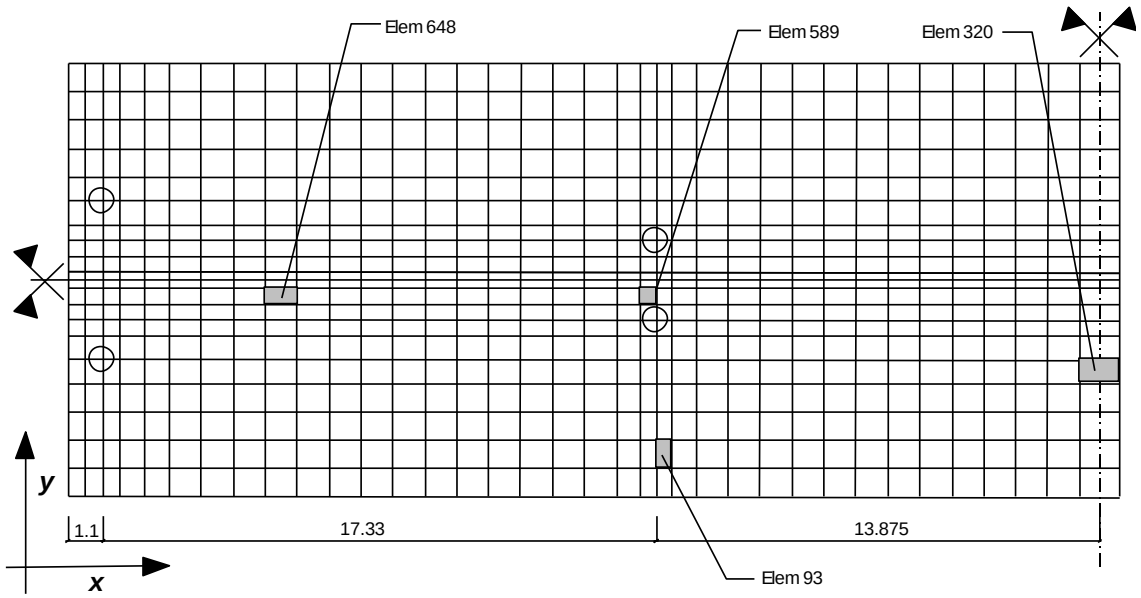


Fig. 7.2-4: Plan of FEM model and considered elements

The adopted shell elements are oriented with the following guidelines:

- local axis 2 is oriented as global axis Y of the deck;
- local axis 3 is oriented in the opposite direction of global axis X of the deck;
- local axis 1 is oriented as global axis Z of the deck.

Positive forces for FEM program output are presented in Fig. 7.2-5:

Copyright fib, all rights reserved. This PDF copy of fib Bulletin 54 is intended for use and/or distribution only within National Member Groups of fib.

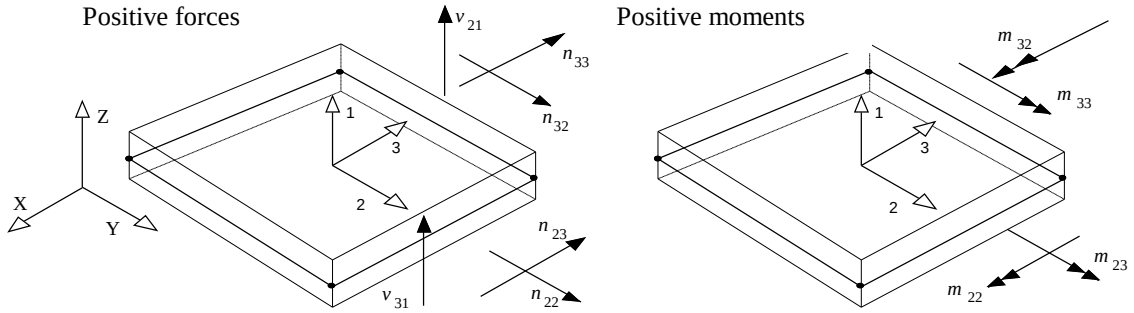


Fig. 7.2-5: Positive forces for FEM elements

(1) Restraints

The external restraints were introduced in the FEM model considering their real geometric dimensions; thus, few nodes were restrained by means of spring elements in order to represent only an individual restraint or support. Fig. 7.2-6 shows a symbolic notation for the external restraints with the nodes involved.

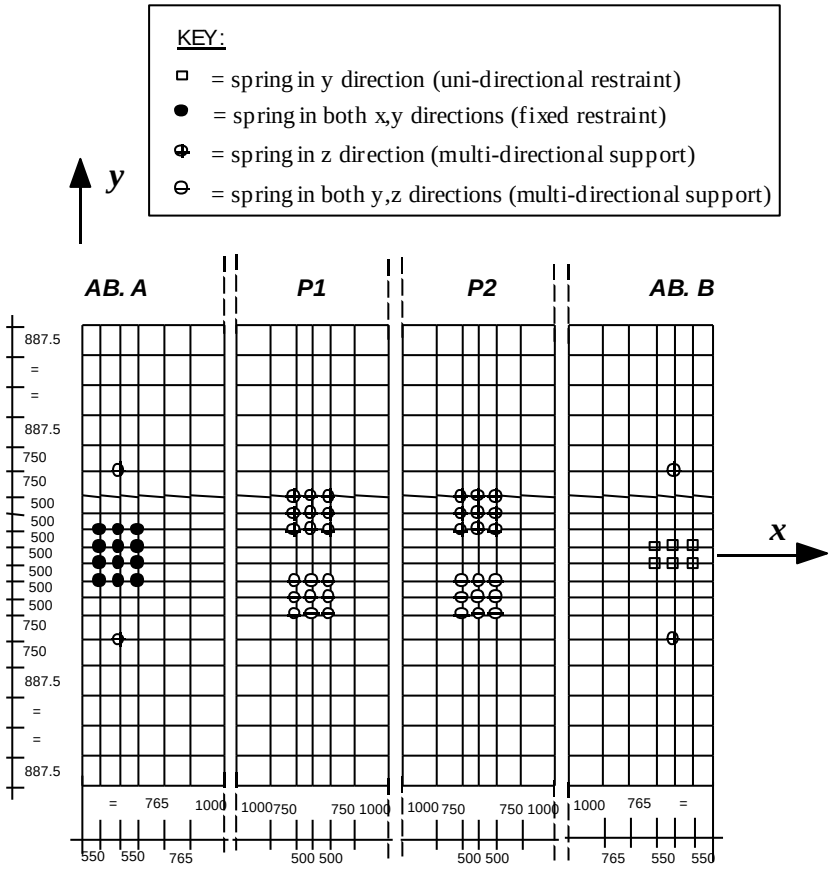


Fig. 7.2-6: External restraints on the FEM model (dimensions in millimetres)

Copyright fib, all rights reserved. This PDF copy of fib Bulletin 54 is intended for use and/or distribution only within National Member Groups of fib.

The elastic constant of the spring restraining elements is calculated to have the same stiffness of the substructure (abutments or piers) on which the slab is rested. For the *x* and *y* directions, it may be assumed that the pier, or the abutment front wall, behaves like a single column fixed at the base and free at his top, so that the relevant $K_{x/y}$ stiffness can be calculated as:

$$K_{x/y} = \frac{3EI}{H^3}$$

where E is the Young modulus, I the inertia and H the height of the column. For the vertical direction, the intrinsic stiffness of pot-bearing is assumed, considering the substructure vertical behaviour to be rigid.

For the sake of simplicity, the calculus of the relevant stiffness is omitted and the final values of the spring constants are reported in Table 7.2-1 .

It can be noted that the previous values refer to the overall stiffness of the restraint, thus the elastic constant of any individual spring element may be obtained by dividing the K values of Table 7.2 -1 by the number of element representing the restraint or the supports.

Location	$K_{x,tot}$ 10^6 kN/m	$K_{y,tot}$ 10^6 kN/m	$K_{z,tot}$ 10^6 kN/m
Abutment A	9.55	178.80	10.02
Pier P1	-	4.74	11.61
Pier P2	-	2.66	11.61
Abutment B	-	2.78	10.02

Table 7.2-1: Stiffness for restraining elements

(2) Prestressing forces

Two rows of prestressing tendons are arranged (in longitudinal and transverse directions) in order to avoid any tensile stress in concrete at service (required by railway code). The initial tensile stress of tendon is: $\sigma_{po,max} = 0.85\, f_{p\,0.1k} = 0.85 \cdot 1600 = 1360$ N/mm^2. The number of tendons is 39 for the longitudinal direction and 64 for the transverse one. Each tendon is built up with 19 strands ∅ 0.6" having an area of 139 mm^2.

Fig. 7.2-7 presents the tendon layout for a half deck, being symmetrically disposed.

Copyright fib, all rights reserved. This PDF copy of fib Bulletin 54 is intended for use and/or distribution only within National Member Groups of fib.

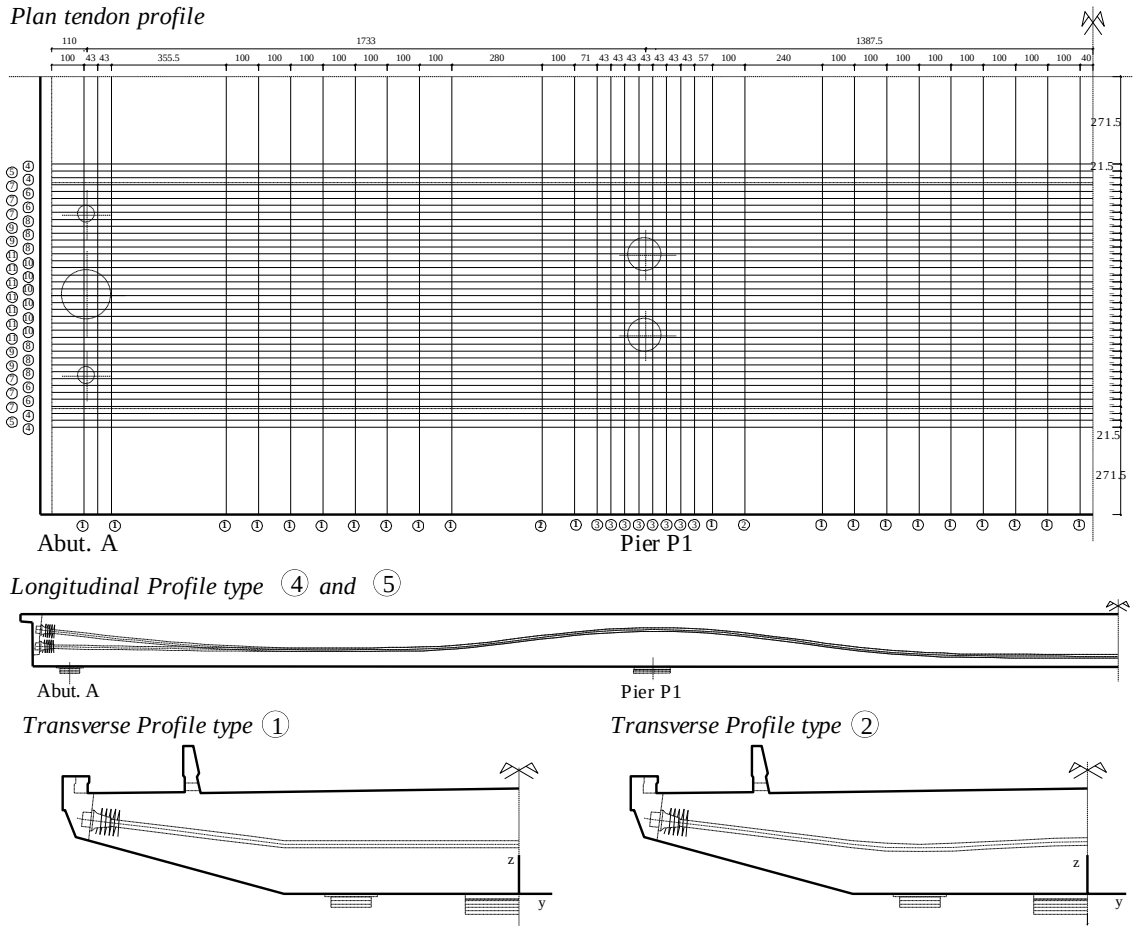


Fig. 7.2-7: Plan and principal section of tendon layout

Immediate losses of prestressing due to friction were evaluated by means of the following expression:

$$\sigma_{po}(x) = \sigma_{po,max} \cdot e^{-\mu(\alpha + k\,x)}$$

with:

$\mu = 0.19$	coefficient of friction between the tendons and their sheathing;
$k = 0.01$ rad/m	unintentional angular deviation.

Prestressing has to be introduced in the FEM model in order to calculate the hyperstatic actions that arise in the structural scheme. Considering prestressing as an external load, it is possible to introduce it by means of two inclined forces at anchorages (representing actions at the extremity) and by means of a system of equivalent loads along the tendon's profile (representing tendon curvature and losses due to friction): these actions per tendon, should be applied consistently at the nodes of FEM model.

The equivalent loads may be calculated by subdividing the tendon profile into elementary segments and evaluating the internal actions which are able to equilibrate the external ones due to end actions deriving from the prestressing.

Copyright fib, all rights reserved. This PDF copy of fib Bulletin 54 is intended for use and/or distribution only within National Member Groups of fib.

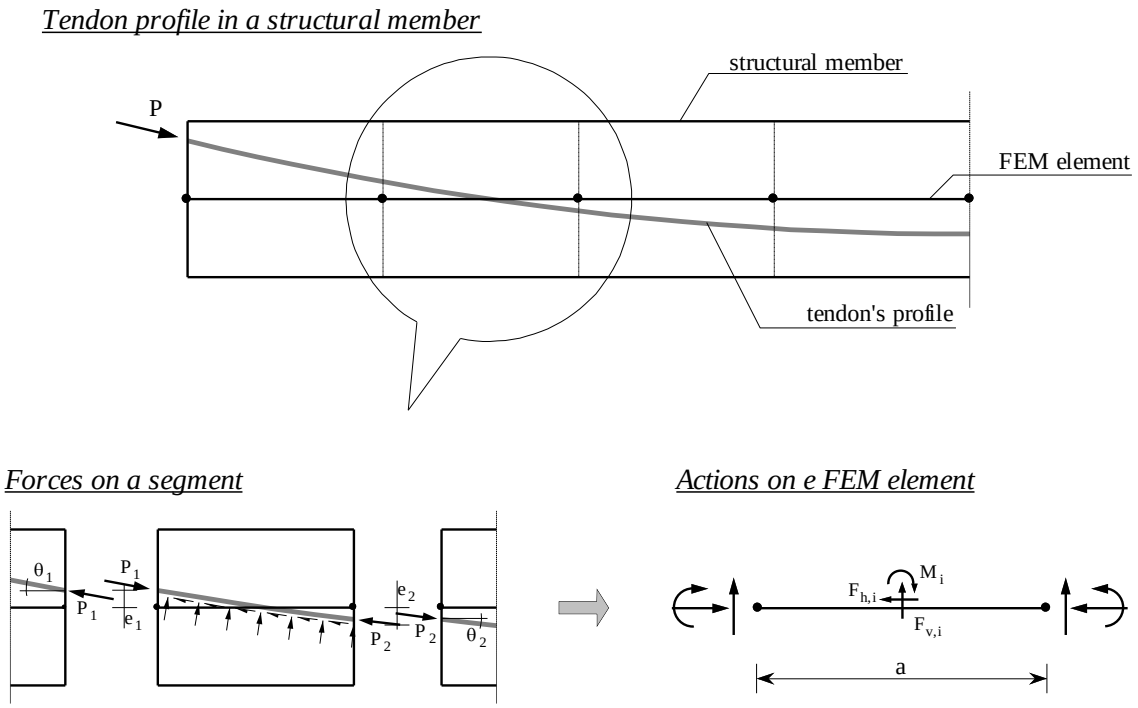


Fig. 7.2-8: Effect of prestressing on a segment and equivalent loads

Fig. 7.2-8 represents the forces acting on a segment of concrete due to a curved prestressing tendon; if the inclination of the cable changes from θ_1 to θ_2 while the prestress force changes from P_1 to P_2 due to friction, the equilibrating vertical and horizontal forces in the i-segment result:

$$F_{v,i} = P_2 \sin\theta_2 - P_1 \sin\theta_1 \quad ; \quad F_{h,i} = P_2 \cos\theta_2 - P_1 \cos\theta_1$$

while the balancing moment is:

$$M_i = (P_2 \cos\theta_2 \, e_2 + P_1 \cos\theta_1 \, e_1) - (P_2 \sin\theta_2 + P_1 \sin\theta_1) \cdot a/2.$$

The above procedure should be repeated for all the segments. It can be noticed that the forces at the end of each segment extremity are the same with opposite signs if the right or the left segment is considered; these forces cancel out themselves with the exception at anchorages. Finally, for each tendon, the forces at the extremity of the cable plus the equilibrating system for each segment, shall be introduced in the FEM model.

The choice of the position of the elementary segments is relative to the kind of element adopted in the FEM model. If beam elements are used, it is possible to introduce a point load (or moment) whether along the element body or at nodes, consequently the segment extremities may be placed indifferently at nodes or at the middle of the element. With shell elements, only nodal forces can be considered so that it is necessary to place segment extremities within two sequential nodes. Furthermore, due to the two-dimensional scheme, one has to consider the transverse position of the tendon that, in general, do not coincide with a nodal alignment. As simple rule, the indications given in Fig. 7.2-9 may be followed.

Copyright fib, all rights reserved. This PDF copy of fib Bulletin 54 is intended for use and/or distribution only within National Member Groups of fib.

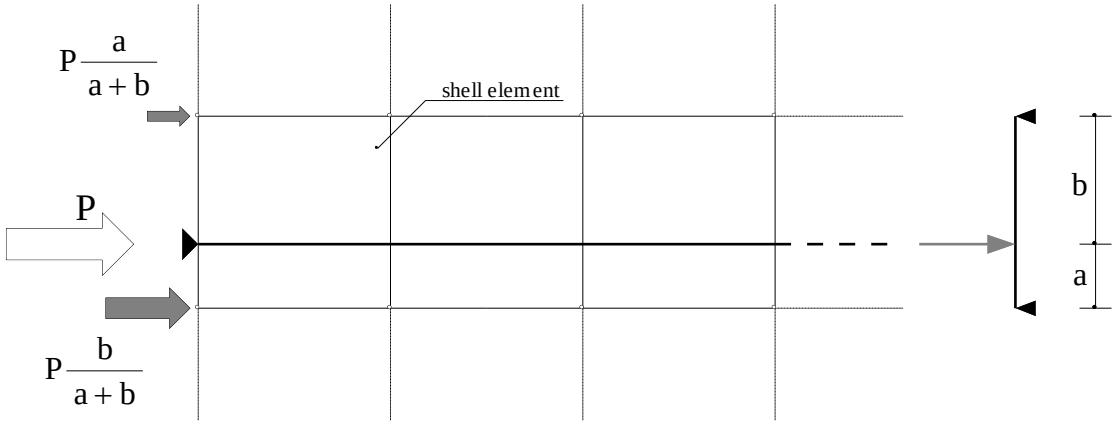


Fig. 7.2-9: Transverse distribution of prestressing

(3) Time-dependent prestressing losses

Time-dependent losses of prestress may be evaluated by means of the following equation:

$$\Delta\sigma_{p,c+s+r} = \frac{\varepsilon_{cs}(t_\infty, t_0)\, E_s + \Delta\sigma_{pr} + \alpha\, \phi(t_\infty, t_0)\,(\sigma_{cg} + \sigma_{cp0})}{1 + \alpha\, \frac{A_p}{A_c}\left[\left(1 + \frac{A_c}{I_c}\, z_{cp}^2\right)\left(1 + 0.8\, \phi(t_\infty, t_0)\right)\right]}$$

where:

$\Delta\sigma_{p,c+s+r}$: loss of initial prestress due to creep and shrinkage of concrete and relaxation of steel, between time t_0 and time t_∞;

t_0 = 28 days: age of concrete at prestressing time;

t_∞ = 25550 days: corresponding to a lifetime of 70 years;

$\varepsilon_{cs}(t_\infty,t_0)$: shrinkage strain at time t_∞, calculated from:

$\varepsilon_{cs}(t_\infty,t_0) = \varepsilon_{cs0} \cdot \beta_s(t_\infty - t_0) = -0.127 \cdot 10^{-3}$

where: $\varepsilon_{cso} = \varepsilon_s(f_{cm}) \cdot \beta_{RH}$ with:

$\varepsilon_s(f_{cm}) = [160 + 10\,\beta_{sc}(9 - f_{cm}/f_{cmo})] \cdot 10^{-6} = 0.000395$

f_{cm} = mean compressive strength of concrete at 28 days = f_{ck} + 8 N/mm^2;

f_{cmo} = 10 N/mm^2;

β_{sc} = 5 for rapid hardening cements;

$$\beta_{RH} = -1.55\left[1 - \left(\frac{RH}{100}\right)^3\right] = -1.018;$$

RH = 70 % relative humidity of the ambient atmosphere;

$$\beta_s(t_\infty - t_0) = \sqrt{\frac{t_\infty - t_0}{0.035 \cdot h^2 + t_\infty - t_0}} = 0.574$$

$h = (2A_c / u) = 1217$ mm notional size of member;

$A_c = 17.43 \cdot 10^6$ mm^2 gross section of the beam;

u = 28640 mm perimeter of the member in contact with the atmosphere;

$\phi(t_\infty,t_0)$: creep coefficient at time t_∞, calculated from:

$\phi(t_\infty,t_0) = \phi_0 \cdot \beta_c(t_\infty - t_0) = 1.5708$

where: $\phi_o = \phi_{RH} \cdot \beta(f_{cm}) \cdot \beta(t_0) = 1.598$ with

Copyright fib, all rights reserved. This PDF copy of fib Bulletin 54 is intended for use and/or distribution only within National Member Groups of fib.

$$\phi_{RH} = 1 + \frac{1 - RH/100}{0.1\sqrt[3]{h}} = 1.281;$$

$$\beta(f_{cm}) = \frac{5.3}{\sqrt{f_{cm}/f_{cmo}}} = 2.556;$$

$$\beta(t_0) = \frac{1}{0.1 + t_0^{0.2}} = 0.488$$

$$\beta_c(t_\infty - t_0) = \left(\frac{t_\infty - t_0}{\beta_H + t_\infty - t_0}\right)^{0.3} = 0.983 \quad \text{with}$$

$$\beta_H = 1.5\left[1 + (0.012\,RH)^{18}\right]h + 250 = 2155 > 1500 \rightarrow 1500.$$

If the improved prediction model of Chapter 3 is used, the following values for $\varepsilon_{cs}(t_\infty, t_0)$ and for $\phi(t_\infty, t_0)$ may be evaluated:

$$\bar{\varepsilon}_{cs}(t_\infty, t_0) = 182.62 \cdot 10^{-6} \quad ; \quad \bar{\phi}(t_\infty, t_0) = 1.5754$$

in good agreement with the previous one, at least for creep value.

$\Delta\sigma_{pr}$: loss of prestressing due to relaxation of steel calculated for a reduced initial tensile stress of $\sigma_p = \sigma_{pgo} - 0.3\,\Delta\sigma_{p,c+s+r}$ (where σ_{pgo} is the effective initial stress in tendons due to dead load and prestressing) and evaluated as percentage by the following formula:

$$\rho_t = \rho_{1000h}\left(\frac{t}{1000}\right)^{0.19} = \rho_{1000h} \cdot 3 \quad \text{where}$$

ρ_t = is the relaxation after t hours; for t > 50 years $\rho_{t.} = \rho_{1000h} \cdot 3$;
ρ_{1000h} = is the relaxation after 1000 hours evaluated from Fig. 7.2.10 ;

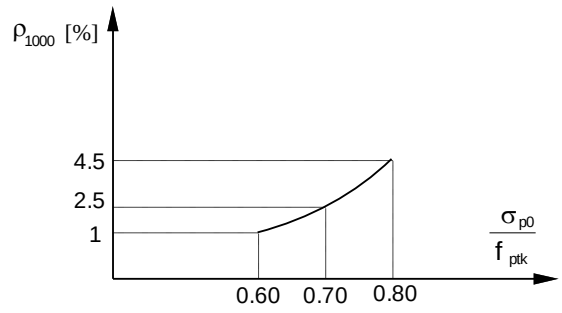


Fig. 7.2-10: Relaxation losses in % at 1000 hours for Class 2

$\sigma_{c.}$: stress on concrete at level of pretensioned steel due to self weight and permanent load;
σ_{cpo} : stress on concrete at level of pretensioned steel due to prestressing;
$\alpha = E_s/E_c$: modulus of elasticity ratio;
A_p : area of prestressing steel at the considered level;
A_c : area of concrete gross section;
I_c : inertia of concrete gross section;
z_{cp} : lever arm between centroid of concrete gross section and prestressing steel.

Copyright fib, all rights reserved. This PDF copy of fib Bulletin 54 is intended for use and/or distribution only within National Member Groups of fib.

Time-dependent losses of prestress should be calculated for each tendon along his profile so that a correct value may be used for each element. As a reference, the maximum values of prestressing losses, as percentage of initial steel tension, are:

longitudinal tendon: 19% at anchorage and 14% at pier axis;
transverse tendon: 18% at anchorage and 12% at midspan.

The effects of losses are taken into account with the same procedure used for the prestressing, but as actions of opposite signs.

7.2.3 Actions

The external loads applied on the structure should be evaluated according to the provisions of EN 1991-2, *Traffic loads on bridges*. As vertical train load the load model LM71 plus the load models SW (SW/0 and SW/2 respectively) were adopted with an α coefficient of 1.1. For the LM71, the four point loads were reduced in an equivalent uniform load by smearing their characteristic value Q_{vk} along the influence length so that a $q_{vk,1}$ may be obtained:

$$Q_{vk} = 1.1 \cdot 250 \cdot \phi_{din} = 319.6 \text{ kN} \quad \rightarrow \quad q_{vk,1} = 319.6/1.6 = 199.75 \text{ kN/m}$$

where ϕ_{din} , the dynamic factor equal to 1.162, is evaluated below.

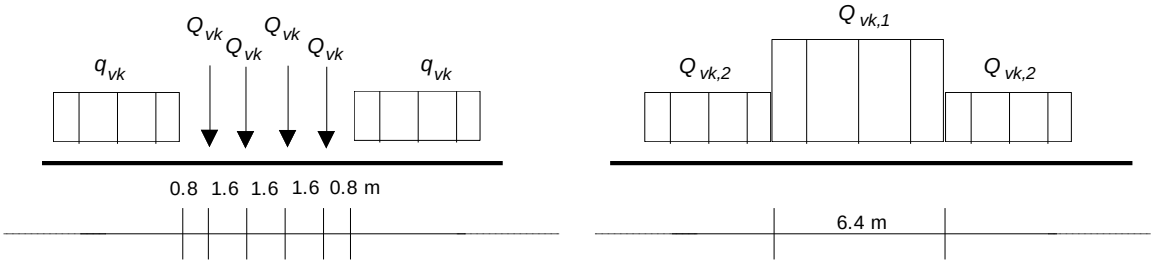


Fig. 7.2-11: Adopted load arrangement for LM71 load model

The uniformly distributed load q_{vk} according to EN 1991-2 is:

$$q_{vk} = 1.1 \cdot 80 \cdot \phi_{din} \quad \rightarrow \quad q_{vk,2} = 102.3 \text{ kN/m}$$

without any limitation in length. Fig. 7.2-11 shows the LM71 arrangement adopted in the calculations.

The load model SW/0 is represented in Fig. 7.2-12 and its characteristic value results:

$$q_{vk} = 1.1 \cdot 133 \cdot \phi_{din} = 170.0 \text{ kN/m}$$

Copyright fib, all rights reserved. This PDF copy of fib Bulletin 54 is intended for use and/or distribution only within National Member Groups of fib.

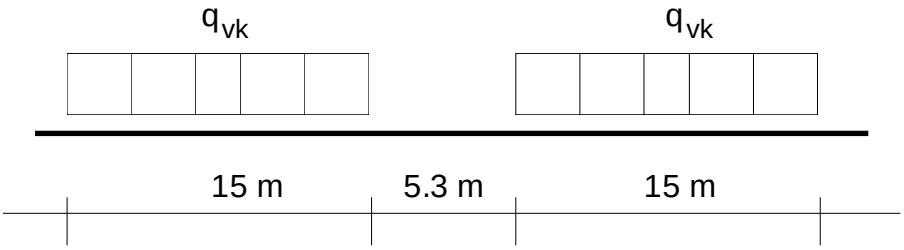


Fig. 7.2-12: Load model SW/0

The load model SW/2 is represented in Fig. 7.2-13 and its characteristic value results:

$$q_{vk} = 1.1 \cdot 150 \cdot \phi_{din} = 174.3 \ \text{kN/m}$$

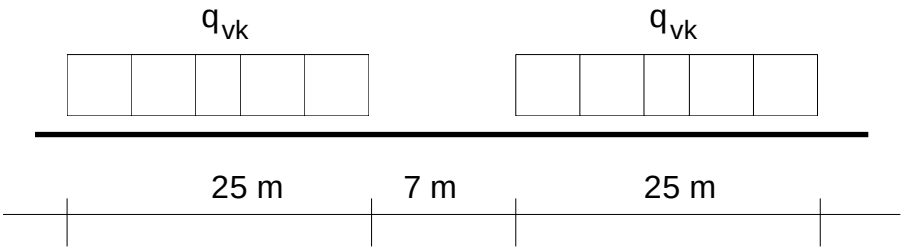


Fig. 7.2-13: Load model SW/2

The previous load model LM71, SW/0 and SW/2 were introduced in the FEM analysis considering a spreading ratio of 4:1 in the ballast and of 1:1 in the concrete up to the middle plane of the slab. In the following the track which has a positive value for the *y* co-ordinate is denoted as the left track , while right track is the other one. Fig. 7.2-14 shows which elements are involved by spreading effects, therefore subjected to variable loads.

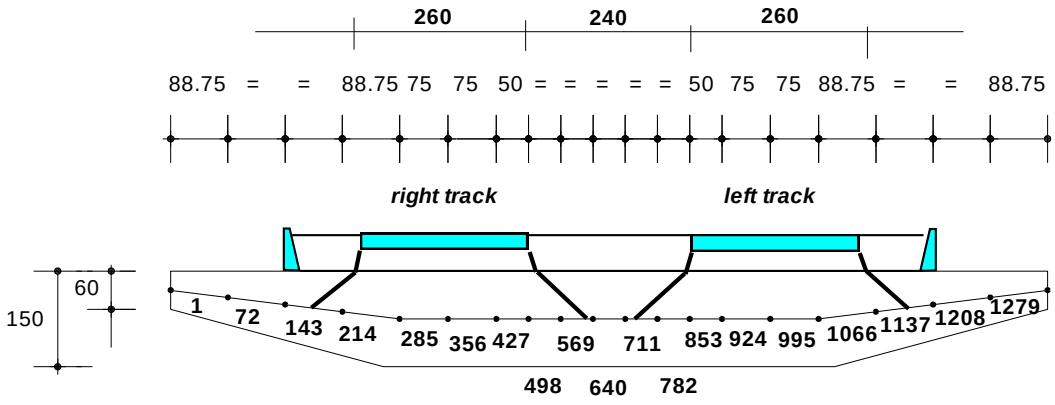


Fig. 7.2-14: Spreading effects on FEM model and loaded elements

The dynamic factor ϕ is calculated by means of the following expression (track with standard maintenance):

$$\phi_3 = \frac{2.16}{\sqrt{L_\phi} - 0.2} + 0.73 = 1.162$$

Copyright fib, all rights reserved. This PDF copy of fib Bulletin 54 is intended for use and/or distribution only within National Member Groups of fib.

where L_ϕ is the *determinant* length defined in the EN 1991-2 as:

$$L_\phi = 1.3\frac{L_1 + L_2 + L_3}{3} = 1.3\frac{17.33 + 27.75 + 17.33}{3} = 27.04\,\text{m}$$

Several other actions, arising from variable loads, should be considered in the analysis (such as traction and braking, centrifugal forces, derailment, wind pressure, differential temperature variation etc.) but, for the sake of simplicity, in these calculations only the following actions were considered (introduced in the mathematical model in different steps):

- STEP 1: Self-weight of the structure: adopting a unit weight value of γ = 25 kN/m^3;
- STEP 2: Prestressing forces at time of tensioning;
- STEP 3: Prestressing forces after time-dependent losses:
  in the calculations, a limit value of tensile stress in tendon equal to 0.6 f_{ptk} after allowance for losses (t_∞) was considered, according to the provisions of the applied railway code to avoid the risk of brittle failure due to stress corrosion.
- STEP 4: Track load, including;
  rails, sleepers and ballast (waterproofing included) evaluated as a cover with a nominal height of 0.8 m and a unit weight of γ = 18 kN/m^3), so that for a width of 9.5 m, a uniformly distributed load results:
  $g_{ballast}$ = 0.8 · 1.8 · 9.5 = 136.8 kN/m;
- STEP 5: Others permanent loads composed by;
  transverse gradient for drain water, assumed as a load of 1.25 kN/m^2 it turns out:
  g_{drain} = 1.25 · 9.5 = 11.875 kN/m;
  ballast retaining walls (with a cross section area of 0.25 m^2 and unit weight of 25 kN/m^3)
  g_{walls} = 25 · 0.25 = 6.25 kN/m for each;
  ducts:
  g_{ducts} = 3 kN/m for each;
  border curbs (with a cross section area of 0.1 m^2 and unit weight of 25 kN/m^3):
  $g_{reinf\ beam}$ = 25 · 0.25 = 6.25 kN/m for each;
  noise barriers:
  $g_{barriers}$ = 8.00 kN/m for each;
- STEP 6: Variable loads for maximum bending moment on first span (x = 6.18 m);
  the applied load is a LM71 model on the left track with the following longitudinal arrangement:



Fig. 7.2-15: LM71 arrangement for Load Step 5

Copyright fib, all rights reserved. This PDF copy of fib Bulletin 54 is intended for use and/or distribution only within National Member Groups of fib.

plus a SW/2 train on the right track with the following longitudinal arrangement:

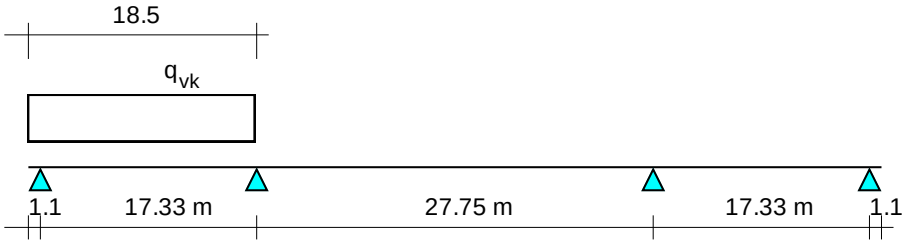


Fig. 7.2-16: SW/2 arrangement for Load Step 5

– STEP 7: Variable loads for minimum bending moment at pier P1 (x = 18.43 m); the applied load is a SW/0 model on the left track with the following longitudinal arrangement:

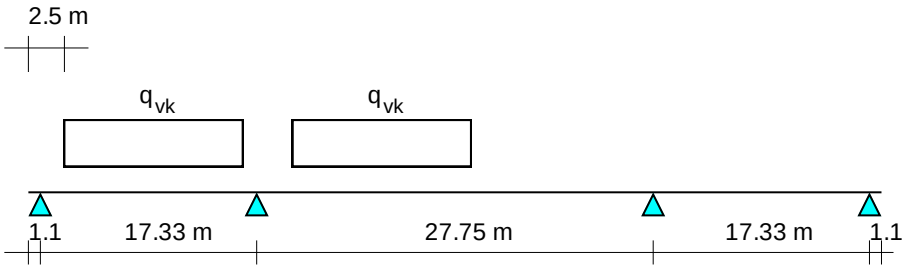


Fig. 7.2-17: SW/0 arrangement for Load Step 6

plus a SW/2 train on the right track with the following longitudinal arrangement:

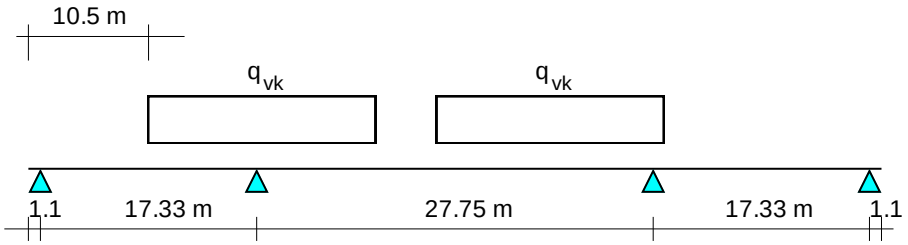


Fig. 7.2-18: SW/2 arrangement for Load Step 6

– STEP 8: Variable loads for max bending moment on second span (x = 32.305 m); the applied load is a LM71 model on the left track with the following longitudinal arrangement:

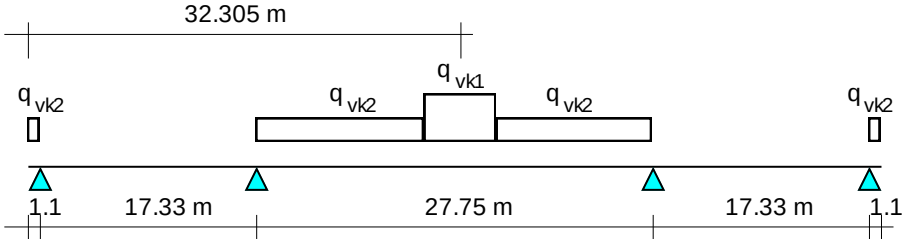


Fig. 7.2-19: LM71 arrangement for Load Step 7

Copyright fib, all rights reserved. This PDF copy of fib Bulletin 54 is intended for use and/or distribution only within National Member Groups of fib.

plus a SW/2 train on the right track with the following longitudinal arrangement:

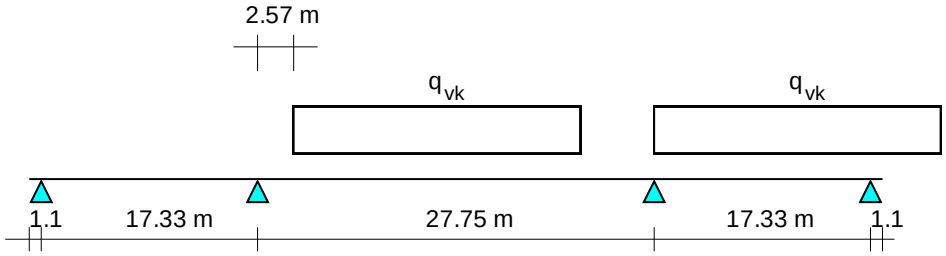


Fig. 7.2-20: SW/2 arrangement for Load Step 7

7.2.4 Combinations of actions

The design values for the external actions were calculated adopting the combinations of loads specified in the applied code as indicated in the symbolic presentation:

– Ultimate Limit State

$$S_d = S\left\{\gamma_{G1}\, G_{1k} + \gamma_{G2}\, G_{2k} + \gamma_p\, P_k + \gamma_Q \left(Q_{1k} + \sum_{i>1} \Psi_{oi}\, Q_{ik}\right)\right\} \qquad (7.2\text{-}1)$$

– Serviceability Limit State: rare combination

$$S_d = S\left\{G_{1k} + G_{2k} + P_k + Q_{1k} + \sum_{i>1} \Psi_{oi}\, Q_{ik}\right\} \qquad (7.2\text{-}2)$$

– Serviceability Limit State: quasi-permanent combination

$$S_d = S\left\{G_{1k} + G_{2k} + P_k + \sum_{i>1} \Psi_{2i}\, Q_{ik}\right\} \qquad (7.2\text{-}3)$$

where:

G_{1k} = characteristic value of the action due to self-weight and permanent loads, ballast excluded;
G_{2k} = characteristic value of action due to ballast self-weight;
P_k = characteristic value of action due to prestress;
Q_{1k} = characteristic value of action due to the base variable action;
Q_{ik} = characteristic value action due to of the other independent variable loads;
γ_1 = partial safety factor of self-weight and permanent loads, ballast excluded, equal to 1.4 for unfavourable effect and 1.0 for favourable effect;
γ_2 = partial safety factor of ballast load equal to 1.8 for unfavourable effect and 1.0 for favourable effect;
γ_P = partial safety factor of prestress load equal to 1.2 for unfavourable effect and 0.9 for favourable effect;
γ_Q = partial safety factor of variable loads equal to 1.5 for unfavourable effect and 0.0 for favourable effect;
Ψ_{0i} = combination factor of variable loads equal to 0.8;
Ψ_{2i} = combination factor of variable loads for quasi-permanent combination at service, equal to 0.6.

Copyright fib, all rights reserved. This PDF copy of fib Bulletin 54 is intended for use and/or distribution only within National Member Groups of fib.

7.2.5 Verification at serviceability limit state

The verification at serviceability limit state is relative to the following conditions:
- stress limitation at tensioning;
- stress limitation at service;
- crack widths;
- deformations.

(1) Verification at tensioning

At time of tensioning, no tensile stress should be present in the extreme fibres of the slab and the maximum compressive stress should not exceed the limit value of 0.6 f_{ck} = 21 N/mm^2. For the sake of simplicity, one reports the verification related to the four elements showed in Fig 7.2-4, as subjected to the higher stress level.

The external actions are calculated adopting the rare combination (7.2-2) with only the load steps 1 and 2. From FEM analysis, the value of n_{22}, m_{22}, n_{33}, m_{33}, n_{23}, m_{23} are evaluated so that the following results:

$$\sigma_{y,t} = \sigma_{22,t} = \frac{n_{22}}{h} - \frac{6\, m_{22}}{h^2}; \qquad \sigma_{y,b} = \sigma_{22,b} = \frac{n_{22}}{h} + \frac{6\, m_{22}}{h^2}$$

$$\sigma_{x,t} = \sigma_{33,t} = \frac{n_{33}}{h} - \frac{6\, m_{33}}{h^2}; \qquad \sigma_{x,b} = \sigma_{33,b} = \frac{n_{33}}{h} + \frac{6\, m_{33}}{h^2}$$

$$\sigma_{xy,t} = \sigma_{23,t} = \frac{n_{23}}{h} - \frac{6\, m_{23}}{h^2}; \qquad \sigma_{xy,b} = \sigma_{23,b} = \frac{n_{23}}{h} + \frac{6\, m_{23}}{h^2}$$

where the subscripts t and b indicate top and bottom fibres, respectively. The angles of principal directions (for which is $\sigma_{xy} = 0$) are:

$$\theta_1 = \frac{1}{2}\arctan\left(\frac{2\,\sigma_{23}}{\sigma_{22} - \sigma_{33}}\right); \qquad \theta_2 = \theta_1 + 90°$$

and the principal stresses result:

$$\sigma_{1,t/b} = \sigma_{22,t/b}\cos^2(\theta_1) + \sigma_{33,t/b}\sin^2(\theta_1) + \sigma_{23,t/b}\sin(2\theta_1)$$

$$\sigma_{2,t/b} = \sigma_{22,t/b}\cos^2(\theta_2) + \sigma_{33,t/b}\sin^2(\theta_2) + \sigma_{23,t/b}\sin(2\theta_2)$$

Copyright fib, all rights reserved. This PDF copy of fib Bulletin 54 is intended for use and/or distribution only within National Member Groups of fib.

Referring to the elements marked in Fig. 7.2-4 one obtains:

Elem.	h [m]	n_{22} [kN/m]	n_{33} [kN/m]	n_{23} [kN/m]	m_{22} [kNm/m]	m_{33} [kNm/m]	m_{23} [kNm/m]
648	1.5	-3091	-13159	6	-225	-2176	0
93	0.963	-7806	-8526	75	743	456	-51
320	1.5	-3516	-10418	1	-45	-812	0
589	1.5	-4280	-10007	-67	653	1945	20

$\sigma_{22,b}$ [N/mm^2]	$\sigma_{33,b}$ [N/mm^2]	$\sigma_{23,b}$ [N/mm^2]	$\sigma_{22,t}$ [N/mm^2]	$\sigma_{33,t}$ [N/mm^2]	$\sigma_{23,t}$ [N/mm^2]	$\theta_{1,b}$ [°]	$\theta_{2,b}$ [°]	$\theta_{1,t}$ [°]	$\theta_{2,t}$ [°]
-2.66	-14.58	0.00	-1.46	-2.97	0.00	0.02	89.98	0.15	89.85
-3.30	-5.90	-0.25	-12.91	-11.80	0.41	-5.48	95.48	-18.17	108.17
-2.46	-9.11	0.00	-2.22	-4.78	0.00	0.01	89.99	0.01	89.99
-1.11	-1.48	0.01	-4.59	-11.86	-0.10	1.29	88.71	-0.77	90.77

$\sigma_{1,b}$ [N/mm^2]	$\sigma_{2,b}$ [N/mm^2]	$\sigma_{1,t}$ [N/mm^2]	$\sigma_{2,t}$ [N/mm^2]
-2.66	-14.58	-1.46	-2.97
-3.27	-5.83	-13.05	-12.15
-2.46	-9.11	-2.22	-4.78
-1.11	-1.48	-4.59	-11.85

which do not exceed the limit.

(2) Verification of limit state of stress limitation in concrete

The serviceability limit states checked in this section are relative only to stress limitation, ensuring that, under service load conditions, extreme concrete stresses do not exceed the corresponding limit for the quasi-permanent and the rare combinations. The limit stresses for concrete are:

- Quasi-permanent combination: compressive stress = 0.4 f_{ck} = 14.00 N/mm^2
- Rare combination: compressive stress = 0.6 f_{ck} = 21.00 N/mm^2

Applying to the structural FEM model the variable loads and combining them according to the railway code provisions, one obtains the maximal stress values at top and bottom fibres that have to be lower than the corresponding limit. One reports the results relative to the four elements indicated in Fig. 7.2-4.

Quasi-permanent combination

Elem.	h [m]	n_{22} [kN/m]	n_{33} [kN/m]	n_{23} [kN/m]	m_{22} [kNm/m]	m_{33} [kNm/m]	m_{23} [kNm/m]
648	1.5	-2420	-10152	4	-236	-1576	4
93	0.963	-6233	-6347	50	589	108	-37
320	1.5	-3539	-7855	2	81	233	4
589	1.5	-2736	-7900	-3	-151	-396	0

$\sigma_{1,b}$ [N/mm^2]	$\sigma_{2,b}$ [N/mm^2]	$\sigma_{1,t}$ [N/mm^2]	$\sigma_{2,t}$ [N/mm^2]
-2.24	-10.97	-0.98	-2.57
-2.65	-5.86	-10.31	-7.37
-2.14	-4.62	-2.58	-5.86
-2.23	-6.32	-1.42	-4.21

Copyright fib, all rights reserved. This PDF copy of fib Bulletin 54 is intended for use and/or distribution only within National Member Groups of fib.

Rare combination

Elem.	h [m]	n_{22} [kN/m]	n_{33} [kN/m]	n_{23} [kN/m]	m_{22} [kNm/m]	m_{33} [kNm/m]	m_{23} [kNm/m]	$\sigma_{1,b}$ [N/mm^2]	$\sigma_{2,b}$ [N/mm^2]	$\sigma_{1,t}$ [N/mm^2]	$\sigma_{2,t}$ [N/mm^2]
648	1.5	-2238	-10270	3	-226	-615	4	-2.09	-8.49	-0.89	-5.21
93	0.963	-6284	-6033	4	577	-133	-62	-2.76	-7.02	-10.29	-5.51
320	1.5	-2604	-7479	7	7	1279	-9	-1.72	-1.58	-1.75	-8.40
589	1.5	-3791	-8243	-55	-689	-1275	-26	-4.36	-8.89	-0.69	-2.09

(3) Verification of serviceability limit state of cracking

The characteristic crack width should be calculated according to the provisions of MC90. It must be noted, however, that from stress calculation neither for the quasi-permanent combination nor for the rare one, the maximum stress is positive (tension). Therefore, no specific reinforcement is required and it is sufficient to arrange the minimum amount of reinforcing steel, able to ensure a ductile behaviour in case of corrosion of prestressing steel.

(4) Deformation

Deformation limitation is carried out to control the maximum vertical deflection for passengers comfort. The limit values δ/L (deflection/span Length) are given by the EN 1991-2 as a function of the span and the train speed. The limit value for maximum vertical deflection is calculated considering a span of 27.75 m (central span) and a train speed over 280 km/h; according to the provisions of the code, the following results:

$$\frac{\delta}{L} = \frac{1}{1600}$$

that should be multiplied by a factor 1.1 for continuous structures. Finally, the following limit may be achieved:

$$\frac{\delta_{lim}}{L} = \frac{1.1}{1600} = \frac{1}{1455}.$$

As a consequence of the transient nature of this event, the elastic deflection, calculated by the FEM model, is relative to the only live load; the check shall be performed loading only one track, reading the maximum deflection in correspondence of the track axis. Having loaded the right track with a LM71 load model plus dynamic allowance, placed in the middle of the central span, the obtained δ/L value is:

$$\frac{\delta_{effective}}{L} = \frac{0.0055}{27.75} = \frac{1}{5045}$$

and it results in a lower value than the corresponding limit.

It can be notice that no further calculation is requested because, due to prestressing effect, the structure remains entirely compressed, so the elastic value, calculated by the FEM analysis, has to be considered.

Copyright fib, all rights reserved. This PDF copy of fib Bulletin 54 is intended for use and/or distribution only within National Member Groups of fib.

7.2.6 Verification of ultimate limit state

Verification at ULS should consider the structure as a whole and its component parts, analysing the resistance of the critical regions. In addition to the analysis of ULS of several shell elements under the relevant combination of internal actions, in this example some case of *detailing* are investigated, i.e.:

- bursting force at anchorage of prestressing tendon;
- spalling force at anchorage of prestressing tendon;
- punching under support plate.

(1) Ultimate limit state of slab

Verification at ULS was performed by adopting the sandwich model for shell elements. The internal actions in a shell element at ULS are shown in Fig. 7.2-21.

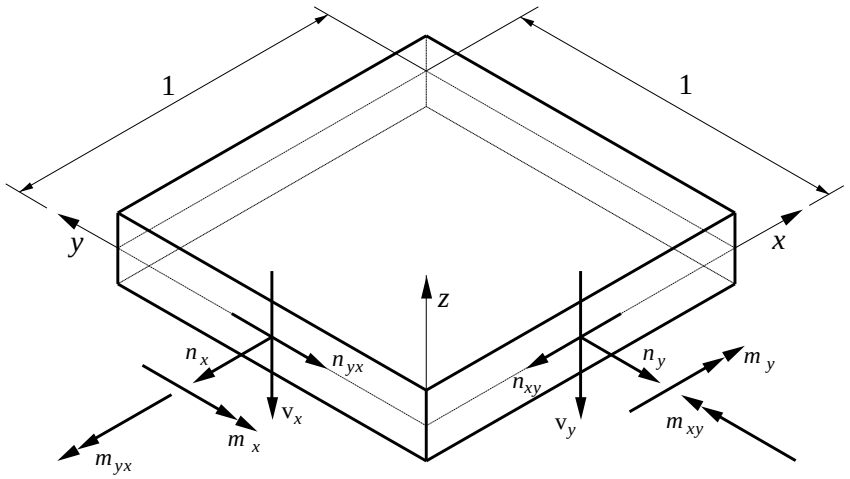


Fig. 7.2-21: Internal actions at ULS in a shell elements

Let us consider in this section only four elements of the whole (see Fig. 7.2-4). The external actions are derived from FEM model using the load step for trains, which leads to the maximum values and combining the results according to the relevant combination formula. For the investigated elements, turns out (in brackets the notation of Fig. 7.2-5):

Elem.	h [m]	$n_{Sd,y}$ (n_{22}) [kN/m]	$n_{Sd,x}$ (n_{33}) [kN/m]	$n_{Sd,xy}$ (n_{23}) [kN/m]	$m_{Sd,y}$ (m_{22}) [kNm/m]	$m_{Sd,x}$ (m_{33}) [kNm/m]	$m_{Sd,xy}$ (m_{23}) [kNm/m]	$v_{Sd,y}$ (v_{13}) [kN/m]	$v_{Sd,x}$ (v_{12}) [kN/m]
648	1.5	-1779	-9096	5	-239	470	-14	-6	-5
93	0.963	-5746	-4610	-63	499	-671	-75	89	-150
320	1.5	-2130	-5922	10	38	3241	-13	20	47
589	1.5	-3865	-7748	-54	-1950	-4274	-41	-1124	-1095

As the first step, one may check if in the inner layer specific shear reinforcement is required or not. In fact, it is possible to calculate the principal shear $v_o^2 = v_x^2 + v_y^2$, on the principal shear direction φ_o (such that $\tan\varphi_0 = v_y / v_x$), and to check that it turn out:

Copyright fib, all rights reserved. This PDF copy of fib Bulletin 54 is intended for use and/or distribution only within National Member Groups of fib.

$$v_0 < v_{Rd1} = 0.12\,\xi\,(100\,\rho\,f_{ck})^{1/3}\;\; d \qquad (7.2\text{-}4)$$

where v_{Rd1} is specified in chapter 6.4.2.3 of MC90 and $\rho = \rho_x \cos^2\varphi_o + \rho_y \sin^2\varphi_o$. If Eq- 7.2-4 is not satisfied, specific shear reinforcement shall be arranged (vertical stirrups) and diagonal compressive forces in concrete shall be checked. According to CEB Bulletin 223, and having set a minimum amount of longitudinal and transverse reinforcement in the bottom and top layer of:

$A_{s,x} = A_{s,y} = 2260$ mm^2/m

placed at 0.07 m from the external face, the following table may be calculated for the elements considered:

Elem.	d [m]	φ_o [°]	ρ_o [-]	v_o [kN/m]	v_{Rd1} [kN/m]	θ [°]	F_{Scw} [kN/m]	F_{Rcw} [kN/m]	A_s/s^2 [mm^2/m^2]	n_{xc} [kN/m]	n_{yc} [kN/m]	n_{xyc} [kN/m]
648	1.43	51.18	0.00158	7	417	26.56	-	-	-	0.0	0.0	0.0
93	0.893	-30.77	0.00253	174	327	26.56	-	-	-	0.0	0.0	0.0
320	1.43	23.14	0.00158	51	417	26.56	-	-	-	0.0	0.0	0.0
589	1.43	45.76	0.00158	1569	417	26.56	3509	13860	1402	763.9	805.6	784.5

with variation of slab components due to v_x and v_y (i.e. n_{xc} , n_{yc} and n_{xyc}) only for element number 589.

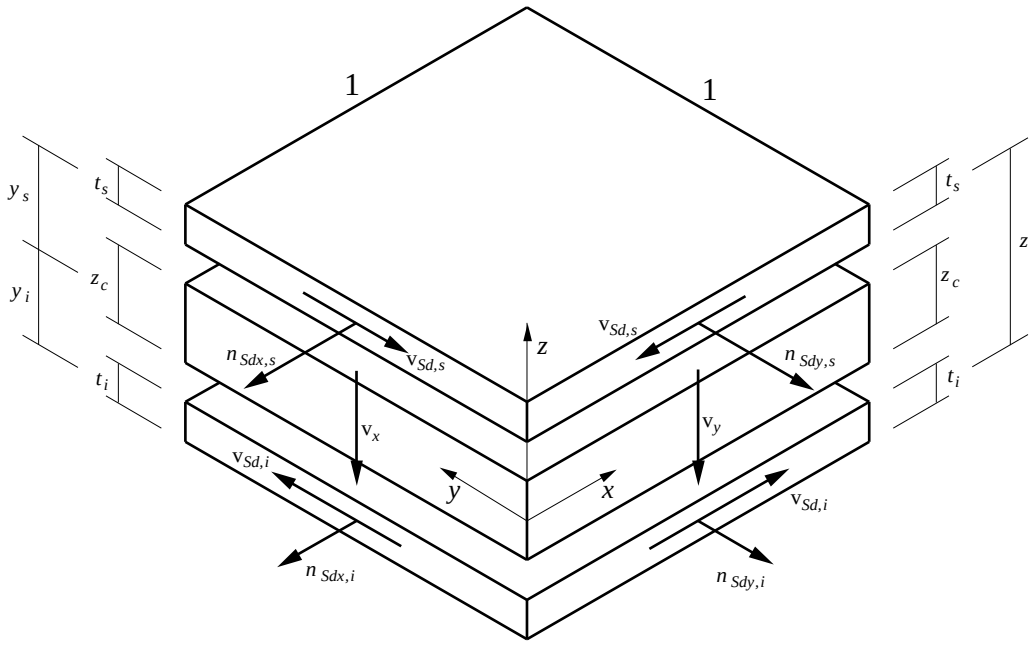


Fig. 7.2-22: Internal forces in the different layers

The outer layers should be designed supposing an initial thickness for both layers not lesser than twice the concrete cover evaluated at the centroid of reinforcement. One assumes:

$t_s = t_i = 2 \cdot 0.07 = 0.14$ m

Copyright fib, all rights reserved. This PDF copy of fib Bulletin 54 is intended for use and/or distribution only within National Member Groups of fib.

so that internal lever arm *z* and in-plane actions may be evaluated for the outer layers of each element by referring to Fig. 7.2-22 and by means of the following equations:

$$n_{Sdx,s} = n_x \frac{z - y_s}{z} + \frac{m_x}{z} + \left(\frac{1}{2}\frac{v_x^2}{v_0}\cot\theta\right) \qquad n_{Sdx,i} = n_x \frac{z - y_i}{z} - \frac{m_x}{z} + \left(\frac{1}{2}\frac{v_x^2}{v_0}\cot\theta\right)$$

$$n_{Sdy,s} = n_y \frac{z - y_s}{z} + \frac{m_y}{z} + \left(\frac{1}{2}\frac{v_y^2}{v_0}\cot\theta\right) \qquad n_{Sdy,i} = n_y \frac{z - y_i}{z} - \frac{m_y}{z} + \left(\frac{1}{2}\frac{v_y^2}{v_0}\cot\theta\right)$$

$$v_{Sd,s} = n_{xy} \frac{z - y_s}{z} - \frac{m_{xy}}{z} + \left(\frac{1}{2}\frac{v_x v_y}{v_0}\cot\theta\right) \qquad v_{Sd,i} = n_{xy} \frac{z - y_i}{z} + \frac{m_{xy}}{z} + \left(\frac{1}{2}\frac{v_x v_y}{v_0}\cot\theta\right)$$

where terms in brackets have to be added if shear reinforcement is required. In the design procedure it is convenient to reach the minimum amount of reinforcement, so that a value of 45° for θ angle may be adopted.

For the chosen elements the following values result:

Elem.	h [m]	t_s [m]	t_i [m]	t_c [m]	y_s [m]	y_i [m]	z [m]	$n_{Sdy,s}$ [kN/m]	$n_{Sdx,s}$ [kN/m]	$v_{Sd,s}$ [kN/m]	$n_{Sdy,i}$ [kN/m]	$n_{Sdx,i}$ [kN/m]	$v_{Sd,i}$ [kN/m]
648	1.5	0.140	0.140	1.220	0.680	0.680	1.360	-713.5	-4893.3	13.0	-1065.1	-4202.2	-7.7
93	0.963	0.140	0.140	0.683	0.412	0.412	0.823	-3479.6	-1489.8	59.3	-2266.7	-3120.5	-122.3
320	1.5	0.140	0.140	1.220	0.680	0.680	1.360	-1093.1	-5344.2	14.8	-1037.3	-577.9	-4.4
589	1.5	0.140	0.140	1.220	0.680	0.680	1.360	307.0	32.7	787.8	-2560.7	-6252.6	726.9

At this stage, each layer may be designed by applying the following equations (θ = 45°):

$$\sigma_c\, t = \frac{v_{Sd}}{\sin\theta\ \cos\theta} \le f_{cd2}\, t \qquad \text{safety verification on concrete side} \qquad (7.2\text{-}5)$$

$$n_{Rdx} = n_{Sdx} + v_{Sd}\cot\theta \qquad \text{required resistance along } x \text{ direction} \qquad (7.2\text{-}6)$$

$$n_{Rdy} = n_{Sdy} + \frac{v_{Sd}}{\cot\theta} \qquad \text{required resistance along } y \text{ direction} \qquad (7.2\text{-}7)$$

from which, if Eq. (7.2-5) results satisfied, the reinforcement areas may be calculated as:

$$A_{sx} = \frac{n_{Rdx}}{f_{yd}} \quad ; \quad A_{sy} = \frac{n_{Rdy}}{f_{yd}}.$$

If concrete strength requirement is not satisfied, an increase layer thickness shall be provided until verification is met; in this case new values for the layer action shall have changed *z* value.

Copyright fib, all rights reserved. This PDF copy of fib Bulletin 54 is intended for use and/or distribution only within National Member Groups of fib.

It can be noted that if n_{Rdx} or n_{Rdy} value are negative, a compression force is present along that direction and no reinforcement is required; if both the n_{Rdx} and n_{Rdy} are negative it is possible to omit the reinforcement in both the directions, but in this case the verification is performed along the principal compression direction in the concrete subjected to biaxial compression, and the checking equation is:

$$\sigma_c\, t = \frac{n_{Sdx} + n_{Sdy}}{2} + \sqrt{\frac{\left(n_{Sdx} - n_{Sdy}\right)^2}{4} + v_{Sd}^2} \le f_{cd1}\, t\,.$$

For the considered elements, one obtains:

	Top Layer Design				Bottom Layer Design			
Elem.	σ_c [N/mm^2]	$f_{cd1/2}$ [kN/m]	A_{sy} [mm^2/m]	A_{sx} [mm^2/m]	σ_c [N/mm^2]	$f_{cd1/2}$ [kN/m]	A_{sy} [mm^2/m]	A_{sx} [mm^2/m]
648	-35.0	-17.1	0	0	-30.0	-17.1	0	0
93	-24.9	-17.1	0	0	-22.4	-17.1	0	0
320	-38.2	-17.1	0	0	-7.4	-17.1	0	0
589	-11.3	-12.0	2518	1887	-45.6	-17.1	0	0

It can be noted that verification for concrete in compression is not satisfied for any layers except for element 589 top layer and element 320 bottom layer. Thus, an increase of layer thickness is required and new values of plate actions are obtained:

Elem.	h [m]	t_s [m]	t_i [m]	t_c [m]	y_s [m]	y_i [m]	z [m]	$n_{Sdy,s}$ [kN/m]	$n_{Sdx,s}$ [kN/m]	$v_{Sd,s}$ [kN/m]	$n_{Sdy,i}$ [kN/m]	$n_{Sdx,i}$ [kN/m]	$v_{Sd,i}$ [kN/m]
648	1.5	0.300	0.240	0.960	0.600	0.630	1.230	-716.6	-5040.8	14.1	-1062.0	-4054.7	-8.8
93	0.963	0.220	0.190	0.553	0.372	0.387	0.758	-3588.5	-1465.5	66.5	-2157.8	-3144.8	-129.4
320	1.5	0.340	0.140	1.020	0.580	0.680	1.260	-1179.8	-5768.3	16.0	-950.6	-153.8	-5.5
589	1.5	0.140	0.430	0.930	0.680	0.535	1.215	708.7	870.1	794.7	-2962.5	-7090.0	720.0

which lead to the following values:

	Top Layer Design				Bottom Layer Design			
Elem.	σ_c [N/mm^2]	$f_{cd1/2}$ [kN/m]	A_{sy} [mm^2/m]	A_{sx} [mm^2/m]	σ_c [N/mm^2]	$f_{cd1/2}$ [kN/m]	A_{sy} [mm^2/m]	A_{sx} [mm^2/m]
648	-16.8	-17.1	0	0	-16.9	-17.1	0	0
93	-16.3	-17.1	0	0	-16.6	-17.1	0	0
320	-17.0	-17.1	0	0	-6.8	-17.1	0	0
589	-11.4	-12.0	3458	3829	-16.8	-17.1	0	0

Copyright fib, all rights reserved. This PDF copy of fib Bulletin 54 is intended for use and/or distribution only within National Member Groups of fib.

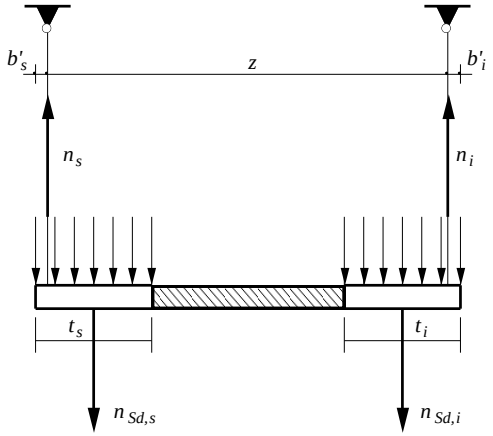


Fig. 7.2-23: Shell element equilibrium in one direction with two reinforcement layers only

Of course, minimum value should be adopted for A_{sx} and A_{sy} if no reinforcement areas are required. For element 589, the A_{sx} and A_{sy} values are required at the centroid of the layer, whereas they are arranged at 0.07 m from the external surface of the slab in an eccentric position with respect to middle plane of the layer; so, the amount of reinforcement provided has to be changed to restore equilibrium conditions. This variation may be assessed with the aid of the mechanism presented in Fig. 7.2-23.

The new forces acting on the reinforcements become:

$$n_s = \frac{n_{Sd,s}\left(h - \frac{t_s}{2} - b_i'\right) + n_{Sd,i}\left(\frac{t_i}{2} - b_i'\right)}{z} \tag{7.2-8}$$

$$n_i = n_{Sd,s} + n_{Sd,i} - n_s \tag{7.2-9}$$

For the checked elements, the following areas were investigated.

	Forces referred to tension steel level				*Top layer reinf*		*Bottom layer reinf*	
Elem.	$n_{s,y}$ [kN/m]	$n_{i,y}$ [kN/m]	$n_{s,x}$ [kN/m]	$n_{i,x}$ [kN/m]	A_{sy} [mm²/m]	A_{sx} [mm²/m]	A_{sy} [mm²/m]	A_{sx} [mm²/m]
648	-702.5	-1070.8	-5026.6	-4063.6	0	0	0	0
93	-3522.0	-2287.2	-1399.0	-3274.3	0	0	0	0
320	-1163.8	-956.1	-5752.3	-159.3	0	0	0	0
589	1503.5	-2242.5	1664.8	-6370.0	3458	3829	0	0

The above procedure should be repeated for all the elements of the structural model finding the amount of reinforcement to provide in the slab; it is useful, to control the structural behaviour and for a best fitted reinforcement layout, to summarise the results in a visual map.

(2) Verification of bursting force

The symmetric prism analogy is used for the calculation of the bursting force, evaluating the height of the prism so that its centroid coincides with the centroid of prestressing tendons. For the sake of simplicity, only the longitudinal direction of prestressing tendon is considered with respect to the vertical plane, but transverse force due to bursting effect should also be calculated in the horizontal plane and for transverse prestressing.

Copyright fib, all rights reserved. This PDF copy of fib Bulletin 54 is intended for use and/or distribution only within National Member Groups of fib.

The design scheme is represented in Fig. 7.2-24, and the most unfavourable situation occurs when a single tendon is tensioned; considering the lower level of tendon (first tensioned) the height of the prism results:

$h_{bs} = 2 \cdot 0.6 = 1.2$ m

and its length, for end anchored tendon, is:

$l_{bs} = h_{bs} = 1.2$ m

while the width follows from the possible enlargement of the anchor plate that may be assumed to be equal to 0.43 m, corresponding to the transverse spacing of longitudinal lower tendons.

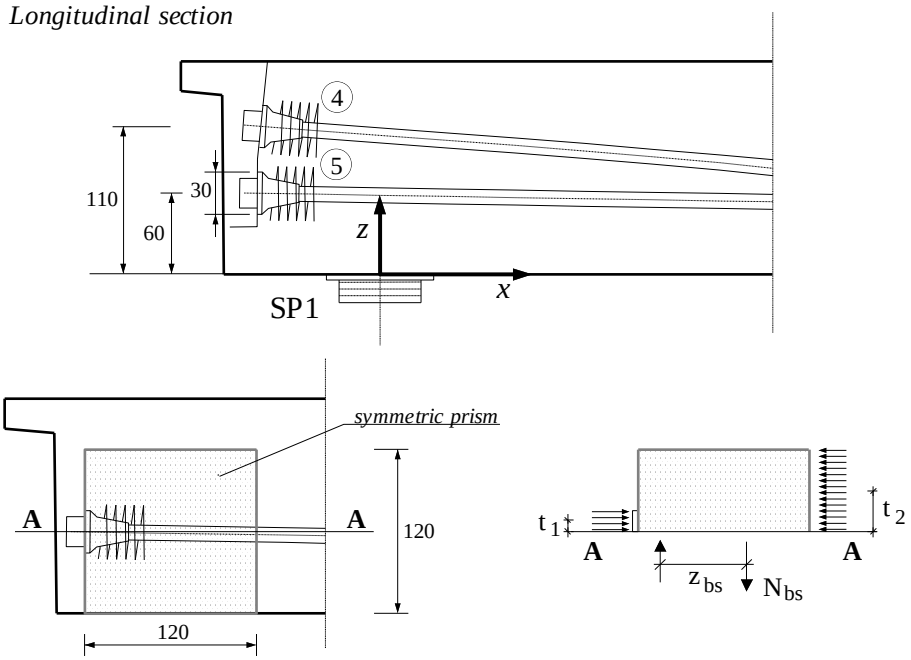


Fig. 7.2-24: Geometric dimensions for bursting calculation

The design force per tendon was evaluated by means of the following equation:

$$F_{Sd} = \frac{f_{ptk}}{1.15} A_{sp} = \frac{1800}{1.15} (139 \cdot 19) \cdot 10^{-3} = 4134 \text{ kN}. \qquad (7.2\text{-}10)$$

The bursting force follows from the moment equilibrium along section A-A:

$$N_{bs} = \frac{0.5 (n_1 + n_2) t_2 - n_1 t_1}{z_{bs}} \gamma_1 F_{Sd} = 852.6 \text{ kN} \qquad (7.2\text{-}11)$$

where:

$t_1 = 0.075$ m distance between the centroid of tendons above section A-A to the centroid of the prism;

$t_2 = 0.300$ m distance between the centroid of concrete stress block above section A-A to the centroid of the prism;

Copyright fib, all rights reserved. This PDF copy of fib Bulletin 54 is intended for use and/or distribution only within National Member Groups of fib.

n_1 , n_2 numbers of tendons above and below section A-A, respectively: considering the anchor plate to be rigid, a value of 0.5 may be assumed;

γ_1 =1.1 supplementary partial safety factor against overstressing by over pumping.

Bursting force shall be resisted by an area of reinforcement steel of:

$A_{s,bs} = N_{bs} / f_{yd} = 1961$ mm^2

distributed within $l_{bs}/3$ to l_{bs} , (i.e. from 0.40 m to 1.20 m) from the anchor plate. Thus the effective area on a meter length, may be found by the following:

$$\frac{A_{s,bs}}{s \cdot s} = \frac{A_{s,bs}}{b \cdot \frac{2}{3} l_{bs}} = \frac{1961}{0.43 \cdot (1.20 - 0.4)} = 5700 \text{ mm}^2/\text{m}^2$$

that may be provided with ties having diameter of 22 mm and spacing both transversally and longitudinally of 250 mm (see Fig. 7.2-25); in fact ∅22/25×25 cm corresponds to 6082 mm^2/m^2 .

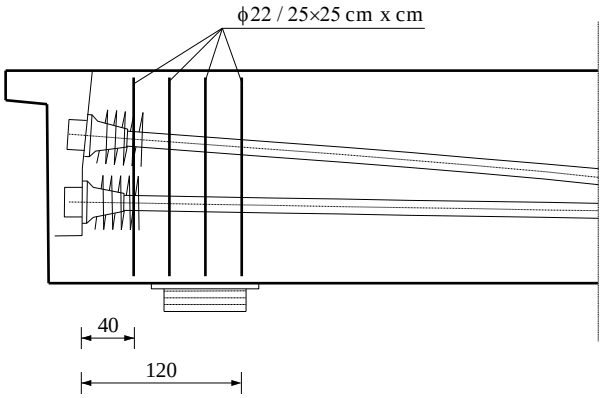


Fig. 7.2-25: Bursting reinforcement arrangement

(3) Verification of spalling force

The spalling force may be calculated with the equivalent prism analogy. As for bursting verification, only the longitudinal direction is considered; furthermore, spalling effects arise if the upper tendons are tensioned first (the eccentricity leads to tension stresses). Thus, a section with a breadth of 0.43 m and a height of 1.50 m has to be verified for one tendon tensioning.

The length of the prism for end anchored tendon, is equal to the overall height of the section, i.e. l_{sl} = 1.50 m. Considering an eccentricity for the upper prestressing tendon of 0.35 m, the extreme stresses at the end of prism length are calculated by means of the beam theory; for a prestressing force F_{Sd} = 4134.0 kN, evaluated with the (7.2-10), they result (negative if compressive):

$$\left.\begin{matrix}\sigma_{top} \\ \sigma_{bottom}\end{matrix}\right\} = F_{Sd}\left(-\frac{1}{0.43 \cdot 1.50} \mp \frac{0.35 \cdot 6}{0.43 \cdot 1.50^2}\right) = \begin{cases} -15.38 \text{MPa} \\ +2.56 \text{MPa} \end{cases}$$

Copyright fib, all rights reserved. This PDF copy of fib Bulletin 54 is intended for use and/or distribution only within National Member Groups of fib.

The section along which no shear force results, is placed at 0.428 m from slab bottom fibre (see Fig 7.2-26) and the moment for equilibrium is:

$$M_{sl} = \frac{2}{3}\sigma_{bottom} \cdot 0.214^2 \cdot 0.43 \cdot 10^3 = 33.61 \text{ kNm.}$$

Assuming $z_{sl} = 0.5\ l_{sl}$ and $b_{sl} = 0.43$ m, the maximum spalling force turns out:

$$N_{sl} = M_{sl} / z_{sl} = 44.81 \text{ kN}$$

Disregarding any concrete tensile resistance, the amount of reinforcement is:

$$A_s = N_{sl} / f_{yd} = 103.1 \text{ mm}^2$$

placed parallel to the end face in its close vicinity.

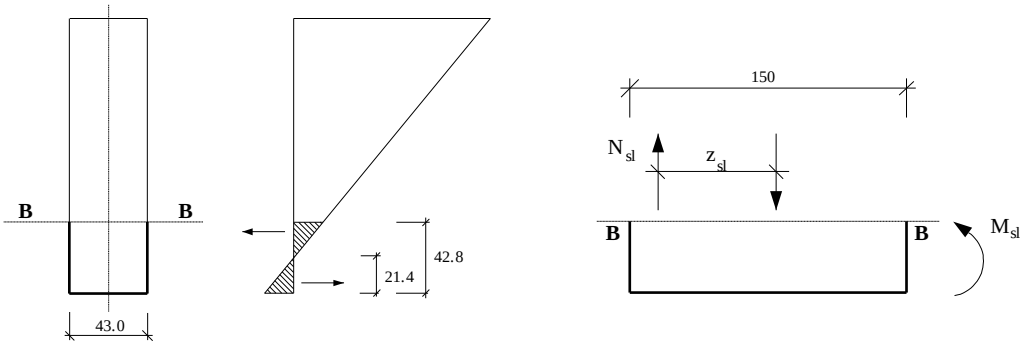


Fig. 7.2-26: Calculation scheme for spalling

(4) Verification of punching action

In the zone near supports high transverse stresses are reached in concrete due to the concentrated load on support plate, which may lead to local crushing. So the punching effect has to be investigated according to the provisions of MC90 for slabs with shear reinforcement. For the sake of simplicity, prestressing effects are neglected and only ordinary reinforcement is taken into account. Furthermore, in this example only one pier support P1 was verified, but all the others should be examined.

The external action results from load combination at ULS according to Eq. (7.2-4), and for pier P1 the higher value results: $F_{Sd} = 16029$ kN.

As the first step one has to verify if the slab is able to carry the punching load, calculating the maximum resistance that should result higher than the applied load; the maximum resistance is evaluated as:

$$F_{Rd,max} = 0.5\ f_{cd2}\ u_0\ d = 0.5 \cdot 12.0 \cdot 3.77 \cdot 1.43 \cdot 10^3 = 32347 \text{ kN} > F_{Sd}$$

where u_0 is the length of the periphery of the circular support plate (see below).

Copyright fib, all rights reserved. This PDF copy of fib Bulletin 54 is intended for use and/or distribution only within National Member Groups of fib.

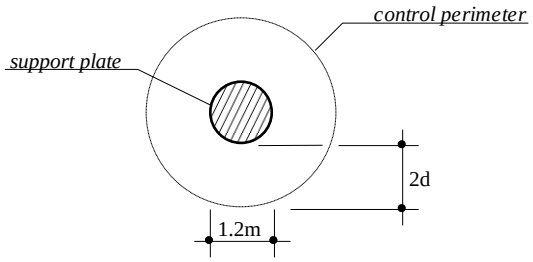


Fig. 7.2-27: Control perimeter for pier P1 supports

As second step, one has to evaluate if transverse reinforcement is requested; the shear stress due to loads at the control perimeter is:

$$\tau_{Sd} = \frac{F_{Sd}}{u_1 \, d} = \frac{16029}{21.74 \cdot 1.43} 10^{-3} = 0.516 \text{ N/mm}^2 \qquad (7.2\text{-}12)$$

where:

d = 1.43 m	effective depth of the slab taken as $(d_x + d_y)/2$;
u_1 = 21.74 m	length of the control perimeter calculated according to Fig. 7.2-27 for a support plate diameter of 1.2 m.

The corresponding stress resistance τ_{Rd} is given in MC90 as:

$$\tau_{Rd} = 0.12 \, \xi \left(100 \, \rho \, f_{ck}\right)^{1/3} = 0.44 \text{ N/mm}^2 \qquad (7.2\text{-}13)$$

with:

$\xi = 1 + \sqrt{200/d} = 1.374$	with d in mm;
$\rho = \sqrt{\rho_x \, \rho_y} = 0.0057$	having disposed an area of 67.1 cm^2/m in the *x* direction and of 98.8 cm^2/m in the *y* direction.

By comparing Eq. (7.2-12) with Eq. (7.2-13) it can be noticed that an amount of shear reinforcement has to be provided, so that the following resistance to punching force results:

$$F_{Sd} \le 0.09 \, \xi \left(100 \, \rho \, f_{ck}\right)^{1/3} u_1 \, d + 1.5 \frac{d}{s_r} A_{sw} \, f_{ywd} \sin\alpha \qquad (7.2\text{-}14)$$

where:

A_{sw}	area of shear reinforcement in a layer around the plate;
s_r	is the radial spacing of the layers of shear reinforcement
α	is the angle between shear reinforcement and the plane of the slab, assumed equal to 90°.

The quantity A_{sw} with Eq. (7.2-14) shall be calculated respecting two additional limits:

$$1.5 \frac{d}{s_r} A_{sw} \, f_{ywd} \sin\alpha \;\ge\; 0.03 \left(100 \, \rho \, f_{ck}\right)^{1/3} u_1 \, d \qquad f_{ywd} \le 300 \text{ N/mm}^2$$

Solving expression (7.2-14) with respect to A_{sw}/s_r and respecting the previous inequalities, the following result is obtained:

Copyright fib, all rights reserved. This PDF copy of fib Bulletin 54 is intended for use and/or distribution only within National Member Groups of fib.

$$\frac{A_{sw}}{s_r} = 8970 \text{ mm}^2/\text{m}$$

that shall be arranged within the control perimeter in a circumferential layout as shown in Fig. 7.2-28. If a radial spacing of 0.72 m is selected, three circumferential layers have to be arranged, and the total area of an individual layer results:

$A_{sw} = 0.72 \cdot 8970 = 6458 \text{ mm}^2$.

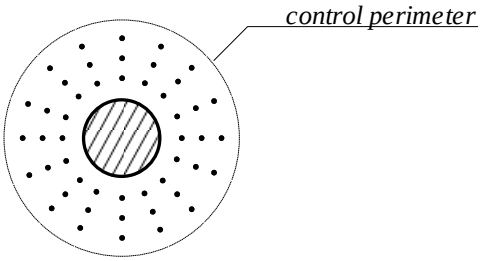


Fig. 7.2-28: Shear reinforcement layout for punching action

References to Section 7.2

CEB Bulletin 141 (1982), *Manual on Bending and Compression*. Comité Euro-international du Béton, Lausanne, Switzerland.

CEB Bulletin 213/214 (1993), *CEB-FIP Model Code 1990*, published by Thomas Telford Ltd., UK. ("MC90")

EN 1991-2: *Traffic loads on bridges.*

Copyright fib, all rights reserved. This PDF copy of fib Bulletin 54 is intended for use and/or distribution only within National Member Groups of fib.

7.3 Deep beams and discontinuity regions

by Kurt Schäfer

7.3.1 Principles and methods of design

(1) Introduction to the design of deep beams and discontinuity regions

(1.1) Definitions and general properties of D-regions

Bernoulli's assumption of linear strain distribution over the cross-section is a basis of the standard design methods for beams, columns and slabs (Chapter 4). However, Bernoulli's hypothesis is in general not valid for the design of deep beams. Fig. 7.3-1 presents some examples from a linear analysis. The span/depth ratio, for which the hypothesis is fairly well applicable, depends on the geometric boundary conditions (cantilever, single span or continuous beam) and the type of loading (distributed or concentrated loads).

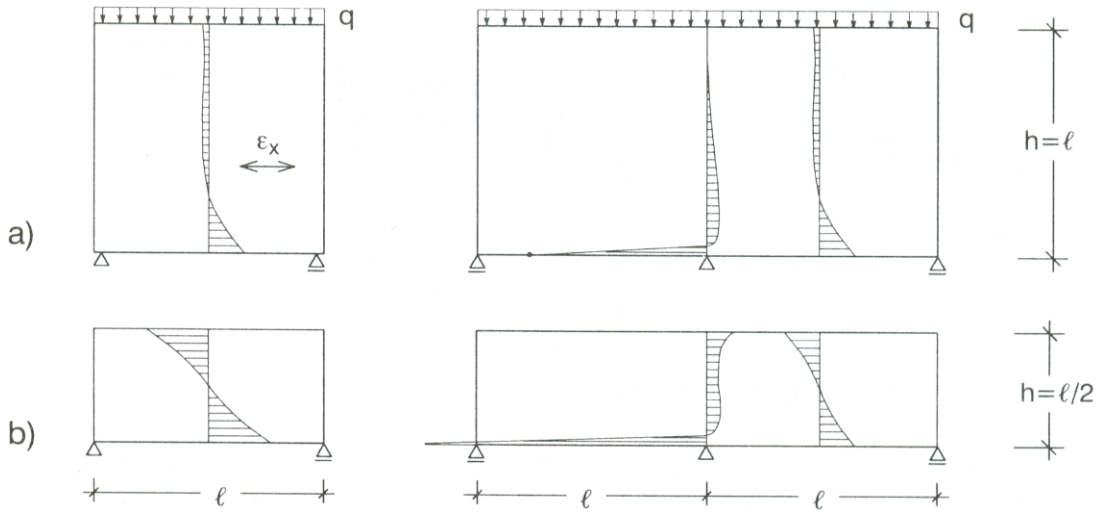


Fig. 7.3-1: Non-linear strain distribution in deep beams depending on l/h and boundary conditions

Unfortunately, the state of stress in such members cannot be derived section by section from the sectional effects *M, N, V*, as is normally the case for elements with small depth as compared to their span. The same applies also to those regions in beams and other members where the regular smooth stress distribution is disturbed due to discontinuities caused by either a member's geometry or concentrated loads. Geometrical discontinuities may be present in the shape of recesses, beam-column connections, openings, and all kinds of re-entrant corners or re-entrant edges between adjacent elements (Fig. 7.3-2 a and c). Statical discontinuities will develop for example from point loads, support reactions and prestressing anchor forces (Fig. 7.3-2 b and c).

For convenience and in recognition of the common mechanical behaviour, the name *D-region* is used for both, Deep beams and Discontinuity regions. The D fits also to Disturbed regions and Details, as discontinuity regions are frequently termed in practise. On the other hand, B-regions (from Bernoulli, Beams, Bending) are those for which the bending theory and standard design methods apply.

Copyright fib, all rights reserved. This PDF copy of fib Bulletin 54 is intended for use and/or distribution only within National Member Groups of fib.

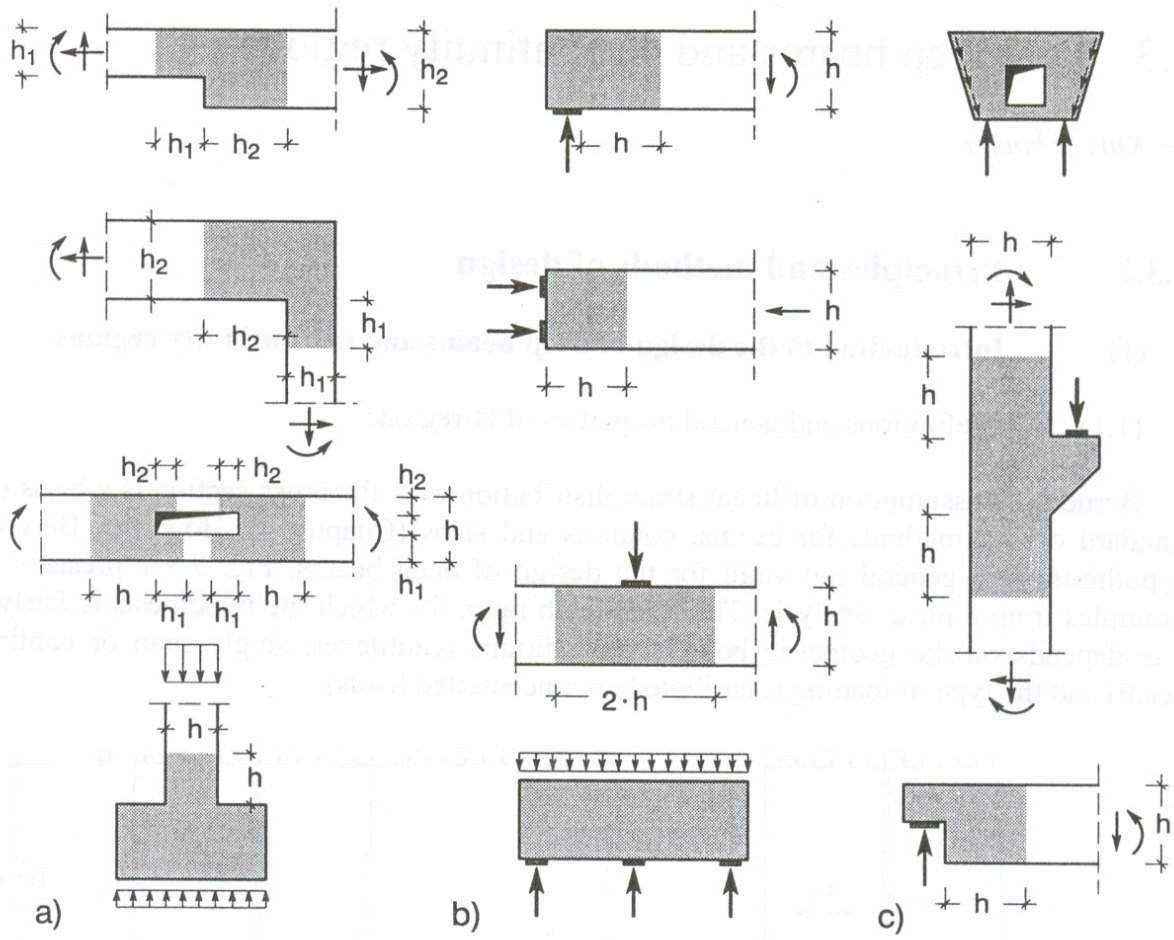


Fig. 7.3-2: D-regions (shaded areas) with nonlinear strain distribution due to: a) Geometrical discontinuities. b) Statical discontinuities. c) Statical and geometrical discontinuities

(1.2) The extent of D-regions

In B-regions, stresses and stress trajectories present a fairly smooth picture compared to their turbulent pattern near discontinuities (Fig. 7.3-3). Stress intensities decrease rapidly with the distance from the origin of the stress concentration, for example an edge, opening or bearing. This behaviour allows an approximate demarcation of B- and D-regions in a structure, according to the following rule:

The D-region is confined to an area extending from the origin of disturbance approximately as far as the thickness of the cross-section (Fig. 7.3-2) [Schlaich, Weischede (1982); Schlaich, Schäfer, Jennewein (1987); Schlaich, Schäfer (2001)]. If the member's depth is different on both sides of a cross-section, as for example in Fig. 7.3-2 a, then the length of the D-region to both sides is accordingly different.

The rule above is based on the Principle of Saint-Venant, which is not precise but good enough to serve as a qualitative aid for identifying regions with disturbed stress flow and for developing the strut-and-tie models. Moreover, the subdivision of a structure into its B- and D-regions is of considerable value for the understanding of the internal forces in the structure. It also demonstrates that simple span/depth ratios are not satisfactory to classify beams, deep beams, short/long corbels, etc. A proper classification of members with respect to their

Copyright fib, all rights reserved. This PDF copy of fib Bulletin 54 is intended for use and/or distribution only within National Member Groups of fib.

mechanical behaviour requires that, besides the geometry, the loading also has to be considered.

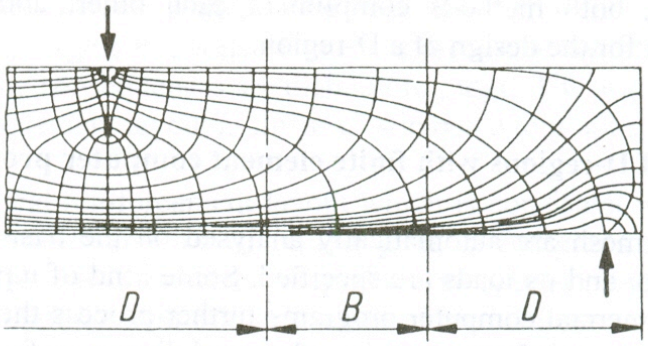


Fig. 7.3-3: Stress trajectories in a B-region and near discontinuities (D-regions)

(1.3) Overview over the design of D-regions

Normally, the D-regions are investigated like in-plane loaded plates. If the flow of forces in the D-region is substantially three-dimensional, it is convenient to investigate the body in orthogonal sections as two-dimensional structures. However, the relationship between the models in different planes must be accounted for by means of the interacting forces or stresses, and the three-dimensional strength capacities for the concrete apply.

Occasionally, it may become necessary to have a closer look at certain areas of the structure by means of local models. To this end, refined models of the specific regions of interest can be used, with the boundary conditions derived from an overall model.

As long as the D-regions remain uncracked, they can be readily analysed with linear-elastic methods, using for example a finite element program. After the formation of cracks, the tensile forces are transferred to reinforcement bars, which for practicality are placed parallel and orthogonal to the structure's edges. Frequently, large tensile forces are concentrated in layers of reinforcement. Thereby the flow of internal forces changes considerably and linear elastic analyses are no longer realistic. If the nonlinear effects are to be realistically considered, the computer analyses turn non-economical and the results are considerably dependent on the skill of the user and his choice of adequate input parameters.

The conventional treatment of D-regions according to 'past experience' or 'good practise', quite often with boundary conditions that are substantially different from reality, cannot be generally satisfactory. It has, indeed, been one of the main reasons for poor performance and failures of reinforced concrete elements.

For a methodical design of D-regions in the cracked state, the internal forces (or stresses) due to loads, prestressing forces and imposed deformations (if applicable) have to be determined and checked against the respective bearing capacities of the concrete and reinforcements.

In practise, two methods are applied for the analysis of the internal forces: linear finite element-programs (FEM) or strut-and-tie models (STM). Both methods have advantages and disadvantages and are preferable in different practical cases. This is discussed in more detail in Sections 7.3.1(2) and 7.3.1(3). Roughly simplifying, it can be summarised that a design based on FEM programs is easier to apply for complicated deep beams, but has drawbacks with concentrated forces, whilst STM are more advantageous for standard cases of deep

Copyright fib, all rights reserved. This PDF copy of fib Bulletin 54 is intended for use and/or distribution only within National Member Groups of fib.

beams and for all D-regions in beams, columns and foundations. STM provide advice also on the anchorage of reinforcement. Fortunately, both methods complement each other, and quite often it is reasonable to combine them for the design of a D-region.

(2) The design of D-regions with finite element computer programs (FEM)

The stresses in the FE mesh are automatically analysed on the basis of linear material behaviour, after the structure and its loads are specified. Some kind of input on the FE-mesh may also be required. Commercial computer programs further process the results to give the principal stresses and necessary reinforcements in orthogonal directions for a chosen grid.

If the results for two different mesh sizes differ considerably, the mesh should be refined. However, in the vicinity of singularities (point loads or re-entrant corners), convergence cannot be achieved, as the theoretical values of stresses approach infinity. Considering plastic behaviour of concrete under high pressures and the reinforcement spacing, a refinement of FE-meshes below that limit would not really improve the design and is impracticable. An upper limit of the mesh size cannot be specified in general, as it depends on the actual structural problem, the type of FE elements used in the program, the reinforcement layout and the importance of stresses in the region considered.

Questions may also arise about how to simplify the real boundary conditions (supports) for the FE-analysis. The results may differ considerably in the vicinity of a support area, if it is represented by either a point support, or a short line support, or several closely spaced point supports, or if a small support element is added to the structure in order to smooth the results in the structure itself [Rückert (1992)]. Again, it is one of the inherent shortcomings of FE-analysis that singularities are difficult to handle with this method and FE results for such areas are not applicable for cracked reinforced concrete.

For the ultimate limit state the reinforcement is proportioned using its design strength f_{yd}. However, the corresponding steel strain is not compatible with the elastic tensile strains analysed for the structure. Furthermore, the concrete will crack in areas with high tensile stresses. Both effects lead to a (relatively modest) redistribution of internal forces in the cracked structure. Although internal forces are somewhat different now than the linear FE-results, a structure so designed is safe, as justified by the lower bound theorem of plasticity (static limit theorem; see Section 4.1.3) and by ample experience.

A limited ductility is necessary for the redistribution of stresses. Therefore, ductility requirements are - besides crack distribution - another reason for providing a minimum reinforcement on all surfaces of concrete structures, in particular deep beams (Section 7.3.2).

The method of designing D-regions with FEM is so far very convenient, giving more or less automatically unique and safe results for the necessary reinforcement everywhere in the structure. The major problems of the method come up with the interpretation of the results and the development of a practical reinforcement layout.

If the structure is a large deep beam, the reinforcement can be equally spaced within strips, for which representative values of required reinforcement are taken from the FE-analysis. But in general it is better to concentrate the reinforcement near the of the structure's edges, which need reinforcement anyhow for crack distribution, for folded plate action, or for other effects not analysed. Such an arrangement of reinforcement is also statically more efficient (compare for example the lever arm z of the standard beam design with the lever arm $2/3 \cdot h$ from an elastic analysis). However, large deviations of the reinforcement layout from the FE-results

Copyright fib, all rights reserved. This PDF copy of fib Bulletin 54 is intended for use and/or distribution only within National Member Groups of fib.

should be avoided, since the consequences are difficult to judge. The arguments in Section 7.3.1(3.2.2) for orienting the reinforcement layout at linear elastic behaviour also apply here.

Finding a practical reinforcement layout that is consistent with the FE-results becomes more difficult with decreasing size of the D-region. In D-regions of linear members and slabs, for example beam-column-connections, it is normally not feasible and not necessary to arrange different strips of reinforcement over the depth of the element. In these cases the strut-and tie models (Section 7.3.1(3)) are, also for other reasons, clearly superior to FE-analyses.

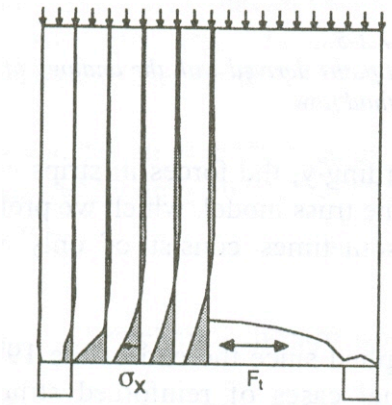


Fig. 7.3-4: Distribution of chord forces in a deep beam from a linear elastic FE-analysis. Horizontal stresses σ_x in vertical sections and resultant tension chord force F_t [Rückert (1992)]

Another problem is the anchorage of reinforcement, for which the (linear) FEM cannot give guidance, since the reinforcement is not modelled at all. It can be rather dangerous to derive anchorage forces and necessary reinforcements near supports or other discontinuities from linear FE-results. As an example, the chord forces in the span of a deep beam are in reality carried on by the reinforcement right into the node over the support, whilst the FEM tends to distribute them in a relatively wide tension field ahead of the node region (Fig. 7.3-4). It is therefore necessary to extend the chord reinforcement determined for the span of a deep beam with its full cross-section into the support nodes and to anchor the reinforcement there for the full force following the rules given in Sections 4.4.4 and 4.5.

(3) Design of deep beams and discontinuity regions with strut-and-tie models

(3.1) Principles of the method

The stresses or inner forces of a structure can be plotted and visualised in the form of trajectories (Fig. 7.3-3). A similar, but not identical mapping of the 'flow of forces' in a structure is possible, using a mechanical analogy between streamlines of fluids and force components in a plate (Fig. 7.3-5) [Fonseca (1995)]. The trajectory patterns or the streamlines of forces, flowing from the loaded edges through the structure into the supports, are indeed very helpful tools in order to correctly understand the load-bearing performance of a given structure, and they provide an instrumental aid for the designer.

However, these patterns are, in general, fairly complicated and, at best, available only for linear-elastic material behaviour. To obtain a more practical model of the structure, the stress trajectories or streamlines of individual compression stress fields can be condensed and straightened to form the struts of a truss model. Accordingly, the forces in strips of parallel

Copyright fib, all rights reserved. This PDF copy of fib Bulletin 54 is intended for use and/or distribution only within National Member Groups of fib.

reinforcement bars can be idealised to form the ties of the truss model, which we prefer to call *strut-and-tie model* (STM), because the models sometimes consist of only very few members.

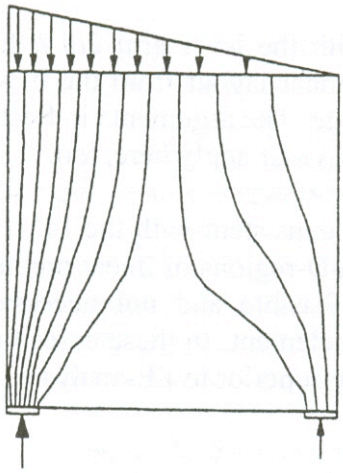


Fig. 7.3-5: Load paths derived with the analogy of force flow and fluid flow

Truss or strut-and-tie models were successfully applied since the end of the 19th century for beams, later on also for corbels and other special cases of reinforced structures. In particular, Swiss and Scandinavian engineers utilised parallel or fan-shaped stress fields to explain the real load bearing capacity of plane reinforced concrete structures by the theory of plasticity [Muttoni, Schwartz, Thürlimann (1997)]. Stimulated by J. Schlaich, the strut-and tie method was generalised and improved to be applicable to all kinds of reinforced concrete members and to entire structures [Schlaich, Weischede (1982); Schlaich, Schäfer, Jennewein (1987); Schlaich, Schäfer (1991); Schlaich, Schäfer (2001)]. Many authors in Canada and USA used similar approaches to trace forces in a structure. The Strut-and-Tie Bibliography of the American Concrete Institute lists about 300 references together with abstracts [ACI (1997)]. Meanwhile such methods are included in many building codes worldwide.

After or parallel with developing a strut-and-tie model, the forces in the struts and ties are determined. Afterwards the struts, ties and nodes (or, to be more precise, the concrete stresses and the reinforcements) are checked or proportioned for the forces derived, with due consideration of reinforcement bends and anchorage of forces (Sections 4.4.4 and 7.3.2). Reinforcement for crack control or nominal reinforcement to assure a reasonable ductile behaviour of the structure complements the design.

The safety of structures designed with stress fields or strut-and-tie models is based on the lower bound theorem of the theory of plasticity. Normally, no analytical check of compatibility conditions is performed for strut-and-tie models.

In order to avoid gross incompatibilities and to reasonably adapt the strut-and tie model to the real behaviour of the structure, the struts and ties of the model should be placed and oriented at the elastic stress pattern (Section 7.3.1(3.2.2)). The elastic stress pattern for the orientation of the model can be derived from a simple linear FE-analysis with a relatively coarse mesh, since the structure's singularities will be treated separately, when dimensioning the nodes of the strut-and-tie model (Section 4.4.4).

Before failure, the structure will adjust its internal forces to the model chosen for its design. However, this process is associated with plastic deformations, which depend on the quality of modelling. Reinforcing bars can endure a great amount of plastic deformation

Copyright fib, all rights reserved. This PDF copy of fib Bulletin 54 is intended for use and/or distribution only within National Member Groups of fib.

without loss of strength, but the concrete's ductility is very limited. Also some types of mesh reinforcement exhibit relatively low ductility [CEB (1993)].

If the model is reasonably oriented at the elastic behaviour, the plastic deformations necessary for stress redistribution will be easily tolerated by the materials. In this case, the plastic deformations are of a similar magnitude as for a design with linear FEM. However, a design based on a poor model can lead to a premature failure of a part of the structure, before it has fully adapted its internal forces to the design model. Furthermore, models that are not oriented at the elastic behaviour are susceptible to wide cracks in the serviceability limit state. To avoid such mistakes, detailed rules for strut-and-tie modelling are given in Section 7.3.1(3.2) and applied thereafter to different types of structures in Sections 7.3.2 - 7.3.5.

Since the design with stress fields is very similar to the strut-and-tie method, the following sections on STM apply in general also to the stress field method. Essential differences will be mentioned.

(3.2) Developing the strut-and-tie model

Developing a suitable model for a given D-region is very instructive but – like other engineering skills – requires some training and experience with the method. The following sections provide guidance for the modelling process and also include some warnings of frequent mistakes. Hastily drawn models rarely satisfy equilibrium, not to speak of compatibility. A systematic approach is therefore strongly recommended.

Three methods of modelling, which may also be combined, are explained: the most instructive one is the *load path method* described in Section 7.3.1(3.2.3). However, this method is not feasible in all cases. It works particularly well if the loads and support reactions are essentially vertical, as in deep beams. Always applicable and to some extent necessary is the method of developing the model from a linear elastic stress pattern (Section 7.3.1(3.2.4)). The fastest method is to adapt a known *typical model* to the special case, if the problems are related (Section 7.3.1(3.2.5)).

(3.2.1) Before modelling begins

As pointed out in Section 7.3.1(1.1), it is useful to identify the B- and D-regions of the structure and to choose division lines in-between them. If the structure contains B-regions, their sectional effects *M, N, V* are to be determined for a suitable static system, e.g. a frame or continuous beam, in the usual way. Thereby the system lines continue straight through the D-regions, e.g. beam-column connections or regions with openings. The sectional effects are used to design the B-regions, following the standard code rules for linear members or slabs (Section 4.4.1).

The internal forces from the B-regions in the chosen borderlines are further needed as loading of the D-regions in those sections. This method allows isolating a D-region from the structure and investigating it separately.

In general, three forces may act in the section between a B- and D-region, as known from the truss model of the beam: Two chord forces, F_c and F_t, and a diagonal compression force F_θ.

$$F_c = M/z + 0.5\ V \cot\theta$$
$$F_t = M/z - 0.5\ V \cot\theta$$
$$F_\theta = V / \sin\theta.$$

Copyright fib, all rights reserved. This PDF copy of fib Bulletin 54 is intended for use and/or distribution only within National Member Groups of fib.

The contribution of the shear force V to the chord forces is necessary for equilibrium. If it is omitted for the compression chord force applied to the D-region (as usually done for B-region design) then problems with the equilibrium of the model forces are to be expected. Another hint: Sometimes it is advantageous to represent the diagonal stress field by two parallel forces with the same resultant.

After the forces from the B-regions and all the other forces acting directly at the D-region are defined (including support reactions), the equilibrium of the isolated D-region should be checked. Unknown or wrong support forces are the most frequent causes of problems with modelling. Distributed loads acting inside the D-region, like weight, may for simplification be replaced by line loads acting at the edges.

(3.2.2) General rules and advice for modelling

a) It is recommended to look for rather simple models with a small number of struts and ties. If necessary, the model can be improved or refined later on.

b) Orienting the model at the elastic behaviour does not mean a perfect mapping of elastic behaviour, but rather adapting the main stream of forces to it. In particular the location and direction of struts with major forces should be oriented at the principal stress flow. Stress fields with low stress intensities may be represented more conveniently.

c) The model ties can be located to give a practical reinforcement layout with due regard to the ease of construction and an effective use of the reinforcement. Straight bars with few bends, arranged parallel and orthogonal to the edges of the member are to be preferred. The edges and surfaces of the structure should be fitted with near-surface reinforcement in order to control cracking. Several parallel bars in a tension stress field may be represented by a single model tie in their centre of gravity. The final reinforcement layout must conform to the model used for its design.

d) The angles θ between struts and ties in a node should be large, at least 45°, whenever possible (Fig. 7.3-6 a). Exceptions from this rule must be tolerated in the very frequent cases where a diagonal compression strut meets two ties which are orthogonal to each other (Fig. 7.3-6 b and c). In such cases reduced compression strengths apply, for example f_{cd2} for the node region (Section 4.4.4(2.3)). Angles smaller than 30° are unrealistic and involve high incompatibility of strains.

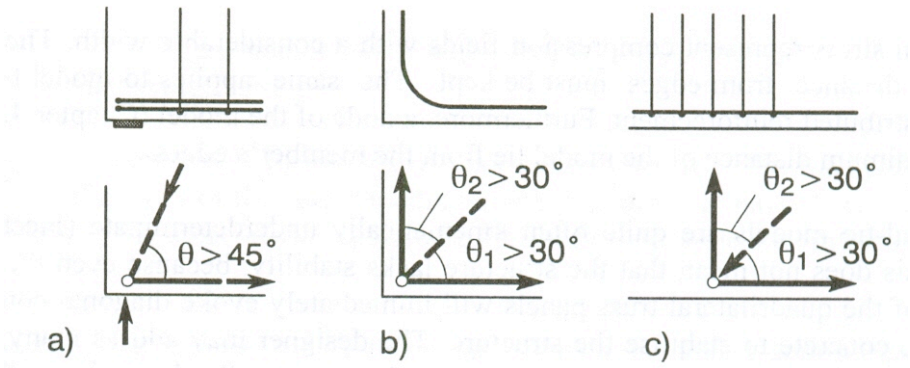


Fig. 7.3-6: Strut angles θ in compression-tension nodes and corresponding reinforcement (nominal reinforcement not shown).[1]
a) Tension in one direction. b) c) Tension in orthogonal directions

[1] In all figures with strut-and-tie models, the struts are drawn as thick dashed lines, the ties as thick solid lines.

Copyright fib, all rights reserved. This PDF copy of fib Bulletin 54 is intended for use and/or distribution only within National Member Groups of fib.

e) Concentrated forces like point loads, support reactions or anchor forces, which are applied to the edge or corner of a member, tend to spread in the member and may be represented according to Fig. 7.3-7 a and b. For point loads located right at the corner or far from the corner the angle of deviation derived from theory of elasticity is:

$\delta = 32.5^0$, corresponding to a strut angle $\theta = 62.5^0$.

This angle gives an idea about the ideal direction of the struts near the origin of concentrated forces and may serve as one clue for the orientation of major struts in the model. However, the stress resultants smoothly change direction with their distance from the origin and the model struts are chosen straight.

f) Depending on the shape and boundary conditions of the whole D-region, some divergence from ideal strut directions is inevitable and acceptable to arrive at a simple model. As an example, for the deep beam in Fig 7.3-7 c, a deviation angle δ up to 45° may be chosen, corresponding to a strut angle $\theta > 45°$ at the support node. For larger span/depth ratios the model in Fig 7.3-7 d with an intermediate vertical tie is more adequate with respect to the strut angle. Both models can also be combined as shown in Fig 7.3-7 e. This is a standard model for many applications, suitable for example for concentrated loads near the support of beams or for corbels and beam-column connections (Section 7.3.4). The statically indeterminate tie force F_w may be reasonably chosen, see paragraph k below), using for example the formula given in Fig. 7.3-7 e. This formula interpolates between $F_w = 0$ for $a < z/2$ and $F_w = F$ for $a > 2z$. The formula takes into account also the effect of a normal force N_{Sd}, (tension positive) which is not shown in the figure. For the design of the support node the angle θ of the resultant strut can be used.

g) Compression struts represent compression fields with a considerable width. Therefore an appropriate distance from edges must be kept. The same applies to model ties which represent distributed reinforcement. Furthermore, a node of the model (Section 4.4.4) may require a minimum distance of the model tie from the member's edges.

h) The strut-and-tie models quite often depict a kinematic mechanism. However, this does not mean that the structure lacks stability, because even the slightest movement of the quadrilateral truss panels will immediately evoke diagonal compressive forces in the concrete to stabilise the structure. The designer may add as many diagonal members to the model as required in order to make it statically determinate. These so-called "zero" members will not carry any significant forces and will not affect the flow of forces, provided that the kinematic model satisfies equilibrium for the given forces.

i) Kinematic models can be applied to one specific load case only. Therefore, the geometry of a kinematic model must be adapted to suit the specific load case. It is advisable to determine the forces in kinematic models already during the modelling process, because the equilibrium conditions for the nodes help to develop the geometry of the model after a few struts and ties have been chosen. The arrangement of reinforcement should ideally be designed to cover various load cases.

j) Contrary to kinematic models, a statically determinate strut-and-tie model will tolerate and cover a number of different load cases, although it is self-evident that one model cannot render an equally perfect representation of the various flows of forces for different load cases.

Copyright fib, all rights reserved. This PDF copy of fib Bulletin 54 is intended for use and/or distribution only within National Member Groups of fib.

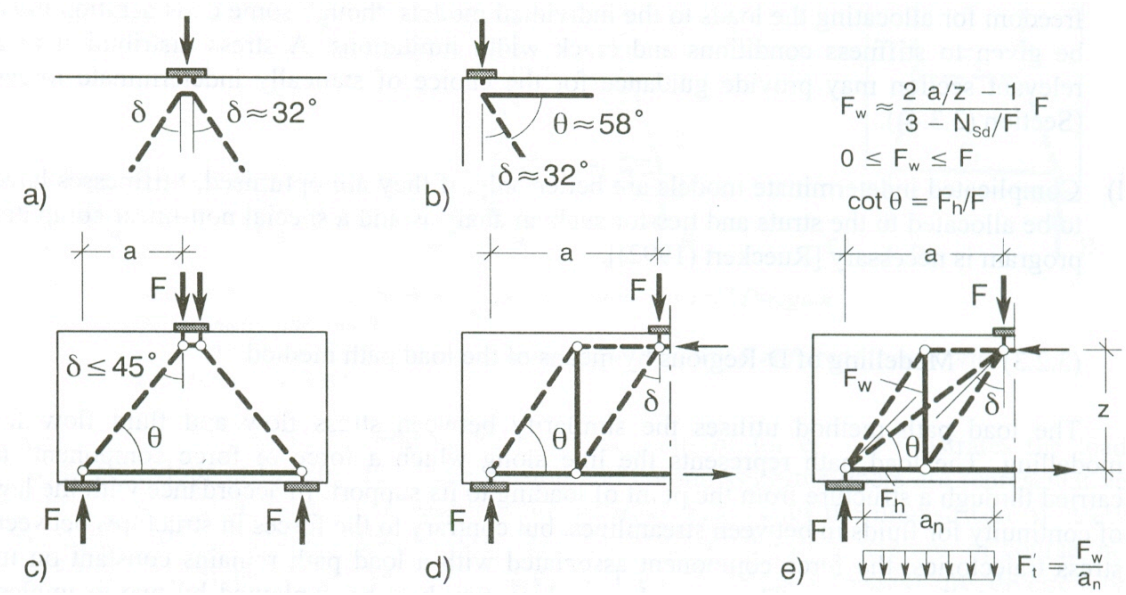


Fig 7.3-7: Change of direction of load paths.
a) Splitting of the concentrated force in order to represent the spreading of stresses.
b) Deviation of a concentrated force applied to a corner (compare Fig. 7.3-6 a).
c) Larger deviation angle δ taking into account the member's shape and its boundary conditions.
d) An intermediate model tie improves the angle θ between resultant struts and tie.
e) Combination of the two previous models

k) For a better representation of the real stress flow it is sometimes appropriate to superimpose two simple models, whereby each model must independently be able to establish equilibrium with part of the load applied (example in Section 7.3.5). There is ample freedom for allocating the loads to the individual models, though some consideration must be given to stiffness conditions and crack width limitations. A stress distribution in a relevant section may provide guidance for the choice of statically indeterminate forces (Section 7.3.1(3.3.4)).

l) Complicated indeterminate models are better only, if they are optimised. Stiffness values have to be allocated to the struts and ties for such an analysis and a special non-linear computer program is necessary [Rückert (1992)].

(3.2.3) Modelling of D-regions by means of the load path method

The load path method utilises the similarity between stress flow and fluid flow for modelling. The load path represents the line along which a force or force component[2] is carried through a structure from the point of loading to its support. In accordance with the law of continuity for fluids in between streamlines, but contrary to the forces in structures between stress trajectories, the force component associated with a load path remains constant on its way through the structure. The general procedure may best be explained by two examples. Further applications are presented in Section 7.3.5.

The D-region shown in Fig. 7.3-8 a is loaded by asymmetric linear stresses q from the adjoining B-region. The stress diagram is subdivided in such a way that the associated resulting loads in the upper part of the structure find their equivalent counterpart on the

[2] More precisely: the component of a force in a chosen direction, e.g. the vertical component of a load.

Copyright fib, all rights reserved. This PDF copy of fib Bulletin 54 is intended for use and/or distribution only within National Member Groups of fib.

opposite side. The pattern that develops when drawing a line to link the opposite forces is the so-called load path (Fig. 7.3-8 b).

It is self-evident that the load paths will not cross each other. The load paths begin and end at the centre of gravity of the corresponding stress diagram, and have there the direction of the applied loads or reactions. They tend to take the shortest possible streamlined way in between.

Considering that concentrated forces tend to spread out as fast as possible in the structure, the resulting load paths will show a pattern which, originating from the supports, will propagate inward and show its maximum curvature near the supports.

Until now, equilibrium has been considered only in the direction of the applied loads. The curvature of the load paths, however, gives rise to deviation forces F_c and F_t which, for the sake of simplicity, are plotted horizontally. Considering that the structure under review is not subject to horizontal loads, it follows that the deviation forces of the two load paths must balance each other.

Next, the horizontal deviation forces are replaced by a strut F_c and a tie F_t. Finally, the load paths are replaced by polygons, the break points of which intersect the resultants of the deviation forces (Fig. 7.3-8 c).

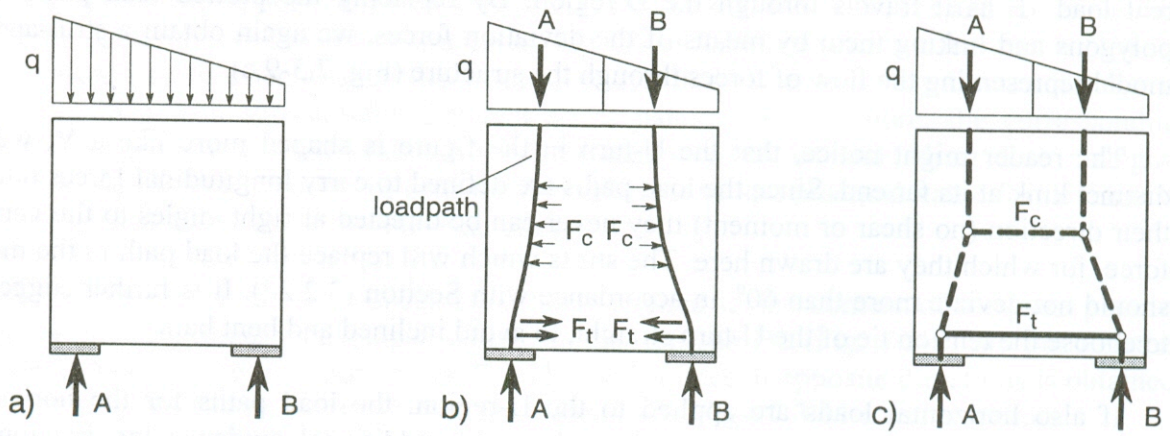


Fig. 7.3-8: Application of the load path method for modelling a typical D-region
a) Geometry and loading.
b) Load paths of the related loads; deviation forces F_c and F_t required for equilibrium.
c) Strut-and-tie model

The model developed in this way reflects the principal paths of forces and illustrates the load bearing behaviour of the structure. The tension and compression members are representative of curved two-dimensional or three-dimensional stress fields with the mainstream of stress orientated in the direction of their centrelines. The nodes of the members are, of course, no real hinges but rather entire regions where the internal forces (stresses) are diverted or introduced (anchored).

The second example shows a D-region which is supported on a B-region and loaded with a concentrated load F on one corner (Fig. 7.3-9 a). Proceeding as described above, the portion of stresses acting on the bottom part of the D-region is isolated in such a way that is in vertical equilibrium with the load F. Then a load path is drawn between F and the resultant of the isolated stresses (Fig. 7.3-9 b).

Copyright fib, all rights reserved. This PDF copy of fib Bulletin 54 is intended for use and/or distribution only within National Member Groups of fib.

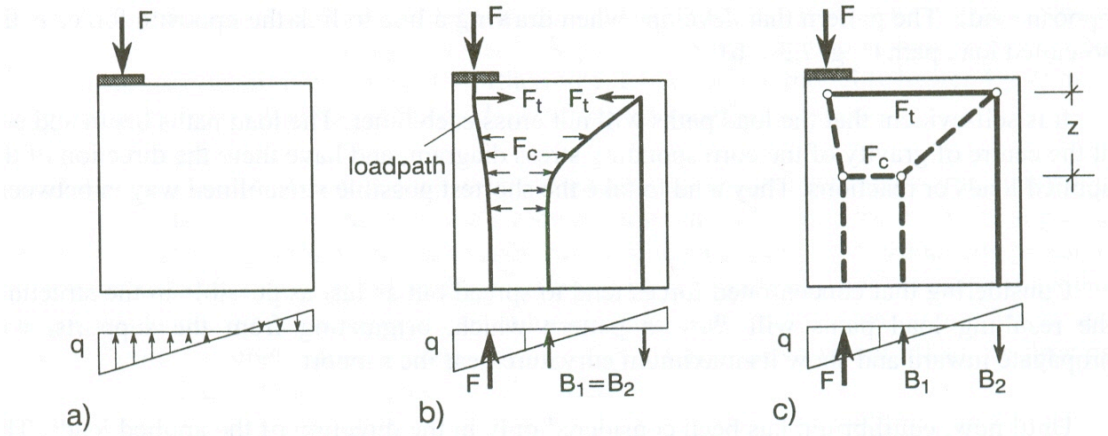


Fig. 7.3-9: Application of the load path method, including a U-turn
a) Geometry and loading.
b) Load paths and deviation forces.
c) Strut-and-tie model

However, there will remain two stress areas acting on the bottom part of the structure, with the resultants B1 and B2. These are equal in magnitude but have opposite directions. Their load path enters the D-region at B1, makes a U-turn and exits at B2. This U-turn of the load path and its associated deviation forces are necessary to equilibrate the deviation forces of the real load F as it travels through the D-region. By replacing the plotted load paths with polygons and linking them by means of the deviation forces, we again obtain a strut-and-tie model representing the flow of forces through the structure (Fig. 7.3-9 c).

The reader might notice that the U-turn in the figure is shaped more like a V, with a distinct kink at its far end. Since the load paths are defined to carry longitudinal forces only in their direction (no shear or moment) they never can be directed at right angles to the vertical force, for which they are drawn here. The struts which will replace the load path in the model should not deviate from the load direction more than 60°, in accordance with Section 7.3.1(3.2.2d). It is further suggested to choose the tension tie of the U-turn straight and parallel to the edge, to avoid inclined and curved bars.

If also horizontal loads are applied to the D-region, the load paths for the horizontal components may be mapped accordingly. They provide additional guidance for drawing the model.

(3.2.4) Developing the model from the elastic behaviour

In principle, a model can always be derived by combining and straightening bands of stress trajectories to form the struts and ties, but this method is suitable only for computer calculations [Rückert (1992)]. Normally, a plot of principal stresses is sufficient to orient the major struts, and the model is then developed according to the principles given in the previous sections (Fig. 7.3-10).

Furthermore, calculated stress distributions for individual sections allow locating important compression struts like F_c in Figs. 7.3-8, 7.3-9 and 7.3-10 more precisely in the centre of gravity of the compressive stress field. Thereby a rough estimate of the centre of gravity is sufficient. Moreover, a modest increase of the internal lever arm z will render the model more realistic and more economic, as are demonstrated by an example in Section 7.3.1(3.2.6).

Copyright fib, all rights reserved. This PDF copy of fib Bulletin 54 is intended for use and/or distribution only within National Member Groups of fib.

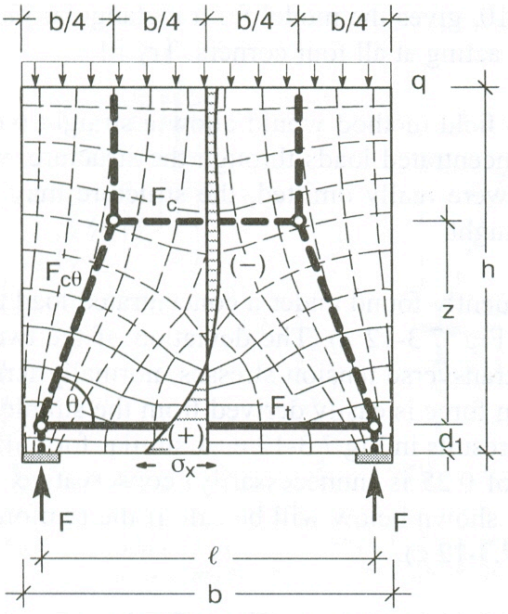


Fig. 7.3-10: Orienting the strut-and-tie model of a deep beam at the theory of elasticity. Linear elastic stress trajectories, stress distribution in the middle section and related strut-and-tie model

(3.2.5) Typical models

Anyone who has spent some time developing strut-and-tie models will observe that some typical models will appear over and over again in many different versions and combinations, even in apparently very different structures, see for example Fig. 16 in [Schlaich, Schäfer, Jennewein (1987)]. The reason for this phenomenon lies in the fact that there exist only a very limited number of discontinuities with substantially different stress patterns. Furthermore, the corresponding models are related to each other and can be easily combined and adjusted to changing geometric proportions. This is of considerable informative and practical value for developing models, as is shown with some examples.

Some typical models for concentrated loads applied to the corners of a square plate or deep beam were already developed above. For reference, the different typical D-regions are given names like D1, D2 etc. If two regions D2 (Fig. 7.3-9) are put together bottom to bottom, the D-region in Fig. 7.3-11 c with forces in opposite directions is obtained. By stretching the length *l* of the region, the typical region D4 appears (Figs. 7.3-11 a and b).

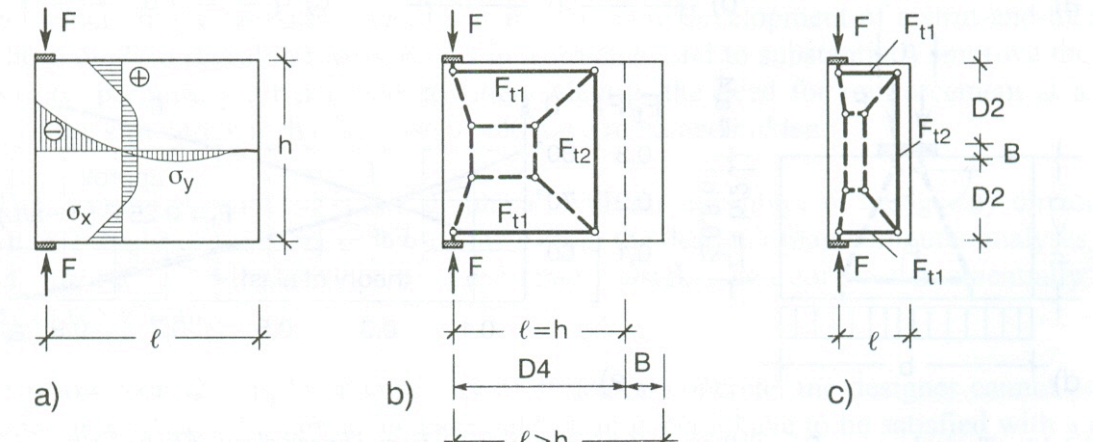


Fig. 7.3-11: Typical region D4: a) Stress diagrams (linear elastic) b) c) Strut-and-tie models for different ratios d/ l

Copyright fib, all rights reserved. This PDF copy of fib Bulletin 54 is intended for use and/or distribution only within National Member Groups of fib.

The same procedure, if applied to Fig. 7.3-10, produces the model for a rectangular plate with point loads acting at all four corners (D8 in [Schlaich, Schäfer (2001)]). Try it!

For these two types of D-regions the stress field method would allow a straight (column-type) strut with constant width to carry the concentrated loads through the structure, with no need for horizontal ties. However, if the ties were really omitted, the structure may fail by shearing off a corner, as major disasters have taught.

Another typical stress situation is very frequently found under a concentrated load applied to a plate or column in its axis of symmetry (Fig. 7.3-12 a). The deviation of the two force components on either side of the axis creates transverse tension stresses, normally termed as splitting tension. The following formula for the total tension force F_t is easily derived from the simple model in Fig. 7.3-12 b, and compared with the elastic results in Fig 7.3-12 e.

$$F_t = 0.25\, F\, (1 - a/b)$$

A similar formula given in the MC90, 3.3.2, with a factor 0.3 instead of 0.25 is (unnecessarily) conservative. A design based on the simple strut-and-tie model shown in Fig. 7.3-12 b is safe if the reinforcement is arranged in accordance with the model (Fig 7.3-12 c).

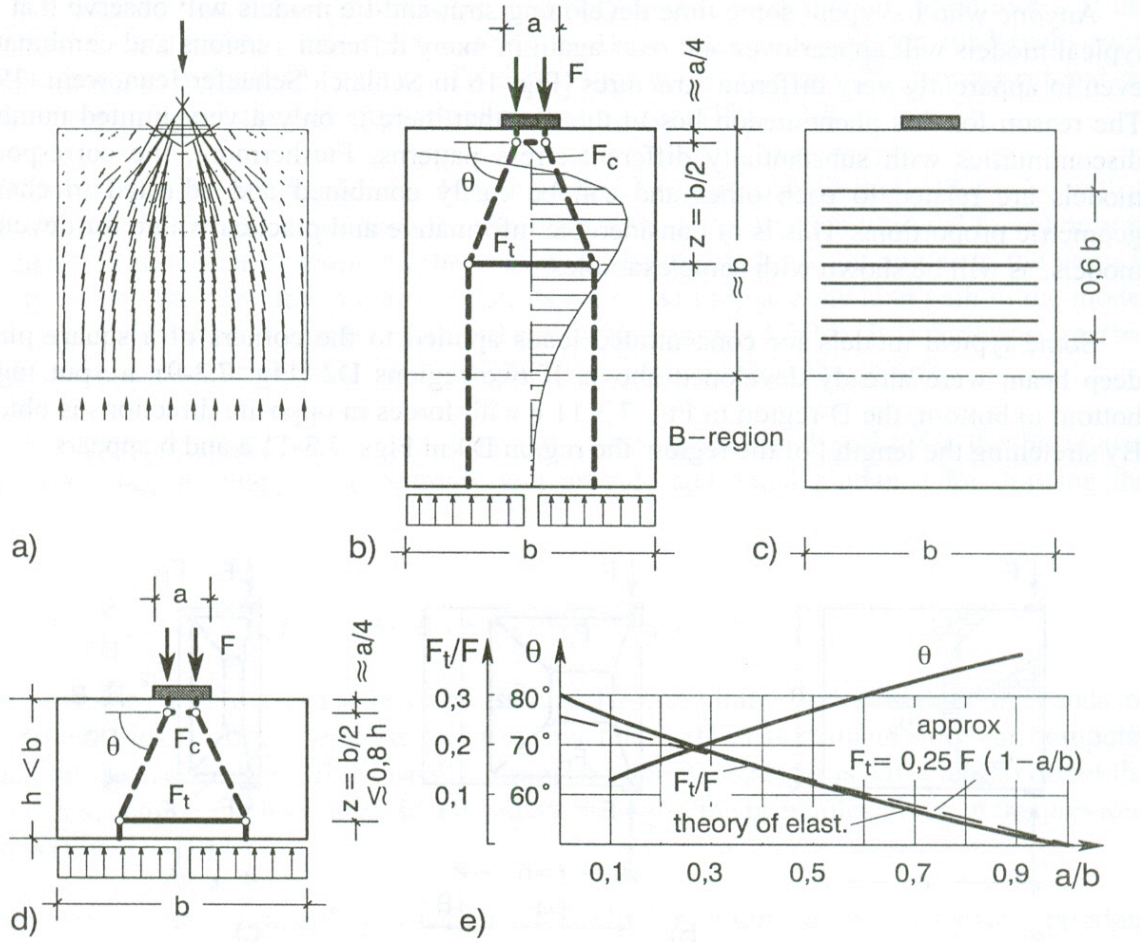


Fig. 7.3-12: Typical region D1. a) Pattern of principal stresses from a linear-elastic FE analysis. b) Strut-and-tie model with diagram of elastic stresses. c) Corresponding reinforcement for splitting tension (nominal reinforcement not shown). d) Strut-and-tie model for b>h. e) Internal force F_t and strut angle θ

Copyright fib, all rights reserved. This PDF copy of fib Bulletin 54 is intended for use and/or distribution only within National Member Groups of fib.

The simple model for the D7-region in Fig. 7.3-13 is obvious. The refined model is drawn here only to show how the individual struts themselves could be modelled with STM in order to examine the transverse tension in the stress field.

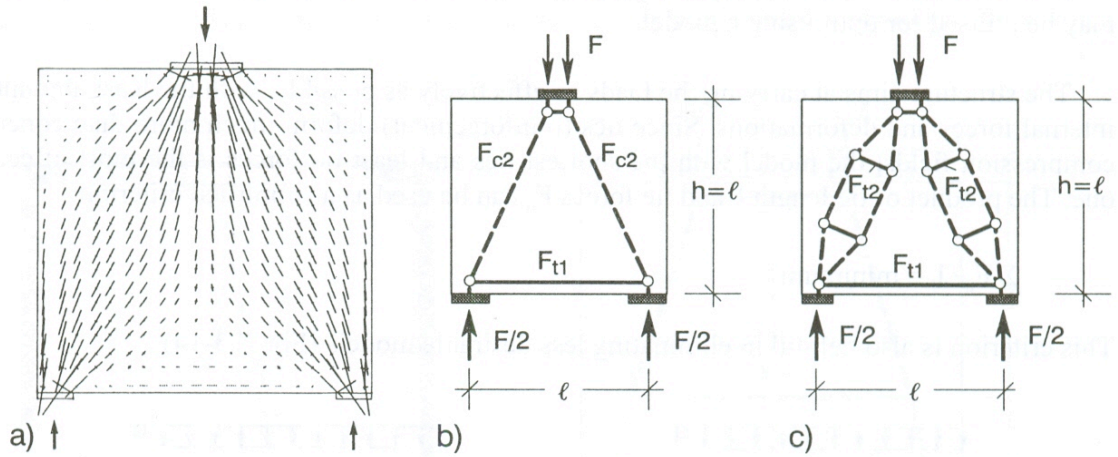


Fig. 7.3-13: Typical region D7. a) Principal stress pattern. b) Simple strut-and-tie model. c) Refined model showing the transverse tension in the struts

(3.2.6) Accuracy and optimisation of the strut-and-tie model

The result of the modelling process is not a unique solution, a fact which is sometimes considered as a major drawback of the strut-and-tie method. The reasons for this non-uniqueness are found firstly in the inherent properties and characteristics of structural concrete itself, the load-bearing behaviour of which is to a large extent influenced by the chosen reinforcement layout. This opportunity should be positively utilized to adapt the structure to the specific requirements of a given case (e.g. absolute dimensions, fabrication, and efficiency).

The second reason lies in the character of the method which is an approximate one. It is only reasonable to expect that a generalized procedure that would also be applicable to complex geometries cannot be as ”accurate” as a method that has been tailored to suit one specific problem and is calibrated from ample experimental feedback, as is the design of beams and plates.

However, even a crude design method that will consistently cover the basic load-bearing behaviour will certainly be more useful and safer than a more or less arbitrary choice of reinforcement in the D-regions. Occasionally, the mere development of a strut-and-tie model will be enough to reveal the weak points in a structure and to substantially improve its details, by permitting for instance, to safely identify the need for reinforcement at a given point of the structure which otherwise would have remained hidden.

The strut-and-tie method is half graphical, with the advantage of being very obvious and intuitive. It requires much more involvement from the designer than computer analyses and it is very instructive. All this helps to avoid major mistakes and essentially contributes to the safety of the structure.

Anyhow, considering the complexity of structural concrete, the designer cannot produce the optimum solution for any given case but will in general have to be satisfied with a design that is just a sufficiently good one. This is a target that an engineer with some experience in strut-and-tie modelling will easily achieve without clear (numerical) criteria for the adequacy of a model.

Copyright fib, all rights reserved. This PDF copy of fib Bulletin 54 is intended for use and/or distribution only within National Member Groups of fib.

In special cases or if a computer program supports the modelling, the following criteria may be utilised for optimising a model:

The structure aims at carrying the loads as effectively as possible, with the least amount of internal forces and deformations. Since ties (reinforcement) deform much more than concrete compression fields, the model with the shortest ties and least tie forces is the most effective one. The product of tie length l_i and tie forces F_{ti} can be used as a simplified criterion:

$$\Sigma F_{ti} \cdot l_i = \text{minimum}$$

where I denotes the number of tie. This criterion is also helpful in eliminating less desirable models (Fig. 7.3-14).

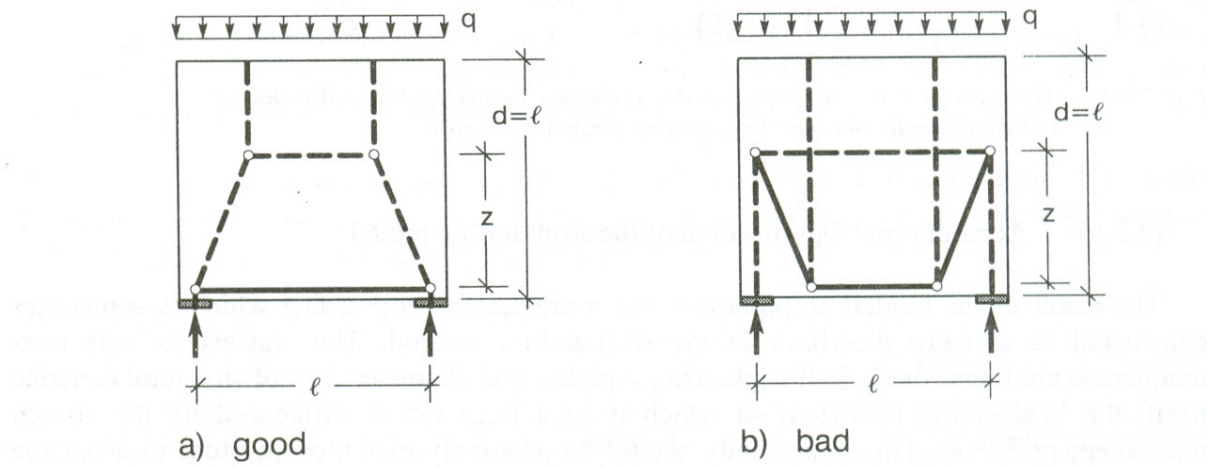


Fig. 7.3-14: Two different strut-and-tie models for the same structure. The good model (a) has shorter ties than the bad model (b)

For the exceptional case that the struts carry very high stresses over a substantial length (not only in the concentrated nodes) and are, therefore, exposed to high mean strains similar to the strain of the tie members, they should be introduced in the optimising criterion:

$$\Sigma F_i \cdot l_i \cdot \varepsilon_{mi} = \text{minimum}$$

where

F_i = force in the strut or tie member i
l_i = length of member i
ε_{mi} = mean strain of member i.

This approach would at the same time allow for the consideration of small strains of individual ties in rarely cracked or uncracked concrete. The above equation has some similarity with the principle of minimum strain energy for linear-elastic behaviour, but is modified for cracked reinforced concrete.

Strut-and-tie models allow a realistic assessment of the real ultimate capacity, if adapted to the crack pattern in the ULS. For example, the crack pattern of the test specimen in Fig. 7.3-15 a reveals, that the compression chord has ultimately shifted to the upper end of the deep beam. Fig. 7.3-15 b shows a strut-and-tie model, which is adapted to the real behaviour and takes into account also the nominal mesh reinforcement by the tie F_{t2}.

Copyright fib, all rights reserved. This PDF copy of fib Bulletin 54 is intended for use and/or distribution only within National Member Groups of fib.

Concluding from this model, 94% of the tested ultimate capacity can be safely carried, while a prediction based on elastic behaviour can explain only 40% of the real capacity. Nevertheless, with respect to crack distribution and rotation capacity, it is recommended not to depart too far from elastic behaviour.

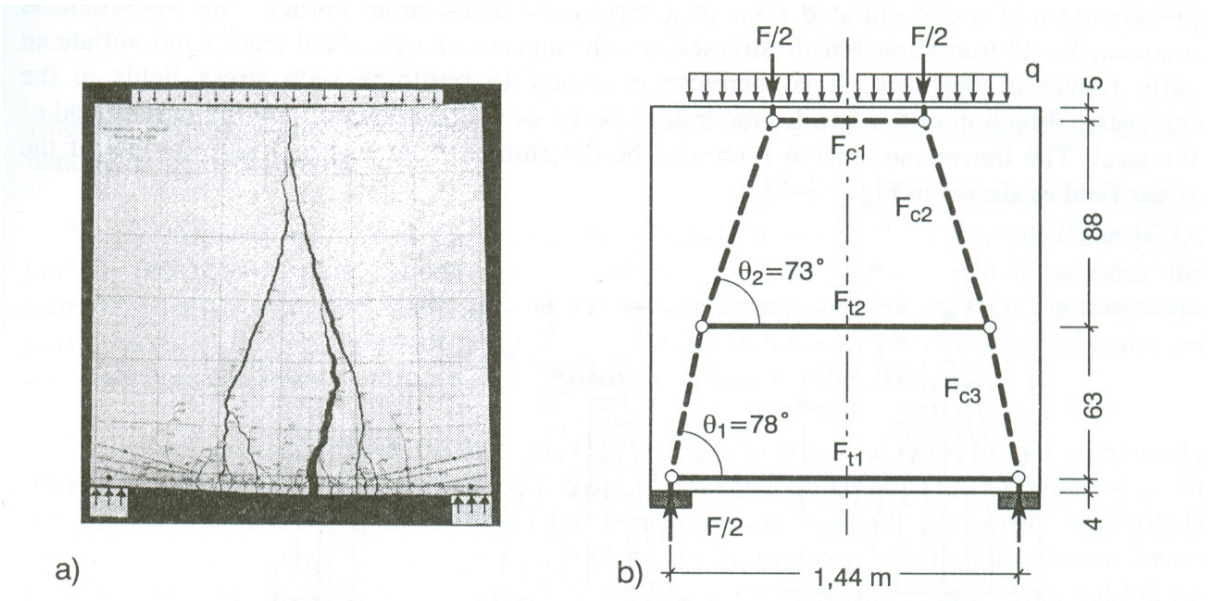


Fig. 7.3-15: Test of a deep beam.
a) Crack pattern before failure. b) Model explaining the ultimate capacity

(3.3) Checking the ties and struts

(3.3.1) Ties

As a general rule, tensile forces should be carried by reinforcing steel or prestressed steel. The necessary area of reinforcement for the ultimate limit state is derived from the design force F_{td} of the model tie and the design yield strength f_{yd} of the reinforcement. It is emphasised again, that the centroid and direction of the steel bars should coincide with the axis of the tie in the model.

For better crack distribution the reinforcement shall be distributed over the width of the tensile zone, which is represented by the model tie. If the model is reasonably oriented at elastic behaviour, crack limitations will in most cases be met by the calculated reinforcement and the minimum surface reinforcements prescribed for deep beams or other members in the code. In case of doubt, a check of crack width can be performed for a critical strip of the structure, which is treated like an independent reinforced concrete tension member.

For the serviceability limit state, sectional effects derived from a linear FEM analysis are normally more realistic and less sensitive to errors, as compared to STM-results.

The risk of wide cracks is particularly important when singular cracks starting from re-entrant corners or point loads intersect the reinforcement steel at acute angles. It is therefore recommended to either choose such a model where the reinforcement intersects the cracks at an angle as close to 90° as possible, or to add diagonal reinforcement, which is neglected in the model for simplification (Fig. 7.3-31). Otherwise, the critical reinforcement should be proportioned for lower stresses.

Copyright fib, all rights reserved. This PDF copy of fib Bulletin 54 is intended for use and/or distribution only within National Member Groups of fib.

(3.3.2) Concrete struts or compression stress fields

Typical for D-regions is the bottle-shaped stress field (Fig. 7.3-16 a) with its bottleneck proceeding into a concentrated node at a support or a re-entrant corner. This stress field is associated with transverse tensile stresses, which can cause longitudinal cracks and initiate an early failure of the strut. It is therefore necessary to reinforce such stress fields in the transverse direction or to consider the transverse tension when determining the failure load of the strut. The transverse tension force can be determined from a strut-and-tie model of the stress field as shown in Fig. 7.3-12.

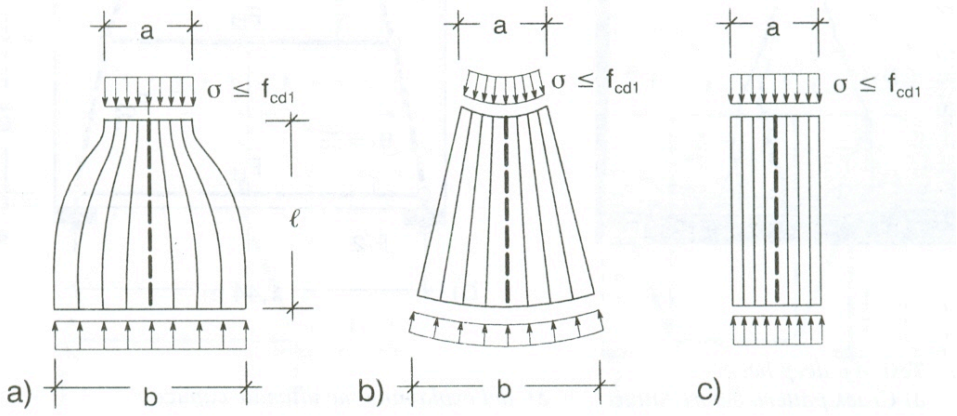


Fig. 7.3-16: The main compressive stress field configurations: a) the "bottle"; b) the "fan"; c) the "prism"

If the stress field has bottlenecks at both ends, as in Fig. 7.3-13, the transverse tension force occurs twice. However, such a stress field can adapt its stress flow to form a slimmer stress field in between the two nodes, resulting in a considerably reduced amount of transverse reinforcement. According to theory of plasticity, even the assumption of a parallel stress field in between the two nodes can be justified, in fact a very common simplification in applications of the stress field method [Muttoni, Schwartz, Thürlimann (1997)]. However, this is far from elastic behaviour and will provoke cracks, which may cause premature failure of the strut if not a minimal amount of transverse reinforcement is provided.

Fan-shaped stress fields (Fig. 7.3-16 b) allow a much better approximation of reality and are also frequently used for applications of theory of plasticity. A nominal transverse reinforcement is recommended also in this case, since stress trajectories tend to be curved in the real structure. The prismatic stress field (Fig. 7.3-16 c) is typical for B-regions and shall be treated like columns or the bending compression zone of beams.

The strength f_{cd1} of the concrete in compression stress fields depends to a considerable extent on the multi-axial state of stress as well as on disturbances from cracks and reinforcement [Collins, Vecchio (1982)]; [Baumann (1988)]; [Collins, Mitchell (1995)]. The MC90 allows in Clause 6.2.2.2 to determine the design resistance of a zone under essentially uniaxial compression to be calculated with a uniform stress diagram over the full area of this zone if appropriately selected. The average stress may be taken as

$$f_{cd1} = 0.85\left[1-\frac{f_{ck}}{250}\right]f_{cd} \qquad \text{for uncracked zones}$$

Copyright fib, all rights reserved. This PDF copy of fib Bulletin 54 is intended for use and/or distribution only within National Member Groups of fib.

$$f_{cd2} = 0.60\left[1-\frac{f_{ck}}{250}\right]f_{cd} \qquad \text{for cracked zones}$$

where the maximum extreme fibre strain is restricted to limits similar to those for the compression zone in beams.

Based on many panel tests carried out by Collins and others, the Canadian Code [CSA (1994)] provides a more refined formula for the concrete strength which includes the transverse tensile strain as a main parameter. Implicating the code-formula for the transverse tensile strain in the concrete strength formula will result in a strong dependence of the concrete resistance on the angle between struts and ties (compare the rules in Section 7.3.1(3.3.2)).

Except for prismatic stress-fields, the design strength of stress fields is, in fact, very rarely needed in practise. The reasons are firstly, that critical concrete stresses in D-regions occur in the regions of concentrated nodes. These are adjacent to the "bottle necks" of the stress fields and are checked with the node design (Section 4.4.4). Furthermore, the parallel stress fields in B-regions are checked otherwise with standard methods for moment, shear and normal forces.

Finally, these standard methods are in practise also frequently applicable to D-regions of beams, frames and other "linear" members.

7.3.2 Deep beams

(1) General

(1.1) Recommendations for the design and reinforcement

For many regular cases of deep beams, the typical strut-and tie models as illustrated in Section 7.3.1(3.2) can be directly applied to determine a suitable layout and the necessary cross-sections of the reinforcement necessary for ultimate load conditions.

For proportioning the reinforcement, it is recommended to begin with the "additional reinforcement" according to subclause 9.5.1.1.2 of MC90, which is 0.2 % of the concrete cross-section in both orthogonal directions. These reinforcements, consisting of relatively thin bars, are arranged on both faces (0.1 % for each face), the horizontal reinforcement normally inside the vertical bars. Straight bars of these reinforcements should overlap near the edges with loop-shaped bars arranged there, or stirrup type reinforcement should be chosen. The surface reinforcements can also be credited to ultimate load conditions and need to be supplemented only locally for major tie forces, in particular for chord forces along the edges. In areas with considerable tensile stresses, where the formation of cracks is to be expected, either from loads or restraints or both, the reinforcement should be designed for crack distribution according to MC90 subclause 7.4 and the rules in Sections 7.3.1(3.2.2) and (3.3.1) above.

Copyright fib, all rights reserved. This PDF copy of fib Bulletin 54 is intended for use and/or distribution only within National Member Groups of fib.

At least two thicker corner bars should be placed along all edges of deep beams, for different reasons not accounted for in the analysis, such as folded plate action or restraints or differential settlement (see Section 7.3.2(2.1), Fig. 7.3-20 a).

Major chord reinforcement along edges should be placed in several layers, to increase the depth u of the node regions over supports and to ease the anchorage of reinforcement there (Section 4.4.4). MC90, subclause 9.2.5.1.1, recommends a depth of 0.12 h or 0.12 l (whichever is less), for the reinforcement in single span deep beams. For the same reasons, additional horizontal loops placed above the chord reinforcement may be necessary at end supports. The support regions of deep beams are normally the critical regions of the structure. They should be detailed and checked very carefully according to the rules outlined in Section 4.4.4.

Model ties at some distance from edges, as for example the chord reinforcement for negative moments in continuous deep beams, represent wide tensile stress fields and should therefore be distributed over a corresponding depth of e.g. 0.6 h, or 0.6 l if $l < h$. Stress-diagrams from a simple linear FE-analysis provide good guidance for the appropriate height and distribution of such reinforcements (see also Fig. 7.3-10, Fig. 7.3-12 and MC90, subclause 9.2.5.2).

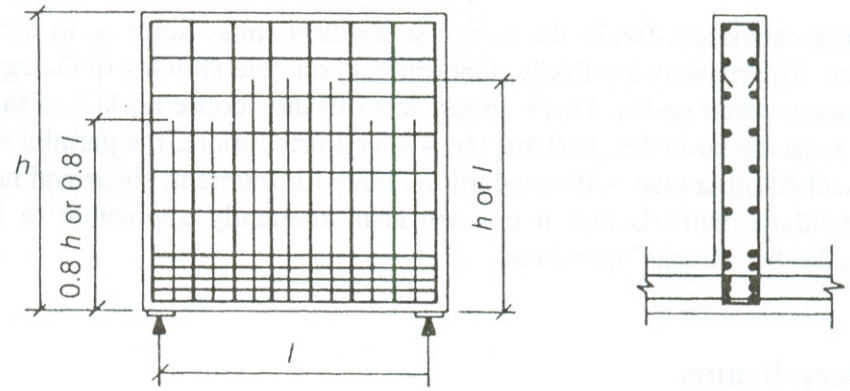


Fig. 7.3-17: Recommended reinforcement layout in a deep beam for loads from a lower floor (schematic) [MC90, Fig. 9.2.7]

Suspended loads, e.g. from a slab at the bottom of the deep beam, call for additional stirrup-type reinforcement in order to hang the load on the compression chord, comparable to the hangers of an arch bridge with suspended deck (Fig. 7.3-17). Concentrated suspended loads may be treated in the same way (Fig. 7.3-18 a, or, if the load is large, bent-up bars may be provided (Fig. 7.3-18 b). These help to avoid reinforcement congestion and reduce the tension chord force.

Copyright fib, all rights reserved. This PDF copy of fib Bulletin 54 is intended for use and/or distribution only within National Member Groups of fib.

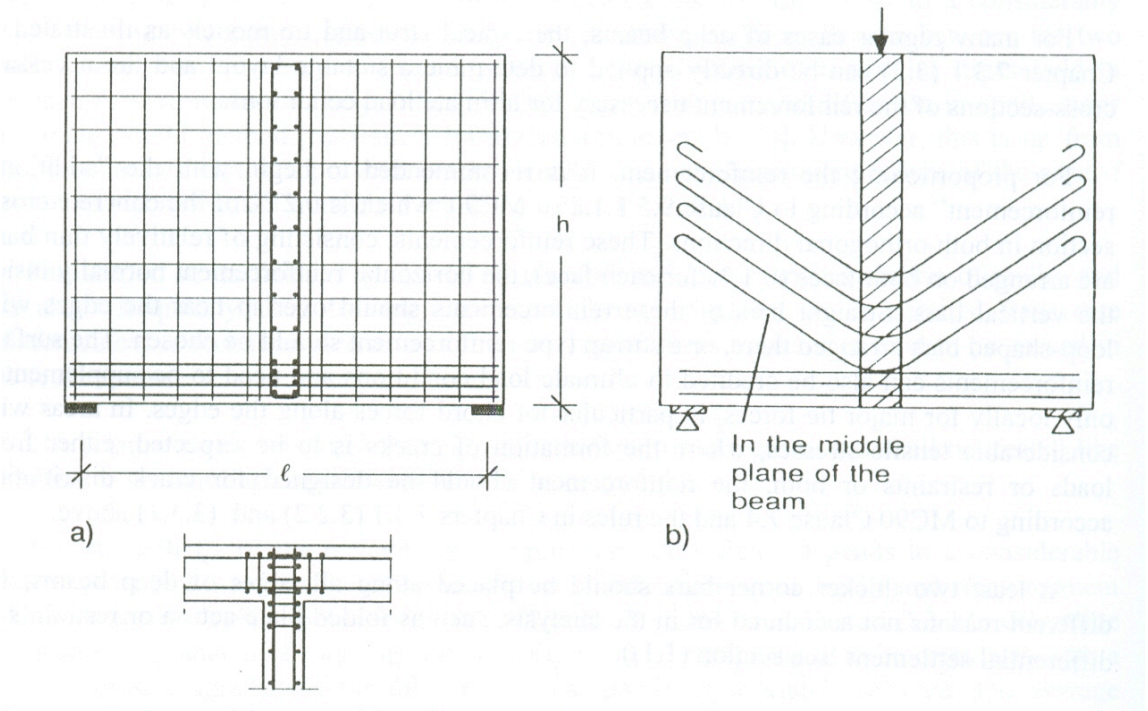


Fig. 7.3-18: Deep beams with hanging reinforcement for indirect support of another deep beam.
a) Vertical hanging reinforcement at the common edge
b) Diagonal hanging reinforcement for vertically distributed load [MC90, Fig. 9.2.8]

Concentrated suspended loads result e.g. from cross-beams that are supported by main beams (indirect support). Three different possibilities of load transfer may be considered:

a) Normally, the cross-beam is assumed to transfer its load to the bottom corners, as if it were supported there by bearings. The support reaction from the cross-beam is then applied as a suspended load to the main beam. The vertical reinforcement for the suspended load should preferably be arranged within the common volume of the two intersecting beams, or very close to it (Fig. 7.3-18 a). Otherwise, considerable additional horizontal reinforcement may be necessary for equilibrium.

b) As an alternative, which avoids the concentrated node in the lower corner, the transfer of shear forces between the two beams can be assumed to be distributed over some depth of the beam. Since the vertical shear is actually transmitted by diagonal concrete compression stresses, horizontal equilibrium at any point of the vertical edge requires horizontal (or diagonal) reinforcements (Fig. 7.3-19 a). These reinforcements need to be placed in accordance with the assumed distribution of shear forces over the depth of the beam, and they must be anchored within the common edge region with loops. They constitute part of the beam's tension chord which has shifted upward near the support as compared with the alternative (a).

   If Fig. 7.3-19 a is turned anti-clockwise by 90°, the similarity to the tension chord of a beam with diagonal compression and stirrups becomes obvious. This is a very typical situation for edges in all kinds of reinforced concrete structures.

c) Another alternative for better distribution of forces near the support is explained by Fig. 7.3-19 b. It has the advantage that the internal lever arm of the chord forces in the span is the same as for the standard case (a). Note that the diagonal concrete stresses in the corner area amount to twice the strut force F_c divided by the (enlarged) cross-section of the strut! The tension forces F_{t2} and F_{t3}, for which additional reinforcements in orthogonal

Copyright fib, all rights reserved. This PDF copy of fib Bulletin 54 is intended for use and/or distribution only within National Member Groups of fib.

directions are to be provided, are equal to the main chord force F_{t1} and the support force V, respectively. Remember also, that the model node indicates the centre of the development length of reinforcement, and that reinforcements must extend beyond the model node by at least half of the development length.

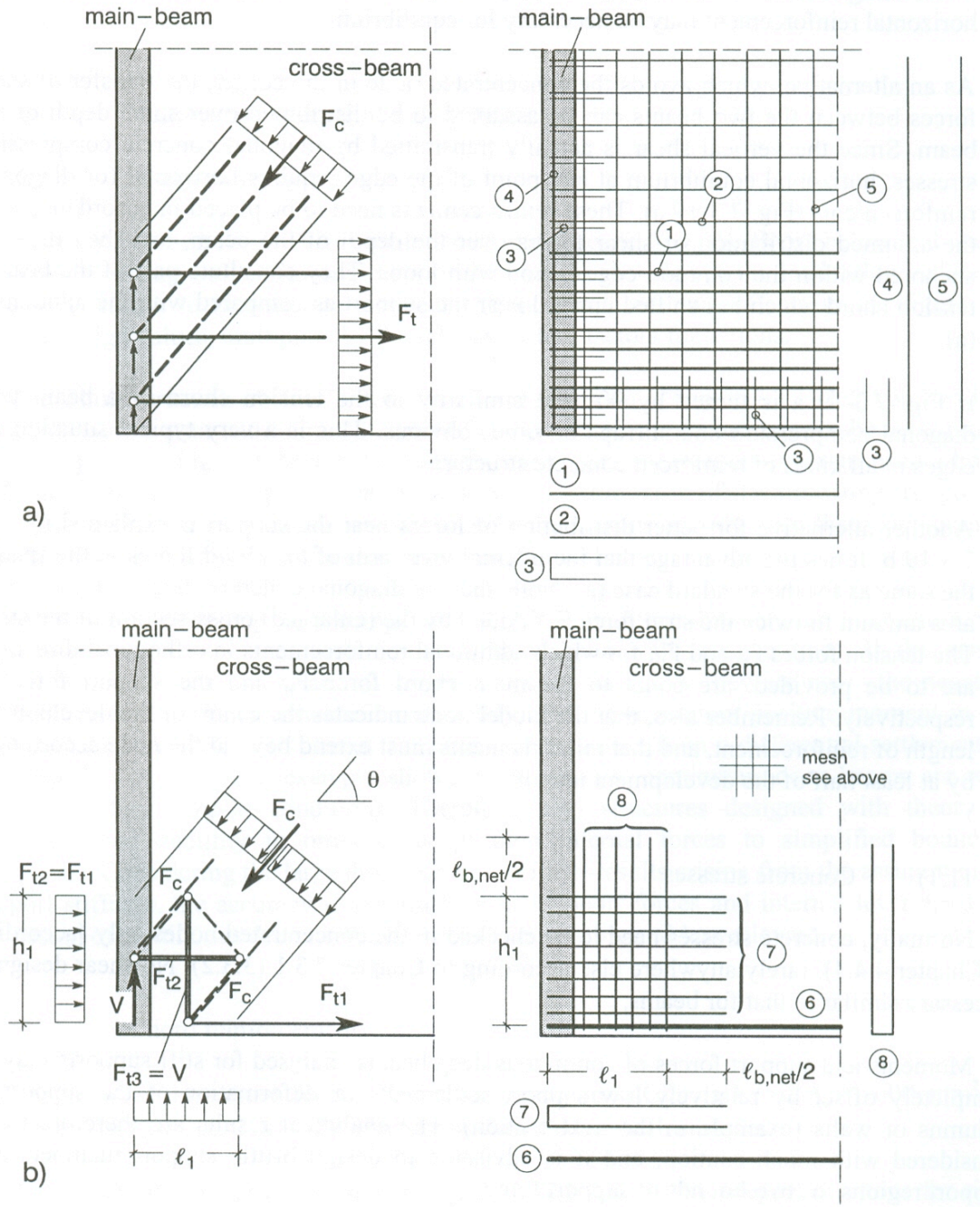


Fig. 7.3-19: Distributed transfer of shear forces between deep beams.
a) Model showing the horizontal reinforcement and the associated upward shift of the tension chord.
b) Another model and the corresponding reinforcement mesh for avoiding a concentrated node in the corner

Copyright fib, all rights reserved. This PDF copy of fib Bulletin 54 is intended for use and/or distribution only within National Member Groups of fib.

(1.2) Concrete stresses in deep beams

Normally, concrete stresses need to be checked in the concentrated nodes only (according to Section 4.4.4), rarely anywhere else according to Section 7.3.1(3.3.2). No shear design is necessary similar to that for beams.

Moments and support forces of continuous deep beams analysed for stiff supports may be completely offset by relatively low support settlements or deformation of the supporting columns or walls (example in the next section). The analytical results are therefore to be considered with much caution, and it is advisable to design brittle support members and support regions for two bounds of support force.

On the other hand, a continuous deep beam has to undergo only very small deformations to adapt its inner forces and support reactions to those from an approximate analysis. A nominal surface reinforcement, as required by code rules, should provide the necessary ductility of the structure.

There was much debate, whether class B steel is sufficiently ductile for the application of plastic methods. MC90, subclause 5.6.3, does not allow type B steel to be used in structures that are designed with statically admissible stress fields, which are the basis of the strut-and-tie method, too. However, the author's opinion on this matter is that for deep beams also welded reinforcement meshes of class B steel can be used as nominal reinforcement, if the design model is reasonably oriented at the elastic behaviour. If there were any danger with respect to steel ductility in deep beams, class B steel ought to be excluded also for continuous deep beams that are designed with linear elasticity (see next section).

(2) Numerical example of a deep beam

(2.1) Structural analysis

The deep beam in Fig. 7.3-20 transfers distributed loads from the floors below and above to three supporting walls. The dead load of the beam is included in the load below, which is safe with respect to hanging reinforcement. Loads and sectional effects in the figure are already design values, multiplied by the relevant safety factors for actions.

The whole structure obviously consists of one D-region (Section 7.3.1(1.1)) and will be designed using a strut-and-tie model. First of all, the support reactions have to be determined. They are given in Fig. 7.3-20 together with the corresponding moment diagram from a linear FEM-analysis for rigid supports (solid line), which is the basis of the following design. As expected, the negative moment of the deep beam is considerably less than the moment obtained from bending theory for slender beams (dotted line).

Much more surprising is a comparison with the moment diagram for a structure, the support of which is a 3 m high column instead of a wall (dashed line). If the elastic deformations of the supports are taken into account – normally they are not – the negative moments over the support disappear completely, and the maximum positive moment in the span increases by a factor of almost 2. These changes result from a differential settlement of less than 0.6 mm (!). The example shows, how sensitive continuous deep beams are with respect to their support conditions. Therefore, also structures designed with theory of elasticity need ductility in order to adapt their internal forces to simplified boundary conditions. Considering the large discrepancies of FEM-results arising from the assumption of support stiffness, the accuracy in determining the support forces and internal lever arms for the design of continuous deep beams becomes questionable and less relevant.

Copyright fib, all rights reserved. This PDF copy of fib Bulletin 54 is intended for use and/or distribution only within National Member Groups of fib.

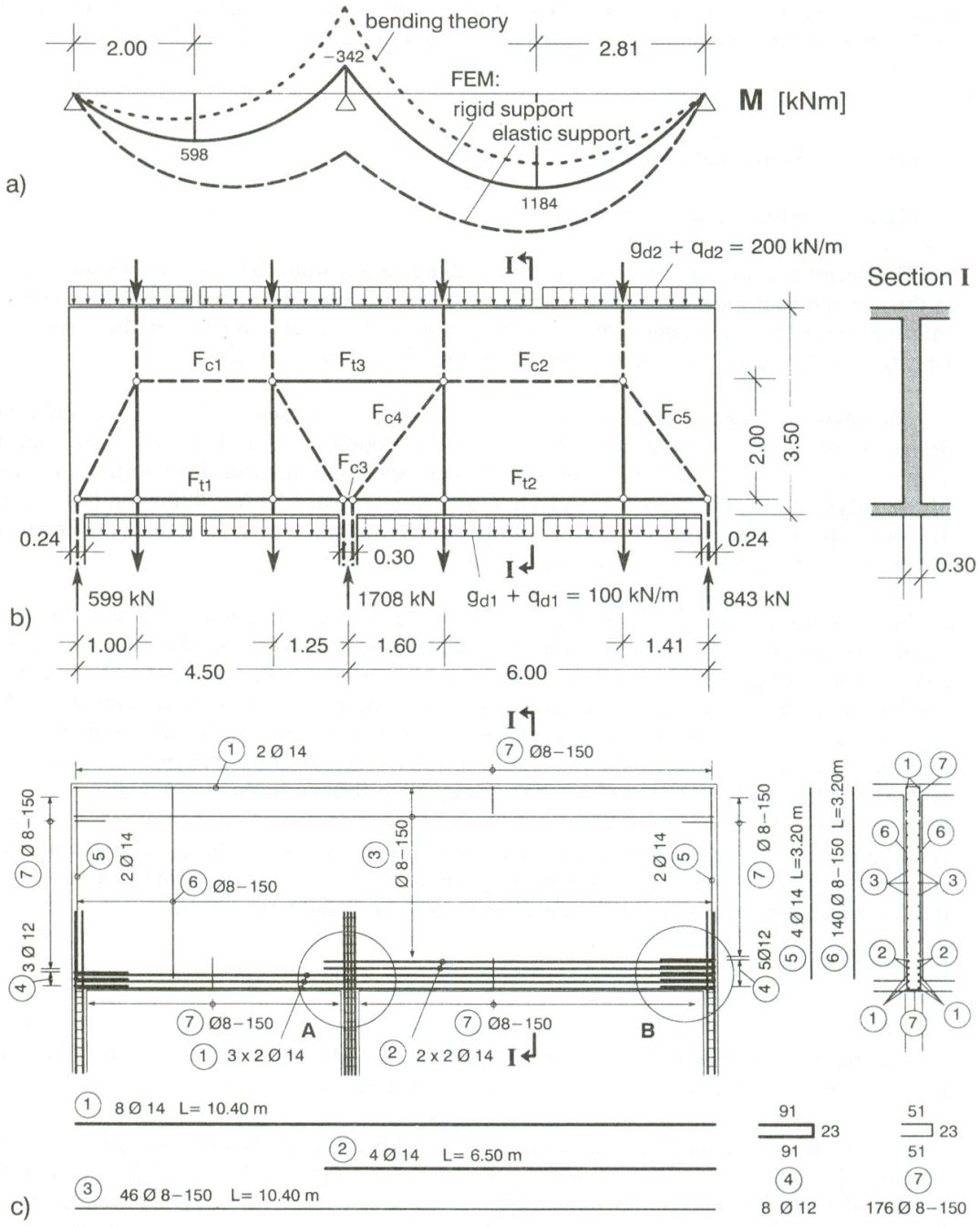


Fig. 7.3-20: Continuous deep beam (concrete C30/37, steel S500). a) Sectional effects. b) Strut-and-tie model. c) Reinforcement

(2.2) Model and reinforcement

The required minimum reinforcement according to MC90 is $0.002 \cdot A_c$ = 600 mm^2/m. Reinforcement meshes ∅ 8 – 150 mm will be provided on both surfaces, where 150 mm is the spacing of bars.

A strut-and-tie model is drawn in Fig. 7.3-20 b, based on the support reactions for rigid support. The model follows from the load path method (Section 7.3.1(3.2.3)). It could also be composed of the two standard models in Fig. 7.3-10 for the two spans and Fig. 7.3-12 (upside

Copyright fib, all rights reserved. This PDF copy of fib Bulletin 54 is intended for use and/or distribution only within National Member Groups of fib.

down) for the interior support. For simplicity, the internal lever arm is chosen to be constant, about 40% of the average span l_m, an assumption which is somewhat conservative for the larger span and safe enough for the smaller span and the support chord (Fig. 7.3-15). Different lever arms could be considered in a refined model [Schlaich/Schäfer (2001)].

The horizontal strut and tie forces can be derived from the equilibrium of the model nodes or, if available, much faster from the moments (Fig. 7.3-12 a) divided by the lever arm.

Using f_{yd} = 500/1.15 = 435 N/mm^2 as design strength, the following chord forces and reinforcements are derived:

$F_{t1} = F_{c1}$ = 598/2.00 = 299 kN $A_{s,\,req}$ = 687 mm^2 → 6 ∅ 14 mm
$F_{t2} = F_{c2}$ = 1184/2.00 = 592 kN $A_{s,\,req}$ = 1363 mm^2 → 10 ∅ 14 mm
$F_{t3} = F_{c1}$ = 342/2.00 = 171 kN $A_{s,\,req}$ = 393 mm^2 → 2 ∅ 8 - 150 mm.

Rules for placing the tensile reinforcement over the supports are given in MC90, subclause 9.2.5.2: The upper strip (Fig. 7.3-21) should be reinforced with a fraction of the required reinforcement that is interpolated between 0% for $l \le h$ and 100% for $l \ge 3\ h$, and some additional reinforcement should be placed near the upper face in cases where $l < h$. In the example, the required chord reinforcement for the negative moment is much less than the minimum mesh reinforcement within any reasonably chosen bandwidth for the reinforcement. Therefore, no extra reinforcement is necessary for F_{t3} (Fig. 7.3-20 b).

The nominal reinforcement is also sufficient to hang the lower slab into the compression chords of the span:

$a_{s,req} = (g_{d1} + q_{d1}) / f_{yd}$ = 100 000 / 435 = 230 mm^2/m
< 670 mm^2/m (2 ∅ 8 - 150 mm)

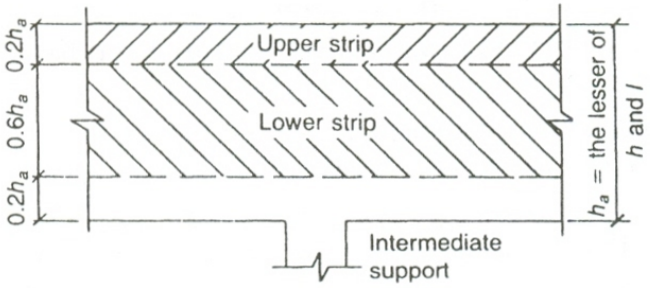


Fig. 7.3-21: Recommended distribution of reinforcement over an intermediate support [MC90, Fig. 9.2.3]

(2.3) Concrete stresses and node regions

Concrete stresses of the deep beam need to be checked only in the node regions with concentrated forces, i.e. the support nodes.

(2.3.1) End supports

Both end support regions are in principle standard compression-tension nodes according to Fig. 4.4-93. Only the end support of the large span will be considered here, as an example (Fig. 7.3-22). This node is particular insofar, as node stresses are quite high and compression reinforcement is necessary to resist the support reaction V_{Sd} = 843 kN.

Copyright fib, all rights reserved. This PDF copy of fib Bulletin 54 is intended for use and/or distribution only within National Member Groups of fib.

The standard node region is determined by the width of the deep beam (b = 0.30 m), the length of the bearing (a_1 = 0.24 m), the depth of the node u, and the strut angle $\theta = 54.9^0$. This angle results from the chosen model or can be evaluated from $\tan\theta = V/H$, where H denotes the tie force to be anchored in the node ($H = F_{t2}$ = 592 kN). The choice of u = 0.42 m corresponds with the recommended width of the tension chord of approximately 0.12 h ($h < l$) in MC90, subclause 9.2.5.1.1.

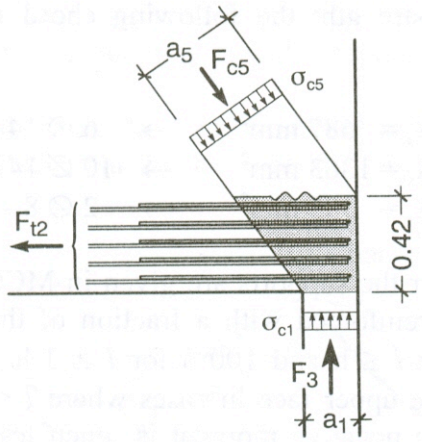


Fig. 7.3-22: End-support-node region of the deep beam in Fig.7.3-20.

(a) Bearing stress

Considering the favourable strut angle and the well distributed chord reinforcement, the design strength $f_{cd1\text{-}2}$ from Eq. 4.4-119 b is applicable as concrete bearing stress σ_{c1} in the support area A_{c1}. The vertical steel bars, 4 ∅16, contribute with their design strength f_{yd} to the total bearing capacity V_{Rd}:

$$V_{Rd} = a_1\, b\, f_{cd1\text{-}2} + A_s f_{yd}$$
$$= 0.24 \cdot 0.30 \cdot 8.6 + 804 \cdot 10^{-6} \cdot 435 = 0.62 + 0.35 = 0.97 \text{ MN} > V_{Sd} = 843 \text{ kN}$$

where

$f_{cd1\text{-}2} = 0.7\,(1\text{-}f_{ck}/250)\, f_{cd} = 8.6$ N/mm^2

$f_{cd} = f_{ck}/\gamma_c = 20/1.5 = 13.3$ N/mm^2

$f_{yd} = f_{yk}/\gamma_s = 500/1.15 = 435$ N/mm^2

(b) Diagonal stress

Next, the average stresses from the diagonal strut force $F_{c5} = V_{Sd}/\sin\theta = 1030$ kN in the node face a_5 will be checked with Eq. 4.4-125. The strut width a_5 can be determined from the chosen geometry of the node region:

$$a_5 = a_1 \sin\theta + u \cos\theta = 0.24 \sin 54.9^0 + 0.42 \cos 54.9^0 = 0.44 \text{ m}$$

$$\sigma_{c2} = F_{c5} / a_5 \cdot b = 1.03 / 0.44 \cdot 0.30 = 7.8 \text{ N/mm}^2 < f_{cd1\text{-}2} = 8.6 \text{ N/mm}^2$$

Copyright fib, all rights reserved. This PDF copy of fib Bulletin 54 is intended for use and/or distribution only within National Member Groups of fib.

(c) Anchorage of reinforcement

In the structure considered, the chord reinforcement cannot be extended beyond the short support length of 240 mm, in contrary, the development length over the support is reduced by 35 mm for the necessary concrete cover. Furthermore, 30 mm allowance will be considered for the length and inaccurate placement of the longitudinal bars. Therefore, only a fraction of the tension chord force F_{t2} = 592 kN can be anchored by the ∅14 mm bars, and 5 additional horizontal loops ∅12 mm will be supplemented in the node region.

Firstly the bond resistance $F_{bd,\varnothing 14}$ of the 10 ∅14 mm bars will be calculated from the surface area of the bars and the design bond strength f_{bd}, following the rules in Section 3.2.4:

$\alpha_1 = 1$ straight bars
$\alpha_2 = 1$ no welded cross bars
$\alpha_3 \cdot \alpha_4 \cdot \alpha_5 = 0.7$ minimum value, taking into account transverse pressure from support
$f_{bd} = 2.25$ N/mm^2
$n = 10$ number of bars
$l_{b,ef} = 0.24 - 0.065 = 0.175$ m effective anchorage length
$\varnothing = 14$ mm

$$F_{bd,\varnothing 14} = n\,\pi\varnothing\, l_{b,ef}\, f_{bd} / \alpha_1\,\alpha_2\,\alpha_3\,\alpha_4\,\alpha_5 = 10\,\pi\cdot 0.014\cdot 0.175\cdot 2.25/0.7 = 0.247\,\text{MN}$$

Accordingly, the loop bars ($\alpha_1 = 0.7$) will contribute

$$F_{bd,\varnothing 12} = n\,\pi\varnothing\, l_{b,ef}\, f_{bd} / \alpha_1\,\alpha_2\,\alpha_3\,\alpha_4\,\alpha_5 = 10\,\pi\cdot 0.012\cdot 0.205\cdot 2.25/0.7\cdot 0.7 = \underline{0.353\,\text{MN}}$$

$F_{bd} = 0.600$ MN
> 0.593 MN

(d) Further consequences of compression reinforcement

The vertical bars from the supporting wall or column must be extended into the deep beam and anchored there with $l_{b,net} \cong 0.8$ m, which is more than $u = 0.42$ m, as assumed so far. If vertical forces are really transmitted over this length, the effective depth u of the node and the width of the tension chord should be adapted accordingly.

In reality, the transmission of forces from the compression reinforcement into the concrete will begin already below the support face a_1, if lateral confinement increases the resistance of the concrete, and it will predominantly occur in the lower part of the transmission length in the deep beam. As a consequence, the concrete stresses in the lower part of the node may increase whilst the steel stresses in the compression reinforcement decrease. It is wise to consider this for the choice of node depth u and the check of nodes with compression reinforcement. The assumption of $u = 0.42$ m $< l_{b,net}$ and the evaluation of the diagonal stress based on that value were conservative in this respect. The same applies to the arrangement of horizontal loops within u for the anchorage of the full tension chord force. Beyond u the nominal horizontal loop reinforcement Ø8–150 mm is sufficient in the example considered. In other cases stronger horizontal loops may be necessary within the development length, as explained by Fig. 7.3-19 a.

Copyright fib, all rights reserved. This PDF copy of fib Bulletin 54 is intended for use and/or distribution only within National Member Groups of fib.

(2.3.2) Inner support node

The node over the inner support of the deep beam is rather complicated (Fig. 7.3-23). Remembering the three standard D-regions included in the model of the continuous deep beam, the inner support node may be considered as a combination of two end-support nodes, one for each span, and a superimposed compression node from the model in Fig. 7.3-12. The diagonal struts are shared by both types of nodes. Accordingly, in the model of Fig. 7.3-20 the horizontal component of the diagonal strut F_{c4} is balanced by the tie force F_{t2}, which belongs to the end-support node, and by the compression force F_{c3}, which is part of a compression node (compare Fig. 4.4-91).

However, it is obvious, that the two tension chords cannot fully anchor their forces within half the column width. Instead, a considerable part of the tension chord forces F_{t1} = 299 kN and F_{t2} = 592 kN is directly balanced through the node region by the continuous chord reinforcement. To preserve equilibrium, the horizontal compression in the node's concrete must increase accordingly. The real horizontal concrete compression force in the node therefore depends on the bond forces with parameters like length of the support, bar diameter and bond properties.

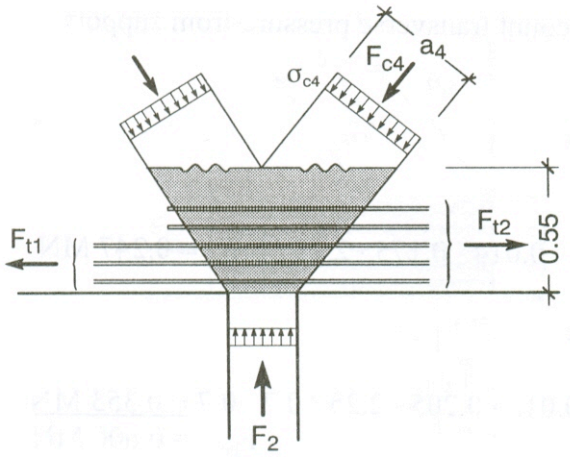


Fig. 7.3-23: Interior support-node regions of the deep beam in Fig. 7.3-20.

In conclusion it can be stated, that the concrete in the node is under biaxial compression, but the horizontal compression is difficult to assess. On the other hand, tensile reinforcement penetrates the node region and is anchored there is to some extent. Therefore, $f_{cd1\text{-}2}$ will again be applied here as design node strength, though f_{cd1} according to Eq. 4.4-119a might eventually be considered.

(a) Bearing pressure

The concrete resistance is

$V_{Rcd} = a_1 \, b \, f_{cd1\text{-}2} = 0.30 \cdot 0.30 \cdot 8.6 = 0.77$ MN.

The remaining part of the support force, 0.94 MN, must be transmitted by compression reinforcement:

$A_{s,\,,req} = 940\,000 / 435 = 2160$ mm^2 $\rightarrow$ $2 \cdot 4 = 8$ ∅20 mm.

Copyright fib, all rights reserved. This PDF copy of fib Bulletin 54 is intended for use and/or distribution only within National Member Groups of fib.

With consideration of the large share of compression reinforcement and transverse tensile stresses due to the anchorage of thick bars, stirrups like those in the column are arranged within the development length.

(b) Diagonal pressure

The check of diagonal pressures at the node surface is analogous to that for the end-support node in Section 7.3.2(2.3.1) above. It will be briefly presented for the strut of the large span:

Strut force $F_{cd4} = 1.22$ MN
Strut angle $\theta = 51.3^0$

Horizontal support length for the diagonal strut of the large span: 0.17 m
Assumed depth of the node region from a pre-calculation: $u = 0.55$ m
Width of the diagonal strut at the node: $a_4 = 0.17 \sin\theta + 0.55 \cos\theta = 0.48$ m
Diagonal stress: $\sigma_{c4} = 1.22 / (0.30 \cdot 0.48) = 8.47$ N/mm^2 < 8.6 N/mm^2 = $f_{cd1\text{-}2}$.

Over the interior support it is not necessary to distribute the chord reinforcement over the total depth u of the node. Those parts of the diagonal strut forces that belong to the compression node equilibrate their horizontal components (e.g. F_{c3}) by direct compression, which works also above the reinforcement layers.

(c) Horizontal node pressure

An upper bound of the horizontal concrete compression can be obtained from the very conservative assumption that the horizontal component $H = F_{c4} \cos\theta$ of the diagonal strut is fully balanced by concrete compressive stresses. Considering the node geometry, the horizontal pressure is less than the diagonal pressure, and therefore needs no numerical check.

(2.4) Concluding remark

The example shows that deep beams, even those with a relatively low reinforcement percentage, may have problems with their support nodes; these are the real critical regions of the structure. Another lesson from the example is that diagonal strut stresses may be more relevant for the design than bearing pressures and horizontal stresses.

7.3.3 Beam-column connections

(1) General behaviour

Beam-column connections are normally checked with standard methods for B-regions (Section 4.4.1(5.2)) applied to the orthogonal sections through the inner corner. The balance of inner forces in between these sections must be taken care of by an appropriate arrangement of reinforcements.

The deflection of the chord forces of the horizontal member into the vertical direction of the columns is shown in the map of principal stresses for pure moment loading and elastic material in Fig.7.2-24 a. The deflection of the chord stresses generates radial stresses σ_2 in the common region of column and beam, here termed as corner region (Fig. 7.3-24 b and c):

Copyright fib, all rights reserved. This PDF copy of fib Bulletin 54 is intended for use and/or distribution only within National Member Groups of fib.

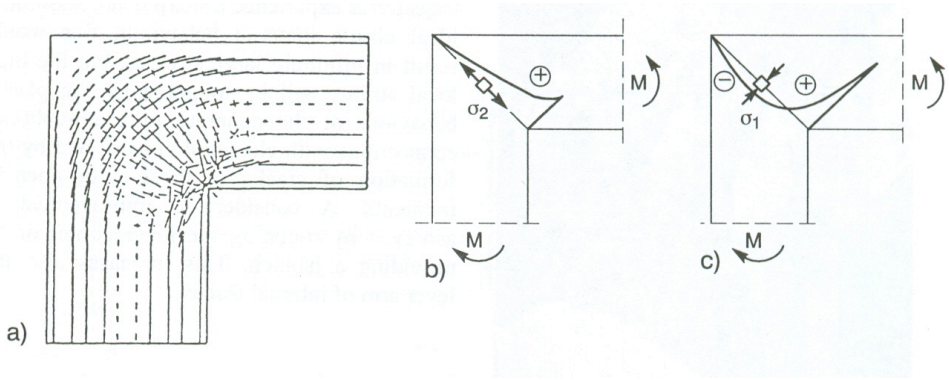


Fig. 7.3-24: Stresses in frame corners from a linear elastic FE-analysis:
a)Principal stresses.
b) and c) Distribution of principal stresses in the diagonal section

The radial stresses are either compressive for negative (closing) moments, or tensile stresses for positive (opening) moments. These tensile stresses are the main cause for a completely different behaviour and accordingly different models for the two cases of moment direction:

Firstly, the concrete in the corner region with opening moment tends to separate in the radial direction and must be tied back to the inner corner by stirrups. If stirrups are arranged in the radial direction of the principal stresses, the congestion of stirrups at the inner corner will complicate the construction. The concrete cover of the curved compression chord cannot be tied back. In beam-column-connections subject to high stresses, the cover will spall before failure (Fig 7.3-25). In such cases it is advisable to neglect the cover, when evaluating the moment resistance in the design sections mentioned above. Note that for the present purposes, concrete cover means all concrete areas which are not tied back to the interior of the corner region, i.e. the regular concrete cover of stirrups plus stirrup diameter plus approx. 1/3 of the distance between the loops or legs of radial ties.

Secondly, the radial tensile stresses weaken the concrete compressive strength of the compression chord. A close look at the map of principal stresses in Fig. 7.3-24 a shows, that the deviation of the stress trajectories of the outer chords begins already before the intersection of beam and column. Therefore, the design sections are affected, too. Besides, the lever arm of internal forces decreases.

For these reasons, beam-column-connections with opening moments carry less moment than undisturbed B-regions with equivalent cross-section and reinforcement. In practical design, this can be taken into account by an effectiveness-factor < 1 for the resisting moment, or by a limitation of the reinforcement percentage. A rough reference for the admissible degree of utilization is the reinforcement percentage $\rho \leq 0.8$ % (for f_y = 500 N/mm^2, concrete C 20/25) in the sections of the frame corner. Sensibly interpreting MC90, the reduced concrete strength f_{cd2} (Eq. 4.4-6) should be applied for opening moments, whilst f_{cd1} (Eq. 4.4-4) is applicable for closing moments.

Another typical feature of the load-bearing behaviour are the peak stresses at the re-entrant corner (Fig. 7.3-24 c) where the trajectories experience a sharp bend. Assuming ideal elastic material behaviour, this would result in infinitely large stresses, but the high local strains will be tolerated by the plastic behaviour of the concrete in beam-column-connections with closing moments, and by the formation of cracks in those with opening moments. A considerable improvement is achieved by rounding the inner corner or by providing a haunch. This also increases the lever arm of internal forces.

Copyright fib, all rights reserved. This PDF copy of fib Bulletin 54 is intended for use and/or distribution only within National Member Groups of fib.

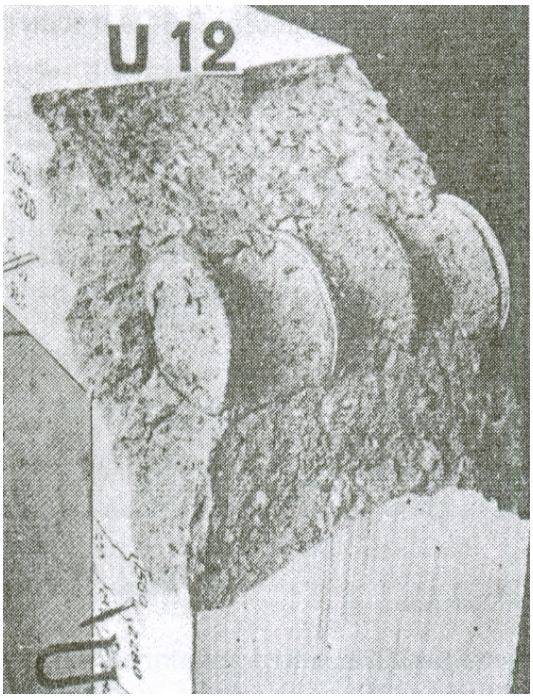


Fig. 7.3-25: Spalling of the compression zone under opening moment [Nilsson (1973)]

(2) Beam-column-connections with negative (closing) moment

(2.1) Elementary models and associated reinforcement for pure moment loading

The simple model as depicted on Fig. 7.3-26 a is applicable only if the internal lever arms of the girder and the column, z_g and z_c, do not differ much in magnitude, and if the entire chord reinforcement of the horizontal and vertical member is extended around the corner.

If the lever arms of girder and column are very different, a truss-type model is appropriate for the corner region, in order to maintain reasonable angles between struts and ties (Fig. 7.3-26 b). The model shows, why additional horizontal reinforcement is necessary in the web of the beam. Omission of it has resulted in severe diagonal cracks extending from the outer column-face towards the inner corner. The horizontal reinforcement (loops or stirrups) is necessary for the anchorage of that part of the column chord force, which exceeds the girder chord force, due to the different lever arms. Assuming strut angles $\theta = 45^0$, the horizontal forces F_{t3} are in total equal to the difference of both chord forces, F_{t2} - F_{t1}. For other strut angles θ, the following formula applies:

$$F_{t3} = (F_{t2} - F_{t1}) \tan\theta.$$

The model provides also information on the necessary anchorage length for the column bars and the large diagonal compression stresses in the corner region.

Copyright fib, all rights reserved. This PDF copy of fib Bulletin 54 is intended for use and/or distribution only within National Member Groups of fib.

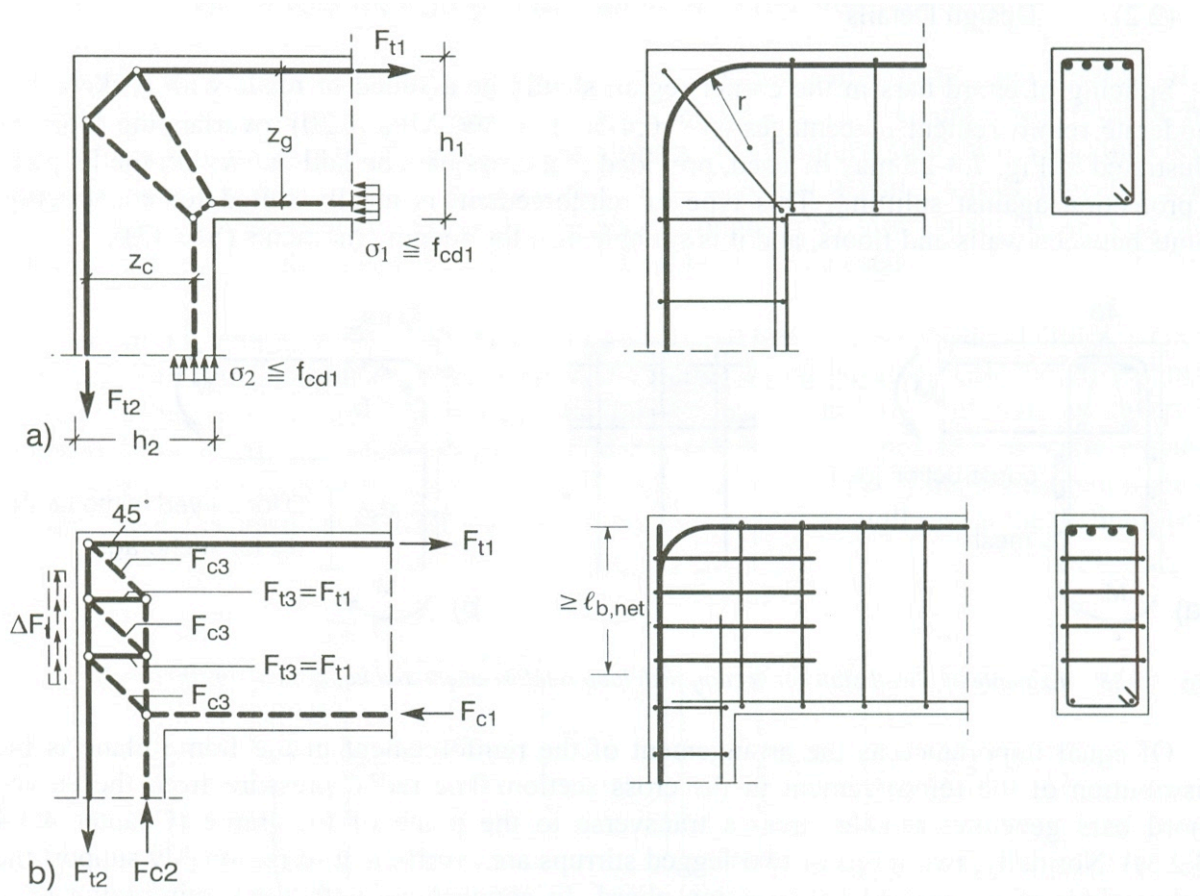


Fig. 7.3-26: Beam-column-connection with closing moment. Model and reinforcement.
a) Almost equal depth of beam and column.
b) Very different depth of beam and column

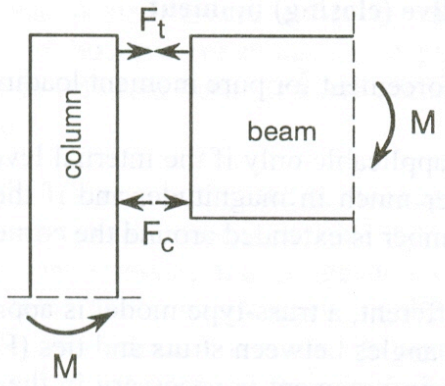


Fig. 7.3-27: Shear in the corner region of a beam-column-connection

Alternatively, the horizontal reinforcement and diagonal concrete stresses can be derived from a standard shear design of the cantilevering part of the column, according to Fig. 7.3-27. The beam's tension chord force F_t acts on the column-end like a concentrated load and is transferred as a shear force through the cantilevering part of the column to the supporting compression chord of the beam. Since chord forces in beams are normally much larger than shear forces, the shear force in the cantilevering column is larger than in any other part of the beam and column! It is amazing that frame structures are usually carefully designed for the

Copyright fib, all rights reserved. This PDF copy of fib Bulletin 54 is intended for use and/or distribution only within National Member Groups of fib.

shear forces in B-region, whilst the more critical shear within the corner region is frequently overlooked, maybe, because it does not appear in the structural analysis of the frame system.

The concentrated compression node in the re-entrant corner needs no extra check, if the standard methods for B-regions were applied to the respective corner sections of the beam and column.

(2.2) Design details

Splicing of chord bars in the corner region should be avoided or made with sockets. For moderate reinforcement percentages (ρ < 0,4 %, f_y = 500 N/mm^2, C20/25) overlapping loops as illustrated in Fig. 7.3-28 may be used, provided that cross bars be laid out within the loops as a protection against splitting. This type of reinforcement is ideally suited for construction joints between walls and floors, and it is suitable also for opening moments (Section 7.3.3(3)).

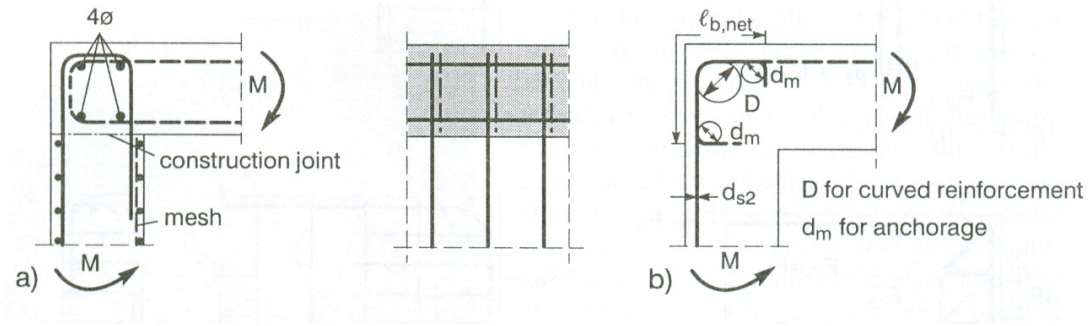


Fig. 7.3-28: Example of a wall-slab connection with loop reinforcement and hooked bars, respectively.

Of equal importance as the arrangement of the reinforcement in the frame plane is the distribution of the reinforcement in the cross section. The radial pressure from the curved chord bars generates tensile stresses transverse to the plane of the frame (Section 4.4.4(3.2.3)). Normally, two loops or two-legged stirrups are insufficient to reasonably support the entire width of the curved compression chord. In connections with thick reinforcing bars, closely spaced stirrups or other transverse reinforcement may be necessary to avoid splitting or spalling of the concrete (Fig. 7.3-29). In particular, the outermost chord bars are to be secured horizontally.

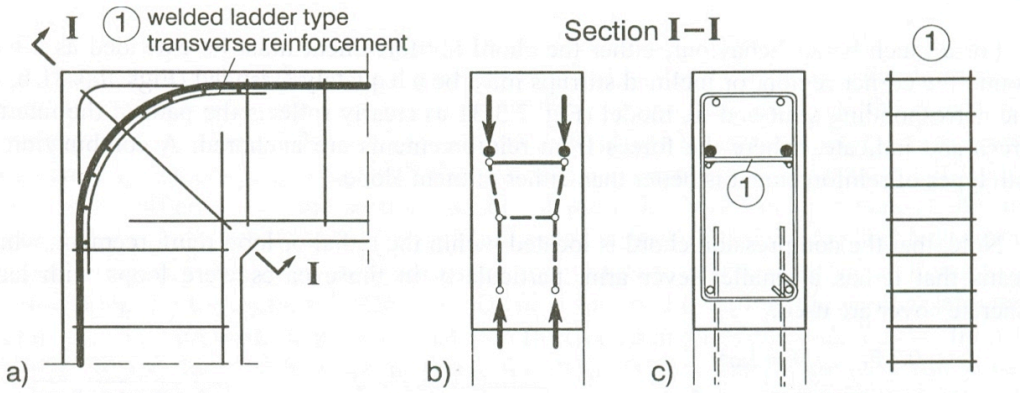


Fig. 7.3-29: Transverse reinforcement of a beam-column-connection with closing moment.
a) View. b) Diagonal section with model. c) Reinforcement.

Copyright fib, all rights reserved. This PDF copy of fib Bulletin 54 is intended for use and/or distribution only within National Member Groups of fib.

Considering the concrete stresses, the bending radius of the chord reinforcement should be chosen large, but on the other hand it should be small enough, to keep the internal lever arm in the diagonal larger than that of the orthogonal sections. It is recommended to choose the radius between 0.6 d_{min} and 0.8 d_{min} where d_{min} denotes the depth of either the girder or the column, whichever is less. The corner region outside the bent chord bars may be secured by a diagonal stirrup or a few thinner chord bars, bent with minimum radius (Fig. 7.3-26 a and 7.3-28).

(3) Beam-column-connections with positive (opening) moment

The model for negative moments (Fig. 7.3-26 a) is not suited (after sign reversal of the forces) for frame corners with positive moments, because reinforcement never shall be bent around a re-entrant corner. If the tension chord bars are continued straight beyond the inner corner, the problem remains how to transfer the large diagonal tensile forces into the chord reinforcements near the inner corner. If any, a very congested reinforcement layout with radial stirrups that enclose the chord reinforcements would have to be used.

The simple model in Fig. 7.3-30 avoids the diagonal ties, but is not suited either, since the tensile chord reinforcements of the beam and column would have to be anchored within the depth of the compression chord near the outer face. In order to effectively divert the compression chord, the reinforcement should enclose it. This is possible to some extent by means of anchor plates or studs or thin loop-shaped bars. A check of the compression-tension-nodes 1 and 2 according to Sections 4.4.4(3.2.2) or 4.4.4(3.2.4) will reveal the difficulties.

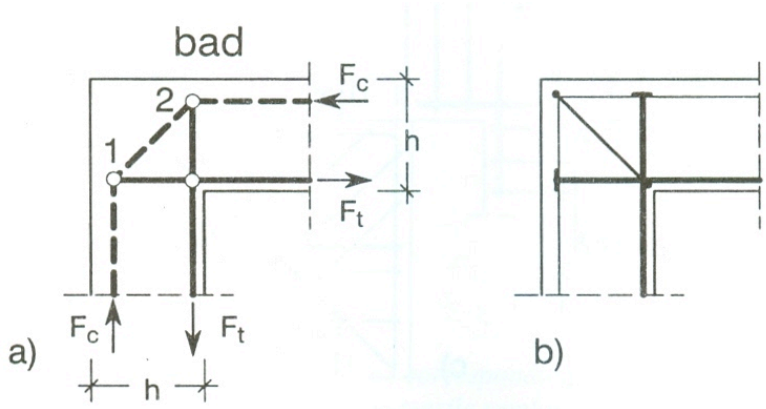


Fig. 7.3-30: Beam column connection with poor performance, feasible only for small positive moments
a) Simple model. b) Corresponding reinforcement.

For a much better behaviour, either the chord reinforcement must be extended as a loop around the corner region, or inclined stirrups must be adequately arranged (Figs. 7.3-31 b or c). The corresponding strut-and-tie model (Fig. 7.3-31 a) clearly reflects the path of the internal forces and indicates where the forces from reinforcements are anchored. A combination of both types of reinforcement is better than either of them alone.

Note, that the compression chord is located within the radial or loop reinforcement, which means that it has a smaller lever arm, particularly in those cases were loops with large concrete cover are used.

Copyright fib, all rights reserved. This PDF copy of fib Bulletin 54 is intended for use and/or distribution only within National Member Groups of fib.

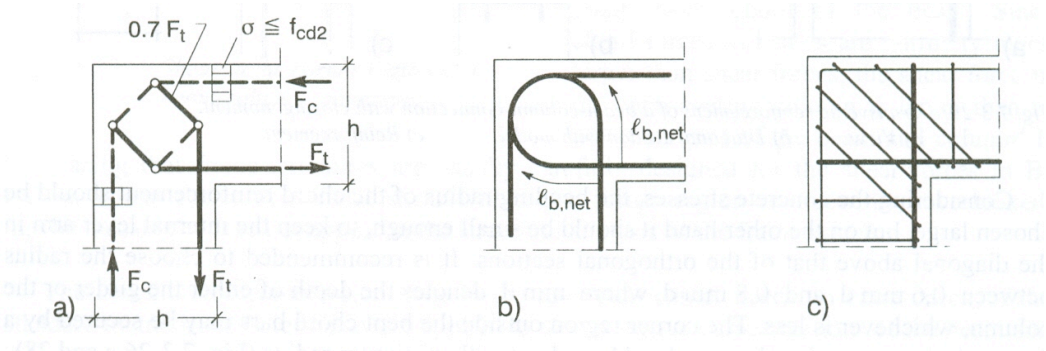


Fig. 7.3-31: Beam column connection for moderate positive moment.
a) Model. b) c) Two alternative reinforcement layouts.

A major drawback of the reinforcement layouts in Fig. 7.3-31 b and c is the divergence (about 45°) of the reinforcement directions in the re-entrant corner from the direction of principal stresses σ_I (Fig. 7.3-24 a). In members with relatively large moments, this may result in severe diagonal cracking which also constricts the compression zone and entails a major reduction in efficiency of the section. Beam-column-joints with inclined bars at the inner corner behave much better, as has been demonstrated in tests (Fig. 7.3-32). The diagonal bars do not reduce the forces in the chord bars, they should be provided in addition to the reinforcement for the sectional effects. As a benefit for good detailing, the moment efficiency factor may be increased, or the higher effective concrete strength $f_{cd1\text{-}2}$ from Eq. 4.4-119b utilised. Inclined bars are advisable for all kinds of re-entrant corners, also those in corbels, stepped beams, half-joints and at openings. They reduce the diagonal crack widths which tend to be particular wide in the corners, due to the discontinuity.

As can be seen from the strut-and-tie model in Fig. 7.3-32a, the tensile force of the diagonal bars continues via the stirrups to the outer compression chord where it is finally anchored. That means that in accordance with the elastic flow of forces (Fig. 7.3-23 a), the stirrups gradually deviate the compression chord also before the corner section. The regions adjacent to the beam-column-joints shall therefore be adequately reinforced with stirrups, apart from the design for shear forces.

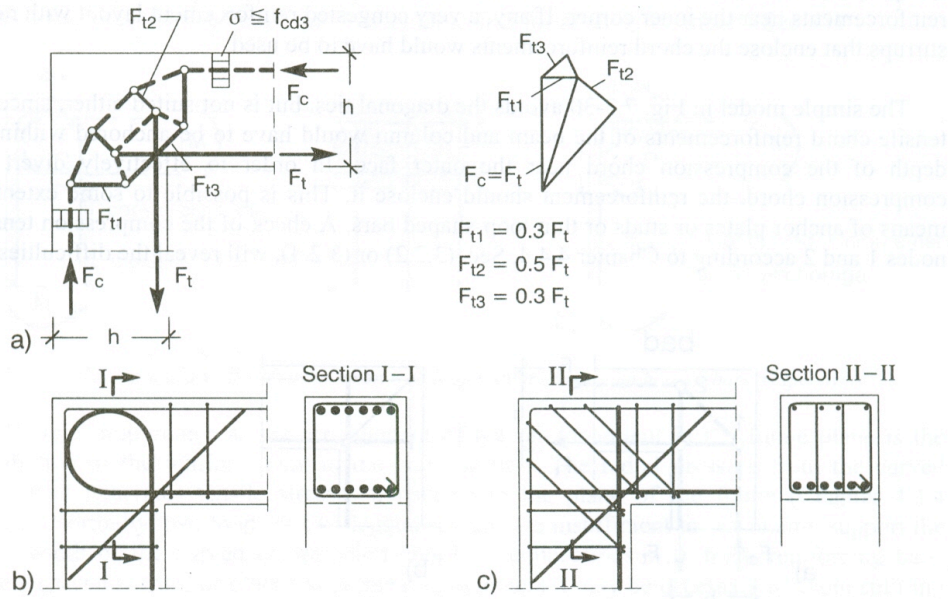


Fig. 7.3-32: Beam-column-connection for large opening moment.
a) Model with force polygon. b) c) Two alternative reinforcement layouts

Copyright fib, all rights reserved. This PDF copy of fib Bulletin 54 is intended for use and/or distribution only within National Member Groups of fib.

(4) Rigid connection of column with continuous beam

For developing the reinforcement layout of joints of three or four members in a frame, it is recommended to split the sectional effects in two or three parts:

a) A moment that is transmitted in the continuous member from one span to the other, like the support moment in a beam over a hinged support. The horizontal reinforcement for this moment is arranged accordingly straight and continuous over the joint.
b) A closing moment that is transmitted from a column to one of the beams. The reinforcement for this moment shall be bent around the corner region as in the equivalent beam-column-joint, Fig. 7.3-26, always "to the other side", e. g. reinforcement from the right hand column side into the beam on the left, and vice versa.
c) An additional opening moment transmitted from a column to the other beam must be considered only if necessary. Reinforcement for this moment is to be placed as explained for the opening beam-column-joint (Section 7.3.3(4)).

Fig. 7.3-33 presents models for different cases together with the equivalent reinforcement layout. The model nodes indicate how and where the anchorage of bars occurs. It is in general not correct to assume the beginning of the development length at the interface of the members!

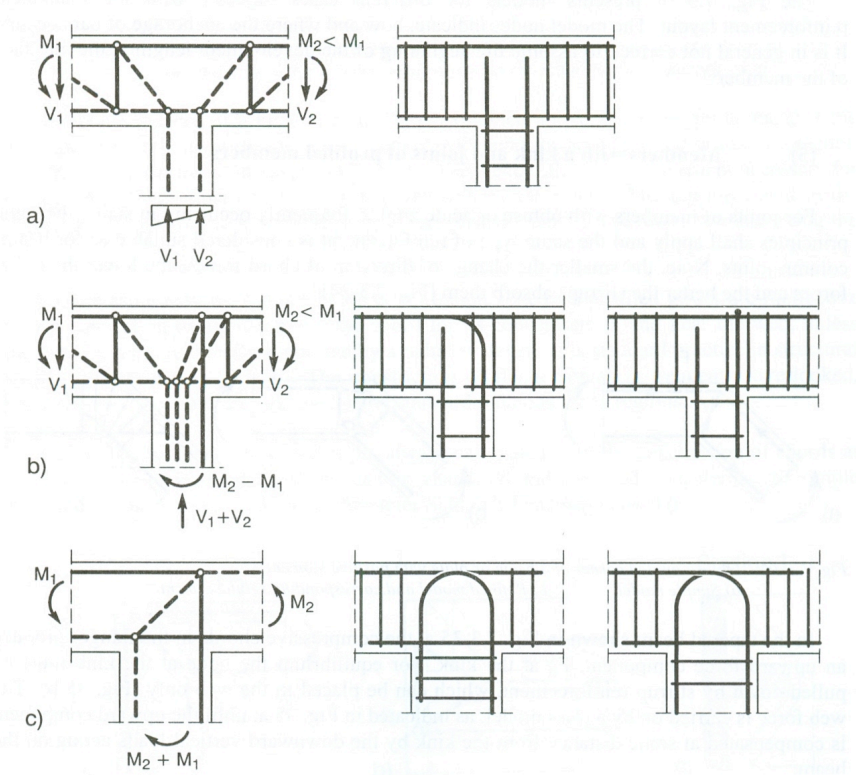


Fig. 7.3-33: Beam-column-joints. Models and corresponding reinforcement layout.
a) For small column moment, no tensile forces in the column.
b) For column with tensile reinforcement.
c) Typical case of a sway frame joint

Copyright fib, all rights reserved. This PDF copy of fib Bulletin 54 is intended for use and/or distribution only within National Member Groups of fib.

(5) Members with a kink and joints of profiled members

For joints of members with obtuse or acute angles, frequently occurring in stairs, the same principles shall apply and the same type of reinforcement is considered suitable as for beam-column-joints. Note that the smaller the change of direction of chord forces, the lower the radial forces and the better the stirrups absorb them (Fig. 7.3-34).

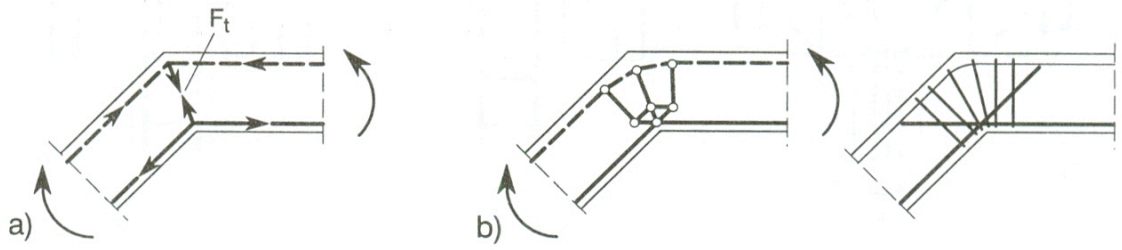


Fig. 7.3-34: Obtuse-angled corner of a beam or plate with positive moment.
a) Simple model. b) Refined model and corresponding reinforcement

In the tapered beam shown in Fig. 7.3-35 a, the compressive chords in the flanges produce an upward force component, F_t, at the kink. For equilibrium the node at the kink must be pulled down by stirrup reinforcement, which can be placed in the web only (Fig. 7.3-35 b). The web force F_t is carried on by a truss model, as indicated in Fig. 7.3-35 a, until the upward component is compensated at some distance from the kink by the downward vertical loads acting on the beam.

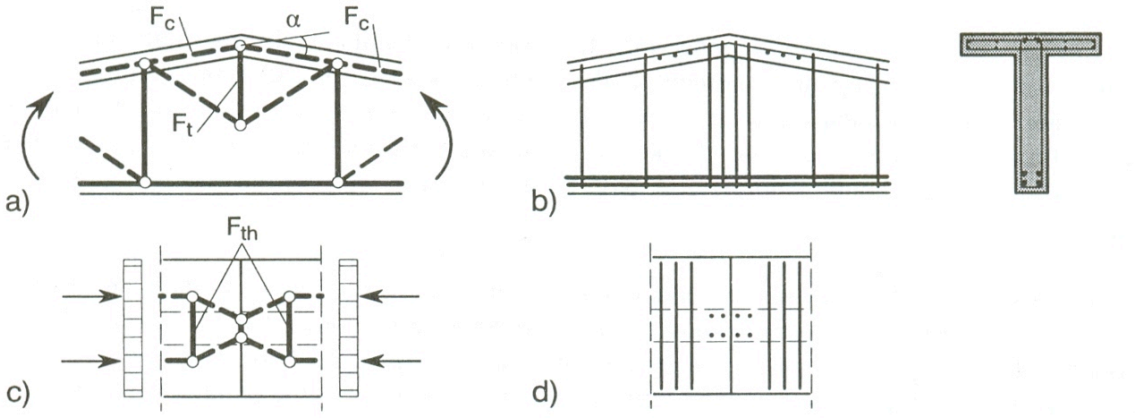


Fig. 7.3-35: Tapered beam with bent top flange:
a) b) Strut-and-tie model and corresponding reinforcement for the bent area in elevation.
c) d) Strut-and-tie model and corresponding reinforcement for the flange near the bent

Since chord- and stirrup-forces must join also in plan (Fig. 7.3-35 c), the compression chord in the flange is narrowed down at the kink, resulting in a concentration of compression stresses over the web. Moreover, the horizontal deviation of these compression stresses will be associated with a tensile force, F_{th}, which calls for horizontal reinforcement in the flange as shown in Fig. 7.3-35 d.

The consequences of a kink in a chord, as explained above, are more pronounced if the angle between the members increases. Flanges will bend in the transverse or radial direction and thus avoid the longitudinal stresses. As a consequence, all the reinforcement necessary for

Copyright fib, all rights reserved. This PDF copy of fib Bulletin 54 is intended for use and/or distribution only within National Member Groups of fib.

the frame moment must be placed in the web or very close to it. The reinforcement in the flanges (or slabs) contributes only towards crack distribution but not towards transmitting the moment.

For the same reasons, flanges in the compression zone of a profiled girder are ineffective near a connection or joint. Instead, the chord forces concentrate in and near the web, unless the radial forces are directly supported by a radial stiffener, as is standard practice in structural steel engineering (Fig. 7.3-36). The constriction of flange forces is frequently overlooked, when the cross sections are designed using standard methods for B-regions.

The transverse tensile forces that are always associated with the constriction of chords at kinks or joints of profiled members can be visualised and analysed with the use of simple strut-and-tie-models (see example in [Schäfer, Schlaich, Jennewein (1991)]).

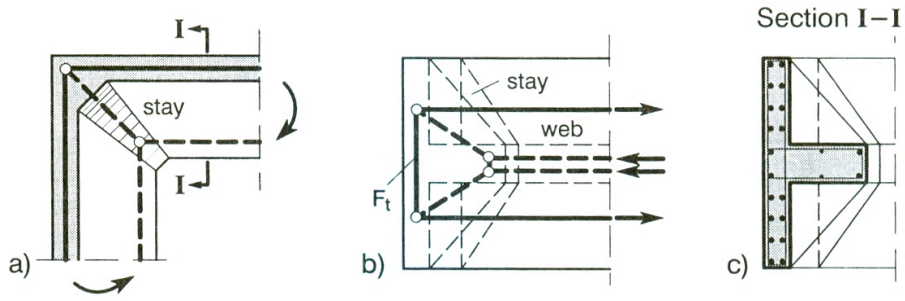


Fig. 7.3-36: Connection of T-beams.
a) Model in the frame plane; b) Top view of the model; c) Cross-section

7.3.4 Corbels

(1) Load bearing behaviour and necessary checks

Similar to a beam-column-connection, the corbel transmits a closing moment to the column below and an opening moment to the column above it (provided the column above exists and can resist such a moment). As for frames, the column sections in the horizontal faces through the corners can be checked with standard methods for their sectional effects M_{Sd}, N_{Sd} and V_{Sd}, though, more rigorously, these faces are well within the D-region with disturbed stress flow.

One essential difference to the beam column-connection is the relatively large shear force in the corbel from its load F_{Sd}, which is transmitted by a diagonal strut from node 1 to a concentrated compression node 2 at the lower corner (Fig. 7.3-37 a). There, the vertical component F_{Sd} of the strut is supported by the compression chord of the column below and the tension chord F_{t2} in the column above. Usually the tension force is comparatively small.

Copyright fib, all rights reserved. This PDF copy of fib Bulletin 54 is intended for use and/or distribution only within National Member Groups of fib.

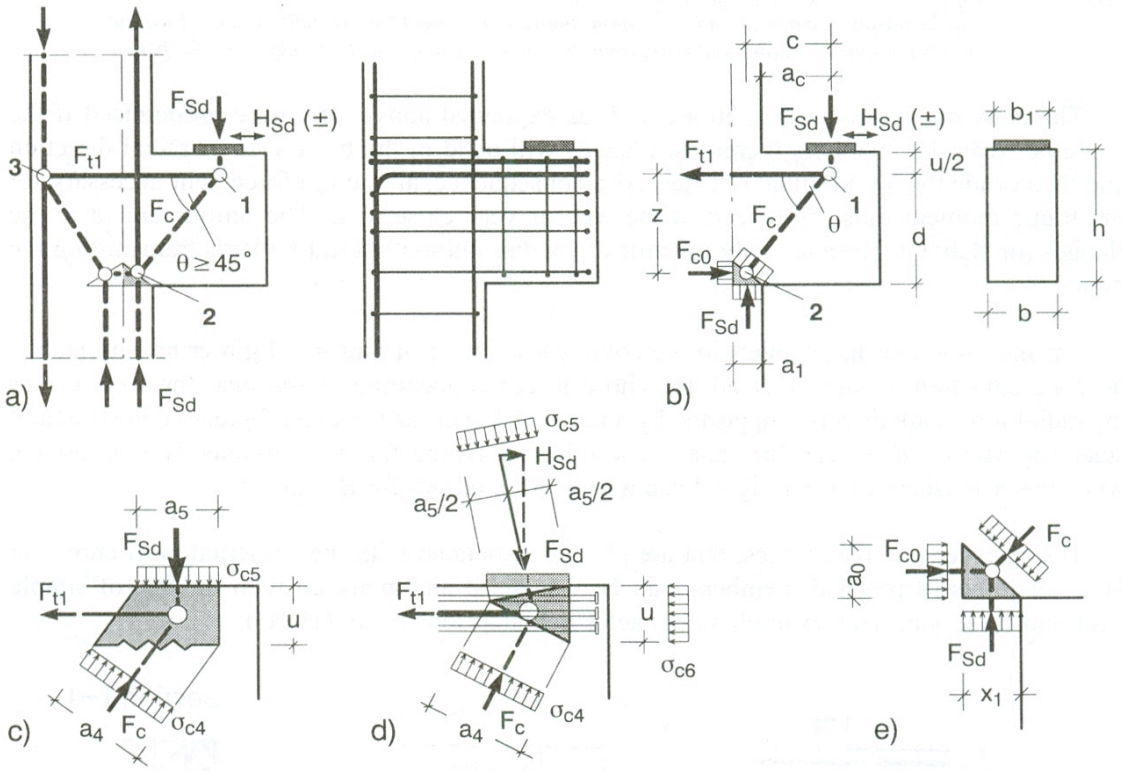


Fig. 7.3-37: Typical corbel.
a) Overall model and corresponding reinforcement.
b) Model of a typical cantilevering part.
c) Standard compression-tension node 1 for vertical load.
c) Idealised hydrostatic node 1 for inclined load and anchorage behind the node region.
e) Detail of the compression node 2 corresponding with b) above

The kinks in the described loadpath of the corbel load result in a horizontal tie F_{t1} in node 1 under the bearing and a horizontal compression force F_{c0} in the supporting node 2. These forces are balanced by a pattern of forces in the column which is almost a mirror image of that in the cantilevering part or the D-region. It can be concluded, that the column region adjacent to the corbel is subject to equivalent stresses, too. Since the overall models of corbel regions are different, depending on the particular loading and boundary conditions of the column above and below, a model of the whole D-region including the column part should be considered for the design [Schlaich, Schäfer (2001)]. It will, in fact, not suffice to simply anchor the main reinforcement behind the column face. With this in mind, the corbel part can be designed as explained in the numerical example in Section 7.3.4(2) below, because it is very frequently of the type shown in Fig. 7.3-37 b.

The example will show that the design for horizontal compression F_{c0} in node 2 and for horizontal tension F_{t1} is identical with the design of a B-region for moment and normal force. It may therefore also be performed using tables or computer routines for beams. Note however, that the design moments are not referred to the column face, but to the relevant vertical section I-I through node 2. This section is determined by the requirement of zero shear force, in order to obtain the maximum chord forces F_{t1} and F_{c0}. As a consequence, the lever arm c of the corbel load F_{Sd} with respect to its support is considerably larger than its distance a_c from the column face, a fact which is frequently overlooked in the literature on corbels and in practical design.

Copyright fib, all rights reserved. This PDF copy of fib Bulletin 54 is intended for use and/or distribution only within National Member Groups of fib.

For the evaluation of forces and stresses, a horizontal force $H_{Sd} \geq 0.2\ F_{Sd}$ from restrained longitudinal deformations of the supported member should also be taken into account.

Nodes are critical points of the structure. Node 1 under the bearing corresponds mechanically to an end-support node turned upside down. For vertical load, it can be designed as a standard compression tension node as shown in Fig. 4.4-92.

To get an idea of an influence of the additional horizontal load component, the hydrostatic node region in Fig. 7.3-37 d will be discussed. It is assumed, that the horizontal tie is completely anchored behind the node, which is not far from reality if anchor plates or studs or loop reinforcement are used. Principal stresses in the node region and in the oncoming struts (including the diagonal strut) will not exceed the node strength if the inclined stresses σ_{c5} under the bearing and the (fictitious) horizontal compression stress σ_{c6} do not exceed it. These stresses should be checked against f_{cd1} in cases with anchorage by anchor plates or $f_{cd1\text{-}2}$ where bond contributes essentially to the anchorage of reinforcing bars.

The relevant inclined constant stress σ_{c5} follows from equilibrium and the node's geometry.

$$\sigma_{c5} = \frac{V_{Sd}}{b\,a_5}\left(1+\left(\frac{H_{Sd}}{V_{Sd}}\right)^2\right).$$

In this formula the node stresses are assumed to be distributed over the whole width b of the corbel. This simplification leads to the same result as a check of the local pressure for the width b_1 of the bearing plate against the increased triaxial strength according to MC90 subclause 6.9.2. However, the code rule is restricted to bearing width $b_1 \geq b/4$.

To preclude any damage to the edges of the corbel the area of support should be smaller than the area enclosed by the chord reinforcement. This holds true also for such cases where a mortar bed is used. Uniform compression across the area of support is best achieved with elastomer supports which, to a certain extent, will also tolerate horizontal displacements and rotations.

The anchorage length of the tension chord in node 1 begins beneath the bearing plate, and in the majority of cases is so short that horizontal loops, welded cross bars or even anchor plates are required. Double headed studs (head diameter 3 times bar diameter) proved very effective as chord reinforcement in corbel tests carried out by Birkle and Ghali in Calgary (2002). The use of bent-down chord bars should be avoided, unless the bearing plate is located well behind the bend.

Node 2 is essentially a compression node, since the vertical compression dominates the tie force from the upper column. All node stresses are safe, because the principal stresses are automatically checked with the standard analyses for B-regions suggested above.

Node 3 is an example for a combination of two types of compression-tension nodes. The horizontal tie force due to the closing frame moment is transmitted by bent bars according to Fig. 4.4-93. The other part of the horizontal tie force, which is associated with to the opening moment from the upper column, causes the compression chord of the upper column to deviate towards node 2. The corresponding horizontal reinforcement should therefore enclose the vertical compression chord of the column. Loops or stirrups are adequate for the anchorage in this case. If all the corbel bars are bent into the column, some additional stirrups must be provided immediately above and below the main corbel reinforcement, to avoid spalling of the concrete near the bend.

Copyright fib, all rights reserved. This PDF copy of fib Bulletin 54 is intended for use and/or distribution only within National Member Groups of fib.

Compression stresses in the diagonal struts do not exceed those in the adjacent nodes. However, the struts will be safe only, if the transverse tensile stresses of the bottle shaped stress-fields are endured by the concrete or if additional web reinforcement is provided (Section 7.3.1(3.3.2)). For the ease of construction, these reinforcements are usually chosen at right angles. Horizontal stirrups are superior to the vertical type for very short corbels. MC90, subclause 6.8.2.2.3, recommends closed horizontal stirrups if $a<z/2$ and closed vertical stirrups if $a>z/2$, or a combination of both in all cases a<z. These reinforcements for the bottle shaped stress fields need not be designed to fully cover the forces derived for linear elastic material behaviour, because the tensile forces will be essentially reduced after cracking, when the stress trajectories straighten between the concentrated nodes. This explains, why different codes of practise give very different rules for the required web reinforcement in corbels.

Under the aspects of crack control, it is prudent to provide an additional diagonal reinforcement near the top corner (compare Fig. 7.3-32 b).

(2) Standard design for a corbel (numerical example)

An overall strut-and-tie-model of the D-region with the corbel is drawn in Fig. 7.3-38 a. It is very similar to the model in Fig. 7.3-36 a, but without an essential moment in the upper column. The projecting part is typical (like Fig. 7.3-37 b) and can be designed as follows:

(2.1) Design of the tension chord and compression node 2

The division line I-I in Fig. 7.3-37 b for the projecting part is determined by the requirement of zero shear force in this section, in order to obtain the maximum chord force F_{t1}. The corresponding support width a_1 for F_{Sd} in node 2 will be derived from the concrete design strength f_{cd1} for compression nodes (Eq. 4.4-119a):

$$f_{cd1} = 0.85\,(1 - f_{ck}/250)\,f_{cd} = 0.85 \cdot (1 - 30/250) \cdot 20.0 = 15.0 \text{ N/mm}^2 \text{ (concrete C30/37)}$$

$$a_1 = F_{Sd} / b\, f_{cd1} = 0.33 / 0.30 \cdot 15.0 = 0.073 \text{ m}$$

With a_1 the lever arm c of the corbel load F_{Sd} is determined:

$$c = a_c + a_1/2 = 0.150 + 0.073/2 = 0.187 \text{ m}.$$

Copyright fib, all rights reserved. This PDF copy of fib Bulletin 54 is intended for use and/or distribution only within National Member Groups of fib.

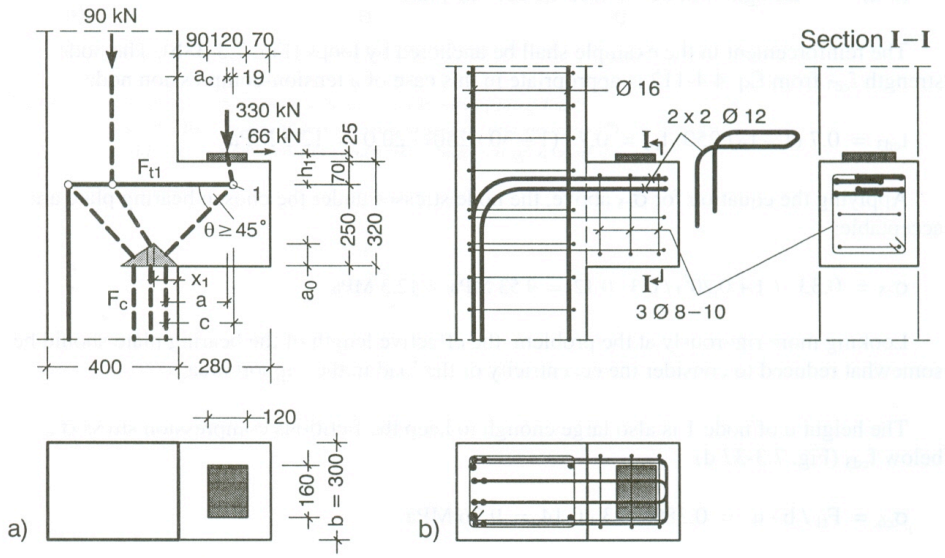


Fig 7.3-38: Corbel (numerical example). Concrete C30, steel S500.
a) Geometry and model b) Reinforcement

The moment due to the corbel load, M_{Sd}, with respect to the chord reinforcement is counteracted in section I-I only by the horizontal compression force F_{c0} in node 2 with the lever arm z. If the necessary vertical depth a_0 = 0.08 m of the compression node is conservatively estimated or approximately known form a pre-calculation, then the horizontal compression stresses σ_{c0} due to F_{co} and the main tension tie F_{t1} can be checked simply by the following equations (notations as in Fig. 7.3-37 and 38):

$z = d - a_0/2 = 0.25 - 0.08 / 2 = 0.21$ m (internal lever arm)

$M_{Sds} = F_{Sd} \cdot a + H_{Sd} \cdot h_1 = 330 \cdot 0.187 + 66 \cdot 0.095 = 68.0$ kNm

$F_{co} = M_{Sds} / z = 68.0 / 0.21 = 323$ kN

$\sigma_{c0} = F_{co} / b \cdot a_0 \leq f_{cd1} = 0.323 / 0.30 \cdot 0.08 = 13.5$ N/mm $< f_{cd1} = 15{,}0$ N/mm^2

$F_{t1} = F_{co} + H_{Sd} = 323 + 66 = 389$ kN

$A_{s,req} = F_{t1} / f_{yd} = 389\,000 / 435 = 894$ mm$^2 \rightarrow 8$ Ø 12 mm steel S500.

Alternatively, the horizontal compression stresses in the compression node 2 and the chord reinforcement may be checked for M_{Sd} and $N_{Sd} = H_{Sd}$ by standard methods for a beam with the cross-section of the corbel.

(2.2) Design of node 1 under the bearing plate

The reinforcement in the example shall be anchored by loops (Fig. 7.3-38 b). The node strength $f_{cd1\text{-}2}$ from Eq. 4.4-119 b is appropriate in this case of a tension-compression node.

$f_{cd1\text{-}2} = 0.7\,(1 - f_{ck}/250)\,f_{cd} = 0.7 \cdot (1 - 30 / 250) \cdot 20.0 = 12.3$ N/mm^2.

Copyright fib, all rights reserved. This PDF copy of fib Bulletin 54 is intended for use and/or distribution only within National Member Groups of fib.

Applying the equation for σ_{c5} above, the node stresses under the chosen bearing plate are acceptable:

$$\sigma_{c5} = 0.33 \cdot (1 + 0.20^2) / 0.3 \cdot 0.12 = 9.53 \text{ N/mm}^2 < 12.3 \text{ N/mm}^2$$

The height u of node 1 is also large enough to keep the fictitious compression stress σ_{c6} below $f_{cd1\text{-}2}$ (Fig. 7.3-37 d):

$$\sigma_{c6} = F_{t1} / b \cdot u \cdot = 0.389 / 0.3 \cdot 0.14 = 9.26 \text{ N/mm}^2 < 12.3 \text{ N/mm}^2.$$

As a consequence, also the stress σ_{c4} in the diagonal strut are acceptable – provided that web reinforcement prevents splitting of the diagonal strut.

Finally, the anchorage length of the reinforcement should be considered, following the code rules. However, it is the author's opinion that loops of thin bars are able to transfer their full yield force by radial pressure in the bend. Essential is that the loops enclose the node region. Crack widths are also not critical for the well distributed reinforcement bars with only 12 mm diameter.

(3) Corbels with suspended or indirect load

Two typical models for suspended loads, applied at the bottom of the corbel, are shown on Figs. 7.3-39 a and b. When combined, these models will render a reinforcement layout that provides a favourable crack distribution pattern and is suitable also for indirect load transfer, for instance from a crane girder (Fig. 7.3-39 c). Note, however, that the contributions of the two models should be selected as a function of the chord forces of the adjoining columns.

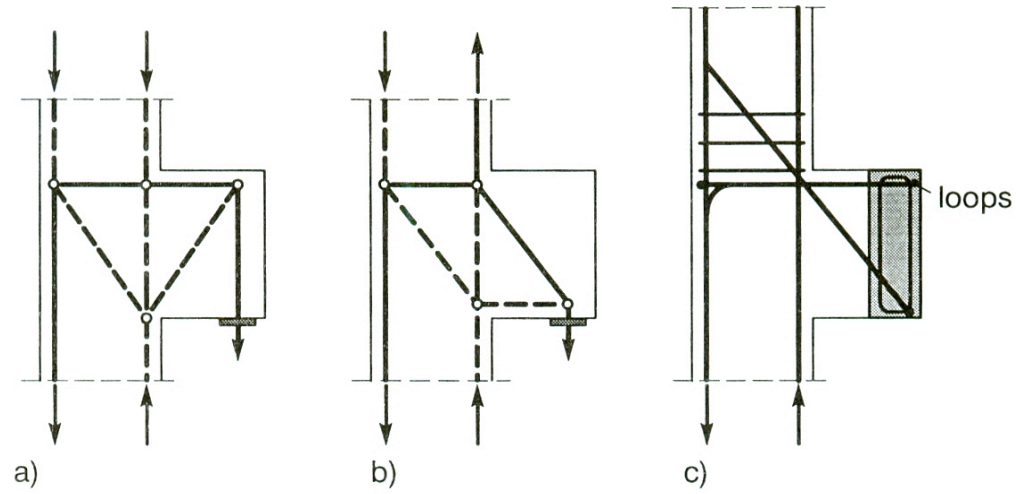


Fig. 7.3-39: Corbels with suspended load or indirectly applied load:
a) and b) Simple models showing possible load-bearing effects.
c) Reinforcement for the combined actions out of a) and b)

Copyright fib, all rights reserved. This PDF copy of fib Bulletin 54 is intended for use and/or distribution only within National Member Groups of fib.

References to Section 7.3:

ACI (1997), *ACI Committee 445 - Shear and Torsion*. Strut-and-Tie Bibliography No. 16.

Baumann, P. (1988), *Die Druckfelder bei der Stahlbetonbemessung mit Stabwerkmodellen.* Thesis, University of Stuttgart.

Birkle, G.; Ghali, A; Schäfer, K. (2002), *Double-headed studs improve corbel reinforcement*. Concrete International. Vol. 24 No.9, pp. 77-84.

CEB Bulletin 213/214 (1993), *CEB-FIP Model Code 1990*, published by Thomas Telford Ltd., UK. ("MC90").

CEB Bulletin 218 (1993), *Ductility – Reinforcement – Progress Report*.

Collins, M. P.; Vecchio, F.: (1982), *The response of reinforced concrete to inplane shear and normal stresses*. Publication No. 82-03, Univ. of Toronto, March 1982.

Collins, M. P.; Mitchell, D. (1995), *Shear and torsion. Chapter 4 of the Concrete Design Handbook*. Canadian Portland Cement Association.

CSA Standard A23.3-94: *Design of Concrete Structures*.

Fonseca, J. (1995), *Zum Bemessen und Konstruieren von Stahlbetonplatten und -scheiben mit Lastpfaden*. Thesis, University of Stuttgart.

Leonhardt, F.; Walther, R. (1966), *Wandartige Träger*. DAfStb H.178, Verlag Ernst u. Sohn, Berlin.

Muttoni, A.; Schwarz, J.; Thürlimann, B. (1997), *Bemessung von Stahlbetontragwerken mit Spannungsfeldern*. Birkhaeuser Basel/Boston/Berlin.

Nilsson, I, (1973), *Reinforced concrete corners and joints subjected to bending moment*. National Swedish Building Research, document D7.

Rückert, K. (1992), *Entwicklung eines CAD-Programmsystems zur Bemessung von Stahlbetontragwerken mit Stabwerkmodellen*. Thesis, University of Stuttgart.

Schäfer, K.; Schlaich, J.; Jennewein, M. (1991), *Strut-and-tie modelling of structural concrete*. IABSE Colloquium Stuttgart.

Schlaich, J.; Schäfer, K. (1991), *Design and detailing of structural concrete using strut-and-tie models*. The Structural Engineer, Vol 69, No. 6.

Schlaich, J.; Schäfer, K. (2001), *Konstruieren im Stahlbetonbau*. Betonkalender 2001, Vol. 2, pp. 311-492. Ernst & Sohn Berlin.

Schlaich, J.; Schäfer, K; Jennewein, M. (1987), *Toward a consistent design for structural concrete*. PCI Journal. V.32 (1987), No.3, pp. 75-150.

Schlaich, J.; Weischede, D. (1982): *Manual for Detailing of concrete structure*. CEB Bulletin 150.

Copyright fib, all rights reserved. This PDF copy of fib Bulletin 54 is intended for use and/or distribution only within National Member Groups of fib.

7.4 Reinforcement layout of typical elements

by Giuseppe Mancini

The following figures represent the reinforcement layout of some typical structural elements, in particular:

- Fig. 7.4-1 to Fig. 7.4-3: Pier of railway viaduct for high speed lines:
- Fig. 7.4-4 and Fig. 7.4-5: Abutment of one highway bridge;
- Fig. 7.4-6 to Fig. 7.4-9: Foundation on piles of the bridge pier pictured in Fig. 7.4-1;
- Fig. 7.4-10 to Fig. 7.4-12: Prestressed beam for highway bridge;
- Fig. 7.4-13 and Fig. 7.4-14: Prestressed slab designed in Section 7.2;
- Fig. 7.4-15 and Fig. 7.4-16: Prestressed slab for highway bridge;
- Fig. 7.4-17 and Fig. 7.4-18: Box culvert.

Copyright fib, all rights reserved. This PDF copy of fib Bulletin 54 is intended for use and/or distribution only within National Member Groups of fib.

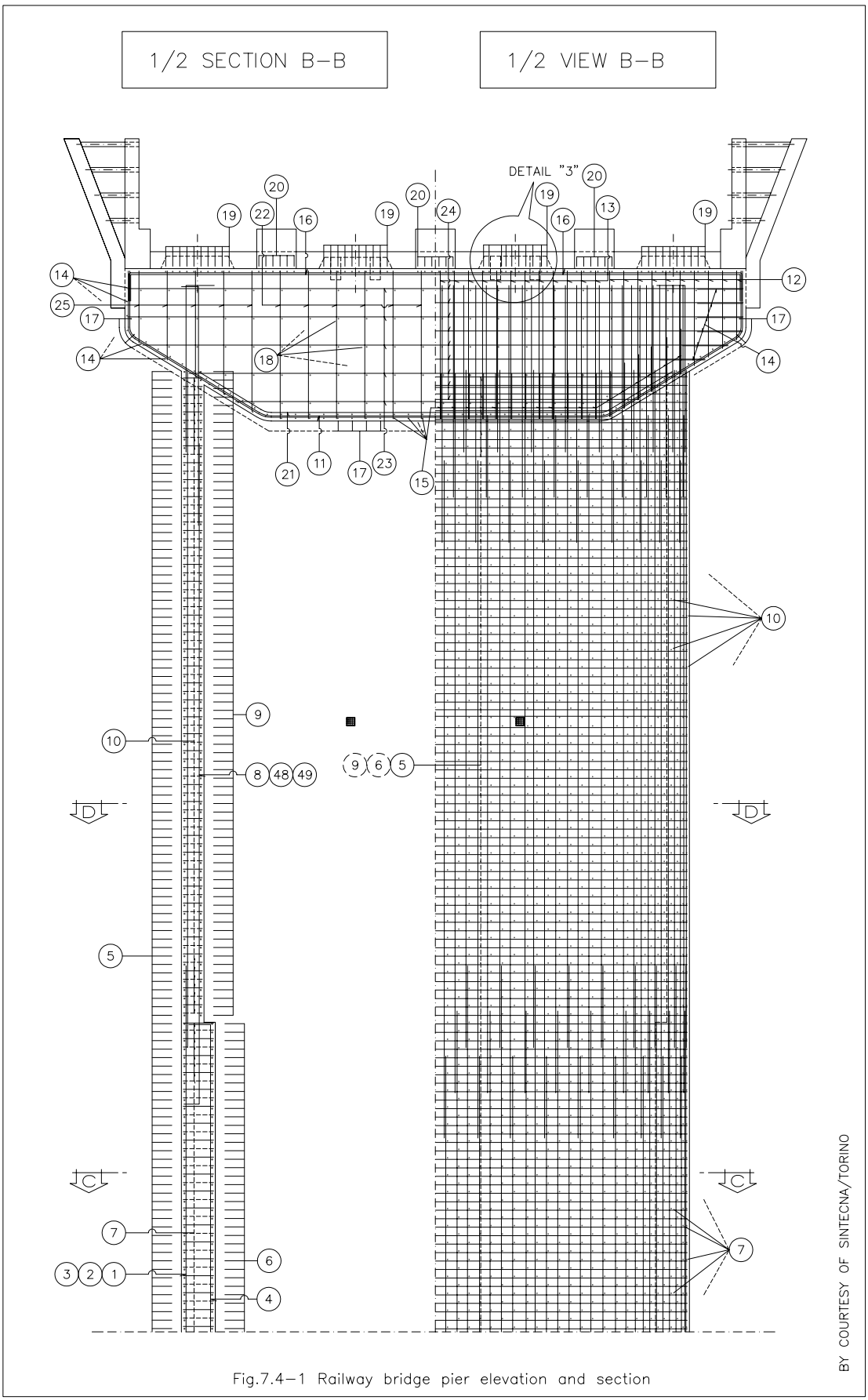


Fig.7.4–1 Railway bridge pier elevation and section

Copyright fib, all rights reserved. This PDF copy of fib Bulletin 54 is intended for use and/or distribution only within National Member Groups of fib.

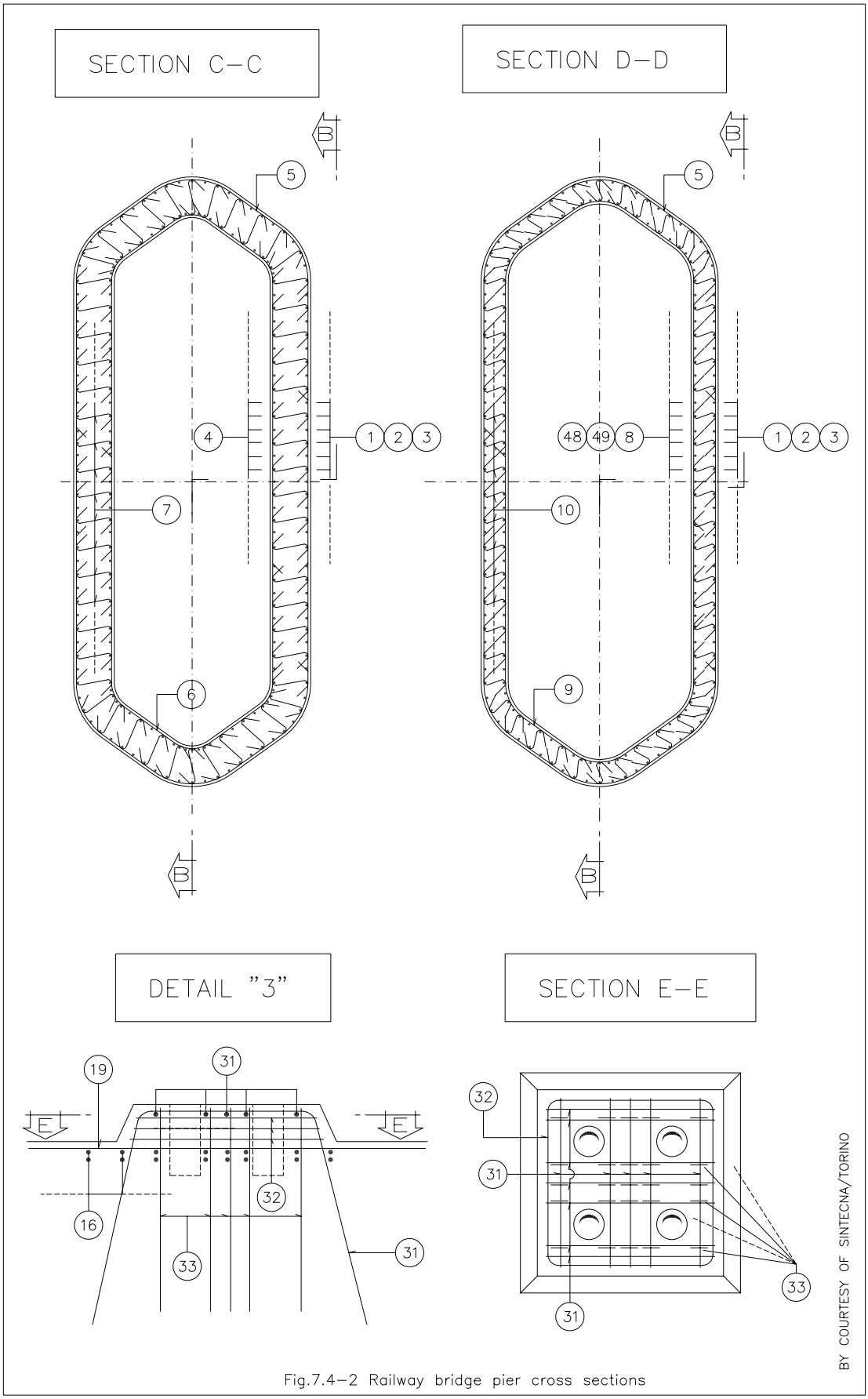


Fig.7.4–2 Railway bridge pier cross sections

Copyright fib, all rights reserved. This PDF copy of fib Bulletin 54 is intended for use and/or distribution only within National Member Groups of fib.

POS.	N.	ø / DIST	LENG. (mm)	SHAPE	L.TOT. (mm)	WEIG. (Kg)
1	36	18 / 600	12000x2 + 3460	2960 500 alternate with pos. 2 e 3 12000 11500 500	988560	1975
2	36	18 / 600	11200+ 12000+ 4260	3760 500 12000 alternate with pos. 1 e 3 10700 500	988560	1975
3	36	18 / 600	10400+ 12000+ 5060	4560 500 alternate with pos. 1 e 2 12000 9900 500	988560	1975
4	108	18 / 200	11760	500 10760 500	1270080	2537
5	134	18 / 150	10800+ 10800+ 6000	200 3770 920 920 3770 200 R=960 R=960 sv.=1200 sv.=910 920 1770 200 200 1770 920 200 5600 200	3698400	7388
6	57	18 / 150	12000 + 10300	200 4920 920 920 2600 200 R=440 R=440 sv.=420 sv.=550 920 5770 200 175 200 920	1271100	2539
7	1566	18 / 300x400	1040	250 540 250	1628640	3253
8	36	18 / 600	12000 + 4560	4260 300 alternate with pos. 48 e 49 11700 300	596160	1191
9	77	18 / 150	12000 + 11570	200 493 920 260 200 R=64 920 R=64 sv.=61 sv.=80 920 514 200 238 920 200	1814890	3625
10	1926	18 / 300x400	840	250 340 250	1617840	3232
11	21	26 / 200	(4350+4350)x2 + (9400+9400)	1000 R=440 sv.=240 1000 1560 1560 5800 R=240 2560 2560 sv.=250 R=44 300 300 sv.=24	760200	3168
12	10 + 10	20 / 250	8060 ÷ 10580	1220 4020 1220 ÷ 800 800 ÷ 2480 2480	186400	460
13	24	20 / 250	10900	4020 2620 820 820 2620	261600	645
14	6 + 6	20 / 250	5600	horizontal bend 790 790 4020	52800	130
15	36	26 / 250	5600	790 790 4020	201600	840
16	21	26 / 200	11850 + 11700	10870 490 10810 490 440 450	494550	2061
17	49	26 / 250	4900	500 500 3900	240100	1001
18	94	20 / 500x500	4400	220 220 3960	413600	1020
19	10 x 4	26 / 125	6200	3960 1120 1120	248000	1034
20	6 x 3	26 / 125	5200	3960 620 620	93600	390
21	21	20 / 200	8400	1300 5800 1300 R=35 R=35 sv.=20 sv.=20	184800	456
22	120	18 / 500x400	3000	190 2620 190	360000	719
23	50	18 / 500x400	7500 ÷ 11300	7100÷10900 200 200	470000	939
24	9 + 9	20 / 250	7500 ÷ 11300	7100÷10900 200 200	169200	417
25	100	18 / 500x400	1540 ÷ 2800	160 1220÷2480 160	217000	433
31	8 x (5+7)	18	3500	980 1260 1260	336000	671
32	8 x 3	18	4780 ÷ 5380	1060÷1210 1060÷1210 270	121920	244
33	8 x 25	18	1400	200 1200	280000	559
48	36	18 / 600	11200 + 5360	5060 300 alternate with pos. 8 e 49 10900 300	596160	1191
49	36	18 / 600	10400 + 6160	5860 300 alternate with pos. 8 e 48 10100 300	596160	1191

Fig.7.4–3 Railway bridge pier reinforcement table

BY COURTESY OF SINTECNA/TORINO

Copyright fib, all rights reserved. This PDF copy of fib Bulletin 54 is intended for use and/or distribution only within National Member Groups of fib.

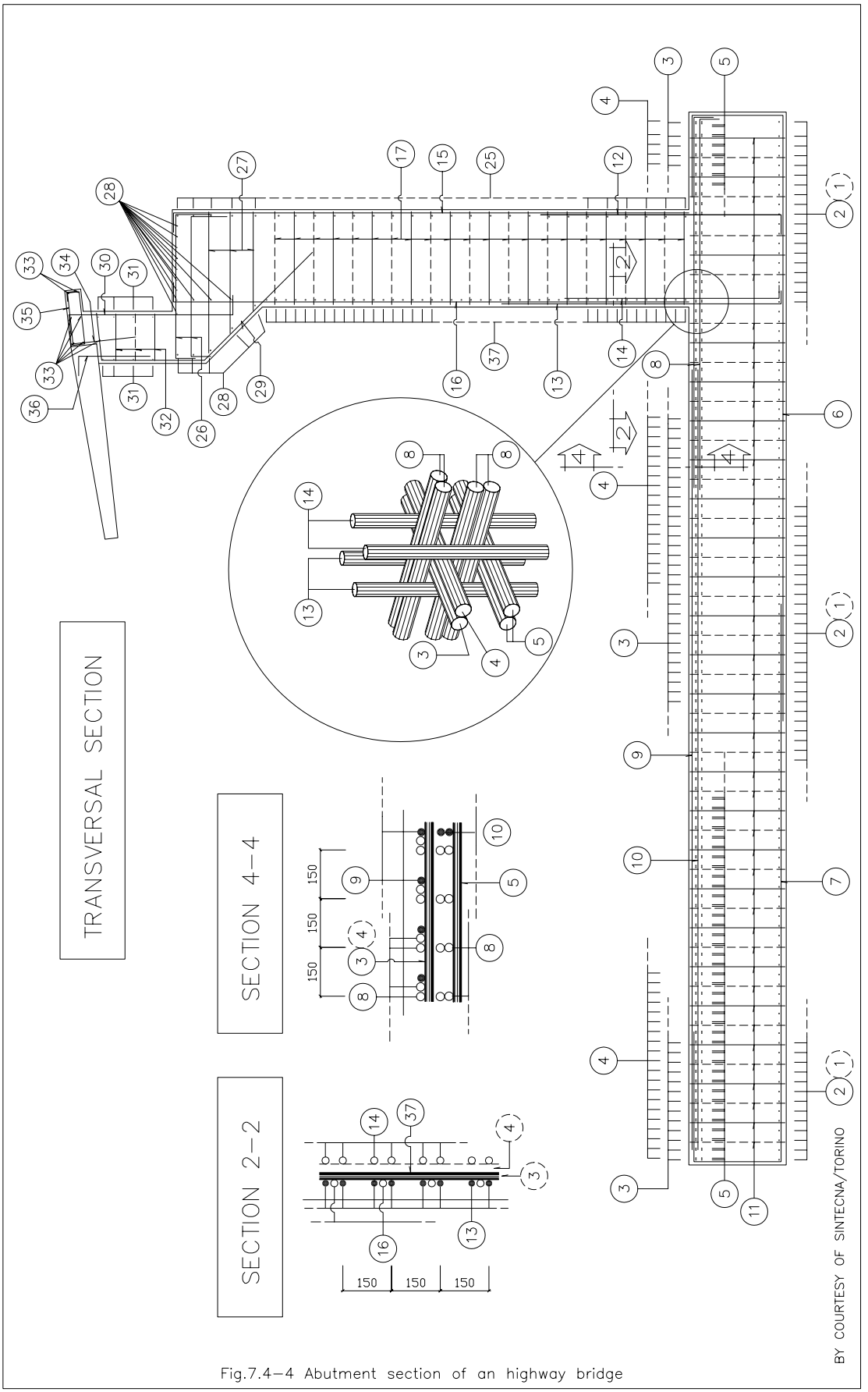


Fig.7.4–4 Abutment section of an highway bridge

POS.	N.	ø / DIST	LENG. (mm)	SHAPE	L.TOT. (mm)	WEIG. (Kg)
1	108 x 2	22 / 150	4000	1300 300 2400	864000	2578.21
2	108	22 / 150	12000	12000	1296000	3867.32
3	108	26 / 150	12000	12000	1296000	5401.46
4	1008 x 2	26 / 150	4500	4200 300	9720000	40051.1
5	108 x 2	26 / 150	3500 + 3500	3500 3500	1512000	6301.7
6	87	22 / 150	12000	1260 9320 1420	1044000	3115.34
7	87	22 / 150	12000	2000 1420 8580	1044000	3115.34
8	87	26 / 150	6000 x 4	5700 300	2088000	8702.35
9	87	16 / 150	12000 + 12000	12000	2088000	3296
10	4 + 4	20 / 900	12000 + 12000	12000	192000	474
11	1170	16 / 300x600	1800	200 1400 200	2106000	3324
12	37	26 / 300	4000	3700 300	148000	616.83
13	60	22 / 150	4500 + 4500	4300 200	540000	1611.38
14	60	22 / 150	3500 + 3500	3300 200	420000	1253.3
15	37 + 6x2	26 / 300	8200	300 7900	401800	1674.62
16	60	22 / 150	8200	300 7900	492000	1468.15
17	352	14 / 300x600	1800	1400 200 200	633600	765.65
25	27	22 / 300	12000	600 600 10800	324000	966.83
26	37x2 + 3x5	22 / 300	3000	2270 250 480 3 additional bars in the bearing support	267000	796.74
27	31 x 3	22 / 300	2800 ÷ 2100	2200÷1500 300 300	227850	679.91
28	17	22	12000	10800 600 600	204000	608.74
29	31	22 / 300	4500	700 107g 1590 150g 2210	139500	416.27
30	37	22 / 300	3000	350 93g 2400 250	111000	331.23
31	4 + 4	16 / 300	12000	10800 600 600	96000	151.52
32	45	12 / 300x600	1000	700 150 150	45000	39.95
33	7	12	12000	10800 600 600	84000	74.58
34	28	16 / 300	1200	200 1000	33600	53.03
35	28	12 / 300	2200	160 180 760 160	61600	54.69
36	14	20 / 600	1200	200 93g 1000	16800	41.43
37	44	22 / 150	12000	10800 600 600	528000	1575.57

BY COURTESY OF SINTECNA/TORINO

Fig.7.4–5 Abutment reinforcement table

Copyright fib, all rights reserved. This PDF copy of fib Bulletin 54 is intended for use and/or distribution only within National Member Groups of fib.

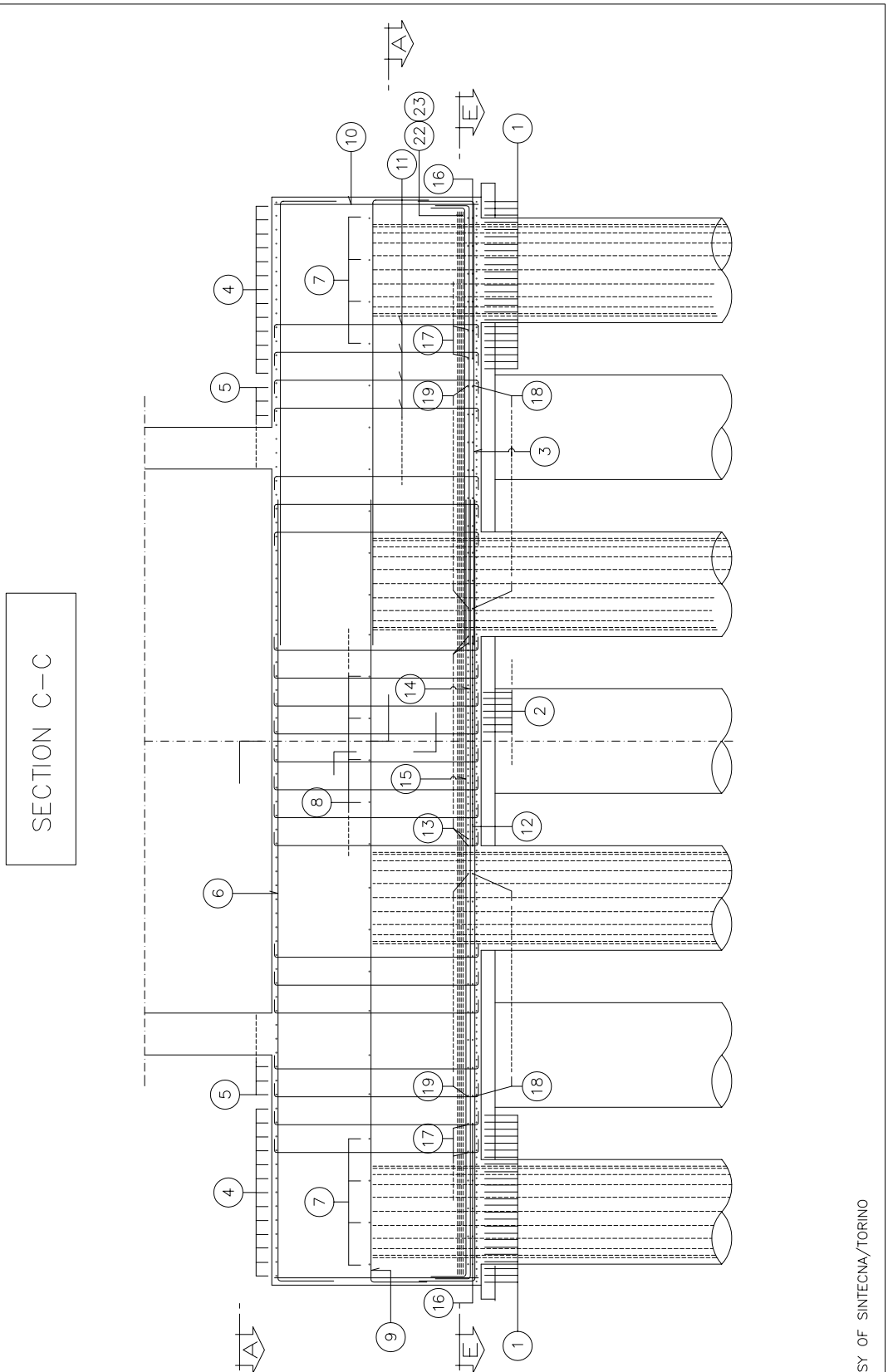


Fig.7.4–6 Pier foundation. Vertical section

Copyright fib, all rights reserved. This PDF copy of fib Bulletin 54 is intended for use and/or distribution only within National Member Groups of fib.

POS.	N.	ø / DIST	LENG. (mm)	SHAPE	L.TOT. (mm)	WEIG. (Kg)
1	25 + 25	26 / 100	2590 ÷ 11160	800 — 990÷9560 — 800	343750	1433
2	105	26 / 100	11420	800 — 9820 — 800	1199100	4998
3	99	26 / 100	(8140÷12000) + (6000÷7200)	800 — 2080 — 800; 7340÷11200 5200÷6400; alternate arrangement	2303730	9601
4	13 + 13	26 / 200	2590 ÷ 11160	990÷9560; 800 — 800	178750	745
5	52	26 / 200	11420	9820; 800 — 800	593840	2475
6	50	26 / 200	(8140÷12000) + (6000÷7200)	7340÷11200 5200÷6400; 800 — 2080 — 800; alternate arrangement	1163500	4849
7	4 + 4	20 / 600	2500 ÷ 8930	1700÷8130; 400 — 400	45720	113
8	18	20 / 600	10620	9820; 400 — 400	191160	471
9	17	20 / 600	(7500÷12000) + (5380÷6000)	7100÷11600 5000÷5600; 400 — 1600 — 400; alternate arrangement	359210	886
10	202	26 / 200	2920	2920	589840	2458
11	710	16 / 400x400	3300	2920; 190; 190	2343000	3698
12	31	26 / 100	10760	500 — 9760 — 500	333560	1390
13	31	26 / 100	10700	500 — 9700 — 500	331700	1382
14	31	26 / 100	12000 + (5300÷6550)	500 — 2080 — 500; 11500 4800÷6050; alternate arrangement	739350	3081
15	31	26 / 100	12000 + (5240÷6500)	500 — 2080 — 500; 11500 4740÷6000; alternate arrangement	735940	3067
16	6 + 6	26 / 400	1230 ÷ 8360	1230÷8360	57540	240
17	6 + 6	26 / 400	1170 ÷ 8300	1170÷8300	56820	237
18	9 + 9	26 / 400	9760	9760	175680	732
19	9 + 9	26 / 400	9700	9700	174600	728
20	8 + 8	26 / 400	10620 ÷ 12000	10620÷12000	180960	754
21	8 + 8	26 / 400	10560 ÷ 12000	10560÷12000	180480	752
22	(31+31) x 2	26 / 200	10400 ÷ 12000	400 — side by side — 400; 9600÷11200	1388800	5788
23	(31+31) x 2	26 / 200	10400 ÷ 12000	430 — side by side — 430; 9540÷11140	1388800	5788
24	(4x2) x 4	26 / 600	3200	3200	102400	427

Fig.7.4–7 Pier foundation. Reinforcement table

BY COURTESY OF SINTECNA/TORINO

Copyright fib, all rights reserved. This PDF copy of fib Bulletin 54 is intended for use and/or distribution only within National Member Groups of fib.

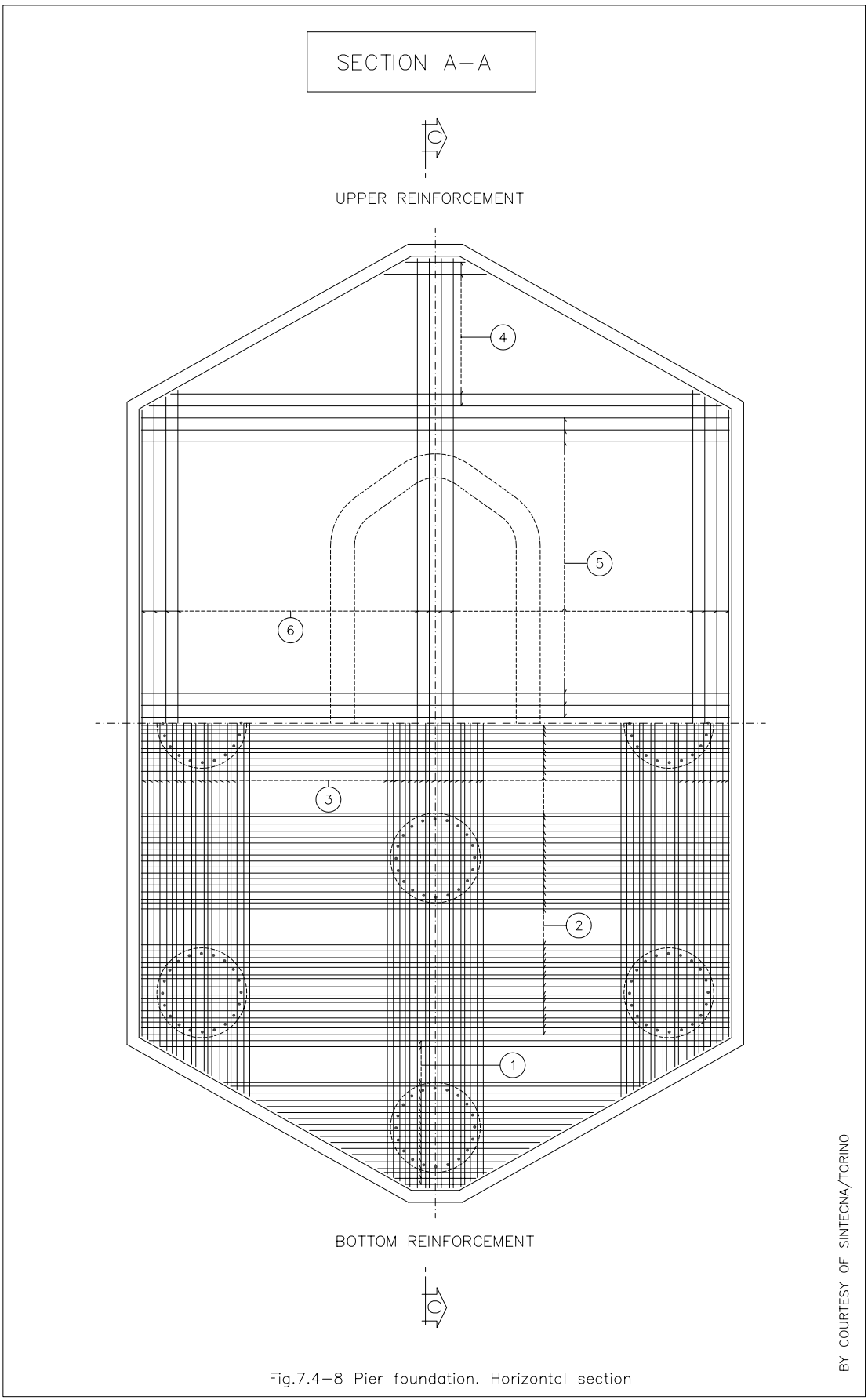


Fig.7.4–8 Pier foundation. Horizontal section

Copyright fib, all rights reserved. This PDF copy of fib Bulletin 54 is intended for use and/or distribution only within National Member Groups of fib.

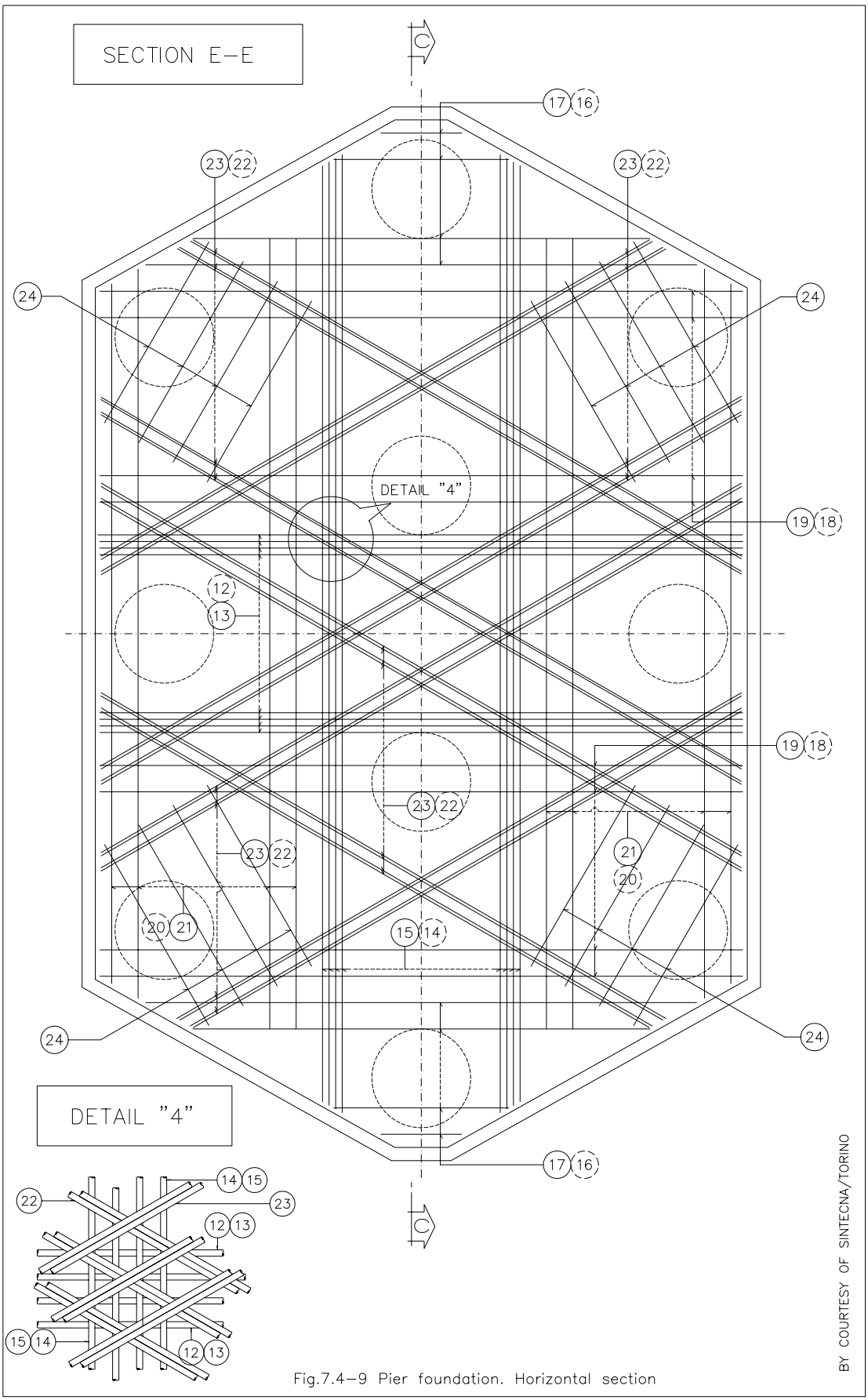


Fig.7.4–9 Pier foundation. Horizontal section

Copyright fib, all rights reserved. This PDF copy of fib Bulletin 54 is intended for use and/or distribution only within National Member Groups of fib.

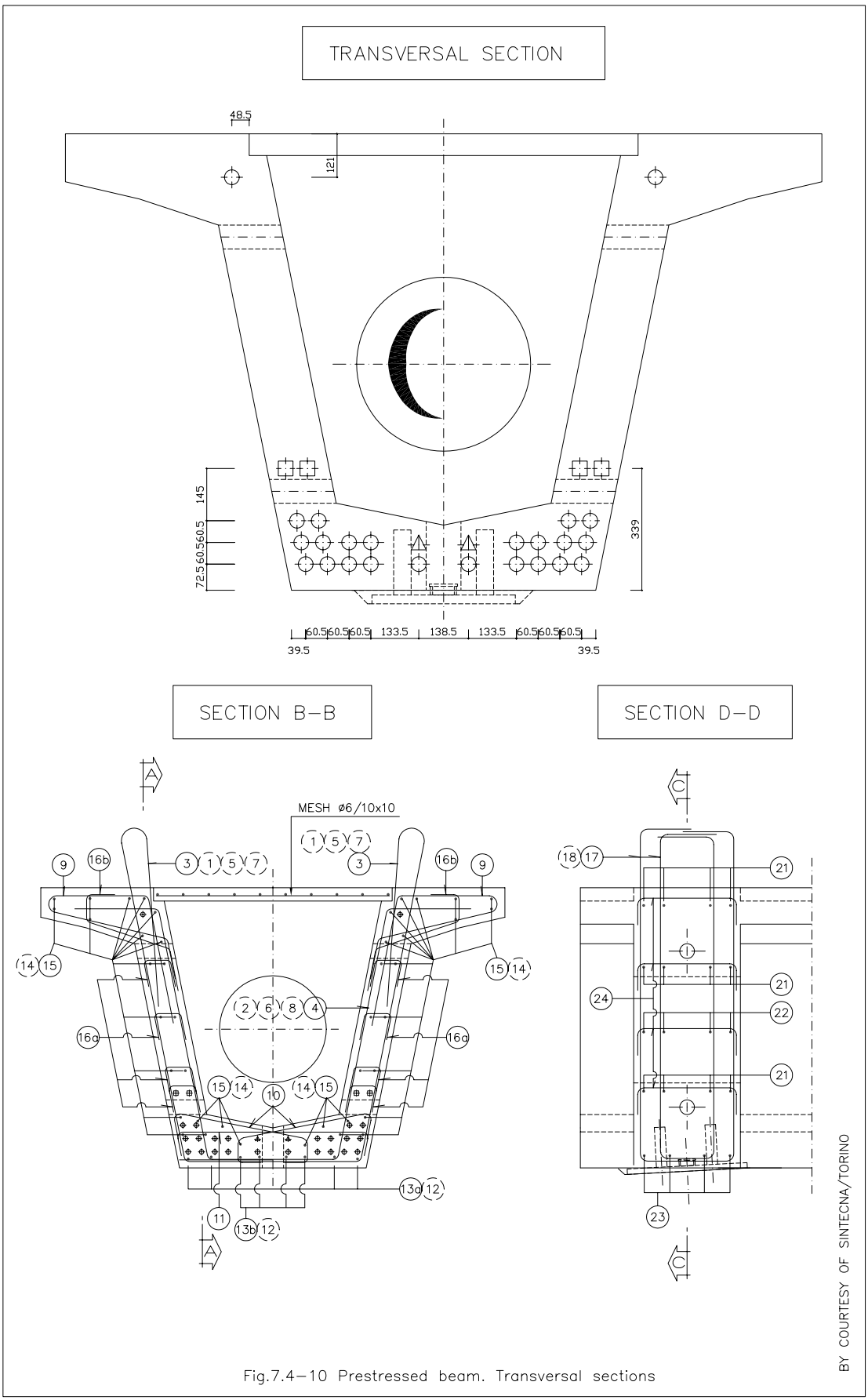
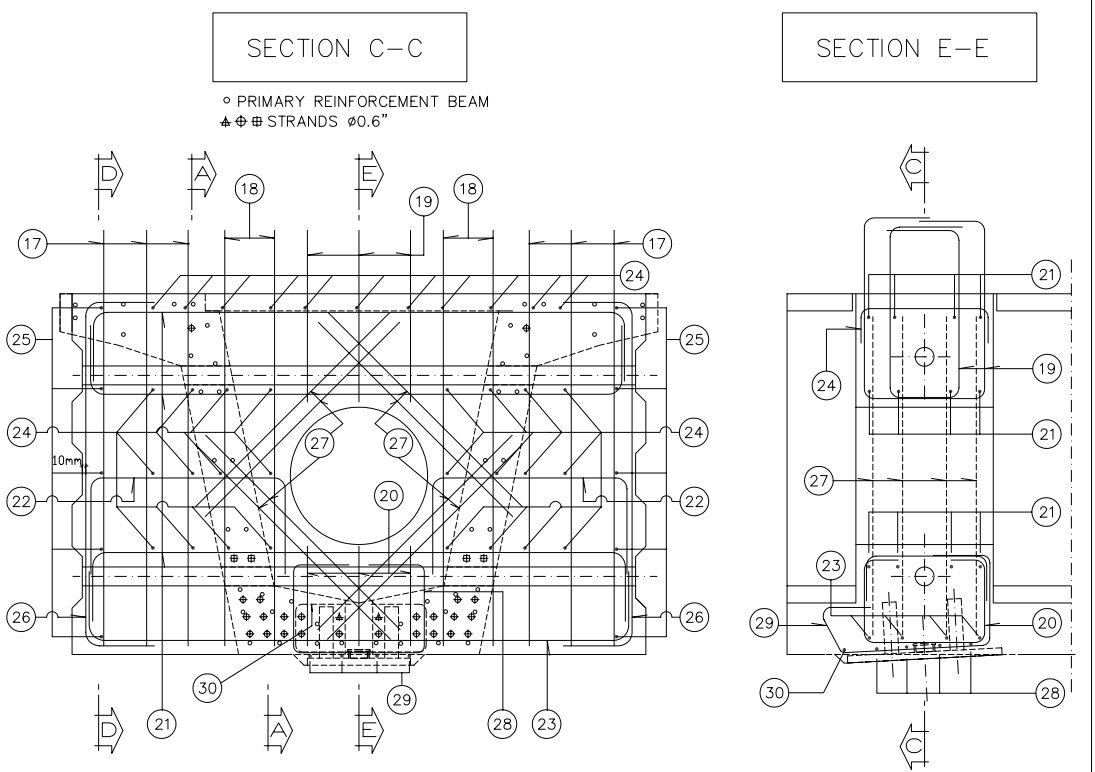


Fig.7.4–10 Prestressed beam. Transversal sections

Copyright fib, all rights reserved. This PDF copy of fib Bulletin 54 is intended for use and/or distribution only within National Member Groups of fib.



POS.	N.	ø / DIST	LENG. (mm)	SHAPE	L.TOT. (mm)	WEIG. (Kg)
1	13 x 2	16 / 100	4600	1220 130 630 30 1220 640	119600	189
2	13 x 2	16 / 100	3000	310 950 310 950 480	78000	123
3	21 x 2	14 / 200	4600	120 1220 640 120 1220 640	193200	233
4	21 x 2	14 / 200	3000	310 950 310 950 480	126000	152
5	25 x 2	12 / 200	4600	100 1220 660 100 1220 640	230000	204
6	25 x 2	12 / 200	3000	310 950 310 950 480	150000	133
7	25	10 / 200	4600	80 1220 680 80 1220 640	115000	71
8	25	10 / 200	3000	310 950 310 950 480	75000	46
9	121 x 2	8 / 200	1500	330 470 s=130 140 430	363000	143
10	121 x 2	8 / 200	800	500 90 100 110	193600	76
11	121	10 / 200	900	700 100 100	108900	67
12	8	10	12000	12000	96000	59
13a	4 + 4	22	11000	2220 980 7800 bend within the web	88000	263
13b	4 + 4	14	8300	410 90 7800	66400	80
14	42	10	12000	12000	504000	311
15	42 + 42	12	7400	100 7300	621600	552

POS.	N.	ø / DIST	LENG. (mm)	SHAPE	L.TOT. (mm)	WEIG. (Kg)
16a	4x121 x 2	8 / 200	290	90 100 113g 87g 100	280720	111
16b	121 x 2	8 / 200	650	100 110 140 300	157300	62
17	(3+3) x 2	14 / 125	3200 + 3000	220 220 190 190 1210 1210 340 200	74400	90
18	(2+2) x 2	18	3200 + 3000	220 220 190 190 1210 1210 340 200	49600	99
19	3 x 2	14 / 150	1800 + 1600	230 230 200 200 500 500 340 200	20400	25
20	3 x 2	14 / 150	1200 + 700	340 180 140 180 290 340	11400	14
21	(4x3)x2	20	1950	1550 200 200	46800	115
22	(4x2)x2	16	940	540 200 200	15040	24
23	4 x 2	22	1950	200 1550 200	15600	47
24	35 x 2	10	600	340 130 130	42000	26
25	(5+5) x 2	10	1000	330 340 330	20000	12
26	(4x2)x2	12	1400	220 960 220	22400	20
27	(8x4)x2	10	800	800	51200	32
28	4 x 2	20	1200	170 170 240 380 240	9600	24
29	4 x 2	20	1250	210 210 260 120 3.4g 127.7g 400	10000	25
30	1 x 2	14	900	160 160 100 380 100	1800	2

BY COURTESY OF SINTECNA/TORINO

Fig.7.4–11 Prestressed beam. Transversal sections and reinforcement table

Copyright fib, all rights reserved. This PDF copy of fib Bulletin 54 is intended for use and/or distribution only within National Member Groups of fib.

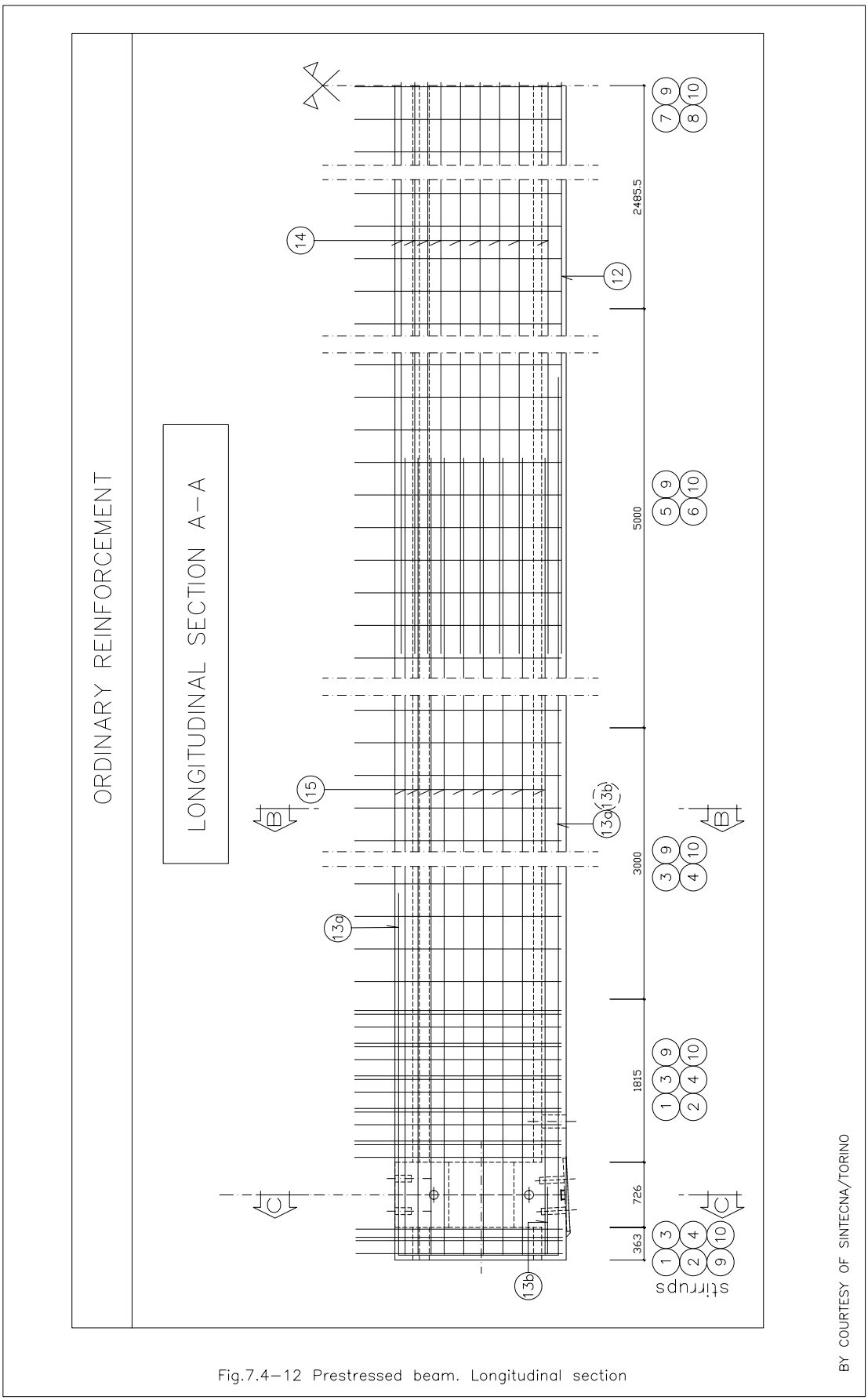


Fig.7.4–12 Prestressed beam. Longitudinal section

Copyright fib, all rights reserved. This PDF copy of fib Bulletin 54 is intended for use and/or distribution only within National Member Groups of fib.

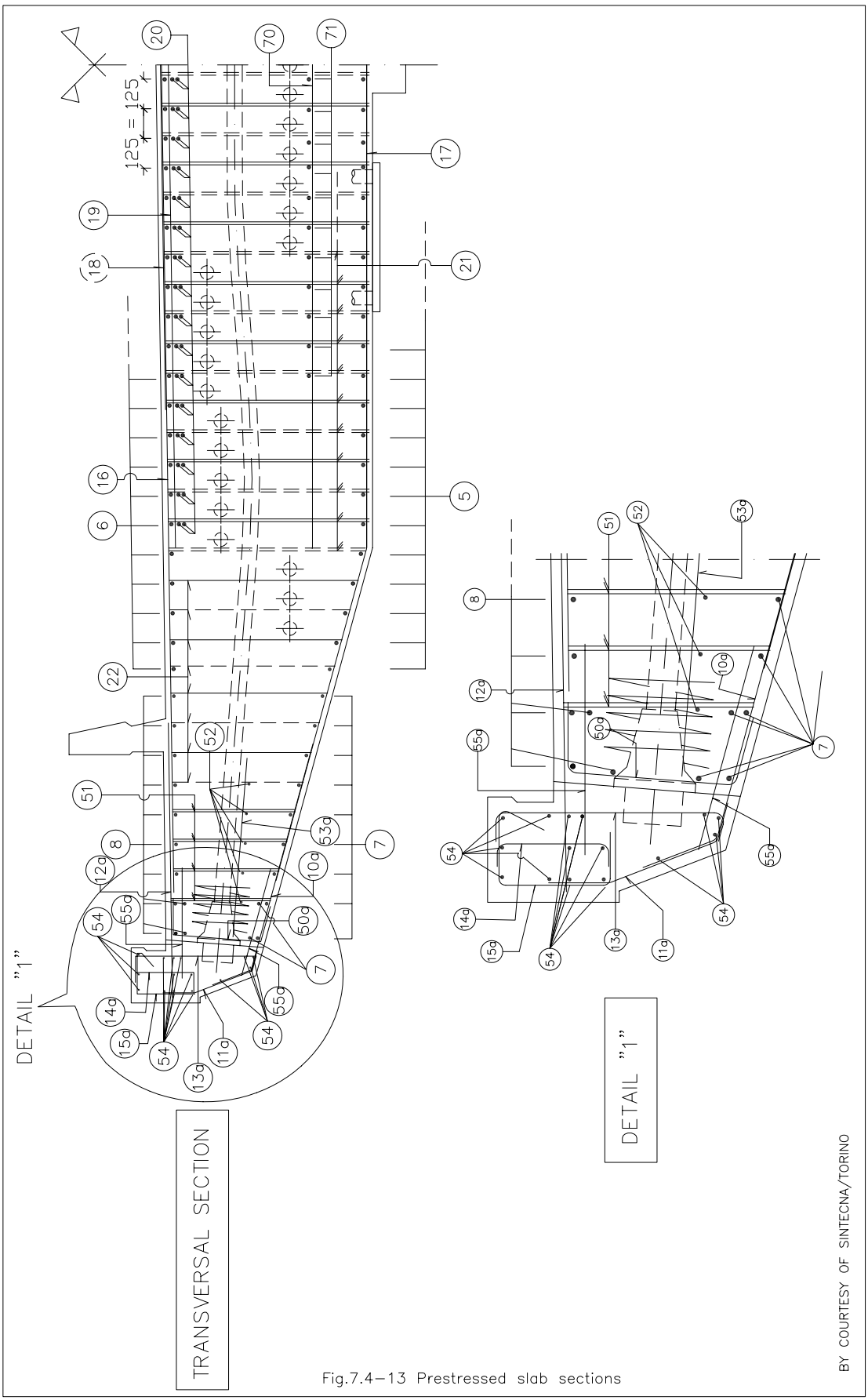


Fig.7.4–13 Prestressed slab sections

Copyright fib, all rights reserved. This PDF copy of fib Bulletin 54 is intended for use and/or distribution only within National Member Groups of fib.

POS.	N.	Ø / DIST	LENG. (mm)	SHAPE	L.TOT. (mm)	WEIG. (Kg)
5	42	22 / 215	7000+ (12000x5)+ 7000	250 12000x5 250 / 6750(1500)(1500)6750	3108000	9274.4
6	42	22 / 215	12000+ (12000x4)+ 12000	11750(1500)(1500)11750 / 250 12000x4 250	3024000	9023.74
7	11 x 2	18 / 215	6000+ (12000x5)+ 6000	250 12000x5 250 / 5750(1170)(1170)5750	1584000	3164.17
8	11 x 2	18 / 215	11400+ (12000x4)+ 11400	11170(1170)(1170)11170 / 230 12000x4 230	1557600	3111.43
10a	10x4 + 17x4	12 / 215	2000 + 2000	bend after tensioning 140g 1700 / 300	432000	383.54
11a	10x4 + 17x4	12 / 215	900	230 176g / 520 / 140g 150	97200	86.3
12a	10x4 + 17x4	20 / 215	2400	horizontal bend 1970 / 180 250	259200	639.23
13a	10x4 + 17x4	16 / 215	1200	160 / 150g 860 / 180	129600	204.55
14a	15x4 + 17x4	16 / 430	700	130 / 420 / 150	89600	141.42
15a	13x4 + 17x4	16 / 215	1150	330 / 420 150g 200 / 200	138000	217.81
16	17 x 2	26 / 215	12000	6000 6000 / 198g	408000	1700.46
17	34 x 2	18 / 107.5	12000	2500 7000 2500	816000	1630.03
18	17 x 2	26 / 215	5000	2500 2500 / 198g (alternate with pos.16)	170000	708.52
19	34 x 2	26 / 107.5	7000	3500 3500 / 198g	476000	1983.87
20	32 x 2	26 / 215	6000 + 6000	6000	768000	3200.87
21	312 x 2	14 / 215x430	(1850÷1800) + (1850÷1800)	1490 ÷ 1440 180 / 180 (disporre a quinconce)	2277600	2752.28
22	120 x 2	16 / 430x430	1350 ÷ 1750	970 ÷ 1370 190 / 190 (disporre a quinconce)	372000	587.14
50a	11x4 + 17x4	20 / 215	1200	270 / 630 109g / 300	134400	331.45
51	201 x 4	18 / 215	1050 ÷ 1240	160 / 150g 730÷920 / 160	920580	1838.93
52	5 x 2	18 / 215	6000+ (12000x5)+ 6000	200 12000x5 200 / 5800(1200)(1200)5800	720000	1438.26
53a	6x4 + 9x4	16 / 430	1500	1300 / 200	90000	142.05
54	15 x 2	14	5200+ (12000x5)+ 5200	200 12000x5 200 / 5000(≥1000) 5000	2112000	2552.17
55a	12x4 + 18x4	12 / 430	1700	790 / 120 / 790	204000	181.11
70	11 x 2	22	6000	6000	132000	393.89
71	22 x 2	22	3000	3000	132000	393.89

BY COURTESY OF SINTECNA/TORINO

Fig.7.4–14 Prestressed slab reinforcement table

Copyright fib, all rights reserved. This PDF copy of fib Bulletin 54 is intended for use and/or distribution only within National Member Groups of fib.

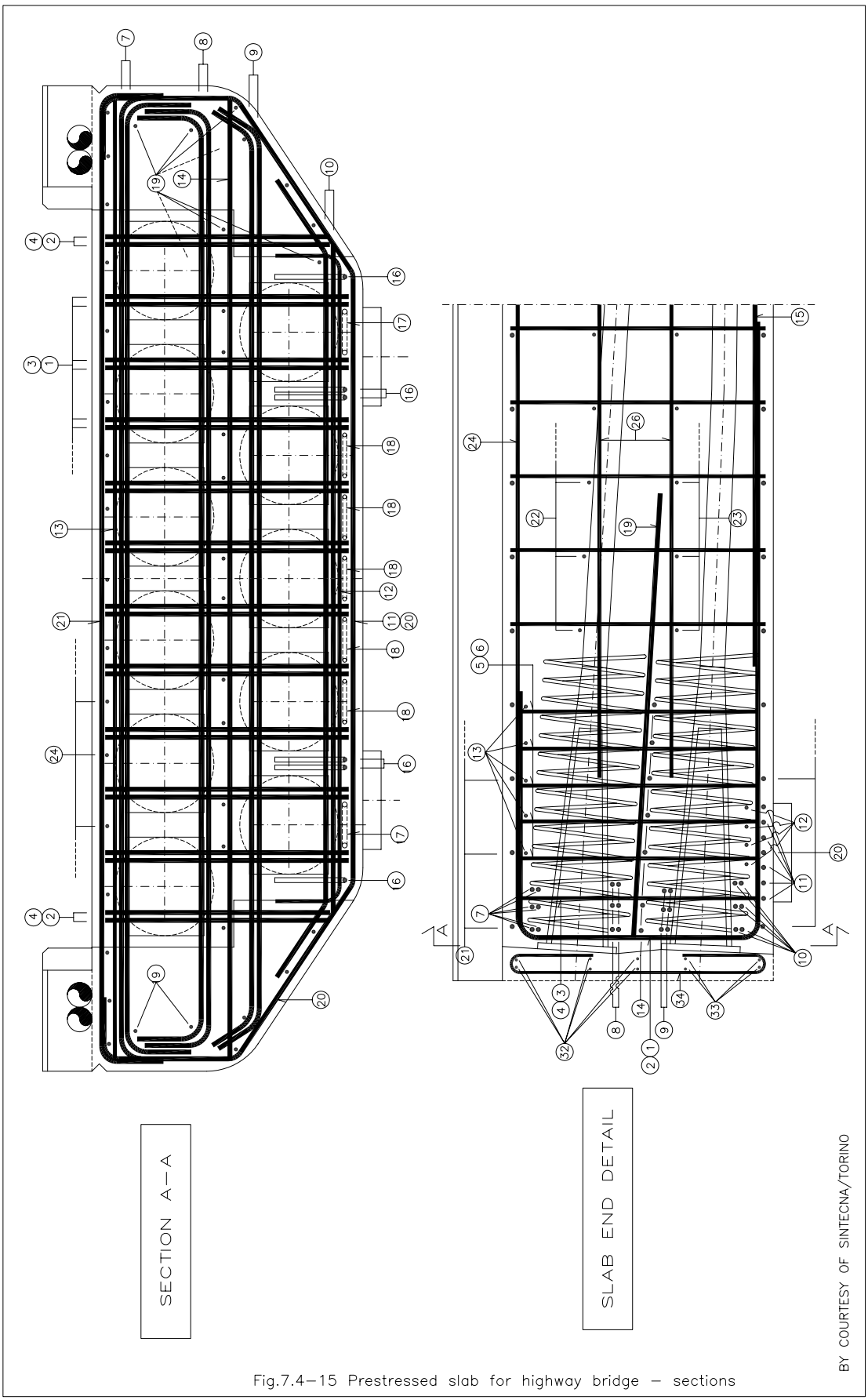
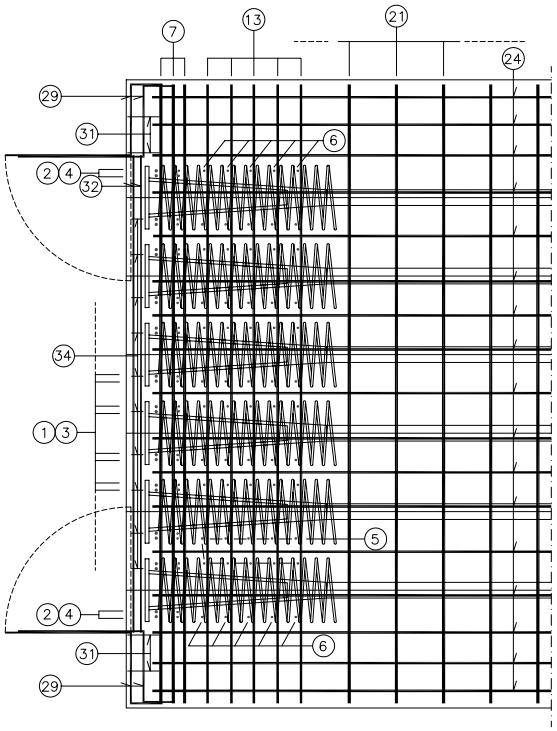


Fig.7.4–15 Prestressed slab for highway bridge – sections

Copyright fib, all rights reserved. This PDF copy of fib Bulletin 54 is intended for use and/or distribution only within National Member Groups of fib.

SECTION B–B



POS.	ø / DIST	SHAPE	LENG. (mm)	N.	WEIG. (Kg)
1	20	125 1000 820 125 2500	4570	20 x 2	451
2	20	125 1000 700 125 2500	4450	4 x 2	58
3	16	60 400 900 60 400	1820	20 x 2	115
4	16	60 400 780 60 400	1700	4 x 2	22
5	16 / 150	60 400 900 60 400	1820	5x 100x 2	287
6	16	60 400 780 60 400	1700	5x 2x 2	54
7	20	125 3730 125 250 3670 250 125 125 180 180	4480 4280	6 6	130
8	20	180 125 125 180 250 3570 250 125 3620 125	4180 4370	6 6	124
9	20	160 100 100 160 160 3480 160 100 3500 100	4000 4020	6 6	119
10	20	350 50 50 350 350 2610 350 50 2690 50	3410 3490	6 6	102
11	20	350 250 50 2400 50	3100	6 + 6	89
12	16	200 200 60 2500 60	3020	4 x 2	38
13	16	60 3840 60 200 200	4360	5 x 2	69
14	20	160 160 125 3720 125	4290	7 x 2	148
15	20	12000 6000 12000 alternate arrangement	12000+ 12000+ 6000	21	1554

POS.	ø / DIST	SHAPE	LENG. (mm)	N.	WEIG. (Kg)
16	20	300 125 2500	2925	6 x 2	87
17	20	250 2500 100	5250	2 x 2	52
18	16	120 2500 100	5120	5 x 2	81
19	16	200 1800	2000	26	82
20	20 / 300	125 250 250 125 470 470 60 800 800 60 2420 50 50	5930	97	1419
21	20 / 300	125 3760 125 250 250	4510	97	1079
22	16 / 300	60 3840 60 140 140	4240	89	596
23	16 / 300	140 140 60 3500 60	3900	89	548
24	16	60 11800 12000 7600 60 140 1100 1100 140 alternate arrangement	12000+ 12000+ 7800	17	853
26	16	12000 12000 6000 1100 alternate arrangement	12000+ 12000+ 6000	12	568
29	12	200 450 800	1450	16 x 2	41
31	12	200 690 840 200	1090 1240	4 4	8
32	12	3040	3040	6 x 2	32
33	12	2550	2550	4 x 2	18
34	12	60 1040 300 300	1760	10 x 2	31

Fig.7.4–16 Prestressed slab for highway bridge – section and reinforcement table

BY COURTESY OF SINTECNA/TORINO

Copyright fib, all rights reserved. This PDF copy of fib Bulletin 54 is intended for use and/or distribution only within National Member Groups of fib.

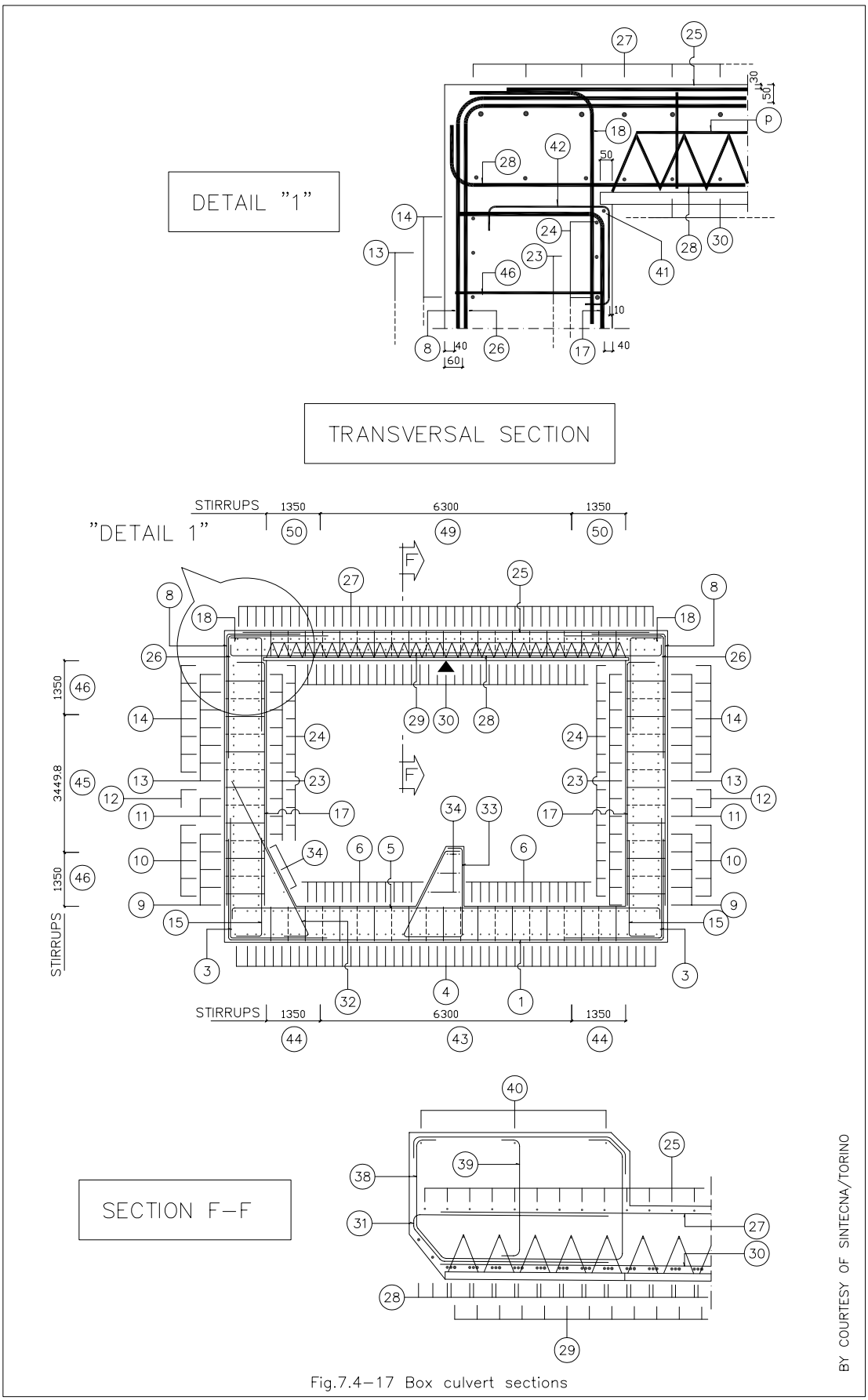
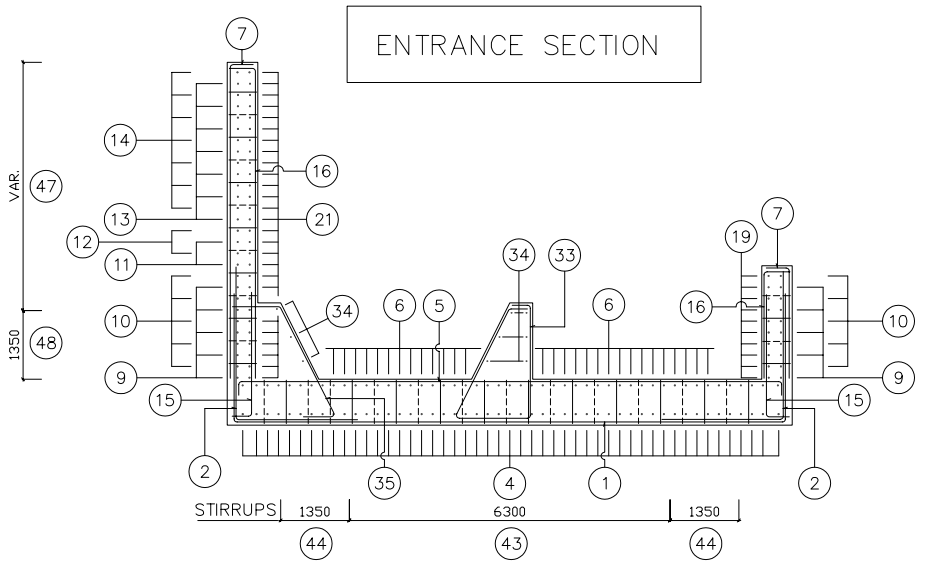


Fig.7.4–17 Box culvert sections

Copyright fib, all rights reserved. This PDF copy of fib Bulletin 54 is intended for use and/or distribution only within National Member Groups of fib.



POS.	N.	Ø / DIST	LENG. (mm)	SHAPE	L.TOT. (mm)	WEIG. (Kg)
1	138	14 / 150	12000	1680 8640 1680	1656000	2001
2	35x2 + 33x2	20 / 150	4000 + 4000	2000 2000 2000 2000	1088000	2683
3	70 x 2	20 / 150	4000	2000 2000	560000	1381.04
4	49	14 / 150	12000+ 12000+ 4000	alternate arrangement 11500 3500 500 12000 500	1372000	1657.94
5	129	18 / 150	9000	8640 180 180	1161000	2319.19
6	49	14 / 150	12000+ 12000+ 4000	500 12000 11500 3500 alternate arrangement 500	1372000	1657.94
7	(35+33) x 2	14 / 177	1800 ÷ 5300	300 1500 ÷ 5000	482800	583
8	70 x 2	14 / 177	6000	1450 4550	840000	1015
9	5 x 2	14 / 300	12000+ 12000+ 4000	300 11700 3700 300 135.6g 12000 64.4g	280000	338.36
10	5 x 2	14 / 300	12000+ 12000+ 4000	300 135.6g 12000 64.4g 300 3700 11700	280000	338.36
11	2 x 2	14 / 300	12000+ 12000+ 1850÷3300	300 135.6g 12000 64.4g 300 1550÷3000 11700	106300	128.45
12	2 x 2	14 / 300	12000+ 12000+ 1850÷3300	300 11700 1550÷3000 300 135.6g 12000 64.4g	106300	128.45
13	7 x 2	14 / 300	12000 + 5650÷11850	300 11700 64.4g 300 135.6g 5350÷11550	290500	351.04
14	7 x 2	14 / 300	12000 + 5650÷11850	135.6g 300 11700 300 5350÷11550 64.4g	290500	351.04
15	138 x 2	14 / 177	2000	300 1700	552000	667
16	(35+33) x 2	12 / 177	1650 ÷ 5300	300 5000 ÷ 1350	472600	420
17	70 x 2	14 / 177	4500	440 4060	630000	761
18	70 x 2	14 / 177	2000	500 1500	280000	338
19	28	12 / 150	2350 ÷ 6900	2050÷6600 300 64.4g	129500	114.97
21	28	12 / 150	2350 ÷ 6900	135.6g 300 2050÷6600	125300	111.24
23	14 + 14	14 / 300	12000 + 2400	11500 1900 500 500 64.4g 135.6g	403200	487.23
24	14 + 14	14 / 300	12000 + 2400	1900 500 64.4g 11500 500 135.6g	403200	487.23
25	69	14 / 150	8000	8000	552000	667.04

POS.	N.	Ø / DIST	LENG. (mm)	SHAPE	L.TOT. (mm)	WEIG. (Kg)
26	69 x 2	26 / 150	4000 + 4000	200 200 200 200	1104000	4601.24
27	48	14 / 150	12000	12000	576000	696.05
28	69	20 / 150	9000 + 9000	180 180 8640 180 180 8640	1242000	3062.96
29	69	22 / 150	6000	6000	414000	1235.39
30	48	14 / 150	12000	12000	576000	696.05
31	48 x 2	14 / 150	3000	57g 1300 450 143g 1250	288000	348.02
32	35	14 / 300	3000	2500 500 66g	105000	126.88
33	69	14 / 300	5000	1760 260 66g 1200 1520	345000	416.9
34	3 x 3	12	12000 + 12000 + 4000	300 11700 3700 300 135.6g 12000 64.4g	252000	223.73
35	18 + 16	14 / 300	3000	600 1700 700 66g	102000	123.26
38	24 x 2	14 / 300	1800 + 2990÷2380	180 1300 140÷80 150 140÷80 490 ÷ 550 140÷80 130÷70 1170 70 ÷ 76 300 1200 590÷650	23040	278.42
39	24 x 2	14 / 300	1000÷940 + 1060÷1000	150÷120 700 ÷ 760 150÷120	48000	58
40	3 x 2	12	9000	180 8640 180	54000	47.94
41	2	16	12000	100 143g 143g 100 11800	24000	37.88
42	69 x 2	8 / 150	1000	400 100 100 400	138000	54.45
43	756 + 181	12 / 300x450	800	140 140 520	74960	665.51
44	376	16 / 300x450	800	140 140 520	30080	474.76
45	118	12 / 300x450	1000	620 190 190	118000	104.76
46	164	16 / 300x450	1000	620 190 190	164000	258.85
47	119	12 / 300x450	600	320 140 140	7140	63.39
48	76	16 / 300x450	600	320 140 140	4560	71.97
49	293	12 / 300x450	700	150 150 400	20510	182.09
50	126	16 / 300x450	700	150 150 400	8820	139.21

BY COURTESY OF SINTECNA/TORINO

Fig.7.4–18 Box culvert section and reinforcement table

Copyright fib, all rights reserved. This PDF copy of fib Bulletin 54 is intended for use and/or distribution only within National Member Groups of fib.

8 Practical aspects

by Konrad Zilch and Angelika Schießl

8.1 Introduction

This chapter deals with the transition from structural design to execution. During the design process, the verification of limit states according to Sections 4.3 and 4.4 is based on the strength or stiffness etc. of members. They depend on material properties and cross-section dimensions. The nature of these quantities is not deterministic but stochastic due to the scatter in the materials used (aggregate, Portland cement) and in the the erection process itself (imperfections, for example precision of formwork, water/cement ratio). So a major point of interest is the deviations of actual properties from nominal values. From the point of structural safety, limiting values for these deviations (*tolerances*) must be defined that are in accordance with the basic assumptions of the safety concept. In order to assure the tolerances defined in design new strategies were developed to achieve a high level of quality in the execution. They are generally known as quality management and are also presented in this chapter. Finally some aspects in the erection of RC and PC structures are described followed by an introduction into prestressing and precast elements and structures.

8.2 Geometric tolerances

8.2.1 Definition and types

The term *tolerance* defines the maximum allowable deviation between an actual geometric quantity of a structural element and its nominal value specified by the designer[1] (Fig. 8.2-1). Under site conditions, certain deviations are inevitable; they may be due to the imperfection of geodetic measurement, the imperfection of formwork and its deformation during casting. They may also be caused by gross errors, but those cannot be treated within the context of tolerances in a reasonable manner. Therefore, they should be excluded by adequate measures of quality control.

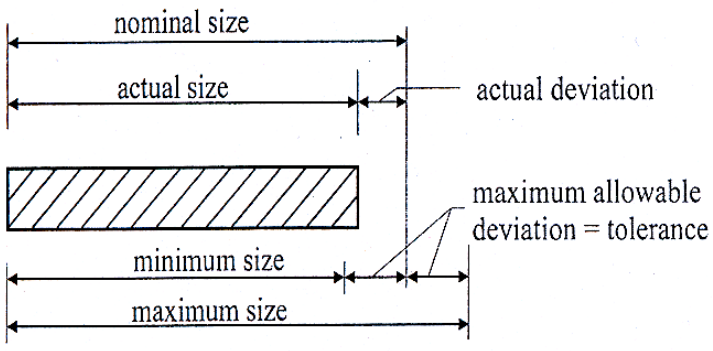


Fig. 8.2-1: Definition of nominal size, deviation and tolerance

[1] Some authors define tolerance as the difference between the maximum and minimum allowable size. Within this chapter, the definition given above will be used.

Copyright fib, all rights reserved. This PDF copy of fib Bulletin 54 is intended for use and/or distribution only within National Member Groups of fib.

Tolerances are criteria that indicate whether an imperfectly executed structure complies with the requirements of safety, durability and serviceability. Their definition is part of the design concept as well as the definition of safety factors. (In this chapter, it will be shown that there is a close connection between tolerances and safety factors.) On the other hand, tolerances are a tool to specify the quality of execution between the client and the executing company.

Geometric deviations (and the corresponding tolerances) may be subdivided into:

- deviations in cross section dimensions,
- deviations in the position of reinforcement,
- deviations in span,
- deviations from perfect shape (curvature) and direction of members,
- deviations in the location of members.

A typical example for an RC member is shown in Fig. 8.2-2. The influence of deviations on structural performance may differ depending on the type of structure, the erection procedure and the specific requirements of serviceability.

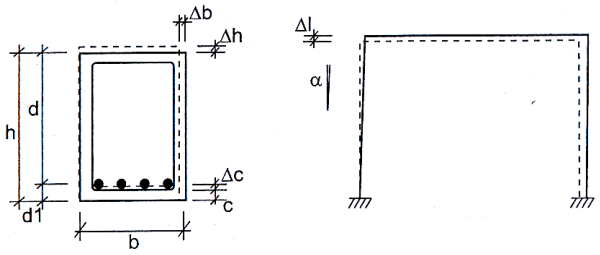


Fig. 8.2-2: Geometric dimensions and deviations of a reinforced concrete member

8.2.2 Effects of tolerances

(1) Effects on safety

Geometric deviations have an influence on structural safety (see Section 4.2) with regard to actions as well as to resistance. A scatter in span may increase the internal forces of a member, but this scatter is usually small compared to the total length and can be neglected in design. In precast structures, however, the deviation in span can reduce the length of support (see Section 8.2.2 (4)) and must be taken into account.

Deviations in cross section dimensions and in the position of reinforcement can cause a considerable decrease of the inner lever arm. Observations on executed structures showed that these deviations do in general hardly depend on total member size [Maaβ, Rackwitz (1980)]. This causes a size dependent coefficient of variation in the cross section dimensions.

Probabilistic calculations show that for a large range of specimen sizes the sensitivity α_i of β to geometric deviations is almost equal to zero. For d < 10 cm the sensitivity increases rapidly indicating a growing influence of geometric deviations on the reliability due to a stochastic size effect. In these cases b and d must be considered fundamental basic variables.

From a theoretical point of view, the strong influence of geometry on the safety of small members would require the use of design values of the cross section dimensions in ULS

Copyright fib, all rights reserved. This PDF copy of fib Bulletin 54 is intended for use and/or distribution only within National Member Groups of fib.

design within the framework of partial safety factors. However, this is undesirable from the practical point of view, as the additional influence on dead load (see below) demands the consideration of upper and lower design values.

Therefore, in MC90 it was decided to introduce the *nominal* values of cross section dimensions into design and cover the uncertainty by an increase of the material safety factors γ_s and γ_c. The calibration of these safety factors can only be performed for assumed reference member dimensions and deviations (see e.g. [Östlund (1991)]). As a practical consequence, the design procedure in MC90 (and in almost any code) is applicable if:

- the dimensions of the members are not below specified minimum dimensions, and
- the deviations are limited to the specified tolerances by an adequate quality assurance.

The minimum dimensions used in MC90 were set to b and h > 80 mm for linear members and h > 100 mm for slabs[2]; the required tolerances are given in Eq. (8.2-3). The verification of smaller members might be performed using design values of the dimensions. The design value of a length a can be derived from:

$$a_d = a_{nom} \pm \Delta a_d \quad \text{with} \quad \Delta a_d = 1.2\Delta a \tag{8.2-1}$$

where Δa is the allowable tolerance.

On the other hand a reduction of safety factors would be justified if either the tolerances are reduced or the cross section dimensions considerably exceed the minimum values. MC90 allows a reduction of γ_s and γ_c by 0.05...0.10 if the standard tolerances are reduced by 50 % and strictly controlled. This reduction might be applied to precast units that are produced under industrial conditions.

An alternative way to handle the size effect is a modification of action effects depending on the member size. German code DIN 1045 (7/88) requires (d in [mm])

$$M^* = M \cdot \frac{150}{d_{nom} + 80}$$

$$N^* = N \cdot \frac{150}{d_{nom} + 80} \tag{8.2-2}$$

for $d_{nom} < 70$ mm.

It would also be possible to use additive safety elements to take into account the effects of tolerances, e.g. the unintentional inclination and curvature in the design of colums (see below).

Apart from the effects on the resistance geometric deviations will also have an influence on the dead load of the structure. This is of considerable importance for concrete structures where the dead load often dominates over the service load. The handling of this uncertainty is difficult due to the fact that the dead load may cause favourable and unfavourable effects. So,

[2] For concrete members, minimum dimensions must also be taken into account due to the fact that common theories regard the composite of aggregate and matrix as a homogeneous continuum. This simplification is only justified in cases where the dimensions of the concrete elements exceed the maximum aggregate size by a factor of at least five.

Copyright fib, all rights reserved. This PDF copy of fib Bulletin 54 is intended for use and/or distribution only within National Member Groups of fib.

the definition and application of upper and lower fractile values of g_k and thus an enormous increase in possible load combinations is required. Fortunately the scatter in density and cross section area is rather small. This allows an introduction of mean values as characteristic values $g_k = g_m$ and generally the assumption that g is fully correlated within the structure. For the determination of the minimum and maximum bending moments in a continuous beam it is sufficient to consider g_d to be constant in all spans with its upper or lower value. This simplification is generally on the unsafe side, but this might be accepted as there is still a sufficient safety margin on the resistance side.

In many cases the effect of geometric deviations on dead loads will be partially compensated by the effects on the bearing capacity. An unintentional increase in the thickness of a slab will not only increase the dead load, but also the inner lever arm (assuming that the concrete cover of the reinforcement remains unchanged) and vice versa. However, this is only true for the considered member. Supporting members, e.g. a beam supporting a slab, will have to carry the increased weight without participating in the increased resistance.

In some special cases where self weight or its scatter within the structure is the dominant action effect additional considerations are required. Fig. 8.2-3 shows a cantilever constructed bridge. The stochastic mean value of the residual moment M_g to be taken by the support is equal to zero. The limiting case of a vanishing correlation of g between the two cantilevers gives an upper bound for the standard deviation of M_g:

$$
\begin{aligned}
&M_g = M_l - M_r \\
&\mu_{Mg} = \mu_{Ml} - \mu_{Mr} = (\mu_{gl} - \mu_{gr}) \cdot \frac{l^2}{2} = 0 \\
&\sigma_{Mg} = \sqrt{\sigma_{Ml}^{\,2} + \sigma_{Mr}^{\,2}} = \sqrt{\sigma_{gl}^{\,2} + \sigma_{gr}^{\,2}} \cdot \frac{l^2}{2} = \sqrt{2} \cdot \sigma_{gl} \cdot \frac{l^2}{2}
\end{aligned}
\qquad (8.2\text{-}3)
$$

It is assumed that the scatter in l can be neglected and that g is normally distributed. Introducing a coefficient of correlation ρ between the dead load on both sides the standard deviation reduces to:

$$
\sigma_{Mg} = \sqrt{\sigma_{Mg}^{\,2} + \sigma_{Mr}^{\,2} - 2 \cdot \rho \cdot \sigma_{Mr} \cdot \sigma_{Ml}} = \sqrt{2} \cdot \sigma_{gl} \cdot \frac{l^2}{2} \cdot \sqrt{1 - \rho} \qquad (8.3\text{-}4)
$$

In any practical case ρ will be between the limits of a full correlation ($\rho = 1$) and no correlation ($\rho = 0$). The estimation of ρ should take into account that the two cantilevers are cast with different formworks by different teams resulting in a rather weak correlation.

Alternatively, the scatter of dead load can be decomposed into a mean scatter of the whole structure g_0 (that could be found by comparison with other bridges) and a local fluctuation Δg within the structure. By definition, the first part is fully correlated within the structure and the second has a mean of zero. Using Eq. (8.2-4) the residual moment is independent of the mean deviation g_0 and only a result of the local fluctuation.

Copyright fib, all rights reserved. This PDF copy of fib Bulletin 54 is intended for use and/or distribution only within National Member Groups of fib.

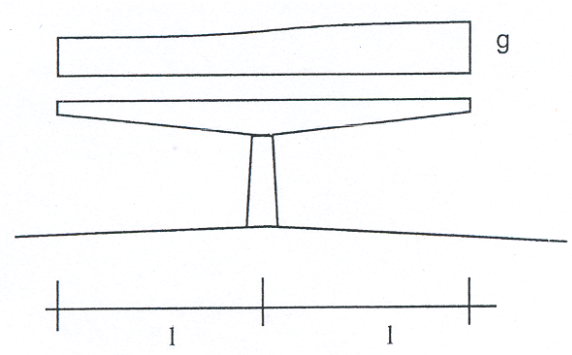


Fig. 8.2-3: Self weight of a cantilever construction

It is obvious that in practical design the required level of safety cannot be achieved by the usual assumption of a full correlation of g. For the verification of static equilibrium the use of upper and lower fractile values in the most unfavourable distribution is required.

A special case of geometric deviations causing action effects are unintentional inclination and curvatures of slender columns, Fig. 8.2-4. Their influence on structural safety is often considerable. In the design procedure, these imperfections must be introduced as design values. The design value of an inclination or curvature cannot be derived from specified tolerances directly, as it is supposed to account for additional non-geometric effects like curvature due to thermal gradients in cases where these effects are not explicitly taken into account.

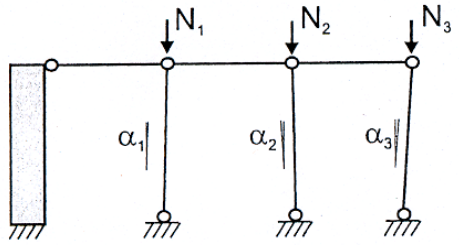


Fig. 8.2-4: Inclinations in a frame system

For single columns, the imperfection must be assumed to have the most unfavourable shape and direction. However, for frames and columns acting in parallel systems this is conservative from a probabilistic point of view. The destabilising force F_i of a column inclined with an angle α_i is:

$$F_i = N_i \cdot \tan\alpha_i \approx N_i \cdot \alpha_i \tag{8.2-5}$$

If the inclination is a random variable with zero mean and N_i is deterministic, the standard deviation of F_i may be evaluated from

$$\sigma_F = N_i \cdot \sigma_\alpha \tag{8.2-6}$$

A full correlation of the inclinations gives a standard deviation for the total horizontal force of

$$\sigma_{F,tot} = n \cdot N_i \cdot \sigma_\alpha \tag{8.2-7}$$

Copyright fib, all rights reserved. This PDF copy of fib Bulletin 54 is intended for use and/or distribution only within National Member Groups of fib.

where n is the number of columns. The assumption that all columns show the design value of the inclination is very conservative.

Assuming that the imperfections are mutually independent, the standard deviation is:

$$\sigma_{F,tot} = \sqrt{\sum N_i \cdot \sigma_\alpha{}^2} = \sqrt{n} \cdot N_i \cdot \sigma_\alpha \tag{8.2-8}$$

In Eq. (8.2-8) a complete lack of correlation is assumed as well as the equality of all acting vertical forces N_i. This is on the unsafe side when there is a systematic error (i.e. some degree of correlation) in the unintentional inclination. In this case, the total variation may be split into a systematic part α_s and a random part α_r. For the systematic and random part Eqs. (8.2-7) and (8.2-8) apply, respectively. The combination of the two parts gives a total standard deviation of the acting horizontal force:

$$\sigma_{F,tot} = N_i \cdot \sqrt{n^2 \cdot \sigma_{\alpha s}{}^2 + n \cdot \sigma_{\alpha r}{}^2} = n \cdot N_i \cdot \sqrt{\sigma_{\alpha s}{}^2 + \frac{1}{n} \cdot \sigma_{\alpha r}{}^2} \tag{8.2-9}$$

Due to the lack of data, the choice of the ratio α_s/α_r is rather arbitrary. The formula given in MC90 is based on the assumption that $\sigma_{\alpha s} = \sigma_{\alpha r}$:

$$\sigma_{F,tot} = n \cdot N_i \cdot \sigma_\alpha \cdot \sqrt{\frac{1}{2} \cdot \left(1 + \frac{1}{n}\right)} \tag{8.2-10}$$

The application of the reduction factor in Eq. (8.2-10) requires averaging and transfer of horizontal forces between columns and horizontal members. The connections must be designed for the maximum possible difference between F_i and the averaged force F_{tot}/n (also considering the case that F_i and F_{tot} have different signs). In structures made of precast elements this transfer may be difficult and may require expensive detailing. Neglecting the averaging effect might be more economic.

(2) Effects on durability

In RC and PC structures reinforcement corrosion is mainly prevented by a concrete cover of adequate thickness and quality (Chapter 5). So, the concrete cover c must be regarded as the most important geometric quantity.

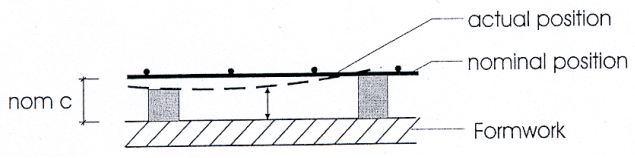


Fig. 8.2-5: Deviations in concrete cover

Copyright fib, all rights reserved. This PDF copy of fib Bulletin 54 is intended for use and/or distribution only within National Member Groups of fib.

In structures cast in situ the variation in c (Fig. 8.2-5) is rather large for various reasons. In beams, the longitudinal reinforcement is fixed to the stirrups. The concrete cover (especially for the top reinforcement) is basically the difference between member size l_c and stirrup size l_w. As stirrups are bent independently from the casting process the scatter in $l_c - l_w$ will generally be larger than the scatter in l_c. In slabs, a stepping on reinforcement during the casting process is inevitable. This reduces the concrete cover especially when the distance between spacers is large and the diameter and stiffness of bars is small.

Many studies have been devoted to the determination of the deviations of concrete cover in precast members and structures cast in situ. Fig. 8.2-6 shows an example for the distribution of deviations measured on several office buildings in Munich in 1975/1976 according to Maaβ and Rackwitz (1980). Surprisingly the mean value of the deviation Δc does not equal zero. The authors assumed that stirrups were bent with smaller dimensions than specified to avoid trouble during the installation of reinforcement that may not fit into the formwork.

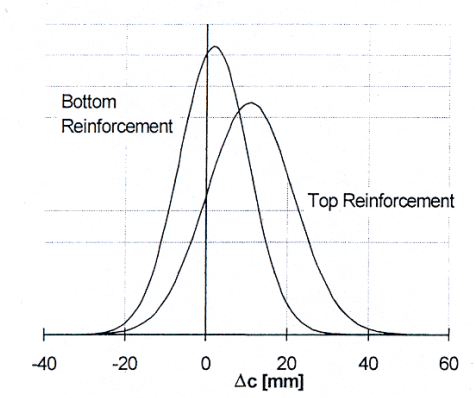


Fig. 8.2-6: Distribution of deviations in c according to Maaβ and Rackwitz (1980)

To achieve an adequate level of reliability for design vs. durability, the required minimum concrete cover defined in Chapter 5 must be compared with a fractile value of the actual cover.

If the standard deviation is set to $\sigma \approx 8...10$ mm and $\mu = 0$ we get:

$$\Delta_{c5\%} = 1.64 \cdot \sigma \approx 15 \text{ mm}$$

$$\Delta_{c10\%} = 1.28 \cdot \sigma \approx 10 \text{ mm} \qquad (8.2\text{-}11)$$

These fractiles are used as additive safety elements for the determination of nominal concrete covers.

The choice of the fractile may be different for different environmental conditions. For interior members, a carbonisation of concrete will generally not cause severe corrosion damage due to the lack of water (see Chapter 5). In this case, a rather high fractile (10%) may be adequate. A lower fractile should be chosen for members subjected to severe environmental conditions. In addition, it would be reasonable to choose Δc depending on the stiffness of reinforcement and on the number and distance between spacers. As this is not

Copyright fib, all rights reserved. This PDF copy of fib Bulletin 54 is intended for use and/or distribution only within National Member Groups of fib.

taken into account in code formulation, special attention should be paid to the type and number of spacers. Recommendations are given in Fig. 8.2-7.

Durability also requires an effective drainage of surfaces subjected to environmental influences like flat roofs. In any case where the inclination of the surface is small, possible deviations must be considered as well as the increase in deformations due to creep and cracking.

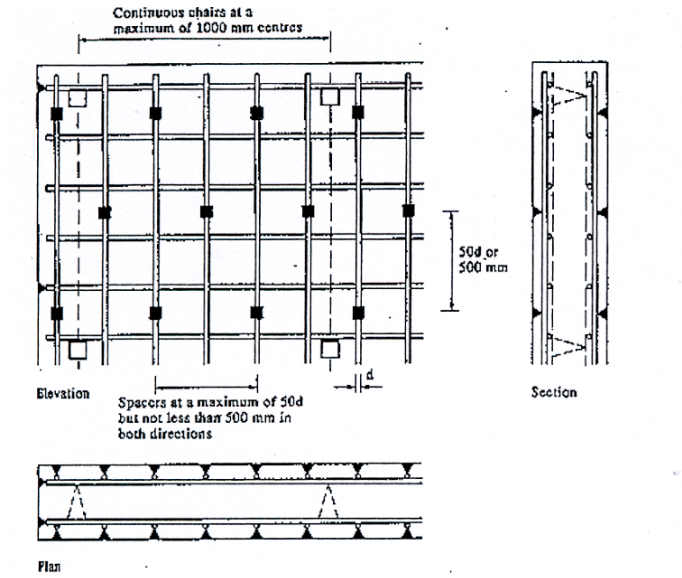


Fig. 8.2-7: Recommended spacing of supports and spacers (according to CEB Bulletin 164)

(3) Effects on serviceability and structural appearance

Human vision is very sensitive to deviations from straight lines and surfaces. As this is a matter of individual perception objective limits and tolerances cannot be found, and the applicability of standards (e.g. German Standard DIN 18202) to an individual case may be doubted. Deviations from smoothness are measured as the maximum distance of a point from a secant line with a certain base length (Fig. 8.2-8).

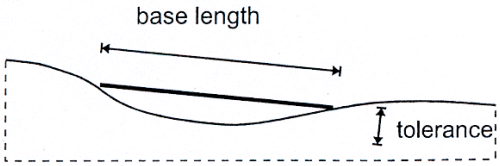


Fig. 8.2-8: Definition of evenness

Tolerances can have a significant effect on later operations in the construction process. As an example, if the surface of a concrete ceiling tile is not even, the thickness of the screed topping have to be increased that a constant minimum height is obtained. This may lead to a significant increase of costs. Considering the fact that the requirements on evenness have a considerable effect on costs (Fig. 8.2-9) it might often be reasonable to define the admissible surface tolerance between client and contractor.

Copyright fib, all rights reserved. This PDF copy of fib Bulletin 54 is intended for use and/or distribution only within National Member Groups of fib.

The tolerances that can be achieved are mostly a function of the stiffness and the correct arrangement of the formwork (see Section 8.5.1). Generally a rough surface finish that can be achieved by the use of unplaned wood planking will be less sensitive. If a sufficient stiffness of the formwork cannot be achieved, imperfections of the member shape can be reduced by a pre-camber of the formwork. A camber might also be used to reduce the visible deformations of the structural member itself, but those member deformations are not relevant to tolerances.

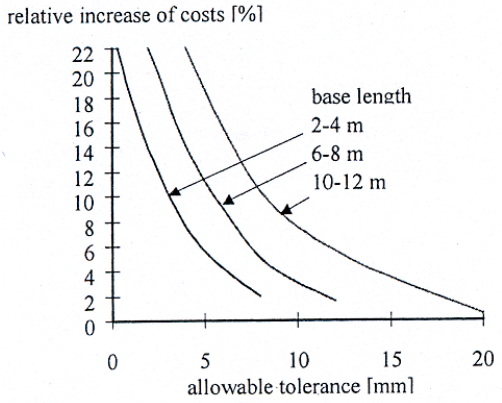


Fig. 8.2-9: Effects of evenness tolerances on structural/ costs according to Tiltmann (1977)

(4) Effects on erection of precast concrete structures

The use of precast elements is attractive in structures where single elements are used repeatedly or where a close schedule demands a quick progress of construction. Their application requires stricter tolerances than those specified for structures cast in situ. During the installation of prefabricated elements deviations cannot be adjusted by adapting the member size as in the case of cast-in-situ concrete. In the worst case, an element may not fit into the allocated position. Specifications for tolerances are given in PCI Journal 1 (1985). In structures where different materials are combined attention must be paid to the fact that the tolerances specified in the relevant product standards may be different.

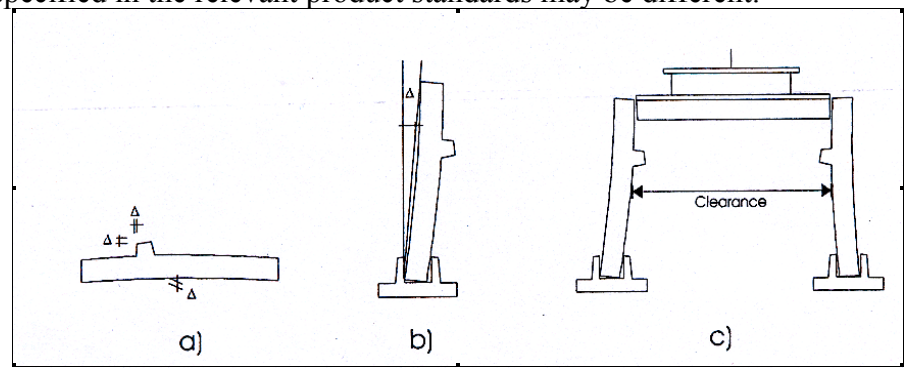


Fig. 8.2-10: (a) Product tolerances, (h) erection tolerances, and (c) effects of clearance

Distinction must be drawn between product tolerances and execution tolerances. Product tolerances are limits for the imperfection of the precast member itself, i.e. its size and shape due to the production in the concrete plant (Fig. 8.2-10). Erection tolerances refer to deviations in the installation on site, i.e. the position and spatial orientation of the members in

Copyright fib, all rights reserved. This PDF copy of fib Bulletin 54 is intended for use and/or distribution only within National Member Groups of fib.

the structure (Fig. 8.2-10 b). The determination of possible total deviations must take into account both types. On the other hand, deviations may reduce the support length of a member (Fig. 8.2-11). The minimum support length is

$$a_{min} = a_1 + a_2 + a_3 \tag{8.2-12}$$

where a_1 may be derived from the limitation of the contact pressure to the strength f_d of either the bearing or the concrete element:

$$F_{sup,d} = a_1 \cdot b \cdot f_d \tag{8.2-13}$$

The terms a_2 and a_3 depend on the concrete cover in the connected members according to Fig. 8.2-11. They are intended to prevent spalling of concrete.

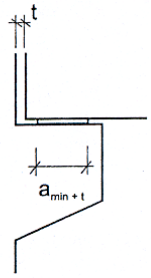


Fig. 8.2-11: Support length of a precast member

This minimum length must be increased to account for the erection tolerances t_e (i.e. the inclination of the column or its deviation from the nominal location in Fig. 8.2-10) and the product tolerances t_p (i.e. the length of the beam and the corbel). The total tolerance of the support length can be derived by the combination (in a stochastic sense) of t_e and t_p:

$$t = \sqrt{t_e^{\,2} + t_p^{\,2}} \tag{8.2-14}$$

The nominal support length is $a_{nom} = a_{min} + t$.

(5) Admissible tolerances

Fig. 8.2-12 shows a comparison between the admissible tolerances according to several European standards and MC90 for different geometric properties. However, one must keep in mind that there is an interaction between tolerances and safety factors or additive safety elements. For this reason tolerances cannot be compared directly.

Copyright fib, all rights reserved. This PDF copy of fib Bulletin 54 is intended for use and/or distribution only within National Member Groups of fib.

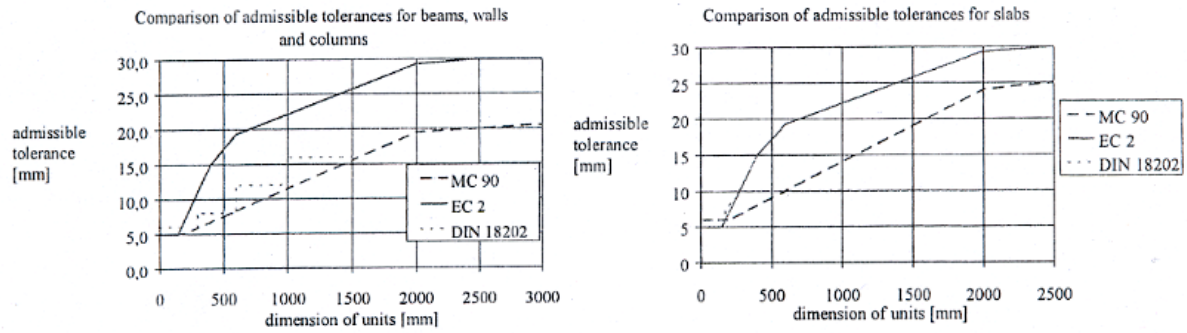


Fig. 8.2-12: Tolerances for the cross section of beams and slab thickness

8.3 Quality requirements for material properties

8.3.1 Variations in material properties

Variations of material properties depend on the kind of product. Civil engineers deal with three kinds of products: natural products (e.g. wood), products made on the construction site (in-situ concrete) or industrially manufactured products (e.g. steel, glass). The quality of natural products can hardly be influenced by mankind and they depend on various conditions (e.g. climate for wood, geological origin for rocks, etc.). However, new technologies have already been developed where the quality of natural products (e.g. boards) is estimated by machines and then an automatic graduation with respect to quality criteria can be made.

In concrete technology, engineers deal with industrially manufactured products (reinforcing and prestressing steel) and with products made on the construction site. Tolerances of these products depend on the properties of the ingredients and on the quality of fabrication. In the following statistical evaluations of variations in material properties (steel and concrete) are shortly presented. It can be seen that the deviations found in the case of industrially manufactured products are significantly lower than in the case of products made on the construction site

Russwurm (1988) gives an example for the coefficients of variation for steel products shown in Table 8.3-1. It can be seen that the coefficients of variation depend on different factors like the examined property, the manufacturer, the production year and also the kind of product. For example prestressing steel which needs to fulfil high requirements with respect to quality has the lowest average coefficient of variation and also the lowest yearly difference in variation. Regarding the entire statistical evaluation the coefficients are found in a range of 0.05 – 0.19.

Copyright fib, all rights reserved. This PDF copy of fib Bulletin 54 is intended for use and/or distribution only within National Member Groups of fib.

Type of steel	manufacturer	property	coefficient of variation in different years of production		
Reinforcing bars	factory 1	R_e [a]	0,066	0,040	0,044
		A_{10} [b]	0,109	0,085	0,060
		ΔA_s [c]	0,016	0,016	0,017
	factory 2	R_e	0,037	0,035	0,043
		A_{10}	0,092	0,124	0,042
		ΔA_s	0,021	0,009	0,019
fabric	factory 1	R_e	0,063	0,064	0,070
		A_{10}	0,134	0,156	0,190
		ΔA_s	0,019	0,019	-
	factory 2	R_e	0,055	0,068	0,072
		A_{10}	0,101	0,163	0,134
		ΔA_s	0,020	0,015	0,019
Prestressing steel (St 1080/1230)		R_e	0,010	0,010	0,013
		A_{10}	0,12	0,07	0,1
		ΔA_s	0,004	0,005	0,005

[a]) $R_e=f_y$: yield strength
[b]) A_{10} : strain at rupture measured on a length of 10 d_s
[c]) ΔA_s: deviation in cross section area

Table 8.3-1: Coefficients of variation of steel products according to Russwurm (1988)

Rackwitz, Müller and Maaβ (1976) carried out an investigation on compression test results of concrete specimens manufactured in different areas in Germany. The objective was to find out if the deviation of actual from nominal strength decreases with increasing quality control. Furthermore, different kinds of concrete production (ready mixed concrete or mixed in-situ) were studied. As a result of a statistical evaluation Rackwitz, Müller and Maaβ concluded that quality control more than the strength class has an effect on the standard deviation of the compression strength. Fig. 8.3-1 gives an idea of the existing scatter in concrete production.

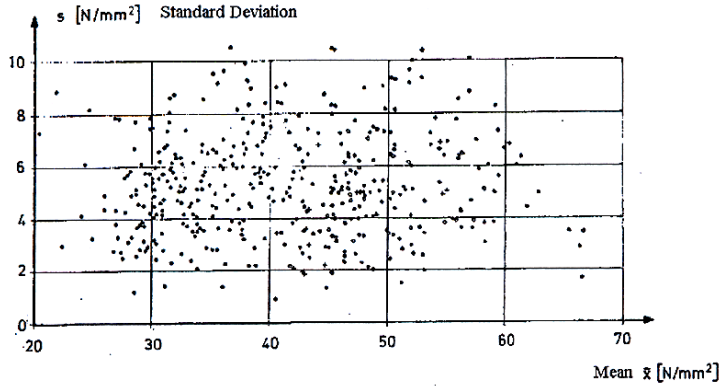


Fig. 8.3-1: Correlation between mean value and standard deviation of the compressive strength according to Rackwitz, Müller and Maaβ (1975)

Copyright fib, all rights reserved. This PDF copy of fib Bulletin 54 is intended for use and/or distribution only within National Member Groups of fib.

But it is important to state that these deviations are not only caused by the material concrete itself but also by a great number of other conditions (place and time of testing, procedure of testing, quality of ingredients, variations in transporting, curing, compaction and temperature, etc.).

Since the study of Rackwitz, Müller and Maaβ was carried out, intensive research was devoted to the development of standardised requirements for concrete production in order to reduce the discrepancy between actual and nominal strength. This is important, because with the introduction of high performance concrete in the European standards, the quality requirements regarding sound production and the later use of a structure are even more pronounced than for normal strength concrete. According to the results of the latest statistical evaluations by for example Hosser and Gensei (1995), König, Soukhov and Jungwirth (1998), test methods and evaluation criteria were developed for the European concrete standard EN 206 (2001) in order to guarantee variations as small as possible.

8.3.2 Control methods of variations in material properties

Design is based on fractile values of material strength. As explained above, it cannot be expected that these characteristic values are reached in every batch of material. From the point of structural safety it is necessary to filter batches of bad quality by suitable test strategies (*tests of conformity*). For practical and economic reasons, tests can only be performed on a small number of specimens. Any conclusion based on the results has a stochastic character. Therefore, criteria for the judgement of concrete quality must be based on statistical methods. The basic hypothesis to be confirmed or rejected is: *The batch of concrete has a 5%-fractile value of compressive strength of x* or, alternatively: *The percentage p of strength values below the required characteristic value within the batch is smaller than 5%.* In general, any test method and criteria will have a probability of acceptance A(p) for a batch with a certain value p.

When the conformity of concrete is tested with the nominal or characteristic values in design, there exists already some experience (*prior information*) with the material. The use of prior information is useful in the judgement of concrete quality as it reduces the uncertainties of the test strategy. For example, the standard deviation of the concrete produced in a specific plant may be known from previous tests.

The test procedure generally includes five steps. At first, the size of the batches has to be defined according to the relevant standards. According to EN 206 (2001) the size of a batch is limited to 400 m^3 or the supply of one week or storey. From this volume of concrete, a certain number of specimens are taken (usually not less than 3). The choice of specimens is usually random, but it may be selective if there is reason to assume that certain sub-volumes (e.g. certain mixes) have a lower quality. Anyway it must be assured that the specimens are independent; for example, it does not make sense to take all specimens from one mix in 100 m^3. The third step is the testing itself and the fourth step is the statistical evaluation of the test results (see below). Based on this evaluation, finally a decision on acceptance has to be made. This may be the most difficult step, as in any case, results are not available during casting as the testing requires hardened specimens. The decision can only be made some weeks after the casting process. That means that in the worst case parts of the structure may have to be demolished and rebuilt.

Copyright fib, all rights reserved. This PDF copy of fib Bulletin 54 is intended for use and/or distribution only within National Member Groups of fib.

Suppose that we have determined the value of a certain material property x (e.g. by a standard cube compression test) on n specimens and received n values x_i. The mean and standard deviation of the sample can be computed as[3]:

$$\overline{x} = \frac{1}{n} \cdot \sum x_i \tag{8.3-1}$$

$$s_n^2 = \frac{1}{n-1} \cdot \sum (\overline{x} - x_i)^2 \tag{8.3-2}$$

The conformity is usually checked by a double criterion of the form

$$\overline{x} \geq f_{ck} + k_1 = f_{ck} + \lambda \cdot s_n \tag{8.3-3}$$

$$x_{min} \geq f_{ck} - k_2 \tag{8.3-4}$$

where both criteria must be fulfilled. A graphical representation of this *operation characteristic* is given in Fig. 8.3-2 where the probability of acceptance is plotted over the percentage of strength values below f_{ck}. For the parameters Λ and k_2 MC90 only gives the general remark that they should be determined by statistical studies. The calibration of the parameters Λ and k_2 can be done by numerical simulations and curve fitting. Generally the choice of parameters includes a contradiction between the economic interests of the producer and the safety requirements of the client. Whereas a high probability of acceptance is economically advantageous for the producer the safety requirements of the client demand conservative values. Generally, Λ.. and k_2 will depend on the amount of available information, i.e. the number of specimens.

An upper limit for the acceptance probability A(p) is given by

$$A(p) \cdot p \leq 0{,}05 \tag{8.3-5}$$

The application of this relation guaranties that the average fractile in batches that have passed the test is above the required value. Another limit is a *total* test performed on the *complete* batch that would give a sharp or deterministic decision. In Fig. 8.3-2 it is shown that this test criterion has the shape of the unit step function. As most tests are destructive the test criterion is hypothetical since it would destroy the complete production.

Any practical test strategy will be less sharp and have a probability of rejection unequal zero for $p < 0$ and of acceptance for $p > 0$. The shaded areas in Fig. 8.3-2 identify the remaining (economic) risk for the producer and the safety risk for the client. With an increasing number of specimens n the operation characteristic will asymptotically approach the unit step. An optimum number of n can be found by minimising the total costs of a possible rejection and tests.

[3] The denominator n-1 in (8.3-2) instead of n (as one might expect) must be attributed to the fact that $\overline{x}$ is only an estimate for the mean value increasing the uncertainty in the test results.

Copyright fib, all rights reserved. This PDF copy of fib Bulletin 54 is intended for use and/or distribution only within National Member Groups of fib.

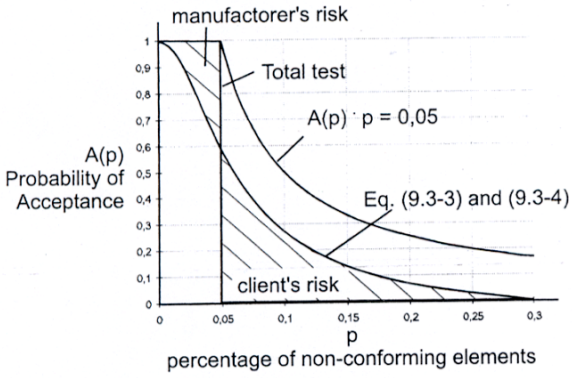


Fig. 8.3-2: Operation characteristic for tests of conformity

In some cases the assessment of the concrete quality in existing structures is required. Testing can be performed by destructive and non destructive methods. The first testing method is based on compressive tests on cores taken from the structure by drilling. The results obtained are representative for the actual behaviour as the concrete tested has been cast and hardened under conditions identical to those of the structure. In many cases, the damage caused by drilling will influence the performance and appearance of members, especially for linear members like beams or columns where the cross section would be severely reduced by the extraction of a core.

Alternatively, concrete strength can be estimated by non-destructive methods like the rebound hammer test. Compared to destructive tests, the reliability of these methods is much smaller as the relevant material property is not measured directly but via related properties like the modulus of elasticity and damping properties. A conversion formula must be based on a regression analysis (Rackwitz, Müller and Maaβ (1976)]. In addition, the results of rebound tests depend strongly on the experience and skills of the performing person. Generally, the correlation between the results of non-destructive tests and the actual concrete strength are rather weak.

8.3.3 Influences of variation in material properties

(1) Effects on safety

Variations in material properties can lead to an overestimated classification in the wrong strength class which may have an influence on the safety of the structure. The most important example to be named is the influence of scatter in strength on the safety of the structure. Especially those structural elements, of which the failure depends merely on the compression strength (columns, walls, support constructions, compressive struts in shear zones of beams, etc.) are concerned. For this reason, regular internal and external quality control is carried out. However, a certain degree of uncertainty in material properties cannot be avoided.

(2) Effects on economy

If deviations result in significant reductions of the required material properties it may come- in the worst case- to demolition and reconstruction of the structural element. If it is proved that the results of the conformity test (see Section 8.3.2) cannot fulfil the required

Copyright fib, all rights reserved. This PDF copy of fib Bulletin 54 is intended for use and/or distribution only within National Member Groups of fib.

design strength, the concrete manufacturer is liable for any damage and any conflict will be solved on his expenses. Therefore the manufacturer will attempt to produce concretes with a certain tolerance upwards to account not only for the uncertainties in the production but also in the test method.

Contrary to this costs and materials may be reduced if excellent quality can be assured and proved. An example is the construction of a bridge across the river Main at Veitshöchheim in 1985 (Fig. 8.3-3) [Naumann et al. (1987, 1988)]. The bridge has a total length of 1280 m with spans of 40 – 61.7 m and an arch of 162 m. The provided concrete strength class was B 45 (corresponding to a C35/45). According to German DIN 1045 12.78 the 5% fractile value β_{WN} (= $f_{cm,cube}$) referring to the cube strength was multiplied with a factor 0.6 to take into account the strength difference between the test specimen and actual structure and the effect of sustained loading ($\beta_R = 0.6\ \beta_{WN}$). Due to special measures in concrete technology (e.g. cooling of fresh concrete) the mean compressive strength after 90 days was 78 N/mm^2 with a standard deviation of only 2.9 N/mm^2 (5%-fractile: 73 N/mm^2). As a consequence of the good quality of the concrete it was agreed by the construction supervision and other experts, that for this case the regulations in DIN 1045 (12.78) were too conservative. It was decided to take this high quality into account by an increase of β_R to 0.7 β_{WN} under consideration of the safety factors according to DIN 1045 (12.78) . This change of β_R due to negligible tolerances in material properties resulted in a significant saving of reinforcement and costs. However, such reductions must be made in a close co-operation between experienced specialists of concrete technology and construction.



Fig. 8.3-3: Main bridge Veitshöchheim

Copyright fib, all rights reserved. This PDF copy of fib Bulletin 54 is intended for use and/or distribution only within National Member Groups of fib.

(3) Effects on serviceability and structural appearance

The aggregates in concrete consist of natural or artificial, mineral substances agglutinated together by the cement matrix. Aggregates take a mean volume in the concrete of about 70% which means that the aggregates are quantitatively the principal components of concrete. Consequently, the elastic modulus of concrete depends to a high degree on the elastic modulus of the aggregates. In DIN 52100 (1990), properties of rocks for normal aggregates for concrete production are given. The elastic moduli of these rocks fluctuate between 2'000 N/mm^2 (siliceous sands) and 100'000 N/mm^2 (diorite and gabbro). These differences also exist in the field. Adjacent gravel pits may provide aggregates of different geological origin resulting in different rock properties (e.g. elastic modulus). In many codes (e.g. EC 2) the secant modulus of elasticity is a function of strength regardless of the type of aggregates used. In MC90 (see also Chapter 3), Table 2.1.5 takes account of the effect of aggregate on modulus of elasticity.

As an example the elastic modulus according to EC2 for a C50/60 independent of the type of aggregate is 37 kN/mm^2. According to MC90 the elastic modulus for a concrete made with basalt aggregate is 46.4 kN/mm^2 and for a concrete made with sandstone aggregates is 27.0 kN/mm^2. So, when using different kinds of aggregates for the same structure, the difference in elastic modulus may result in higher deflections (up to 40%). Therefore, if concrete structures are sensitive to deflections (e.g. incremental launching, cantilevered construction bridge), it is substantial to consider an aptitude test before execution starts.

8.4 Quality management

8.4.1 General

It has been shown in the previous sections, that adequate quality in planning and execution is essential to avoid variations in material properties and geometry. Poor quality may result in damage and an increase of risk and costs. Therefore, all parties included in a building project (building owner, building contractor and staff) shall be involved in the assurance of quality. This idea is described in detail by various organisations and authors, as for example by CEB 234 (1990), DBV (1985), Jungwirth (1984): The building owner is obliged to specify the requirements to be fulfilled by the structure in detail. Quality means, that the building contractor tries to satisfy these requirements. Quality assurance is realised by systematic operations and control, which are summarised in a quality assurance system (quality management system, respectively). The objective is feedback between all parties involved in the construction progress and well functioning communication.

Technical circumstances are in a steady progress and specialisation increases proportionally. So, one process (e.g. placing, tensioning and grouting of a tendon) may require a number of different, qualified specialists. Therefore, the objective of a quality management system is to record and to co-ordinate the different processes. Quality assurance shall not only be gained by control but also by increasing the individual and personal responsibility of all parties involved in the building process. As a consequence a quality management system can attribute to organisational and qualitative efficiency and economy. As a long time effect other companies and financing institutions, respectively, are attracted to participate and invest in new projects.

Copyright fib, all rights reserved. This PDF copy of fib Bulletin 54 is intended for use and/or distribution only within National Member Groups of fib.

8.4.2 Concept of quality management

Each project in the construction industry is different in many aspects: the location, the logistics, the erection process (complexity, subcontractors, etc.) and the work schedule (time to be taken for construction) have to be planned and organised individually. Therefore quality management has to be adjusted for each particular project. Because of this specific peculiarity of the construction industry quality management systems consist of two parts:

Project quality documentations can be regarded as a result of project quality planning. The concept and the content have to be developed for each singular project or case including specific procedures or instructions. The length and level of details depends on the size of the project and of the company, respectively. If more participants are involved (owner, designer, material supplier, etc.) a quality agreement should be made to provide a co-ordination of each project quality planning and documentation. Special attention should be drawn to the ~ interfaces between the participants. However, adequate project quality planning does not mean unnecessary formalism but flexibility and communication of all parties.

Company quality systems can be considered as a permanent organisational framework for practical work performance – independent of any particular project. These company quality systems are developed by each company under consideration of ISO 9000 providing general rules and generic concepts. However, it is not possible to standardise company quality systems since they have to be adjusted to the specific objectives and functions of the company. The concept of the company quality system should be summarised in a quality manual which is available for external bodies (partners in joint ventures, approved certifiers, etc.). In addition general procedures and work instructions should also be contained in a company quality system describing organisational or technical processes and particular work items, respectively. The structure of a quality management system can be seen in Fig. 8.4-1.

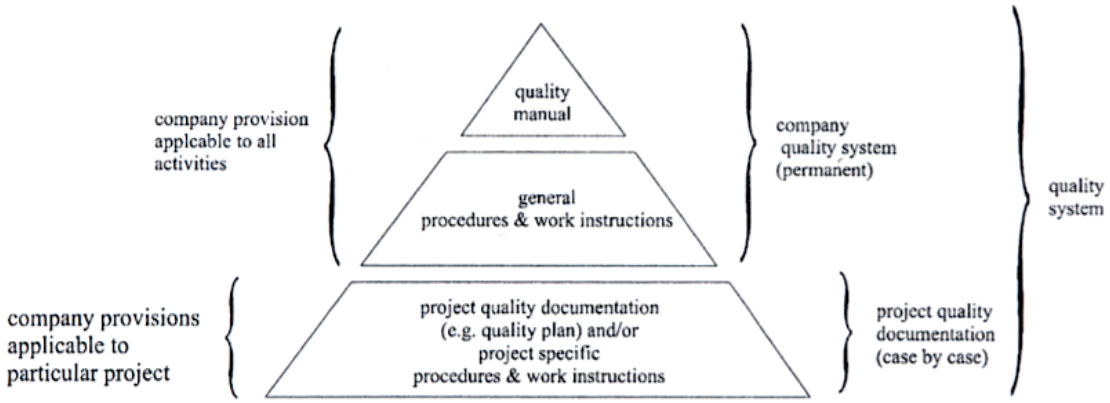


Fig. 8.4-1: Structure of quality systems in the construction industry [Jungwirth (1984)]

Since many middle class construction companies are replaced by big companies surveying of the entire company system becomes more and more complicated. Therefore it is important to implement quality management systems in the company structure by experienced and qualified personal. The quality management system must be flexible and has to be adjusted to the particular structure of the company. Transparency should be provided and everybody should have good access if information is required. The management of the company must introduce and demonstrate the system. All employees should be involved in

Copyright fib, all rights reserved. This PDF copy of fib Bulletin 54 is intended for use and/or distribution only within National Member Groups of fib.

the quality system and the responsibility of each should be increased with respect to his function. The theoretic aspects of the quality management system should be explained in training programs. Quality management is a continuous learning process, because it develops with respect to the progress of the company.

8.4.3 Quality assurance plan

The content of a quality assurance plan depends on the extend of the individual quality system. With regard to MC90 important topics are:

- *Organisation*: Design, construction and maintenance has to be co-ordinated in advance. The participants of one building project have to be determined and the functions, authority and responsibilities of each have to be defined and specified (e.g. by names or qualification). The interrelation of all participants who manage, perform and control work affecting quality have to be assured.

- *Planning*: The building process should be planned and described to achieve a systematic and faultless performance.

- *Design control*: Procedures should be established and maintained to identify input requirements, to perform and verify design, and to record the design changes.

- *Document control*: Important documents which are related to the quality of the project should be reviewed and approved regularly. Also, it has to be assured that documents are available at the right places at the right time.

- *Procurement*: Measures should be taken, that the services procured and the products delivered are in accordance with the specified requirements.

- *Production and construction*: Regular control is performed to guarantee good quality in production and construction (materials, equipment, processes and procedures, personnel, suppliers, utilities, etc.)

- *Records*: Performance quality records which prove that execution is performed according to the agreements and requirements, respectively. These records should be available for all parties for an agreed period after completion of the project.

These elements should be contained in a quality assurance plan. It has to be decided by the executives which elements correspond to the particular construction project and if complements have to be added.

In addition, a very important tool to assure quality is checklists to check individual and common processes. They should be established prior to the construction in collaboration with all participants and accompany the entire building process. The checklists should be distributed to all parties contributing to a special process and during the building progress, parties should compare the checklists. This measure promotes communication and an overview of the construction process.

Copyright fib, all rights reserved. This PDF copy of fib Bulletin 54 is intended for use and/or distribution only within National Member Groups of fib.

8.4.4 Quality control

(1) General

Since quality management depends to a high degree on the company and the particular project, quality control has to be defined according to the company quality system and to the project quality documentation. When a quality control system is established different parameters should be considered: first of all, the degree of control depends, of course, on the technical complexity and on the extend of the structure to be built. The client and the building contractor (or the building owner) should then define the intended degree of control. However it is important to adjust the degree of control to all participants involved in the project. Ideally, the quality control should base on experience and correspond to the company quality system. If the degree of control is defined, the building contractor has to inform the responsible personnel and discuss how to successfully implement control into the building process. A more detailed description of quality control is given in MC90.

(2) Phases of control

The definition of quality control should contain the phases where it is important to control the building process. The first process to be controlled is the planning and the design phase. In this phase, calculation models, drawings, descriptions and necessary requirements should be controlled and discussed between architect, design engineer, building owner and building contractor. If communication exists already in the planning phase, misunderstandings between the theoretical and the practical side can be avoided and defaults might be discovered in advance.

When the construction process starts, the quality and the completeness of the supplied materials and components, respectively, should be controlled- before the construction process starts as well as during construction. In the execution phase it is important to limit deviations to the specified tolerances. Therefore, the quality of workmanship should be controlled and documented regularly. Also, it is important to control the interfaces of different construction processes executed at the game time and to assure good communication between all participants.

When the structure is completed the final acceptance of the structure has to be controlled and documented. In addition, a control system for the future should be determined and organised.

(3) Types of control

In quality control there are two defined types of control: production control and compliance control. However, both types of control are somehow interconnected: production control relates to production and execution processes and it applies to raw materials, components of production and execution. Control can be performed by testing (also preliminary testing) but also by inspecting. Production control has the objective to discover and avoid defaults in advance – before a bad quality product is accomplished. But especially in a complex construction process, it is important not only to control during the process but

Copyright fib, all rights reserved. This PDF copy of fib Bulletin 54 is intended for use and/or distribution only within National Member Groups of fib.

also after the construction process: Therefore, compliance control relates to the results of the production and execution processes. Compliance control is applicable to all stages of the building processes since it is important to include results of singular steps as much as possible in the quality control system. So, it is proposed to control the results of promotion, design, production and execution.

(4) Control levels

To assure independent and neutral control there have to be two control levels. Internal control has to be defined by the building contractor and to be performed by the producer and supplier, respectively. Internal control should be integrated in the production process (production control) but also include regular documentation of results (compliance control). However, internal control is only performed during the building process and not when it comes to final acceptance of the product. The controlling body has to be trained and a high degree of independence has to be guaranteed.

External control is made by the client or by another body acting for the client. External control is important to guarantee a constant good quality of single results during the building process (compliance control). As a consequence the final acceptance is only the conclusion of a steady control process. In cases of reliable certified production, external control may be reduced to inspections, identification of the product and verification of the certificates.

8.5 Aspects in erection of RC and PC structures

8.5.1 General

The erection of in situ RC and PC structures can be subdivided into certain procedures shown in Fig. 8.5-1. Especially for costly projects it is important to determine a time schedule and a construction progress chart and to co-ordinate the individual building procedures already in the planning phase.

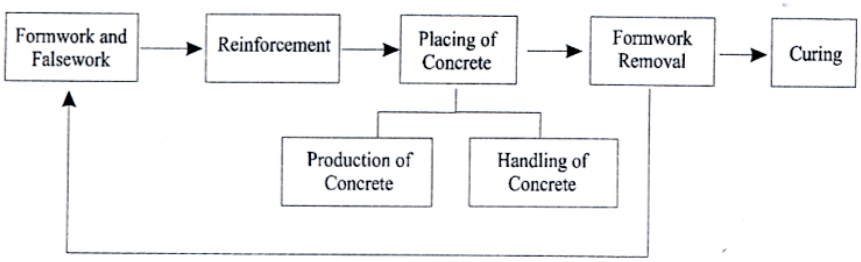


Fig. 8.5-1: Concreting procedures

Fig. 8.5-2 shows the co-ordination of the individual processes at the example of a bridge. It can be seen that the columns are built first followed by the construction of the superstructure: after the arrangement of the scaffold and the formwork, the bridge is reinforced, casted, cured and prestressed. When an adequate strength is attained the bridge is striked and the scaffold and the formwork are moved forward. The formwork consists of

Copyright fib, all rights reserved. This PDF copy of fib Bulletin 54 is intended for use and/or distribution only within National Member Groups of fib.

elements which can be adapted to the length of the different spans and consequently be reused.

8.5.2 Formwork and falsework

A major advantage of concrete compared to other materials is the possibility to form monolithic structures of almost any size and shape. On the other hand, this requires a support of concrete by formwork and falsework during its hardening process. For standard situations like slabs and columns in office or residential buildings there is a huge variety of standardised formwork systems. However, the design and construction of formwork and scaffolds for engineering structures like bridges, towers and high-rise building is a task comparable to the design of the structure itself.

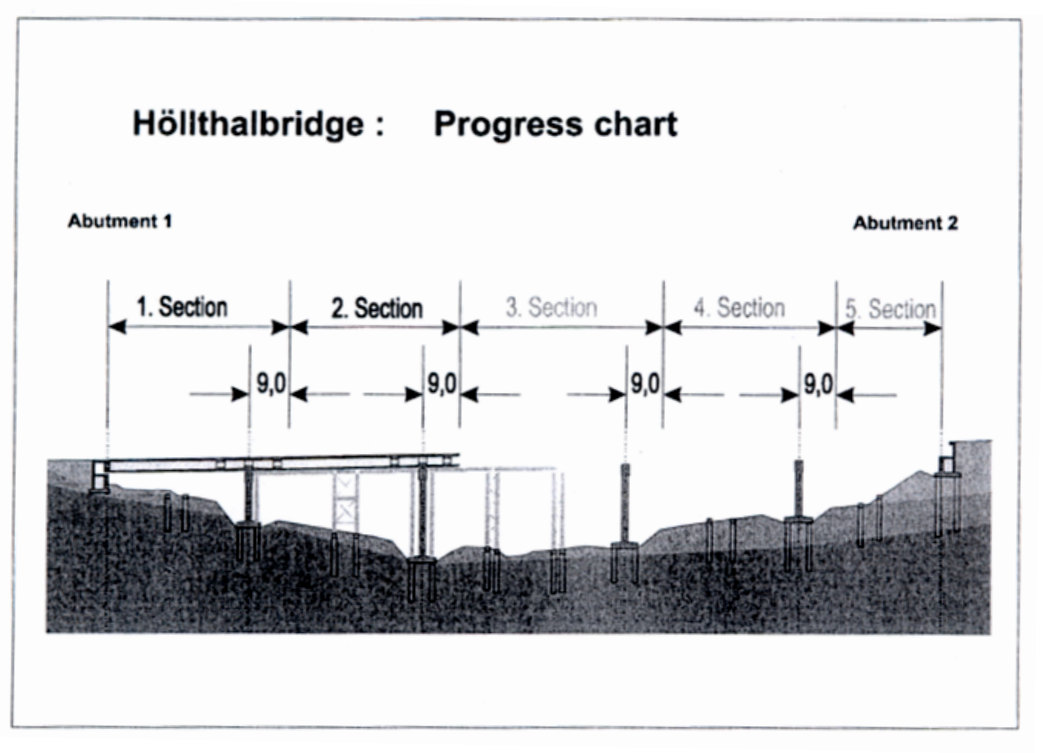


Fig. 8.5-2: Progress chart of the Höllthalbridge

(1) Formwork

In concrete structures, formwork plays an important role in terms of economy. Berner (1999) estimates that formwork and falsework takes 50% of all wages and 30% of the total costs for the preliminary building works. So, an optimal use and reuse of formwork material may result in a noticeable saving of total costs. For this reason the formwork industry is very innovative and more and more prefabricated formwork elements and systems are used. For a maximum reuse of the formwork it is advised to choose the game dimensions of footings, columns, and beams. In addition columns and the corresponding supporting elements should be adjusted to each other and be chosen that cut-outs are possibly avoided.

Copyright fib, all rights reserved. This PDF copy of fib Bulletin 54 is intended for use and/or distribution only within National Member Groups of fib.

Formwork must assure the proper shape of the concrete structure within the specified tolerances. This requires a strict limitation of deformations and as a consequence careful design and consideration of the applying loads. Before hardening concrete causes a horizontal pressure on the formwork that depends on the rate of placement, consistency of concrete and the kind of compaction. Fig. 8.5-3 shows the distribution of pressure. In the upper parts pressure can be assumed to act as hydrostatic

$$P_{hyd} = \gamma_c \tag{8.5-1}$$

where γ_c is the unit weight of fresh concrete. With the beginning of the solidification of concrete the increase of p with x will be slowed and finally stopped, and after hardening concrete will be able to carry its own weight without lateral pressure (though the pressure will still act in a stiff formwork, as the system of concrete and formwork is fixed in a compressed state). For practical design, simplified distributions are used (Fig. 8.5-3). The values h_s and h_h are

$$h_s = v \cdot t_s \qquad h_h = v \cdot t_h \tag{8.5-2}$$

where v is the rate of casting in [m/h], t_s/t_h the beginning of solidification/hardening in [h]. For h_s and h_h see the relevant codes [German DIN 18218 or ACI Guide to formwork for Concrete (1988)]. For special casting techniques, e.g. where concrete is pumped from the base, p can exceed the hydrostatic pressure.

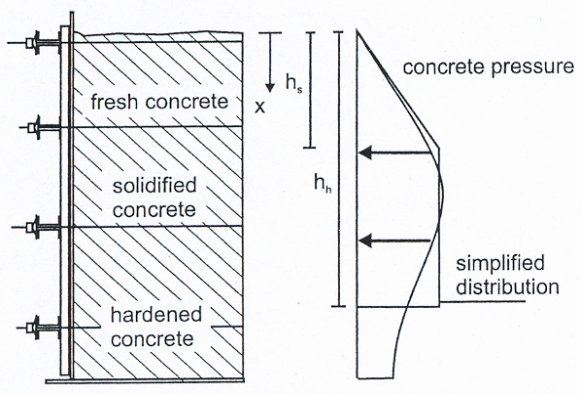


Fig. 8.5-3: Horizontal pressure of concrete

In the planning process the architect has to define the finish of the concrete structure. This choice depends on the kind of structure and on the visibility of the structural element. The parameters of exposed concrete to be varied are the colour (almost white to a dark grey-depending mainly on the cement and the water/cement ratio) and the structure of the concrete surface. According to the demands of the architect or other requirements (low production time, high degree of reuse, technical demands) the kind of formwork is chosen:

- Planed and unplaned planking is the traditional formwork material. The advantage of this type of formwork is, that the desired surface finish can be influenced by quality of the surface of the planking. As a consequence the degree of tolerances and the structure of the future concrete surface can be determined and the planking can be treated accordingly. Another advantage is that wood is very well suited for absorbing

Copyright fib, all rights reserved. This PDF copy of fib Bulletin 54 is intended for use and/or distribution only within National Member Groups of fib.

the bleeding water at the concrete surface. As a consequence the concrete shows a good quality with regard to durability. In terms of economy planking has the disadvantage that it normally can be used only once. In the case of unplaned planking, special attention has to be drawn to the fact to use a good quality form oil, otherwise singular wood fibres may adhere to the finish which should possibly be avoided in case of architectural concrete.

- Plywood sheets can be manufactured by building workers on site or be ordered by special formwork suppliers. Formwork suppliers offer ready-made formwork systems but they also design the formwork system for individual projects. Sheet materials are available in all different kinds: plywood sheets from law cost untreated materials to high cost resin film coated boards. Therefore, the advantages and disadvantages depend on the material used. However, when considering large-purpose panels for repeated use, high costs may be justified, because good quality of the panels results in an increase of using times. A disadvantage of many plywood sheets is that the absorbing properties are poor. This may result in a bad concrete surface especially, when a concrete with high w/c-ratio is placed.

- Metal panels are normally used in bigger projects because otherwise they are too expensive in purchase. On the other side they can be reused for a very long time. So often, they are used for permanent construction, e.g. for precast concrete elements. When metal panels are used on site cranes are needed for their transportation and placing. Mostly, they are used in special constructions, like for example as glide formwork.

(2) Falsework

From the point of structural safety, scaffolds are very sensitive to errors in design and execution as may be seen from the rather large number of failures during construction (compared to the number of failure during service). This may be attributed to several facts:

The dominant action effect on falsework is the dead weight of concrete. As explained in Section 8.2.1, for the dead weight the characteristic value is generally set equal to the mean value. Therefore, the characteristic value of loads will be reached or even exceeded with a very high probability by definition. In structures under service conditions a considerable part of the (nominal) action is usually the live load with a low probability of being exceeded during lifetime. So the design loads on the structure may be considered more or less fictitious whereas the design loads during construction are realistic.

For economic and practical reasons the connections between the elements of the scaffold are often hinges resulting in statically determined systems and loaded close to their limit. Unlike most other structures, the nominal capacity is very close to the actual capacity whereas RC structures usually have some hidden reserves not taken into account in design like monolithic connections considered as hinges, additional reinforcement, etc.

Finally it must be said that due to the fact that they are only temporary constructions falsework quite often is not designed and executed with the required precaution.

Copyright fib, all rights reserved. This PDF copy of fib Bulletin 54 is intended for use and/or distribution only within National Member Groups of fib.

The vertical actions of fresh concrete can easily be calculated from its density and. the member size. However, when concrete is dropped from a certain height it might be necessary to consider the dynamic effects of falling concrete. For the design of the scaffold, transitory states must be taken into account as the loading of single fields in a continuous beam. If the scaffold is sensitive to this (e.g. scaffolds for arches) or if it would be uneconomic to design for this most unfavourable combination, it is possible to apply the concrete load in an order that avoids this combination. However, in this case the casting sequence must be prescribed precisely by the designer.

In many cases the relevant criterion for the design of scaffolds is not the strength, but the stiffness. The estimation of stiffness must take into account shear deformations, deformations in connections of the scaffold and a settlement of the foundation. Wooden scaffolds may also show significant deformations due to drying shrinkage or swelling. To adjust unavoidable deformations the formwork may be banked. The required camber must be determined by an adequate calculation of formwork deformation and not be chosen to large, as a negative sag is often less desirable than a positive one.

The amount of required scaffold material also depends on the period of striking. In general, this will depend on the development of concrete strength. As loading of concrete at early ages may lead to extended micro cracking and increased creep, generally having a strong influence on the serviceability and durability, criteria for striking cannot be derived from ULS considerations alone.

8.5.3 Curing

The last important step in the concrete production is curing. In practice curing is often underestimated since the benefits with regard to short-time-effects are barely obvious. But with regard to long time effects (especially to guarantee an adequate durability of a structure), adequate curing should be performed after placing of the concrete.

According to Spear (1983) curing can be defined as a procedure for insuring the hydration of cement in outer concrete layers (concrete skin). Powers (1947) found out that the process of cement hydration stops below a relative humidity of 80%. Consequently if fresh concrete is exposed to a relative humidity below 80% the concrete strives for humidity equilibrium with the environment. In other words, the water evaporates since the internal humidity is adapted to the environmental conditions. Direct exposure to sun or wind accelerates this process, especially close to the surface. As a result, the hydration of concrete in the surface layers slows down or even ceases. Although this reduction of hydration rate does not mean a significant loss in the overall strength of the structure, it may result in a high porosity of the surface layer. Consequently, the concrete is more susceptible to abrasion and, when exposed to unfavourable environmental conditions, also to carbonisation. For the sake of avoidance it is important to provide adequate curing of the concrete.

Curing means to keep the concrete moist or avoid drying. For the practical engineer it is important to know, how long the concrete has to been cured. The duration depends on several factors:

- curing sensitivity of the concrete as influenced by its composition,
- concrete temperature,

Copyright fib, all rights reserved. This PDF copy of fib Bulletin 54 is intended for use and/or distribution only within National Member Groups of fib.

- ambient conditions during and after curing,
- exposure conditions of the finished structure.

The curing concept given in the Model Code 90 is related to the rate of development as a function of w/c ratio and class of cement (MC90, Table d.11)) and the environmental conditions (MC90 Table d.l0). The minimum curing duration is determined as a function of the rate of development of impermeability and the environmental conditions. The minimum duration time is then described in days.

In the new European standard generation there has been developed a new curing concept. According to Grübl (1996), concrete properties with regard to durability are influenced by three material parameters:

- water-cement ratio,
- binder,
- hydration degree.

In EN 206, first an environmental class has to be determined to which the concrete structure will be exposed. These classes describe the environment as a function of carbonation corrosion, chloride corrosion, freeze/thaw cycle, chemical attack and abrasion. According to the environmental classes, limiting values for composition and properties of concrete are provided (maximum w/c ratio, minimum strength class of concrete, minimum cement content and minimum air pores content). By using this concept which considers the material parameters w/c ratio and binder, a good quality concrete mix with regard to durability (carbonisation, strength and compaction) can be achieved.

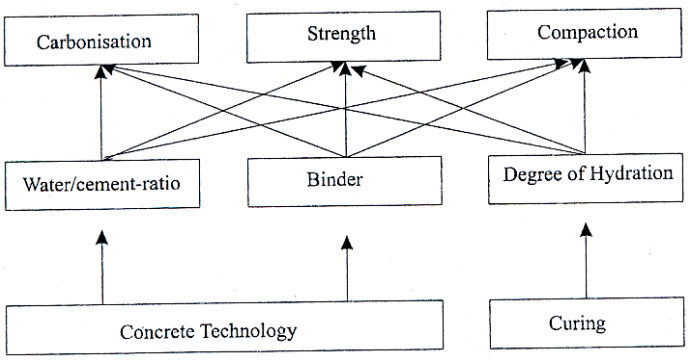


Fig. 8.5-5: Dependency of the properties which materially determine the durability of concrete on the technological parameters according to Grübl (1996)

Fig. 8.5-5 shows that w/c ratio and binder are covered by the concrete technology. The idea of the new curing concept is now, to determine curing as a function of degree of hydration. As a consequence it is possible to assure that the concrete on the construction site - especially in the surface layers- corresponds to the composition specified by the concrete technology. As criterion to judge the degree of hydration the strength has been chosen, because compared with carbonisation and compaction, more experience and testing methods are available.

In the curing concept of the European standard the duration of curing is defined in days. The concrete should have a certain strength related to the 28-day strength when the curing

Copyright fib, all rights reserved. This PDF copy of fib Bulletin 54 is intended for use and/or distribution only within National Member Groups of fib.

duration is finished. This strength ratio is a function of climate conditions (humid, moderate, dry and very dry) defined by the average relative humidity of a certain region. This has the background that hydration does not cease at the end of curing if there is a certain water supply given by a humid environment. Therefore, the duration of curing at a high outside relative humidity can be shorter compared to dry environments. As a consequence, the environmental conditions as used in the old codes (e.g. MC90) are not required any more. When the strength ratio is determined the time of curing can be chosen as function of strength ratio as presented in Fig. 8.5-6.

The next question was how this concept can be realised in design and how the strength of the concrete at a certain time can be tested on site, if great accuracy is required. The easiest case for the designer is to determine the duration of curing according to a table which directly gives the days of duration as a function of climate and strength development of the concrete. The values given in this table are determined with respect to the concept described above. Of course, these values are on the safe side. Duration time can be saved, if a more accurate method is applied. For this method the exact duration, at which the concrete achieves the demanded strength ratio at a temperature of 20°C, needs to be known (e.g. to be determined by aptitude tests). In cases of deviation, the influence of temperature on strength development has to be considered. This is possible by applying so-called maturity junctions, which describe the relation between strength development and temperature.

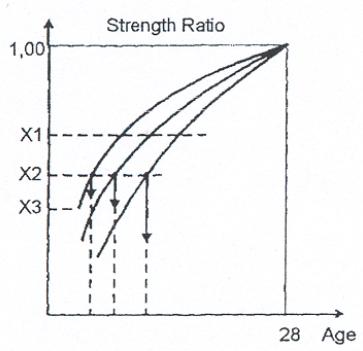


Fig. 8.5-6: Strength developments of European concretes with a w/c ratio of 0.6 according to Grübl (1996)

There are two exceptions deviating from the concept that concrete has to be cured until a certain strength ratio has to be developed. The first exception is made for structures not exposed to any moisture (e.g. interior members). In these cases, curing may be reduced to 12 maturity hours. The other exception concerns surfaces which need exceptionally high resistance against abrasion. In this case the respective strength ratio is increased by a factor 0.2.

8.6 Prestressing

Prestressing leads to an improved behaviour in the serviceability limit state. Stiffness will be increased and cracking can be avoided under severe environmental conditions. So prestressing has become an important construction method even though planning and execution of prestressed structures requires a higher technical input and experience than reinforced concrete structures. This is manifested by the fact that the quality standards for the manufacture of prestressing devices but also for the execution of prestressed structures are

Copyright fib, all rights reserved. This PDF copy of fib Bulletin 54 is intended for use and/or distribution only within National Member Groups of fib.

very high. However the widely spread use and the gained experience has lead to a huge variety of different prestressing devices and prestressing methods (see Section 3.2), as well as to sophisticated design models. In the following some important aspects are described when planning and executing prestressed structures.

8.6.1 Time of prestressing

In many cases the use of prestressed structures requires further considerations during construction. It should be kept in mind that under construction prestress may become the dominant action effect before the full dead load and service load is applied. So, the transient states may be decisive in design or require a certain prestressing procedure.

Post-tensioned structures can either be prestressed in one or several steps to avoid increased unfavourable combinations of prestress and external loads. For prestressing in one step it is important that the concrete should have hardened to a certain degree to avoid increased creep by early microcracking and subsequent losses of prestress. The age of concrete when prestress may be applied depends on the strength development and therefore on the type of cement and the temperature and curing conditions. However the strength should be sufficient to support the applied prestress (proved by hardening tests). In general, these strength values are given in approval documents. The required strength for full application of prestress should be at least 80% to 90% of 28 days strength.

In the case of greater compact cross sections it is advised to consider several steps of prestressing. Considerable internal stresses may occur because of the non-uniform distribution of hydration heat and shrinkage strains causing cracking of the concrete that has not yet its full strength. To avoid this a low percentage of prestress can already be applied in the first days. It is important though not to exceed a certain percentage of the low early strength of concrete (as already mentioned before up to 20%). The remaining prestress can then be fully applied after an adequate hardening time. In many cases it may be useful to apply prestress step by step. The degree of prestress that is applied in the first step can be chosen to equilibrate the already installed dead load and then be increased according to the advance of the construction process.

8.6.2 Effects of prestressing during construction

Structures are often prestressed to such degree that dead loads are taken by the generated prestressing force. Before the removal of the scaffold, at least parts of the prestress must be applied to take the dead loads and as a consequence to avoid the appearance of too high stresses resulting in cracking or even failure. In general the prestressing forces will cause deformations of the concrete member and thus a considerable redistribution of the forces within the scaffold. Depending on the stiffness ratio of the concrete member and the scaffold[4] it may come to unfavourable effects.

[4] The stiffness of the scaffold depends on many parameters (e.g. the number of flying shores, the stiffness of the flying shores, settlements, the stiffness of the scaffold girder) and is therefore difficult to determine.

Copyright fib, all rights reserved. This PDF copy of fib Bulletin 54 is intended for use and/or distribution only within National Member Groups of fib.

In general distinction can be made between a very stiff scaffold construction and a rather elastic one. In Fig. 8.6-1, three examples are shown where problems may occur. In Figure 8.6-1 a, the scaffold is very stiff. So the dead weight of the concrete member applied during casting does not result in a deformation of the scaffold. So if a prestressing force exceeding the dead load is applied the member will be lifted off the scaffold. Thus, the whole dead load will be activated to reduce the unfavourable effects of the prestress.

However, in cases where the scaffold is rather elastic (Fig. 8.6-1 b) the deformations due to prestressing will hardly reduce the supporting forces from the scaffold (spring back effect). In the limiting case $EI_{conc} / Ei_{scaf} \rightarrow \infty$, no dead weight will act on the member as it is still carried by the scaffold girder. The member is therefore subjected to prestressing effects alone. This leads to moments equal to the ones caused by dead load but of opposite sign and requires adequate consideration in design.

In the last example (Fig. 8.6-1 c) the scaffold girder is supported by three columns taking the dead weight of the concrete member. If the deformations of the scaffold remain small, the game phenomena as shown in the first example may happen. The concrete member rises in such way that the whole weight has to be taken by the outer columns. So, if the columns are only dimensioned for 1/4 F it may come to a collapse of the scaffold system.

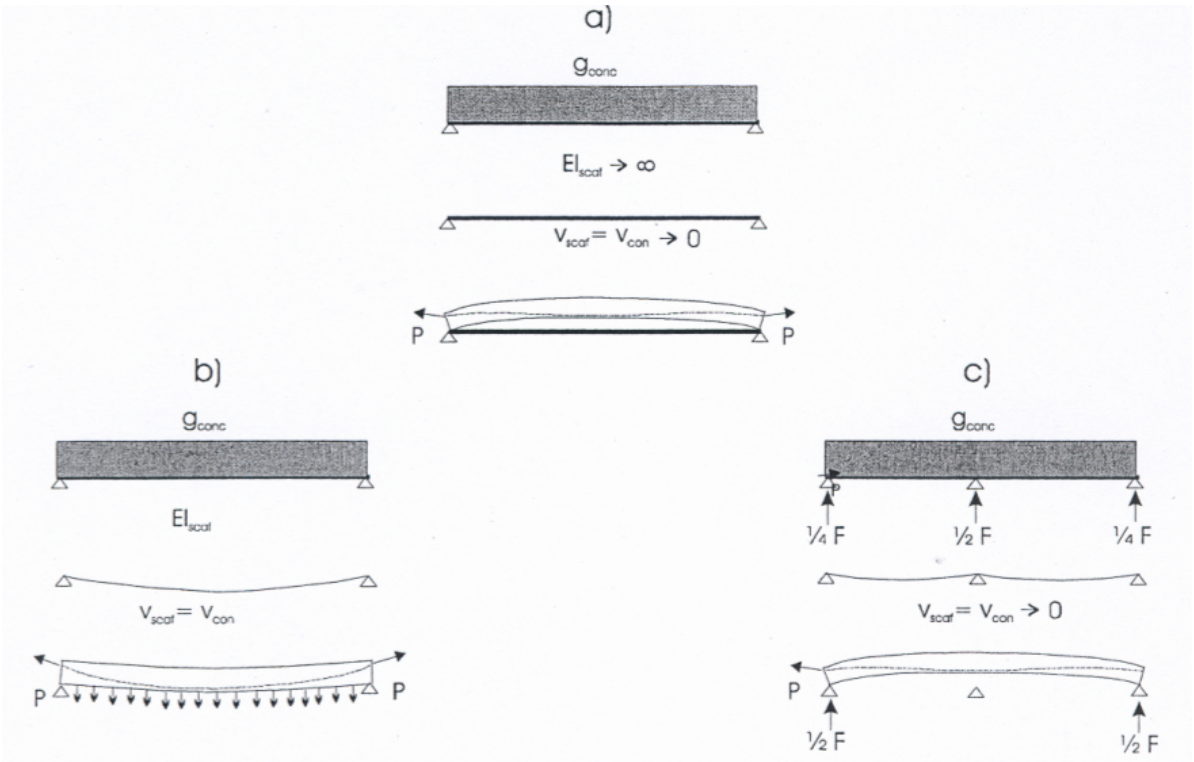


Figure 8.6-1: Prestressed beam on a) stiff scaffold, b) elastic scaffold and c) scaffold supported by columns

It can be seen that prestressing is a susceptible construction method. In many cases the design engineer has to calculate and design not only for the final condition of the structure but also for transient situations. Especially in bridge design noticeable inner redistributions of forces and stresses occur and lead to different statical systems. The engineer should be aware of this and consider all transient conditions during construction.

Copyright fib, all rights reserved. This PDF copy of fib Bulletin 54 is intended for use and/or distribution only within National Member Groups of fib.

8.7 Precast elements and structures

8.7.1 General

MC90 defines that *precasting of structural elements derives from the philosophy of industrialisation of the production processes, aimed at improving economy and quality of buildings.* In precast plants a higher quality level is possible because of the constant production conditions (e.g. weather conditions, temperature, aimed concrete strength), lower production costs (reduction of costs for formwork and falsework) and lower production time (parallel production of wall- and floor systems, production during winter).

When using precast elements it is important to choose an adequate modular co-ordination. The choice depends on the function of the building - the module of a parking garage is different than that of a hospital. According to the modular co-ordination the dimensions of the precast elements (cross-section, length) can then be determined. In this respect it is also important to determine the allowable tolerances (see also Section 8.2.2(4)). In the dimensioning process transport and erection play also an important role. The size of members is limited by the size of transport vehicles but should be as large as possible for financial reasons.

After transport of the precast elements to the construction site they are connected. Special attention should be paid to an adequate bracing of the structure. Columns (for 1 or 2 floors) or wall panels, frames, bracings or cores (for more than 2 floors) can be used for horizontal bracing possibly jointed to stiff ceiling panels – the arrangement of bracing elements should be planned and executed according to the accepted rules.

Generally analysis and design of precast structures should be carried out with respect to the ultimate and serviceability limit state requirements of in-situ structures. Modifications or supplementary requirements are given in MC90 or other Codes (e.g. ENV 1992-1-3). In analysis special attention should be paid to the following aspects:

- the behaviour of structural units as such (this may be important in transitory situations),
- the behaviour of structural assemblies, in particular with regard to actual deformability, strength and fatigue resistance,
- the uncertainties influencing restraints and force transmission between elements, that may depend on errors in geometry and in the positioning of units and bearings,
- all external and internal actions intervening in all phases (e.g. possible changes of the statical system); some non-conventional conditions may be envisaged (e.g. for dimensioning against overall instability, explosions, impacts, progressive collapse).

In design the limit states have to be verified but it is also important to consider an easy and reliable assembly and maintenance of the precast elements and the connections. In addition, the designer should account for all static and dynamic transitory situations occurring for example during transport (verification for combinations of actions such as wind, dead weight and possible superimposed loads during assembly). Since the quality of precast elements is usually very high, MC90 allows a reduction of the partial safety factors γ_c (only for precast elements, not for joints) and γ_s provided that there is a complete quality assurance system supervised by an independent control body. Reduction values are given in MC90.

Copyright fib, all rights reserved. This PDF copy of fib Bulletin 54 is intended for use and/or distribution only within National Member Groups of fib.

Nowadays the precast industry offers a great number of different elements as well as whole system units (floor systems, wall systems, beam and column systems and segmental systems). For these systems, design criteria and detailing rules have been developed which are generally approved by the building authorities and which are specified in standards for precast elements (e.g. ENV 1992-1-3). In this chapter these precast systems will not be further treated.

8.7.2 Joints

Cast-in-situ structures are manufactured by a whole casting process. Precast structures are manufactured by single elements which are connected later to an entire structure. The connecting devices are usually determined and designed during the planning process and then somehow installed during the manufacturing process (e.g. fixed at the formwork). For smaller loads they can also be applied afterwards. According to MC90 the design of joints should be based on the following assumptions:

- the joint is able to accommodate the relative displacements needed to mobilise the resistance of the joint,
- the joint is able to resist all action effects resulting from the analysis of the structure as a whole as well as those resulting from the analysis of the individual members,
- the strength and deformability of the joints secure a robust and stable behaviour of a structure as a whole,
- account is taken of the tolerances anticipated in manufacture and erection.

The resistance and stiffness of these joints is often generally approved or can be determined by analytical models or experimental tests. With regard to the different action effects to be transmitted the following joints are distinguished:

- compression joints (dry joints, bedded joints),
- shear joints (plane joints, key joints),
- flexural and tensile joints (reinforced joints, welded joints).

References to Chapter 8

ACI (1988), *Guide to Formwork for Concrete*. Journal of the ACI Vol. 85 No. 5, pp. 530-562.

Bemer, F. and Koch, M. (1999), *Schalen, Rüsten, Bewehren - Wettbewerbsfähigkeit durch Senkung der Fertigungsdauer*. Bauingenieur, 4/99, April, S3-S7.

CEB Bulletin 164 (1985), *Industrialisation of Reinforcement in Reinforced Concrete Structures*. Comité Euro-international du Béton, Lausanne, Switzerland.

CEB Bulletin 213/214 (1993), *CEB-FIP Model Code 1990*, published by Thomas Telford Ltd., UK. ("MC90").

CEB Bulletin 234 (1997). *Quality Management, Guidelines for the implementation of the ISO standards of the 9000 series in the construction industry*. Comité Euro-international du Béton, Lausanne, Switzerland.

DBV (1985), *Merkblatt Qualitätssicherung* (Fassung Dezember 1985), DBV-Merkblatt-Sammlung, Deutscher Betonverein E. V., Eigenverlag, 3. Ausgabe Mai 1991.

Copyright fib, all rights reserved. This PDF copy of fib Bulletin 54 is intended for use and/or distribution only within National Member Groups of fib.

DIN 1045/88, *Beton und Stahlbeton, Bemessung und Ausftihrung.* Normenausschuss Bauwesen (NaBau) im DIN Deutsches Institut für Normung e. V.

EN 206 (2001), *Concrete - Performances, production and conformity*. European Committee for Standardization (CEN), Brussels.

ENV 1992-1-1: 1991, *Design of concrete structures*. European Committee for Standardization (CEN), Brussels.

Grübl, P. (1996), *European concept of the Curing of Concrete*. Concrete Precasting Plant and Technology, No. 10/96.

Hosser, D., GenseI B. (1995), *Kritische Bewertung der Statistik beim Konformitätsnachweis der Betondmckfestigkeit nach prEN 206*, SchIussbericht DBV 162, Braunschweig.

Jungwirth, D. (1984), *Bauausführung, Bauorganisation - Qualitätssicherung*. Beton + Fertigteil- Technik, Heft 5, pp.332-336.

König, G., Soukhov D., Jungwirth F. (1998), *Sichere Betonproduktion für Stah1betontragwerke*, Schluβbericht DBV 1998.

Maaβ, G., Rackwitz, R. (1980), *Maßabweichungen bei Ortbetonbauten*. In: Beton- und StahIbetonbau No. 1.

Naumann, G., Springenschmid, R., Zilch, K. (1987): *Betontechnologische Besonderheiten beim Bogen*. Beton- und StahIbetonbau. Vol. 82, no. 9, pp. 229-233, published by Ernst & Sohn Verlag

Naumann, G., Wiest, R., and Zilch, K. (1988): *Konstruktion, Berechnung und Bau der Maintalbrücke Veichthöchheim*. Ernst & Sohn Verlag, Vol. 83, no. 1, pp. 19-22.

Östlund, L. (1991), *An Estimation of - Values. In: Reliability of Concrete Structures*. CEB Bulletin 202, Comité Euro-international du Béton, Lausanne, Switzerland.

PCI Journal 1 (1985), *Tolerances for Precast and Prestressed Concrete*. PCI Committee on Tolerances.

Powers, T. C (1947), *A discussion of cement hydration in relation to the curing of concrete*. Publication no. RX25, Portland Cement Association, Skokie, 12 pp.

Rackwitz, R., Müller, K. F., and Maaβ, G. (1976), *Berichte zur Sicherheitstheorie der Bauwerke. Teil 1: Untersuchungen für ein stochastisches Modell der Betonduckfestigkeit sowie zum Qualitätsangebot von Beton. Laboratorium für den konstruktiven Ingenieurbau (LKI)*, Technische Universität München, Heft 13.

Russwurm, D. (1988), *Partial factors of safety for structural materials. Betonwerk + Fertigtei l- Technik*, Heft 10, pp. 30-36

Tiltmann, K. O. (1977), Was *kostet die Genauigkeit im Betonfertigteilbau. Baugewerbe*, Heft 5, pp. 21-26.

Spears, R. E. (1983), *The 80 per cent solution to inadequate curing problems*. Concrete international 5, No. 4, pp. 15-18.

Copyright fib, all rights reserved. This PDF copy of fib Bulletin 54 is intended for use and/or distribution only within National Member Groups of fib.

Annex: List of notations

Roman lower case letters:

$1/r$	curvature of a section of an element
$1/r_{(g)}$	curvature due to g
$1/r_{(g+q)}$	curvature due to g and q
$1/r_{0(g+q)}$	instantaneous (initial) curvature due to g and q
$1/r_1$	curvature of an uncracked concrete section (state I)
$1/r_{1r}$	curvature in state I under cracking moment
$1/r_2$	curvature of a cracked concrete section (state II)
$1/r_{2r}$	curvature in state II under cracking moment
$1/r_{ts}$	tension stiffening correction for curvature
a	deflection; aggregate content in concrete
a_c	elastic deflection (calculated with rigidity $E_c I_c$)
b	breadth of compression zone or flange
b_{red}	reduced breadth of web
b_x	smaller side dimension of a rectangular section
b_y	greater side dimension of a rectangular section
b_w	breadth of web
c	concrete cover; concentration of a substance in a volume element; cement content in concrete
c_1	column dimension parallel to the eccentricity of the load
c_2	column dimension perpendicular to the eccentricity of the load
c_{min}	minimum concrete cover
c_{nom}	nominal value of concrete cover (= c_{min} + tolerance)
c_s	the transverse rib spacing, i.e. the distance between the centres of two consecutive transverse ribs measured parallel to the axis of the bar
d	effective depth to the centroid of main tension reinforcement
d’	effective depth to compression reinforcement
d_{max}	maximum aggregate size
e	load eccentricity
e_0	first order eccentricity (= M_{Sd} / N_{Sd})
e_{01}	smaller value of the first order eccentricity at one end of the considered element
e_{02}	greater value of the first order eccentricity at one end of the considered element
e_{tot}	total eccentricity
f_{bd}	design value of bond stress
f_c	cylinder compressive strength of concrete
f_c^*	cylinder compressive strength of concrete under triaxial loading (confined strength), reduced concrete strength due to transverse tension
f_{cc}	cylinder compressive strength of concrete under uniaxial stress
f_{cd}^*	design compressive strength of concrete under triaxial loading (confined strength), reduced design concrete strength due to transverse tension
f_{cd}	design value of f_c
f_{cd1}	average design strength value in an uncracked compression zone
f_{cd2}	average design strength value in a cracked compression zone
$f_{cd,fat}$	design fatigue reference strength of concrete under compression

Copyright fib, all rights reserved. This PDF copy of fib Bulletin 54 is intended for use and/or distribution only within National Member Groups of fib.

f_{ck}	characteristic value of f_c
$f_{ck,cf}$	value of f_{ck} of confined concrete
$f_{ck,cube}$	characteristic value of cube compressive strength of concrete
$f_{ck,fat}$	fatigue reference compressive strength
f_{cm}	mean value of compressive strength f_c at an age of 28 days
f_{ct}	axial tensile strength of concrete (determined according to RILEM CPC 7)
f_{ctd}	design value of f_{ct}
f_{ctk}	characteristic value of f_{ct}
f_{ctm}	mean axial tensile strength
$f_{ct,fl,m}$	mean flexural tensile strength (at T = 20°C)
$f_{ct,sp,m}$	mean splitting tensile strength
f_d	design value of strength
$f_{p0,1}$	0,1% proof stress of prestressing reinforcement
$f_{p0,2}$	0,2% proof stress of prestressing reinforcement
$f_{p0,1k}$	characteristic 0,1% proof stress
$f_{p0,2k}$	characteristic 0,2% proof stress
f_{pt}	tensile strength of prestressing reinforcement
f_{ptd}	design tensile strength of prestressing reinforcement
f_{ptk}	characteristic tensile strength of prestressing reinforcement
f_{py}	tension yield stress of prestressing reinforcement
f_{pyd}	design value of tension yield stress of prestressing reinforcement
f_{pyk}	characteristic value of tension yield stress of prestressing reinforcement
f_R	relative (or projected) rib area
f_t	tensile strength of non- prestressing reinforcement
f_{tk}	characteristic value of tensile strength of non- prestressing reinforcement
f_y	tension yield stress of non- prestressing reinforcement
f_{yc}	yield strength of steel in compression
f_{ycd}	design strength of steel in compression
f_{yd}	design value of tension yield stress of non- prestressing reinforcement
f_{yk}	characteristic value of tension yield stress of non- prestressing reinforcement
g_d	design value of distributed permanent load
h	overall depth of member, total height; notional size of a member ($2\ A_c/u$; u: perimeter in contact with the atmosphere)
h_b	depth of beam
h_f	depth of flange
h_l	the longitudinal rib height, i.e. the distance from the highest point of the rib to the surface of the core measured normal to the axis of the bar
h_s	the transverse rib height, i.e. the distance from the mid- point of the considered segment on the rib to the surface of the core measured normal to the axis of the bar
Δh_w	height of water column
i	radius of gyration, number of longitudinal ribs
j	the length of the pitch of the longitudinal rib on twisted bar
k	the number of the rows of the transverse ribs around the perimerer
l	design span, effective span, length of an element, thickness of a penetrated section
Δl	measured elongation between two measuring points
l_0	design lap length; effective length (of columns); distance between measuring points
l_b	basic anchorage length

Copyright fib, all rights reserved. This PDF copy of fib Bulletin 54 is intended for use and/or distribution only within National Member Groups of fib.

l_{bp}	basic anchorage length of pretensioned reinforcement
l_{bpd}	design anchorage length of pretensioned reinforcement
l_{bpt}	transmission length of pretensioned reinforcement
$l_{b,min}$	minimum anchorage length
$l_{b,net}$	design anchorage length
l_{ch}	lever arm characteristic length (fracture parameter)
l_p	development length for prestressing reinforcement
l_{pl}	plastic length (region in which tensile strain is larger than yield strain)
Δl_{pl}	residual elongation after unloading
$l_{p,max}$	length over which the slip between prestressing steel and concrete occurs
$l_{s,max}$	length over which the slip between steel and concrete occurs
l_t	transmission length
m	moment per unit width (out-of-plane loading); mass of substance flowing; degree of hydration; the number of transverse ribs in one row over the distance considered
n	number of bars, number of load cycles; force per unit width (in-plane-loading)
n_{Ri}	number of cycles leading to failure at stress levels $S_{i,min}$ and $S_{i,max}$, respectively
n_{Si}	number of cycles applied at constant minimum and maximum stress levels $S_{i,min}$ and $S_{i,max}$, respectively
p	local gas pressure; the number of segments on transverse rib considered
q	distributed variable load
q_d	design value of distributed variable load
r	radius
s	slip (relative displacement of steel and concrete cross-sections); shear slip (at interfaces); spacing of bars; coefficient which depend on the strength class of cement
s_{max}	maximum bar spacing
s_r	distance between cracks; radial spacing of layers of shear reinforcement
s_{rm}	mean spacing between cracks
t	time, age, duration; thickness of thin elements
t_0	age at loading
t_s	concrete age at the beginning of shrinkage or swelling
t_T	effective concrete age
u	length of a perimeter; component of displacement of a point
u_0	length of the periphery of the column or load
u_l	length of the control perimeter for punching
u_{ef}	length of the perimeter of A_{ef}
u_n	length of the control perimeter for punching outside a slab zone with shear reinforcement
v	shear force per unit width (out-of-plane loading), component of displacement of a point
w	crack width; component of displacement of a point, water content in concrete
w_c	crack width for $\sigma_{ct} = 0$
w_k	calculated characteristic crack width
w_{lim}	nominal limit value of crack width
x	depth of compression zone, distance
z	internal

Copyright fib, all rights reserved. This PDF copy of fib Bulletin 54 is intended for use and/or distribution only within National Member Groups of fib.

Greek lower case letters:

α	coefficient, reduction factor
α_e	modular ratio (E_s / E_c)
α_E	coefficient which depends on the type of aggregete
α_{es}	coefficient which depends on the type of cement
$\alpha_{e,p}$	modular ratio (E_p / E_c)
$\alpha_{e,sec}$	secant modular ratio ($E_{s,sec}$ / $E_{c,sec}$)
α_{sT}	coefficient of thermal expansion for steel
α_T	coefficient of thermal expansion in general
β_1	coefficient characterizing the bond quality of reinforcing bars
$\beta_c(t,t_0)$	coefficient to describe the development of creep with time after loading
$\beta_{as}(t)$	function to describe the development of autogenous shrinkage
$\beta_{RH}(RH)$	coefficient to take into account the effect of rel. humidity on drying shrinkage
$\beta_{ads}(t-t_s)$	function to describe the time development of drying shrinkage
β_s	transverse rib inclination i.e. the angle between the centre line of the transverse rib and the longitudinal axis of the bar
γ	safety factor
γ_c	partial safety factor for concrete material properties
$\gamma_{c,fat}$	partial safety factor for concrete material properties under fatigue loading
γ_F	partial safety factor for actions
γ_G	partial safety factor for permanent actions
γ_Q	partial safety factor for variable actions
γ_s	partial safety factor for the material properties of reinforcement and prestressing steel
$\gamma_{s,fat}$	partial safety factor for the material properties of reinforcement and prestressing steel under fatigue loading
δ_{ii}	node displacement
ε	strain
ε_c	concrete compression strain
ε_c*	concrete compression strain under triaxial stress
ε_{cm}	average concrete strain within $l_{s,max}$
ε_{c0}	concrete strain at peak stress in compression
$\varepsilon_{cc}(t)$	concrete creep strain at concrete age $t > t_0$
$\varepsilon_{ci}(t_0)$	stress dependent initial strain at the time of stress application
$\varepsilon_{cn}(t)$	total stress independent strain at a concrete age t (= $\varepsilon_{cs}(t) + \varepsilon_{cT}(t,T)$)
$\varepsilon_{cs}(t,t_s)$	total shrinkage or swelling strain at concrete age t (t in days)
$\varepsilon_{cs}(t,t_s)$	total shrinkage or swelling strain at concrete age t (t in days)
$\varepsilon_{cas}(t,t_0)$	autogenous shrinkage at time (t in days)
$\varepsilon_{cds}(t,t_0)$	drying shrinkage at time (t in days)
$\varepsilon_{caso}(f_{cm})$	notinal autogenous shrinkage coefficient
$\varepsilon_{cds}(f_{cm})$	notinal drying shrinkage coefficient
$\varepsilon_{c\sigma}(t)$	total stress dependent strain at a concrete age t (= $\varepsilon_{ci}(t_0) + \varepsilon_{cc}(t)$)
ε_{ct}	concrete tensile strain
$\varepsilon_{cT}(t,T)$	thermal strain at a concrete age t
ε_{cu}	ultimate strain of concrete in compression
ε_{d0}	strain of prestressed reinforcement corresponding to P_{d0}
ε_{pu}	total elongation of prestressing reinforcement at maximum load

Copyright fib, all rights reserved. This PDF copy of fib Bulletin 54 is intended for use and/or distribution only within National Member Groups of fib.

ε_r	strain at the onset of cracking
ε_s	steel strain
ε_{s1}	steel strain in uncracked concrete
ε_{s2}	steel strain in the crack
ε_{sm}	mean steel strain
$\Delta\varepsilon_{sr}$	increase of steel strain in cracking state
ε_{sr1}	steel strain at the point of zero slip under cracking forces
ε_{sr2}	steel strain in the crack under cracking forces (σ_{ct} reaching f_{ctm})
ε_{sT}	thermal strain of steel
ε_{su}	ultimate strain of non- prestressing reinforcement at maximum load
$\Delta\varepsilon_{ts}$	increase of strain by the effect of tension stiffening
ε_u	total elongation of reinforcing steel at maximum load
ε_{uk}	characteristic total elongation of reinforcing steel at maximum load
ε_{yd}	design yield strain of non - prestressing reinforcement (= f_{yd} / E_s)
ε_ν	transverse contraction
ζ	ratio of bond strength of prestressing steel and high-bond reinforcing steel
η	viscosity
θ	angle between web compression and the axis of a member; rotation
θ_f	angle between inclined compression in a flange and the axis of the member
λ	slenderness ratio (= l_0 / i); span/depth ratio
μ	coefficient of friction, relative bending moment
ν	relative axial force
ν_c	Poisson's ratio of concrete
ν_s	Poisson's ratio of steel
ν_{Sd}	relative design axial force (= N_{Sd} / $A_c f_{cd}$)
ρ	ratio of (longitudinal) tension reinforcement (= A_s/bd)
$\rho_{s,ef}$	effective reinforcement ratio (= $A_s/A_{c,ef}$)
ρ_t	relaxation after t hours
ρ_w	ratio of web reinforcement (= $A_{sw}/b_w s \cdot \sin\alpha$)
σ	stress
$\chi\ (t,t_0)$	ageing cooeficient
$\sigma_1,\sigma_2,\sigma_3$	principal stresses
σ_c	concrete compression stress
σ_{cd}	design concrete compression stress
σ_{ct}	concrete tensile stress
$\sigma_{c,cf}$	compression stress of confined concrete
$\sigma_{c,max}$	maximum compressive stress
$\sigma_{c,min}$	minimum compressive stress
$\sigma_{p0}\,(x)$	initial stress in prestressing reinforcement at a distance x from anchorage device
$\sigma_{p0,max}$	maximum tensile stress in prestressing reinforcement at tensioning
σ_{pcs}	tendon stress due to prestress after all losses (due to creep and shrinkage)
σ_{pd}	tendon stress under design load
$\Delta\sigma_{Rsk}(n)$	stress range relevant to n cycles obtained from a characteristic fatigue strength function
σ_s	steel stress
σ_{s2}	steel stress in the crack
σ_{sE}	steel stress at the point of zero slip

Copyright fib, all rights reserved. This PDF copy of fib Bulletin 54 is intended for use and/or distribution only within National Member Groups of fib.

σ_{sr2} steel stress in the crack under crack loading (σ_{ct} reaching f_{ctm})
$\Delta\sigma_{Ss}$ steel stress range under the acting loads
$\Delta\sigma_p$ loss of prestress
σ_{sw} stirrups stress
τ_b local bond stress
τ_{bm} mean bond stress
$\tau_{fu,d}$ ultimate design shear friction capacity
τ_{max} maximum value of bond stress
τ_{Rd} resistance to shear stress (design value)
τ_{Sd} applied shear stress (design value)
$\psi\ (t,t_0)$ relaxation coefficient
ω mechanical reinforcement ratio
ω_{sw} mechanical ratio of stirrup reinforcement
ω_v volumetric ratio of confining reinforcement
ω_w volumetric mechanical ratio of confining reinforcement
ω_{wd} design volumetric mechanical ratio of confining reinforcement

Roman capital letters:

A total area of a section or part of a section (enclosed within the outer circumference)
A_1 section area in state I (taking into account the reinforcement)
A_c area of concrete cross section or concrete compression chord
$A_{c,ef}$ effective area of concrete in tension
A_{core} effectively confined area of cross-section in compression
A_{ef} area enclosed by the centre-lines of a shell resisting torsion
A_p cross-sectional area of prestressing reinforcement
A_s cross-sectional area of reinforcement
A_s' cross-sectional area of compressed reinforcement
A_{sh} cross-sectional area of hoop reinforcement for torsion
A_{sl} cross-sectional area of longitudinal reinforcement
A_{st} cross-sectional area of transverse reinforcement
A_{sw} cross-sectional area of shear reinforcement
$A_{s,cal}$ calculated cross-sectional area of reinforcement required by design
$A_{s,ef}$ cross-sectional area of reinforcement provided
$A_{s,min}$ minimum reinforcement area
C_{eq} the equivalent carbon value
D fatigue damage, diffusion coefficient
$D^{el}(t)$ system of deformations in the associated elastic problem
D_{lim} limiting fatigue damage
E modulus of elasticity
E_c modulus of elasticity for concrete
$E_c(t_0)$ modulus of elasticity at the time of loading t_0
E_{ci} tangent modulus of elasticity at a stress σ_i (at T = 20°C)
$E_{c,sec}$ secant modulus of elasticity at failure for uniaxial compression ($E_{c,sec} = f_{cm}/|\varepsilon_{c0}|$)
E_p modulus of elasticity of prestressing steel
E_s modulus of elasticity of steel
$E_{s,sec}$ secant modulus of elasticity of steel
F force, applied load or load effect

Copyright fib, all rights reserved. This PDF copy of fib Bulletin 54 is intended for use and/or distribution only within National Member Groups of fib.

F_b	bond force transmitted along the transmission length
F_c	strut force (compression force)
F_d	design value of action
F_{pt}	tensile load of prestressed reinforcement
$F_{p0,1}$	characteristic 0,1% proof -load
$F_{Sd,ef}$	effective concentric load (punching load enhanced to allow for the effects of moments)
F_t	tie force (tension force)
F_{ud}	ultimate dowel force
G	permanent action
G_F	fracture energy of concrete
G_{F0}	base value of fracture energy (depending on maximum aggregate size)
G_{inf}	favourable part of permanent action
G_{sup}	unfavourable part of permanent action
H	horizontal force, horizontal component of a force
I	second moment of area
I_1	second moment of area in state I (including the reinforcement)
I_2	second moment of area in state II (including the reinforcement)
I_c	second moment of area of the uncracked concrete cross-section (state I)
$J(t,t_0)$	creep function or creep compliance representing the total stress dependent strain per unit stress
K_g	coefficient of gas permeability
K_w	coefficient of water permeability
L	span, length of an element
M	bending moment; maturity of concrete
M_r	cracking moment
M_{Rd}	design value of resistant moment
M_{Sd}	design value of applied moment
M_u	ultimate moment
M_y	yielding moment
N	axial force, number of cycles to failure (fatigue loading)
N_r	axial cracking force
N_{Rd}	design value of resistance to axial force
N_{Sd}	design value of applied axial force
P_{d0}	design value of prestressing force (initial force)
$P_{k,inf}$	lower characteristic value of prestressing force
$P_{k,sup}$	upper characteristic value of prestressing force
P_m	mean value of prestressing force
Q	variable single action
$R(t, t_0)$	relaxations function
R	resistance (strength); bending radius; universal gas constant
R_d	design resistance
RH	ambient relative humidity
RH_0	100% relative humidity
S	load effect (M, N, V, T); absorption coefficient
ΔS_{cd}	stress range under fatigue loading
$S_{cd,max}$	design value of maximum compressive stress level (fatigue loading)

Copyright fib, all rights reserved. This PDF copy of fib Bulletin 54 is intended for use and/or distribution only within National Member Groups of fib.

$S_{cd,min}$	design value of minimum compressive stress level (fatigue loading)
$S_{c,max}$	maximum compressive stress level (fatigue loading)
$S_{c,min}$	minimum compressive stress level (fatigue loading)
S_d	design value of load effect (M, N, V, T)
$S^{el}(t)$	system of stresses in the associated elastic problem
T	temperature, torsional moment
ΔT	temperature change
T_{Rd}	design value of resistance to torsional moment
T_{Sd}	design value of applied torsional moment
$T_{Sd,eff}$	effective design value of applied torsional moment
V	shear force; volume of gas or liquid
V_{Rd}	design value of resistance to shear force
V_{Sd}	design value of applied shear force
$V_{s,trans}$	volume of closed stirrups or cross-ties
V_u	ultimate shear force
W_1	section modulus in state I (including the reinforcement)
W_2	section modulus in state II (including the reinforcement)
W_c	section modulus of the uncracked concrete cross-section (state I)
$W_{c,cf}$	volume of confined concrete
W_e	external work
W_i	internal work

<u>others:</u>

ø	nominal diameter of steel bar
$ø_n$	equivalent diameter of bundles containing n bars
$ø_p$	diameter of prestressing steel (for bundles equivalent diameter)
$\phi\ (t,t_0)$	creep coefficient
ϕ_0	notional creep coefficient
Θ_{pl}	plastic rotation capacity
$\sum U$	total perimeter of rebars

Copyright fib, all rights reserved. This PDF copy of fib Bulletin 54 is intended for use and/or distribution only within National Member Groups of fib.

fib *– fédération internationale du béton – the International Federation for Structural Concrete – is grateful for the invaluable support of the following National Member Groups and Sponsoring Members, which contributes to the publication of* ***fib*** *technical bulletins, the Structural Concrete Journal, and* ***fib****-news.*

National Member Groups

AAHES - Asociación Argentina del Hormigón Estructural, Argentina
CIA - Concrete Institute of Australia
ÖVBB - Österr. Vereinigung Für Beton und Bautechnik, Austria
GBB - Groupement Belge du Béton, Belgium
ABCIC - Associação Brasileira da Construção Industrializada de Concreto, Brazil
ABECE - Associação Brasileira de Engenharia e Consultoria Estrutural, Brazil
fib Group of Canada
CCES - China Civil Engineering Society
Hrvatska Ogranak ***fib***-a (HOFIB) - Croatian Group of ***fib***
Cyprus University of Technology
Ceska betonarska spolecnost, Czech Republic
Dansk Betonforening DBF - Danish Concrete Society
Suomen Betoniyhdistys r.y. - Concrete Association of Finland
AFGC - Association Française de Génie Civil, France
Deutscher Ausschuss für Stahlbeton, Germany
Deutscher Beton- und Bautechnik-Verein e.V. – dbv, Germany
Technical Chamber of Greece
Hungarian Group of fib, Budapest Univ. of Tech. & Economics
The Institution of Engineers (India)
Management and Planning Organization, Iran
IACIE - Israeli Association of Construction and Infrastructure Engineers
Consiglio Nazionale delle Ricerche, Italy
JCI - Japan Concrete Institute
PCEA - Prestressed Concrete Engineering Association, Japan
Administration des Ponts et Chaussées, Luxembourg
Betonvereniging - ***fib*** Netherlands
New Zealand Concrete Society
Norsk Betongforening - Norwegian Concrete Association
Chancellery of the Polish Academy of Sciences
Committee of Civil Engineering, Concrete Structures Section, Poland
GPBE - Grupo Portugês de Betão Estrutural, Portugal
Society For Concrete and Prefab Units of Romania
Technical University of Civil Engineering, Romania
Association for Structural Concrete (ASC), Russia

Association of Structural Engineers, Serbia
Slovak Union of Civil Engineers
Slovenian Society of Structural Engineers
ACHE - Asociacion Cientifico-Técnica del Hormigon Estructural, Spain
Svenska Betongföreningen, Sweden
Délégation nationale suisse de la ***fib***, IS-BETON, EPFL, Switzerland
ITU - Istanbul Technical University, Turkey
Research Inst. of Build. Constructions, Ukraine
fib UK Group
ASBI - American Segmental Bridge Institute, USA
PCI - Precast/Prestress. Concrete Institute, USA
PTI - Post Tensioning Institute, USA

Sponsoring Members

Preconco Limited, Barbados
Liuzhou OVM Machinery Co., Ltd., China
Consolis Technology Oy Ab, Finland
Fachverband Beton- u. F. B.-W. e. V., Germany
FIREP Rebar Technology GmbH, Germany
MKT Metall-Kunststoff-Technik GmbH, Germany
Larsen & Toubro Ltd., ECC Division, India
Sireg S.P.A., Italy
Fuji P. S. Corporation Ltd., Japan
Kajima Corporation, Japan
Obayashi Corporation, Japan
Oriental Construction Co.Ltd., Japan
P. S. Mitsubishi Construction Co., Ltd., Japan
PC Bridge Company Ltd., Japan
SE Corporation, Japan
Sumitomo Mitsui Construct. Co. Ltd., Japan
BBR VT International Ltd., Switzerland
SIKA Services AG, Switzerland
VSL International Ltd, Switzerland
PBL Group Ltd., Thailand
CCL Stressing Systems Ltd., United Kingdom
Strongforce Engineering PLC, United Kingdom

fib Bulletins published since 1998

N°	Title
1	Structural Concrete – Textbook on Behaviour, Design and Performance; Vol. 1: Introduction - Design Process – Materials Manual - textbook (244 pages, ISBN 978-2-88394-041-3, July 1999)
2	Structural Concrete – Textbook on Behaviour, Design and Performance Vol. 2: Basis of Design Manual - textbook (324 pages, ISBN 978-2-88394-042-0, July 1999)
3	Structural Concrete – Textbook on Behaviour, Design and Performance Vol. 3: Durability - Design for Fire Resistance - Member Design - Maintenance, Assessment and Repair - Practical aspects Manual - textbook (292 pages, ISBN 978-2-88394-043-7, December 1999)
4	Lightweight aggregate concrete: Extracts from codes and standards State-of-the-art report (46 pages, ISBN 978-2-88394-044-4, August 1999)
5	Protective systems against hazards: Nature and extent of the problem Technical report (64 pages, ISBN 978-2-88394-045-1, October 1999)
6	Special design considerations for precast prestressed hollow core floors Guide to good practice (180 pages, ISBN 978-2-88394-046-8, January 2000)
7	Corrugated plastic ducts for internal bonded post-tensioning Technical report (50 pages, ISBN 978-2-88394-047-5, January 2000)
8	Lightweight aggregate concrete: Part 1 (guide) – Recommended extensions to Model Code 90; Part 2 (technical report) – Identification of research needs; Part 3 (state-of-art report) – Application of lightweight aggregate concrete (118 pages, ISBN 978-2-88394-048-2, May 2000)
9	Guidance for good bridge design: Part 1 – Introduction, Part 2 – Design and construction aspects. Guide to good practice (190 pages, ISBN 978-2-88394-049-9, July 2000)
10	Bond of reinforcement in concrete State-of-art report (434 pages, ISBN 978-2-88394-050-5, August 2000)
11	Factory applied corrosion protection of prestressing steel State-of-art report (20 pages, ISBN 978-2-88394-051-2, January 2001)
12	Punching of structural concrete slabs Technical report (314 pages, ISBN 978-2-88394-052-9, August 2001)
13	Nuclear containments State-of-art report (130 pages, 1 CD, ISBN 978-2-88394-053-6, September 2001)
14	Externally bonded FRP reinforcement for RC structures Technical report (138 pages, ISBN 978-2-88394-054-3, October 2001)
15	Durability of post-tensioning tendons Technical report (284 pages, ISBN 978-2-88394-055-0, November 2001)
16	Design Examples for the 1996 FIP recommendations *Practical design of structural concrete* Technical report (198 pages, ISBN 978-2-88394-056-7, January 2002)
17	Management, maintenance and strengthening of concrete structures Technical report (180 pages, ISBN 978-2-88394-057-4, April 2002)

N°	Title
18	Recycling of offshore concrete structures State-of-art report (33 pages, ISBN 978-2-88394-058-1, April 2002)
19	Precast concrete in mixed construction State-of-art report (68 pages, ISBN 978-2-88394-059-8, April 2002)
20	Grouting of tendons in prestressed concrete Guide to good practice (52 pages, ISBN 978-2-88394-060-4, July 2002)
21	Environmental issues in prefabrication State-of-art report (56 pages, ISBN 978-2-88394-061-1, March 2003)
22	Monitoring and safety evaluation of existing concrete structures State-of-art report (304 pages, ISBN 978-2-88394-062-8, May 2003)
23	Environmental effects of concrete State-of-art report (68 pages, ISBN 978-2-88394-063-5, June 2003)
24	Seismic assessment and retrofit of reinforced concrete buildings State-of-art report (312 pages, ISBN 978-2-88394-064-2, August 2003)
25	Displacement-based seismic design of reinforced concrete buildings State-of-art report (196 pages, ISBN 978-2-88394-065-9, August 2003)
26	Influence of material and processing on stress corrosion cracking of prestressing steel – case studies. Technical report (44 pages, ISBN 978-2-88394-066-6, October 2003)
27	Seismic design of precast concrete building structures State-of-art report (262 pages, ISBN 978-2-88394-067-3, January 2004)
28	Environmental design State-of-art report (86 pages, ISBN 978-2-88394-068-0, February 2004)
29	Precast concrete bridges State-of-art report (83 pages, ISBN 978-2-88394-069-7, November 2004)
30	Acceptance of stay cable systems using prestressing steels Recommendation (80 pages, ISBN 978-2-88394-070-3, January 2005)
31	Post-tensioning in buildings Technical report (116 pages, ISBN 978-2-88394-071-0, February 2005)
32	Guidelines for the design of footbridges Guide to good practice (160 pages, ISBN 978-2-88394-072-7, November 2005)
33	Durability of post-tensioning tendons Recommendation (74 pages, ISBN 978-2-88394-073-4, December 2005)
34	Model Code for Service Life Design Model Code (116 pages, ISBN 978-2-88394-074-1, February 2006)
35	Retrofitting of concrete structures by externally bonded FRPs. Technical Report (224 pages, ISBN 978-2-88394-075-8, April 2006)
36	2006 *fib* Awards for Outstanding Concrete Structures Bulletin (40 pages, ISBN 978-2-88394-076-5, May 2006)
37	Precast concrete railway track systems State-of-art report (38 pages, ISBN 978-2-88394-077-2, September 2006)
38	Fire design of concrete structures – materials, structures and modelling State-of-art report (106 pages, ISBN 978-2-88394-078-9, April 2007)

N°	Title
39	Seismic bridge design and retrofit – structural solutions State-of-art report (300 pages, ISBN 978-2-88394-079-6, May 2007)
40	FRP reinforcement in RC structures Technical report (160 pages, ISBN 978-2-88394-080-2, September 2007)
41	Treatment of imperfections in precast structural elements State-of-art report (74 pages, ISBN 978-2-88394-081-9, November 2007)
42	Constitutive modelling of high strength / high performance concrete State-of-art report (130 pages, ISBN 978-2-88394-082-6, January 2008)
43	Structural connections for precast concrete buildings Guide to good practice (370 pages, ISBN 978-2-88394-083-3, February 2008)
44	Concrete structure management: Guide to ownership and good practice Guide to good practice (208 pages, ISBN 978-2-88394-084-0, February 2008)
45	Practitioners' guide to finite element modelling of reinforced concrete structures State-of-art report (344 pages, ISBN 978-2-88394-085-7, June 2008)
46	Fire design of concrete structures —structural behaviour and assessment State-of-art report (214 pages, ISBN 978-2-88394-086-4, July 2008)
47	Environmental design of concrete structures – general principles Technical report (48 pages, ISBN 978-2-88394-087-1, August 2008)
48	Formwork and falsework for heavy construction Guide to good practice (96 pages, ISBN 978-2-88394-088-8, January 2009)
49	Corrosion protection for reinforcing steels Technical report (122 pages, ISBN 978-2-88394-089-5, February 2009)
50	Concrete structures for oil and gas fields in hostile marine environments State-of-art report (36 pages, IBSN 978-2-88394-090-1, October 2009)
51	Structural Concrete – Textbook on behaviour, design and performance, vol. 1 Manual – textbook (304 pages, ISBN 978-2-88394-091-8, November 2009)
52	Structural Concrete – Textbook on behaviour, design and performance, vol. 2 Manual – textbook (350 pages, ISBN 978-2-88394-092-5, January 2010)
53	Structural Concrete – Textbook on behaviour, design and performance, vol. 3 Manual – textbook (390 pages, ISBN 978-2-88394-093-2, December 2009)
54	Structural Concrete – Textbook on behaviour, design and performance, vol. 4 Manual – textbook (196 pages, ISBN 978-2-88394-093-2, October 2010).
55	*fib* Model Code 2010, First complete draft – Volume 1 Draft Model Code (318 pages, ISBN 978-2-88394-095-6, March 2010)
56	*fib* Model Code 2010, First complete draft – Volume 2 Draft Model Code (312 pages, ISBN 978-2-88394-096-3, April 2010)

Abstracts for *fib* Bulletins, lists of available CEB Bulletins and FIP Reports, and an order form are available on the *fib* website at www.fib-international.org/publications.